UVR8 FUNCTION IN A NATURAL SOLAR ENVIRONMENT

Kirsten Findlay

Submitted in fulfilment of the requirements for the degree of Doctor of Philosophy

Institute of Molecular, Cell and Systems Biology
Faculty of Biomedical and Life Sciences
University of Glasgow

September 2015

Abstract

In a natural outdoor environment plants have to react to a variety of signals including Ultraviolet-B (UV-B) light. UV-B light was long believed to be a stressor to plants, but recent research has shown that a stress response to UV-B is unusual in natural solar environments. The UV-B photoreceptor in plants, UV RESISTANCE LOCUS8 (UVR8), has also been identified and studied in both purified protein and controlled growth room conditions. It has been established that UVR8 is a dimer in the absence of UV-B and monomerises after UV-B absorption, initiating UV-B photomorphogenesis. However, while these studies were excellent for uncovering the mechanism of photoreception, they were undertaken in UV-B naïve plants, typically with only one or two *Arabidopsis thaliana* ecotypes, and used short term UV-B exposure. In a natural solar environment, plants are exposed to UV-B over the entirety of their lifetime. This study aims to investigate the effect of long term UV-B exposure on UVR8 and what factors might affect a plant's response to UV-B other than UV-B fluence rate.

Under controlled growth room conditions, the long term effect of varying ecologically relevant fluence rates of UV-B on UVR8 was investigated. It was found that in the absence of UV-B no monomerisation occurred, as expected. While monomerisation was observed in plants that had received long term UV-B treatment, UVR8 did not act as an off/on dimer-to-monomer switch. Instead a balanced photoequilibrium between dimer and monomer was observed. This was confirmed in a natural solar environment, although the photoequilibrium was far more variable, suggesting that factors other than UV-B fluence rate, such as temperature, were having an effect on the photoequilbrium.

Further investigation demonstrated that the REPRESSOR OF UV-B PHOTOMORPHOGENESIS (RUP) proteins were involved in maintaining the photoequilibrium of UVR8. Additionally, temperature was affecting the UVR8 photoequilibrium via the RUP proteins as the regeneration rate of UVR8 differed between different temperature environments. *A. thaliana* ecotype also played a role on the balance of the UVR8 photoequilibrium. Ecotypes from higher altitudes seemed to be less sensitive to UV-B than low altitude ecotypes in

establishing a photoequilibrium. However, different ecotypes of *A. thaliana* show variation in many diverse physiological ways, for example seed dormancy or trichome density. Hence the variation in UVR8 photoequilibrium between ecotypes of different altitudes was not necessarily adaptive.

To determine the role of environment in UV-B photoreception, 855 *A. thaliana* ecotypes that had been fully sequenced by the 1001 Genomes Project were categorised based on six different genes involved in UV-B photoreception, UVR8, ELONGATED HYPOCOTYL 5 (HY5), HY5 HOMOLOG (HYH), CONSTITUTIVELY PHOTOMORPHOGENIC 1 (COP1), RUP1 and RUP2. By grouping the non-synonymous changes seen in these genes by continent, country, latitude, longitude and altitude it was possible to determine how different genes vaired based on geography, UV-B environment and both. HYH did not differ based on any of the investigated criteria. HY5 and COP1 did vary based on geographical location. UVR8, RUP1 and RUP2 changed based on geographical location and UV-B environment. Furthermore, there were some amino acid substitutions that were more common in high UV-B environments than elsewhere.

This study has shown how long term exposure to a signal may change the molecular response to that signal. Furthermore, it has highlighted that several factors can affect the response of a single protein. New information has been obtained, both on the response of UVR8 in a natural environment and on the genetic variation of the UV-B haplotype in *A. thaliana* with respect to adaptation to the environment. Further work is required to determine other factors that cause the variability in the UVR8 photoequilibrium in a natural solar environment and to investigate how the amino acid changes in the UV-B haplotype affect the UVR8 photoequilibrium.

Table of Contents

Figures and Tables

CHAPTER 1:

CHAPTER 2:

CHAPTER 3:

CHAPTER 4:

CHAPTER 5:

APPENDIX:

Acknowledgements

Firstly, I would like to thank my supervisor Prof. Gareth I. Jenkins. He has not only provided encouragement, advice and invaluable support throughout my Ph.D, but taught me how to become an independent and self-sufficient researcher. I valued how you pushed me outside of my comfort zone in the lab but also listened to my ideas and let me set the course of my research. Thanks also to Prof. John M. Christie, who was always available for discussion and helped me sort out my ideas and gave many helpful suggestions. I also want to thank Dr Eirini Kaiserli, who challenged my assumptions and encouraged me to keep going, the discussions we had made me a better scientist.

This Ph.D would not have been possible without all of the excellent lab colleagues and friends I have made during my research. Thank you to Dr Catherine Cloix, Dr Katherine Baxter, Dr Bobby Brown and Peggy Ennis for helping me get started in a new lab, giving me protocols and helping me troubleshoot. Thanks to Dr Christos Velanis, for keeping me company through my timecourses and always reminding me that I could do another Ponceau. Thank you to Bhavana for sharing tea with me and chatting to me about non-science. It was so good to get a break and get to know you. Thank you to Dr Ashutosh, Kirsty McInnes, Lisa Blackwood, Dr Monika Heilmann, Dr Jan Peterson, Aranza Díaz Ramos, Jaynee Hart, Xingyang Liao, Vicky Millen and William Rooney for making the lab a fun place to work, for helping me out and encouraging me when I was down. Thank you to everyone in the Bower Building for making me feel at home. I also need to thank the BBSRC for funding my work.

I would also like to thank Graeme Sneddon, I miss our morning coffee breaks where we discussed our research. You reminded me that I was still a good person and a good scientist even when my experiments weren't working. My family deserve thanks for listening to me talk about my research patiently, without your kind words this would have been so much harder.

Finally, I would like to thank my incredible fiancé Victoria Gerrie. I have so much to thank you for I can't include it all here. You supported me, celebrated with me, commiserated with me and became my proof reader and editor in this final stretch. I couldn't have survived this without you.

Abbreviations

35S	Cauliflower mosaic virus 35S promotor
ABRC	*Arabidopsis* Biological Resource Center
ATM	ataxia telangiectasia-mutated
ATP	Adenoside triphosphate
ATR	ataxia telangiectasia-mutated and RAD3-related
BLAST	basic local alignment search tool
BSA	bovine serum albumin
BRET	bioluminescence resonance energy transfer
BRZ	brassinosteroids
bZIP	basic leucine zipper
CCE	Cryptochrome C-terminal extension domain
CD	circular dichroism
CDF	cycling DOF factor
CHS	chalcone synthase
CHUP	chloroplast unusual positioning
CIB	cryptochrome-interacting basic-helix-loop-helix
CLS	cytoplasmic localisation signal
CO	constans
COP	consitutively photomorphogenic
CRY	cryptochrome
CV	column volume
cv.	cultivar
DAS	DQXVP-Acidic-STAESSS motif
DDB	damaged DNA binding
DNA	deoxyribonucleic acid
DOF	DNA-binding with One Finger
DTT	1,4-Dithiothreitol
DWD	DDB1 binding WD40 Domain
EDTA	theylenediaminetetraacetic acid
EFO	early flowering by overexpression
FAD	Flavin adenine dinucleotide
FKF	flavin-binding Kelch Repeat F-box
FLC	flowering locus C

FMN	Flavin mononucleotide
FRET	Förster resonance energy transfer
FT	flowering locus T
GA	gibberellic acid
GAF	cGMP-specific phosphodiesterases adenylyl cyclases and FhiA domain
GEF	guanine nucleotide exchange factor
GFP	green fluorescent protein
GI	gigantea
GLM	generalised linear modelling
GSH	glutathione
HFR	long hypocotyl in far-red
HKRD	histidine-kinase-related domain
HRP	horseradish peroxidase
HY	elongated hypocotyl
HYH	HY5 homolog
IPTG	isopropyl-beta-D-thiogalactopyanoside
JA	jasmonic acid
JAC	J-domain protein required for chloroplast accumulation response
kDa	kilo Dalton
LAF	long after far-red
LB	Luria broth medium
LFR	low-fluence responses
LKP	LOV Kelch Protein
LOV	light oxygen voltage
LWL	low white light
MAPK	mitogen-activated protein kinase
MKP	MAPK phosphatase
mRNA	messenger ribonucleic acid
MS	Murashige and Skoog salts
MTHF	5,10-methenultetrahydrofolate
NASC	The European *Arabidopsis* Stock Centre
NCBI	National Center for Biotechnology Information
NLS	nuclear localisation signal
NPH	non-phototropic hypocotyl
OD	optical density
OX	over-expressor

PΦB	phytochromobillin
PAGE	polyacrylamide gel electrophoresis
PAR	photosynthetically active radiation
PAS	Per-ARNT-Sim
Pfr	far-red light absorbing form of phytochrome
PHOT	phototropin
PHY	phytochrome
PHR	photolyase-homologous region
PIF	phytochrome interacting factor
PKS	phytochrome kinase substrate
PMI	plastid movement impaired
PMSF	phenylmethylsulphonylfluoride
Pr	red light absorbing form of phytochrome
PRR	pseudo-response regulator
QTL	quantitative trait loci
rbcL	ribulose-1,5-bisphosphate carboxylase large subunit
RCC	regulator of chromatin condensation
RING	really interesting new gene
RNA	ribonucleic acid
ROS	reactive oxygen species
RUP	repressor of UV-B photomorphogenesis
SDS	sodium dodecyl sulfate
SE	standard error
SNLS	subnuclear localization signal
SPA	suppressor of phyA
SUMO	small ubiquitin-related modifier
TAIR	The *Arabidopsis* Information Resource
TBS	Tris buffered saline
TBS-T	Tris buffered saline Triton-X
TBS-TT	Tris buffered saline Triton-X Tween
TEMED	N,N,N',N'-tetramethylethane-1,2-diamine
TOC	timing of CAB expression
Tris	Tris(hydroxymethyl)aminomethane
UV	ultraviolet
UVR	UV resistance locus
VLFR	very-low fluence responses

v/v	volume/volume
w/v	weight/volume
WT	wild-type
ZTL	Zeitlupe

Chapter 1: Introduction

1.1 Plants in their environment

Throughout their lives, plants are subject to many different signals that dictate both when and how they grow (Chen, *et al*. 2004). As sessile organisms, reacting to environmental signals with some plasticity is important. The ability to react appropriately to different environmental signals can be a matter of survival for plants. Not only does reaction to these signals include stress responses, but can also have developmental effects (Frohnmeyer and Staiger, 2003, Hideg, *et al*. 2013). There are many different environmental signals that can provoke a response in plants; including temperature, salt concentration in the soil, water availability, gravity and light (Trewavas and Malhó, 1997). These external factors do not directly change the growth of plants; instead they are detected and monitored by a variety of sensors within the plant that can cause changes in the chemical composition of the cell, leading to changes in morphology (Trewavas and Malhó, 1997). If the way that plants sense signals from their environment and how they respond to them is understood, this will allow greater understanding of the way that plants grow, allowing the morphology of plants to be potentially controlled or enabling the protection of plants from stresses.

1.1.1 Signal based responses

As previously mentioned plants grow in response to a variety of signals. These signals can either regulate the development of the plant to better suit its environment or induce stress. Whether a signal causes a stress response or a developmental change depends partly on the kind of environment that a plant has evolved in. This is the reason that many plants have latitude restricted populations (Sexton, *et al*. 2009). A species will have a limited range based on a variety of abiotic and biotic factors such as temperature or other climatic conditions (Sexton, *et al*. 2009). This example is true, in varying forms, for most of the signals that plants receive - what is too much for one plant may be too little for another.

1.1.2 Stress

Stress can occur at any time during a plant's lifetime. Many different environmental factors can be a stress: nutrient concentration in the soil; water availability; salt concentration in the soil; the temperature (including freezing and fire stress); light intensity and wavelength (Smirnoff, 1998). There are three options available for a plant to deal with stress: they can try to avoid the stress; acclimate to a stress or adapt to a stress (Angers, *et al*. 2010, Smirnoff, 1998, Vinocur and Altman, 2005).

1.1.2.1 Acclimation

Acclimation is when a plant is exposed to a stress and responds to protect itself. The ability to change in response to a stress also provides extra protection in the event of a stress worsening after the initial exposure. There are lots of different signals that can cause this. For example, cold and freezing acclimation can be triggered by both a slow decrease in temperature and the transition from long to short days (Guy, 1990, Thomashow, 1999, Thomashow, 2001). Another point about acclimation is that not all plants will adjust their responses to the same degree, and some won't change their growth responses at all (Osmond, *et al*. 1987). An interesting example of this is plants that are able to withstand -196°C, the equivalent to liquid nitrogen, when appropriately introduced to gradual reductions in temperature (Burke, *et al*. 1976). A further example is the ability of some species to escape anaerobic stress through vertical growth (Visser, *et al*. 2003). Acclimation can also occasionally cause cross-tolerance to different stresses (Chalker-Scott and Scott 2004). This is because the changes that occur to protect against one stress can protect against another. Therefore it is important to understand how the stress is affecting the plant, what actions the plant takes to protect itself against damage and how the responses could affect other stresses the plant may experience.

1.1.2.2 Adaptation

Adaptation to a stress is when a plant is genetically prepared to deal and cope with a stress. For example, there are many plants that are regularly flooded and therefore unable to respire, however their adaptations and then further acclimation allow them to cope with this stress for far longer than other plants

that do not have specific adaptations (Perata, *et al*. 2011). Adaptation to a stress also impacts on the degree to which a plant can acclimate to a stress and occasionally the type of response the stress triggers.

1.1.3 Signal directed growth and development

Plants receive signals every day of their lives, whereas stresses are not necessarily (although they certainly can be) continuous. Plants use these signals to interpret their environment and to direct their growth patterns accordingly. Nutrient concentration in the soil will affect root growth. Gravity affects the direction in which a newly germinated seedling grows. Sunlight or lack thereof affects the direction of growth of plants, the circadian rhythm of a plant and flowering time among other responses (Clerget, *et al*. 2012, McClung, *et al*. 2002, Pedmale, *et al*. 2010). Indeed, as plants are photo-autotrophs, light is one of the most important signals during a plant's life. If there is not enough light, the plant will be unable to photosynthesize and will die; if the sunlight is too intense it could damage the chloroplasts and photosynthetic apparatus and stop photosynthesis. The direction of sunlight is important, as is the wavelength. The length of day is also a key factor in the flowering time of plants (Boccalandro, *et al*. 2004, Clerget, *et al*. 2012, Imaizumi, *et al*. 2005, McClung, *et al*. 2002). Light signals are monitored by a range of photoreceptors, whose signalling pathways overlap to control different aspects of plant development and stress response and which respond to different wavelengths of light (Chen *et al*. 2004, Christie, 2007, Deng, *et al*. 1994, Devlin, *et al*. 2007, Heijge and Ulm, 2012, Li, *et al*. 2011, Möglich, *et al*. 2010, Yu, *et al*., 2010). These photoreceptors are vital to photomorphogenesis within the plant (Boccalandro, *et al*. 2004, Pedmale, *et al*. 2010).

1.2 Photomorphogenesis

Photomorphogenesis is the response of plants to light both morphologically and through gene expression (Wu, 2014). Plants can react to the duration, quantity, quality and direction of light and do so by using different photoreceptors (Kami, *et al*. 2010). These photoreceptors react to different wavelengths of light and produce different responses, although there is cross-talk between the different photoreceptor pathways (Brosche and Strid, 2003, Fuglevand, *et al*. 1996, Jian

and Li, 2015, Wade, *et al*. 2001). Without these photoreceptors it would be impossible for plants to survive.

1.3 Red light and its pathways

Red and far-red light (625-750nm) and the effect it has on plants is well documented. The response of plants to red light and the red light photoreceptor were first described in the 1920s and they have been intensively studied since that time (Li, *et al*. 2011).

1.3.1 Phytochrome: the red light photoreceptor

Phytochrome (PHY) was the first described plant photoreceptor. 'Phyto' is derived from the Greek for plant and chrome from the Greek for colour. Phytochrome was first used to describe the pigment that controlled photoperiod detection in the 1920s and in the 1950s it was used to describe the photoreceptor that responds to red and far-red light (Li, *et al*. 2011, Vierstra and Zhang, 2011). Over time, the initial knowledge of Phytochrome was expanded, showing that there is not only one Phytochrome but several: differing in function; the intensity of light that is detected and interactions with other proteins (Chen, *et al*. 2004, Deng, 1994, Li, *et al*. 2011, Vierstra and Zhang, 2011).

1.3.1.1 The Phytochrome family

In *A. thaliana* there are five Phytochromes designated phyA through to phyE (Chen, *et al*. 2004, Deng, 1994, Li, *et al*. 2011, Möglich, *et al*. 2010, Vierstra and Zhang, 2011). These have different, although overlapping, roles throughout the plant's life in directing developmental and photomorphogenic responses. The Phytochromes are classified as two groups according to their stability in light. PhyA is a light labile protein and is most abundant in dark conditions (Deng, 1994, Li, *et al*. 2011, Möglich, *et al*. 2010). Upon exposure to red or white light, phyA is degraded and the concentrations of it in the cell decrease dramatically (Deng, 1994, Li, *et al*. 2011, Möglich, *et al*. 2010). The other Phytochromes, phyB through to phyE are photo-stable and are found in light grown plants (Deng, 1994, Li, *et al*. 2011, Möglich, *et al*. 2010). Of these, phyB is the most abundant (Li, *et al*. 2011).

Aside from being either light labile or light stable, the Phytochromes also differ in the fluence rate of red light that they respond to. PhyA causes very-low-fluence responses (VLFRs); phyB and phyE cause low-fluence responses (LFR); red light high-irradiance responses are caused by phyB and phyC; far-red light high-irradiance responses are caused by phyA and end of day far red light and the red to far-red light ratio is sensed by phyB, phyD and phyE (Li, *et al.* 2011). All of these Phytochromes then act under different conditions to help the plant to develop correctly and undergo photomorphogenesis.

1.3.1.2 The structure of Phytochrome

Phytochromes consist of an N-terminal and C-terminal domain attached to each other via a hinge (Li, *et al.* 2011, Möglich, *et al.* 2010, Vierstra and Zhang, 2011). These domains can be further subdivided: the N-terminal domain into four sub-domains and the C-terminal domain into two sub-domains. The N-terminal domain contains an N-terminal extension, a Per-ARNT-Sim (PAS) domain, a cGMP-specific phospodiesterases adenylyl cylcases and FhiA (GAF) domain to which the external chromophore binds and a PHY domain (Li, *et al.* 2011, Möglich, *et al.* 2010, Vierstra and Zhang, 2011). The C-terminal domain contains a PAS-related domain consisting of two PAS repeats and a histidine-kinase-related domain (HKRD) (Li, *et al.* 2011, Möglich, *et al.* 2010, Vierstra and Zhang, 2011).

Phytochromes are homodimers and assemble in the cytosol with an external chromophore, phytochromobillin (PϕB) (Deng, 1994, Li, *et al.* 2011, Möglich, *et al.* 2010, Vierstra and Zhang, 2011). The PϕB is linked to the Phytochrome via a thio-esther linkage (Li, *et al.* 2011, Möglich, *et al.* 2010). The PϕB allows the Phytochrome to convert between an inactive red light absorbing form of phytcohrom (Pr), a form that absorbs maximally in red light to an active far-red light absorbing form of phytochrom (Pfr), a form that absorbs maximally in far-red light (Chen, *et al.* 2004, Deng, 1994, Li, *et al.* 2011, Möglich, *et al.* 2010, Vierstra and Zhang, 2011). The conversion is triggered by red light causing a Z to E isomerization within the PϕB as shown in Figure 1-1 (Li, *et al.* 2011, Möglich, *et al.* 2010).

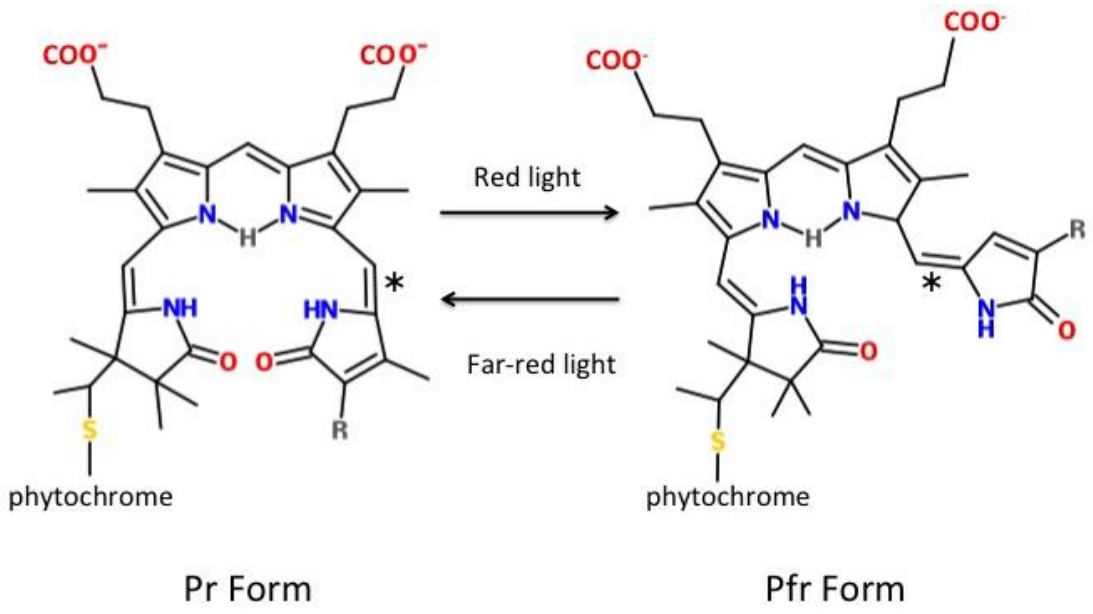

Figure 1-1: The structure of the Phytochrome chromophore. Upon absorption of red light, the * bond switches from Z to E configuration, causing the chromophore to switch from the Pr form to the Pfr form. This is reversible upon absorption of far-red light or prolonged exposure to darkness (Figure adapted from (Möglich *et al*. 2010)).

Phytochromes are photoreversible, once in the Pfr form they will revert to the Pr form after prolonged darkness, which is relatively slow, or from exposure to far-red light, the quicker alternative (Chen, *et al*. 2004, Deng, 1994, Li, *et al*. 2011, Möglich, *et al*. 2010, Vierstra and Zhang, 2011).

1.3.1.3 Phytochrome function

As previously mentioned, there are five Phytochromes and these interact to regulate the development of plants in response to red and far-red light. Red light controls several different physiological responses through the Phytochromes such as seedling germination, de-etiolation, shade-avoidance and the circadian clock (Chen, *et al*. 2004, Deng, 1994, Li, *et al*. 2011, Möglich, *et al*. 2010, Vierstra and Zhang, 2011). PhyA responds to far-red light while phyB through phyE are active under red light (Li, *et al*. 2011). Phytochromes are photoreversible and act like a switch (Li, *et al*. 2011, Vierstra and Zhang, 2011). This in conjunction with five photoreceptors that respond to different fluence rates of light allows for intricate control of red-light development.

1.3.2 The Phytochrome signalling pathway

Phytochromes control many different developmental features within plants, and there are many different signalling pathways that include Phytochrome including the de-etiolation pathway described here.

In dark-grown seedlings the majority of Phytochrome is phyA. After exposure to red light, phyA undergoes a configuration change from the Pr to the Pfr form. The Pfr form of phyA is rapidly degraded. The half-life of Pfr phyA is 1 to 2 hours compared to the few days of Pr phyA. However if phyA absorbs far-red light in Pfr form, it will change back to Pr form and initiate photomorphogenesis. It does this by suppressing the Phytochrome Interacting Factors (PIFs), transcription factors which cause skotomorphogenesis or etiolation (Li, *et al*. 2011). In conjunction with this, phyB can absorb red light that causes the suppression of the PIFs and the E3 ubiquitin ligases Constitutively Photomorphogenic 1 (COP1) and Suppressor of phyA (SPA) (Boccalandro, *et al*. 2004, Kircher, *et al*. 2004, Li *et al*. 2011, Yi and Deng, 2005). COP1 and SPA repress the transcription factors involved in photomorphogenesis in darkness (Boccalandro, *et al*. 2004, Li, *et al*. 2011, Seo, *et al*. 2003, Yi and Deng, 2005). With these repressed, the transcription factors Elongated Hypocotyl 5 (HY5), HY5 Homolog (HYH), Long After Far-Red1 (LAF1) and Long Hypocotyl in Far-Red (HFR1) can initiate photomorphogenesis and also repress skotomorphogenesis (Figure 1-2) (Boccalandro, *et al*. 2004, Li, *et al*. 2011).

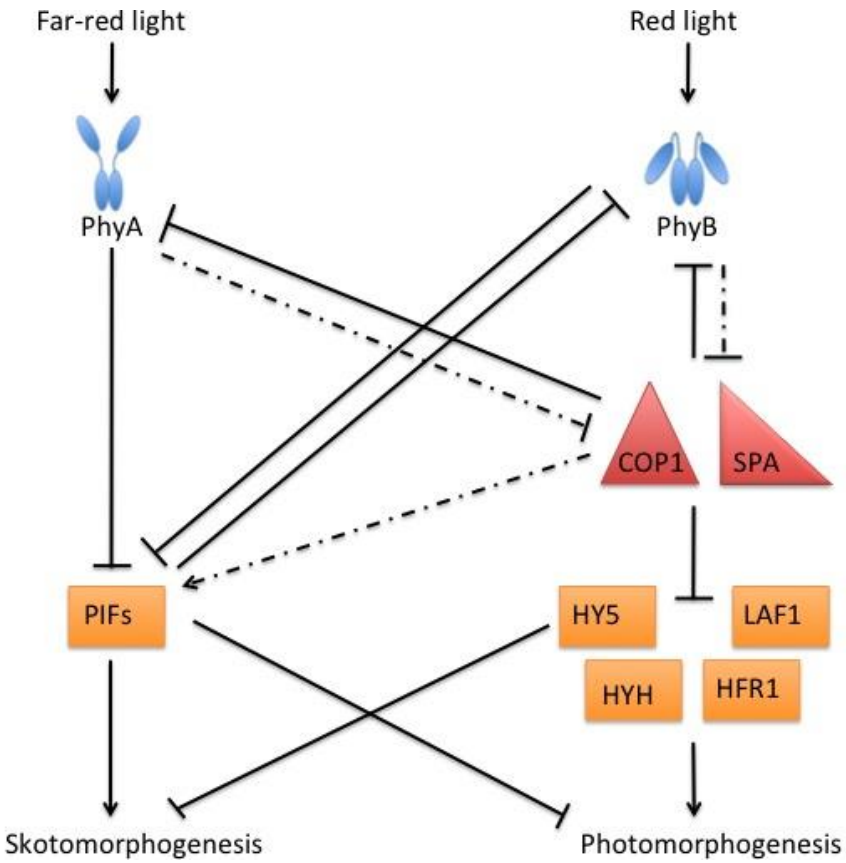

Figure 1-2: A simplified model of the Phytochrome de-etiolation pathway. Red or far-red light is sensed by either phyA or phyB, this causes the repression of the E3 ubiquitin ligases, COP1 and SPA and repression of the PIFs. This leads to an increase in the transcription factors HY5, LAF1, HYH and HFR1 with the eventual outcome of supressed de-etiolation and the initiation of photomorphogenesis. (Figure modified from (Li, *et al.* 2011)).

1.4 Blue and Ultraviolet-A (UV-A) light and its pathways

There are several different classes of photoreceptor that perceive blue and UV-A light. Cryptochromes were discovered in 1993 and since that time there have been two documented Cryptochromes (CRY) in *A. thaliana*, delegated CRY1 and CRY2 (Chen, *et al.* 2004, Devlin, *et al.* 2007, Yu, *et al.* 2010). Phototropins (PHOT) were first identified in 1997. There are currently two described Phototropins, phot1 and phot2 (Christie, 2007, Devlin, *et al.* 2007, Liscum, *et al.* 2003). There is also the Zeitlupe family of blue light photoreceptors. There are three of these proteins known as Zeitlupe (ZTL), Flavin-binding, Repeat F-box1 (FKF1) and Light, Oxygen, Voltage (LOV) Kelch Protein 2 (LKP2) (Devlin, *et al.* 2007, Imaizumi, *et al.* 2005, McClung, *et al.* 2002, McClung, *et al.* 2011, Somers, 2001).

1.4.1 Effects of blue and UV-A light on plants

Blue light controls a plethora of different developmental and photomorphogenic responses. These responses include, but are not limited to, phototropism, leaf positioning, inhibition of hypocotyl growth in seedlings transferred from darkness to light, the entrainment of the circadian clock, inhibition of stem elongation and floral inhibition (Banaś, *et al.* 2012, Christie, 2007, Devlin, *et al.* 2007, Liscum, *et al.* 2003, Imaizumi, *et al.* 2005, McClung, *et al.* 2002, McClung *et al.* 2011, Pedmale, *et al.* 2010, Somers, 2001, Yu, *et al.* 2010).

1.4.2 Cryptochrome: a blue light photoreceptor

The Cryptochrome protein was first investigated during the 1980s and it took until 1993 for Cryptochrome to be described as a blue light photoreceptor (Yu, *et al.* 2010). 'Crypto' is Greek for hidden, so Cryptochrome means 'hidden colour'. There have been two described Cryptochromes in *A. thaliana*: cry1 and cry2 (Liscum, *et al.* 2003, Yu, *et al.* 2010). Cryptochromes are found not only in plants, but also in bacteria and animals (Liscum, *et al.* 2003).

1.4.2.1 The structure of Cryptochrome

Cry1 was first identified in the 1980s as HY4, when this protein was sequenced it was shown to have sequence similarity to a deoxyribonucleic acid (DNA) photolyase (Yu, *et al.* 2010). However, experimentation showed that cry1 lacked

any photolyase activity, and instead bound a flavin adenine dinucleotide (FAD) chromophore (Chen, *et al*. 2004, Yu, *et al*. 2010). All Cryptochromes share homology in their N-terminal region, a Photolyase-Homologous Region (PHR) (Möglich, *et al*. 2010, Yu, *et al*. 2010). The C-terminal of Cryptochromes also has a shared region of varying lengths known as the Cryptochrome C-terminal Extension (CCE) domain (Möglich, *et al*. 2010, Yu, *et al*. 2010). The CCE domain is 180 residues in cry1 and 110 residues in cry2 (Möglich, *et al*. 2010, Yu, *et al*. 2010).

The PHR domain is the region of Cryptochromes that binds the FAD chromophore (Möglich, *et al*. 2010, Yu, *et al*. 2010). Interestingly, the PHR domain shows greater similarity in Cryptochromes of the same type between species than in Cryptochromes of different types within species (Yu, *et al*. 2010). The most conserved region of the PHR domain is the area that binds the FAD chromophore (Yu, *et al*. 2010). Cryptochrome binds its chromophore non-covalently. It is unclear whether cry3 is a Cryptochrome-like protein which is more likely to be involved in DNA repair. However, cry3 can also bind a second chromophore, 5,10-methenyltetrahydrofolate (MTHF) (Yu, *et al*. 2010). It is unclear if cry1 is also able to bind MTHF.

The CCE domain shows no sequence similarity between animals and plants (Yu, *et al*. 2010). Within plants there is a conserved DQXVP-Acidic-STAESSS (DAS) motif, however this motif is not found within algae (Yu, *et al*. 2010). The CCE is an unstructured region of the protein, but is important for function as mutations within this region impair function (Yu, *et al*. 2010). It has been hypothesized that the CCE domain may change conformation in response to light, changing its interaction with the PHR domain (Yu, *et al*. 2010, Liscum, *et al*. 2003). Alternatively it may be an effector modulator that causes a change in interaction caused by light based conformational change (Liscum, *et al*. 2003).

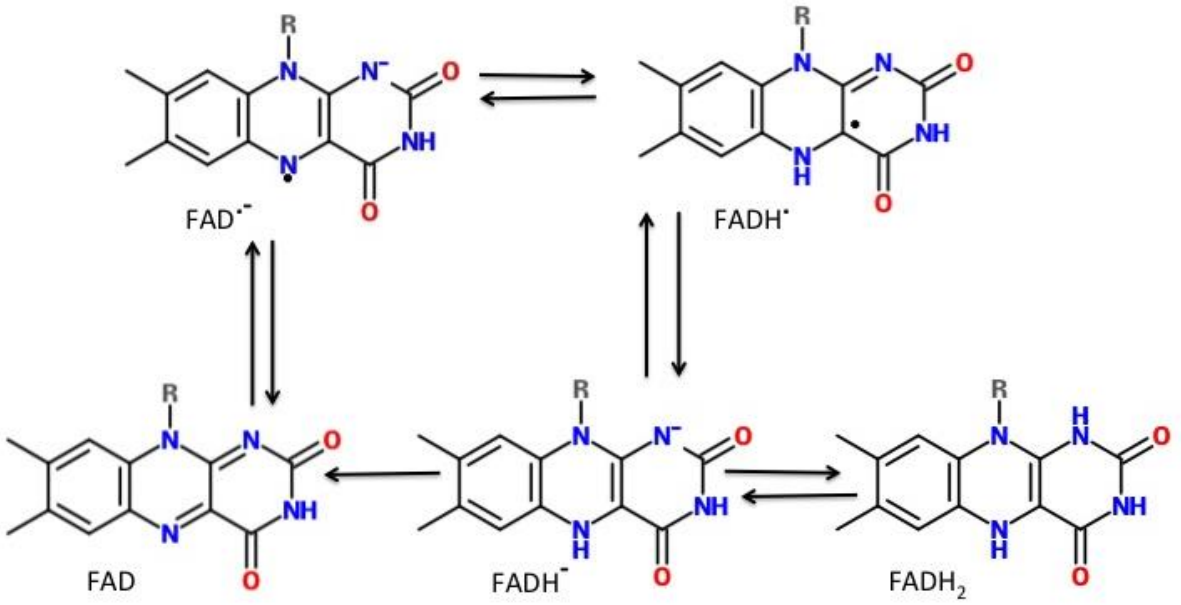

Figure 1-3: The redox equilibrium of FAD, FADH and $FADH_2$. It is hypothesized that upon absorption of blue light FAD shifts redox equilibrium to flavosemiquinone $FAD^{\bullet -}$ or $FADH^{\bullet}$. These can be further reduced to flavohydroquinones $FADH^{-}$ or $FADH_2$. Oxidisation can then occur and the photocycle of FAD is completed.

Exposure to blue light allows Cryptochromes to change conformation and auto-phosphorylate, which activates the protein or allows dimerization and the ability for Cryptochromes to interact with downstream proteins: for example, binding with the E3 ubiquitin ligase COP1 or the blue light inhibition of CONSTANS (CO) (Yu, *et al*. 2010). The details of the role of FAD in the light based change of Cryptochromes are still under debate. Current hypotheses suggest that oxidised FAD absorbs blue light and becomes a semi-reduced $FADH^{\bullet}$ or a semiquinone radical $FAD^{\bullet -}$. After this it is hypothesized that in darkness the semiquinone can be oxidised to return to the FAD form (Figure 1-3) (Yu, *et al*. 2010).

1.4.2.2 The function of Cryptochrome

Up to 25% of the genes in *A. thaliana* have changed levels of expression under blue light (Yu, *et al*. 2010, Liscum, *et al*. 2003). It is hypothesized that the cry1 and cry2 regulate the majority of these (Yu, *et al*. 2010). There is of course overlap and cross talk between the genes that are regulated by cry1 and cry2 and also by other signalling pathways (Yu, *et al*. 2010, Liscum, *et al*. 2003,

Wade, *et al*. 2001, Brosche, 2003). The Cryptochromes regulate expression at both the transcriptional and post-translational stages (Yu, *et al*. 2010).

1.4.2.2.1 The Cryptochrome signalling pathway

Although Cryptochromes were discovered in *A. thaliana*, their signalling pathways and in particular their role in the circadian clock are best understood within *Drosophila* and mouse models (Yu, *et al*. 2010). Within plants there is a working model that in response to blue light both cry1 and cry2 suppress the E3 ubiquitin ligases COP1 and SPA (Figure 1-4) (Boccalandro, *et al*. 2004, Yu, *et al*. 2010).

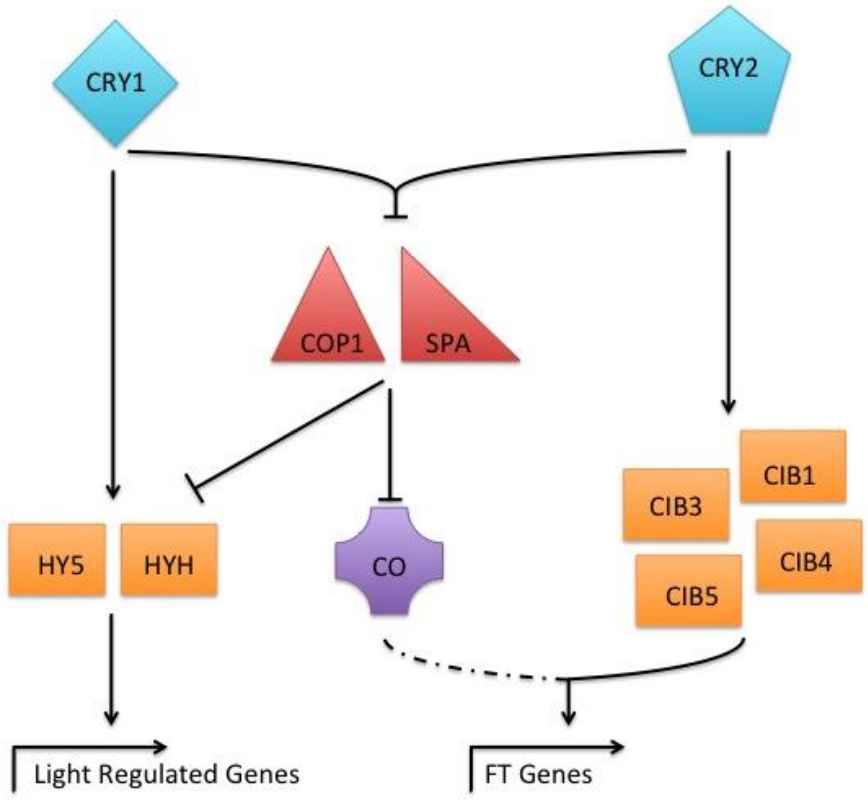

Figure 1-4: The current signal transduction model for cry1 and cry2 in A. thaliana. Both cry1 and cry 2 suppress E3 ubiquitin ligases COP1 and SPA. This allows for the up-regulation of HY5, HYH and CO. Cry2 also up-regulates the transcription factors Crytopchrom-interacting basic helix-loop-helix 1 (CIB1), CIB3, CIB4 and CIB5. Depending on interaction with circadian proteins light regulated genes or flowering time genes are up-regulated.

In dark conditions COP1 and SPA degrade the photomorphogenic transcription factors HY5 and HYH as well as the CO protein involved in flowering (Yu, *et al*. 2010, Liscum, *et al*. 2003, Boccalandro, *et al*. 2004). Once their degradation is inhibited following illumination, these proteins are free to up-regulate

photomorphogenic genes and flowering time genes respectively (Yu, *et al*. 2010). Cry1 also directly up-regulates HY5 while cry2 up-regulates the flowering time transcription factors Cryptochrome-Interacting Basic-helix-loop-helix 1 (CIB1), CIB3, CIB4 and CIB5 (Yu, *et al*. 2010). Depending on the circadian clock, fluence rate and exposure time, different light regulated genes are up-regulated leading to differential development (Yu, *et al*. 2010, McClung, *et al*. 2002, McClung, *et al*. 2011).

1.4.3 Phototropins: a blue and UV-A light photoreceptor

Phototropins were first described in 1997, although their effects had been noted far earlier (Chistie, 2007). Phototropins are named for their primary function, the regulation of phototropism, 'photo' meaning light and 'tropism' meaning turning, they are the proteins that cause plants to turn towards light. There are two described Phototropins phot1 and phot2 (Christie, 2007, Pedmale, *et al*. 2010, Banaś, *et al*. 2012, Liscum, *et al*. 2003). Generally Phototropins are involved in light dependent processes that increase the productivity of photosynthesis or protect from light based damage.

1.4.3.1 The structure of Phototropins

Phototropins belong to the cAMP-dependent protein kinase, cGMP-dependent protein kinase and phospholipid-dependent protein kinase (AGC) family of proteins (Christie, 2007). They have two major domains. The N-terminal domain contains two LOV domains, each of around 110 amino acids (Christie, 2007). These domains are part of the PAS superfamily. This region of the protein is the photosensory domain and binds the external chromophore Flavin Mononucleotide (FMN) (Christie, 2007, Pedmale, *et al*. 2010). The LOV2 domain is the region where photoreception primarily occurs (Pedmale, *et al*. 2010, Christie, 2007). The C-terminal of Phototropins is a serine protein kinase involved in autophosphorylation of the protein and possibly signal transduction (Christie, 2007).

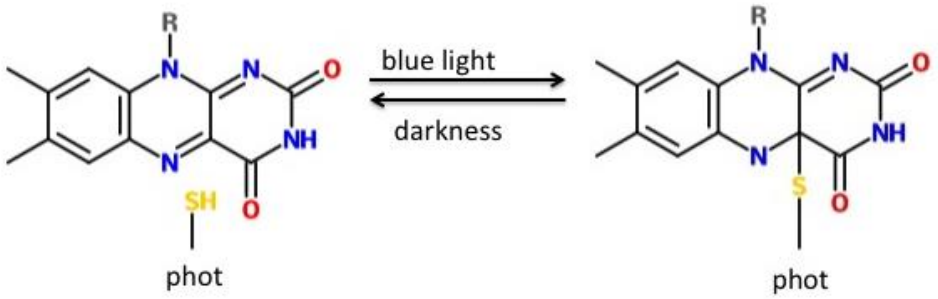

Figure 1-5: The response of FMN to blue light. The external Flavin Mononucleotide (FMN) chromophore becomes covalently attached to the LOV domain of Phototropin via a sulphide bridge after exposure to blue light. This is fully reversible in darkness.

After exposure to blue light the FMN chromophore, which is positioned within a cavity of the LOV domain, composed of a β-sheet and two α-helices of the LOV domain, becomes covalently bound via a sulphide bridge to Phototropin (Figure 1-5) (Pedmale, *et al*. 2010, Christie, 2007). This is the active signalling form of Phototropin. The covalent binding of FMN is reversible in darkness in the period of seconds rather than minutes so Phototropins are continually cycling between active and inactive forms (Pedmale, *et al*. 2010, Christie, 2007).

1.4.3.2 The function of Phototropin

Phototropins regulate many of the light dependent reactions of plants. Phototropism, leaf movement, leaf expansion, stomatal opening and chloroplast accumulation are regulated by both phot1 and phot2 (Liscum, *et al*. 2003, Pedmale, *et al*. 2010, Christie, 2007, Banaś, *et al*. 2012). Phot2 reacts to higher fluence rates of blue light and regulates chloroplast avoidance (Christie, 2007). Phot1 is able to sense lower fluence rates of blue light and controls hypocotyl growth inhibition and messenger ribonucleic acid (mRNA) stability (Christie, 2007).

1.4.3.2.1 The Phototropin signalling pathway

The overall structure of the Phototropin signalling pathway is complex, especially as parts, such as the mechanism by which Phototropin regulates the auxin gradient that leads to phototropism, are unknown. It is known that the LOV2 domain regulates the autophosphorylation of Phototropin and that autophosphorylation causes a structural change in Phototropin (Pedmale, *et al*.

2010, Christie, 2007). The residues that are autophosphorylated depend on whether the light perceived was of a high or low fluence rate. Once the Phototropin has been exposed to blue light an α-helix joining the light sensing N-terminal domain to the C-terminal serine protein kinase domain becomes disordered causing the C-terminal domain and the N-terminal domain to separate like a hinge (Pedmale, *et al*. 2010, Christie, 2007). This could potentially allow for a substrate to bind and be phosphorylated.

There have been several proteins discovered to be associated with Phototropins *in vivo* and the candidates for a signal transduction pathway are slowly being assembled. Non-Phototropic Hypocotyl 3 (NPH3) is a protein that putatively serves as a scaffold to the plasma membrane and is required for phototropism (Christie, 2007). Another protein, PHYTOCHROME KINASE SUBSTRATE 1 (PKS1), which is also required for phototropism, binds both NPH3 and phot1 (Christie, 2007). Chloroplast Unusual Positioning 1 (CHUP1), Plastid Movement Impaired 1 (PMI1), PMI2, PMI5 and J-domain protein required for chloroplast accumulation response 1 (JAC1) are required for correct chloroplast positioning (Christie, 2007, Banaś, *et al*. 2012). Further experimentation will presumably shed light on the details of the Phototropin signalling pathway.

1.4.4 Zeitlupe family: blue light photoreceptors

The Zeitlupe family consists of three proteins, Zeitlupe (ZTL), (FKF1) and LOV Kelch Protein 2 (LKP2) (McClung, 2011, Somers, 2011, McClung, *et al*. 2002, Devlin, *et al*. 2007, Imaizumi, *et al*. 2005). These proteins are involved in the degradation of proteins within the circadian clock. ZTL and FKF1 show some photoreception, ZTL as light input to the circadian clock and FKF1 in detecting long days and control of flowering (McClung, 2011, Somers, 2001, Devlin, *et al*. 2007). Double and triple mutant plants for these three proteins show that there is some redundancy between them (McClung, 2011, Somers, 2001).

1.4.4.1 The structure of Zeitlupe proteins

The Zeitlupe family of proteins show a great deal of similarity, with 70-80% amino acid similarity. There are three conserved domains between the proteins of this family (Somers, 2001). An N-terminal LOV domain of around 110 amino

acids and shows most similarity (40% sequence similarity) to the LOV domains of phot1 (Somers, 2001). There is also an F-box domain of around 45 amino acids (Somers, 2001). F-boxes are widely found throughout plants and animals. There is also a C-terminal Kelch domain. There are seven Kelch repeats that form a seven bladed β-propeller (Somers, 2001). ZTL mutants contain an aspartate to asparagine mutation within this region, stressing its importance for function (Somers, 2001). The majority of sequence dissimilarity within the Zeitlupe family proteins is at the N-terminus and between the three domains (Somers, 2001).

1.4.4.2 The Zeitlupe family function and signalling pathway

The Zeitlupe proteins are involved in the input and regulation of the circadian clock, an extremely complex signalling pathway (McClung, 2011, Somers, 2001, McClung, 2002, Imaizumi, *et al*. 2005). In particular they are involved in the evening loop of the circadian clock (McClung, 2011, McClung, *et al*. 2002). ZTL is stabilised by GIGANTEA (GI), the interaction between GI and ZTL is enhanced by blue light (McClung, 2011, McClung, et al 2002). In darkness ZTL dissociates from GI and degrades Timing Of CAB expression 1 (TOC1) and Pseudo-Response Regulator 5 (PRR5) (McClung, 2011, McClung, *et al*. 2002). This shows that ZTL provides a blue light input to the circadian clock of *A. thaliana* (McClung, 2011, McClung, *et al*. 2002).

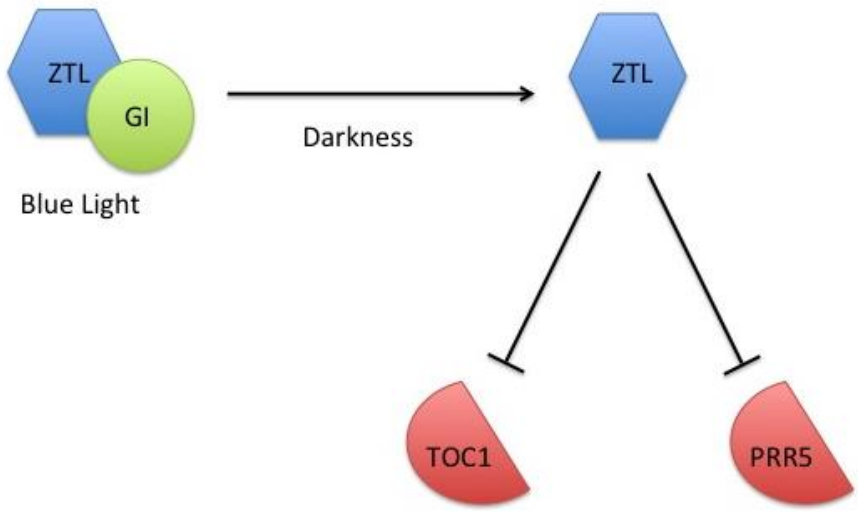

Figure 1-6: A simplified view of the role of ZTL within the circadian clock.

The FKF1 protein is involved in the photoperiodic timing of flowering (Imaizumi, *et al*. 2005). An FKF1 mutant plant will flower late (Imaizumi, *et al*. 2005). The transcription factor Cycling DNA-binding with One Finger (DOF) Factor 1 (CDF1), which suppresses CO expression, is degraded by FKF indirectly regulating the expression of CO (Imaizumi, *et al*. 2005). The expression of CO is also upregulated by FKF1 via an unknown mechanism (Imaizumi, *et al*. 2005).

Currently, LKP2 does not have an identified photoreception role like ZTL and FKF1, nevertheless there is redundancy between these three proteins, as the triple mutants have a more pronounced effect on the circadian clock than *ztl* or *ztlfkf1* mutants alone (McClung, 2011, McClung, *et al*. 2002).

1.5 Ultraviolet-B (UV-B) light and its pathways

UV-B light is defined as light with a wavelength between 280-315nm (Commission International de l'Eclairage) and it has a variety of effects on plants. It has long been known that there was a UV-B photoreceptor, but there was discussion over whether an already known photoreceptor sensed and reacted to UV-B light or whether there was a unique and independent UV-B photoreceptor. This was resolved in 2011 when UV RESISTANCE LOCUS8 (UVR8) was confirmed to be the UV-B photoreceptor and not just a signalling factor downstream of the photoreceptor as previously thought (Christie, *et al*. 2012, Rizzini, *et al*. 2011, Wu, *et al*. 2012). However, UVR8 is not the sole receptor of UV-B light as will be discussed below.

1.5.1 The UV-B stress pathway

UV-B does not just act as a photomorphogenic trigger. High fluence rates of UV-B are harmful to plants as it causes damage to DNA, proteins, phospholipids, photosynthetic reactions and protein synthesis (González Besteiro, *et al*. 2011, Gao and Zhang, 2008, Beggs, *et al*. 1985, Apel and Hirt, 2004). High fluence rates of UV-B are therefore considered stresses. The response to UV-B stress includes the expression of defence, stress and wound genes (Jenkins, 2009). The UV-B stress pathway also negatively regulates the UV-B photomorphogenic pathway (Ulm, *et al*. 2004).

There are three ways in which the UV-B stress signalling pathways are activated. None of these are specific UV-B responses. The first of these is signalling in response to DNA damage (Jenkins, 2009, Müller-Xing, *et al*. 2014). After exposure to short wavelengths of UV-B or high fluence rates of UV-B DNA can become damaged. In particular, exposure causes cyclobutane pyrimidine dimers (CPDs) and (6-4)-photoproducts (64PPs) to form (Jenkins, 2009, Britt, 2004). DNA damage always occurs under UV-B light conditions but only accumulates when plants are unable to repair the damage. The majority of DNA damage is repaired by blue light induced photolyases. More serious DNA damage includes double strand breaks. These can be repaired by light independent proteins like the Ataxia telangiectasia-mutated (ATM), which senses DNA double-strand breaks and Ataxia telangiectasia-mutated and Rad3-related (ATR), which senses single-stranded DNA (Jenkins, 2009, Garcia, *et al*. 2003). ATM and ATR initiate signalling for DNA repair. Indeed ATR mutant plants are hypersensitive to UV-B (Culligan, *et al*. 2006, Garcia *et al*. 2003, Jenkins, 2009).

The second non-specific UV-B signalling pathway involves the production of Reactive Oxygen Species (ROS) (Wrzaczek, *et al*. 2010, Mackerness, *et al*. 2001, Apel and Hirt, 2003, Müller-Xing, *et al*. 2014). ROS are produced in response to a variety of stresses including UV-B (Wrzaczek, *et al*. 2010, Mackerness, *et al*. 2001, Apel and Hirt, 2003). They are highly reactive and destructive in cells and can cause oxidative damage to the cell. However there is also evidence that they are released in a directed manner at certain times during a plant's development, such as during fruit ripening. In addition, different ROS initiate different responses (Jenkins, 2009). Under UV-B stress plants produce superoxide radicals, although the origin of these ROS is still unknown (Jenkins, 2009). High fluence rates of UV-B induce genes that protect against high levels of ROS. There is also evidence of gene expression regulated by ROS in response to UV-B (Wrzaczek, *et al*. 2010).

High fluence rates of UV-B also induce genes involved in pathogen response or wound response via an increase in jasmonic acid (JA), ethylene or salicylic acid (Kazan and Manners, 2011, Jenkins, 2009). These are all signalling molecules

involved in the pathogen response pathways. Furthermore, as previously mentioned, ROS are also induced, and these can induce defence genes.

Investigation into the role of ROS suggests that at low UV-B fluence rates the ROS are produced but that the pool of antioxidants such as ascorbate, Glutathione (GSH), xanthophylls and α-tocopherol is large enough to protect against damaging oxidation (Hideg, *et al*. 2013). At higher stressful UV-B fluence rates the pool of antioxidants is not large enough to cope with the increase in ROS production, leading to UV-B stress damage (Hideg, *et al*. 2013). As previously mentioned plants are able to acclimate to stresses and this includes UV-B stress. If a plant is exposed to a low, chronic dose of UV-B this results in a dramatic increase in the amount of antioxidants the plant produces. For example, spinach that was exposed to a low UV-B dose for two weeks had a 2.7 fold increase in ascorbate levels and an eight fold increase in α-tocopherol (Hideg, *et al*. 2013). Clearly this vast increase in antioxidant levels would prepare the plant for a further, previously stressful, now negated UV-B dose.

UV-B stress is now considered to be the exception rather than the rule, especially in natural solar environments (Hectors, *et al*. 2007, Hideg, *et al*. 2013 and Robson, *et al*. 2014). However a great deal of how plants react to differing UV-B levels depends a lot upon which plant is being studied. There is variation in UV-B sensitivity even among different *A. thaliana* ecoptypes (Cooley, *et al*. 2001, Torabinejad and Caldwell, 2000). Between differing species of plants it can be no surprise that there is even more variation. Conifers, for example have to deal with accumulative damage, as they do not shed and regrow their leaves yearly (Jordan, 1996). The sensitivity of trees to UV-B has been observed to be species and growth form specific. When different species of tree were given supplemental UV-B radiation over a number of years, photosynthetic activity decreased in *Fagus sylvatica* after three years, but only after five years in *Fraxinus excelsior, Betula pendula, Tilia cordata, Quercus robur* and *Acer pseudoplanatus* (Sedej, 2014). However, in *Acer rubrum* photosynthetic activity increased after three years exposure to supplemental UV-B in addition to normal solar levels of UV-B (Sedej, 2014).

It must also be taken into account that the plant will change over time in response to UV-B. While factors such as epicuticular waxes and leaf hairs can affect how UV-B will transmit and penetrate the leaf, the composition of the leaf, such as increases in flavonoid produced in response to UV-B will change the effect of UV-B throughout the plant's lifetime. Furthermore these changes will have a knock on effect on how Photosynthetically Active Radiation (PAR) is distributed throughout the leaf (Jordan, 1996). Once again, species plays a role in UV-B transmittance through leaves, UV-B penetrates 150 μm into *Chenopodium album* leaves but only 17 μm into *Picea pungens* leaves (Jordan, 1996).

It is not only the response of the plant and the plant species, cultivar or ecotype that affects response to UV-B stress, the presence or absence of other stressors also plays a role. For example, the crop plant *Zea mays* is stressed by natural solar levels of UV-B when also under nutrient stress; when the plant is well fertilised it is not stressed by UV-B (Hideg, *et al*. 2013). Similarly, exposure to UV-B can provide cross-tolerance to other stresses. When *Pisum satium, Nicotiana tabacum* cultivar (cv) Petit Havanna SR1 and *Pinus pinea* were acclimated to UV-B they had a greater ability to withstand subsequent drought stress (Hideg, *et al*. 2013).

1.6 UVR8: The UV-B Light Photoreceptor

UVR8 is the only known photoreceptor for UV-B photomorphogenesis (Christie, *et al*. 2012, Rizzini, *et al*. 2011, Wu, *et al*. 2012). It absorbs UV-B light at extremely low fluence levels and causes transcriptional responses within a very quick time period. UVR8 is able to re-dimerise in darkness within three hours *in vivo*. UVR8 causes the flavonoid biosynthesis pathway to be activated; it provides some degree of pathogen resistance as well as other photomorphogenic responses that help acclimate the plant against UV-B and oxidative stress (Brown and Jenkins, 2008, Christie, *et al*. 2012, Favory, *et al*. 2009, Kliebenstein, *et al*. 2002, Wargent, *et al*. 2009, Wu, *et al*. 2012, Wu, *et al*. 2011).

1.6.1 The structure of UVR8

UVR8 has a different structure to the other described photoreceptors in that it does not bind a chromophore (Christie, *et al*. 2012, Wu, *et al*. 2012). It is a

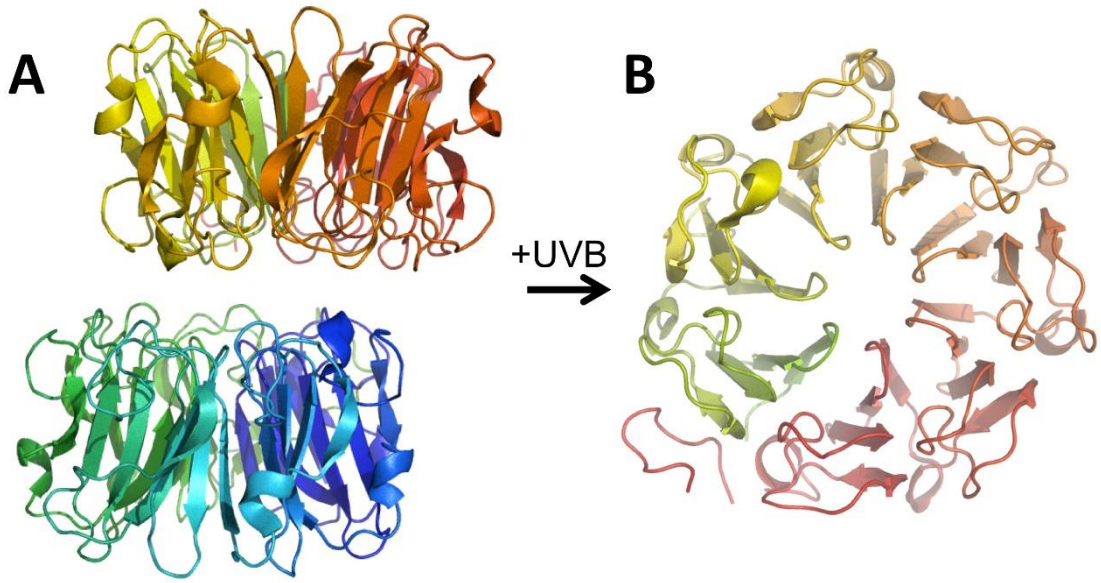

Figure 1-7: The structure of UVR8. View of the UVR8 dimer (A) and close up of the UVR8 monomer (B). The UVR8 Monomer shows a seven-bladed β-propeller structure. The central cavity is water filled. The dimer monomerises when exposed to UV-B light. Re-dimerisation occurs in the absence of UV-B.

seven bladed β-propeller that switches between a dimer in dark conditions to a monomer when excited by UV-B light (Figure 1-7) (Christie, *et al*. 2012, Wu, *et al*. 2012).

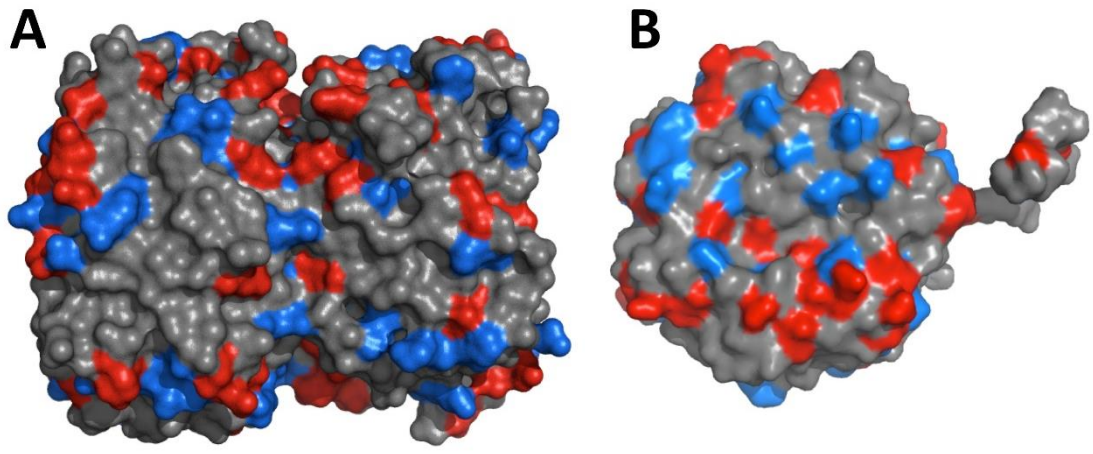

Figure 1-8: The surface charge of UVR8. Surface of UVR8 Dimer (A) and Monomer showing the dimer interface (B). The UVR8 dimer interface is composed of two charged patches that sit opposite each other, positive to negative. In this figure positive amino acids are shown in blue, negative amino acids are shown in red.

The cavity in the centre of each monomer propeller is water filled (Christie, *et al*. 2012, Wu, *et al*. 2012). Furthermore the dimer interface shows a very interesting distribution of charge with one large negative and one large positive patch (Christie, *et al*. 2012, Wu, *et al*. 2012). In the dimer these charged patches sit opposite each other like the poles of batteries within a torch (Figure 1-8).

A network of salt bridges, primarily arginine/aspartate bridges but also arginine/glutamate, are found across the dimer interface and hold the dimer together (Figure 1-9) (Christie, *et al*. 2012, Wu, *et al*. 2012). The closer these salt bridges are to the internal chromophore discussed below, the more vital they are to the stability of the dimer (Christie, *et al*. 2012, Wu, *et al*. 2012).

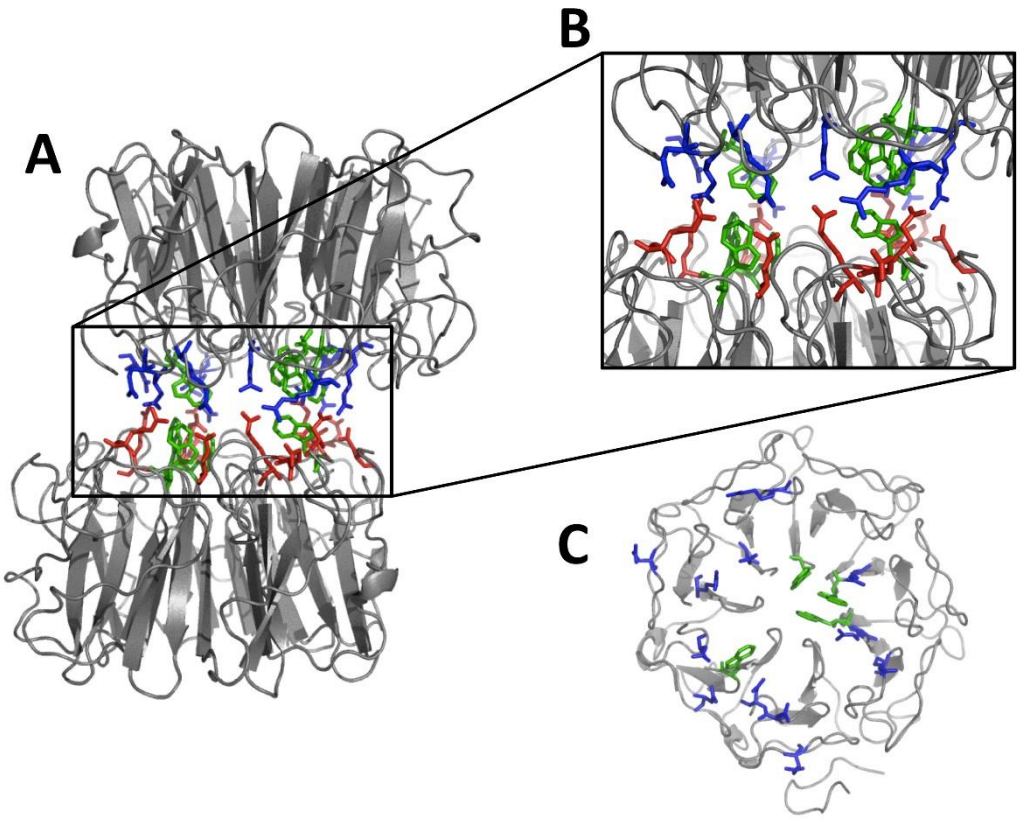

Figure 1-9: The salt network formed in the UVR8 dimer interface. The UVR8 Dimer (A) is held together by a network of salt bridges (B). The arrangement of the amino acids involved in the salt bridges on the dimer interface is shown in (C). The photorecepting tryptophan pyramid is shown in green.

Overall its genetic sequence shows a similarity to human Regulator of Chromatin Condensation 1 (RCC1), which is a guanine nucleotide exchange factor (GEF) for Ran proteins and is involved in controlling the cell cycle and mitosis

(Kleibenstein, *et al*. 2002). Although there is around 35% identity between RCC1 and UVR8 there are significant differences, both in sequence and in function. The seven bladed structure is highly conserved, partly because of a selection of structurally vital glycine and proline residues (Kleibenstein, *et al*. 2002). The majority of these are also conserved in UVR8, giving it a similar propeller structure (Figure 1-10).

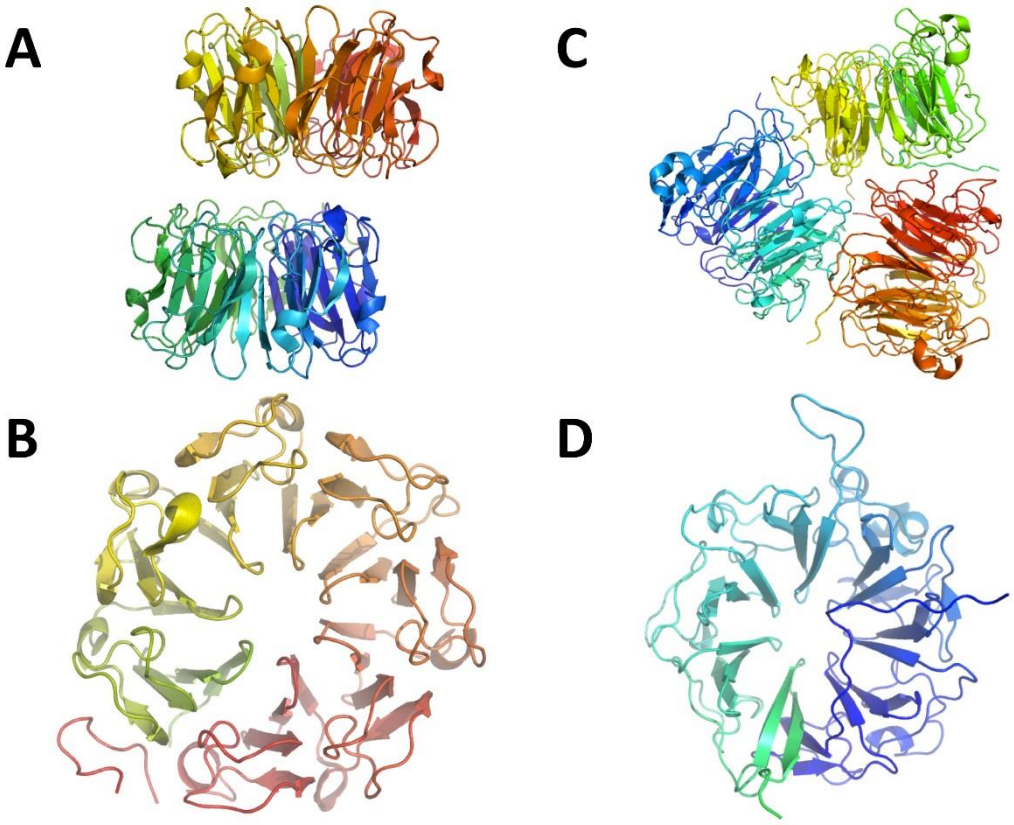

Figure 1-10: A comparison of the structures of UVR8 and RCC1. Comparison of the UVR8 dimer (A) and Monomer (B) structure to the RCC1 Trimer (C) and Monomer (D) structure.

However, although UVR8 also contains eight of the amino acids considered necessary for RCC1 Ran GEF activity, there are also many amino acids that affect the Ran GEF activity of RCC1 that are not conserved in UVR8 (Kleibenstein, *et al*. 2002). Furthermore, *rcc1* mutant yeast and mammalian cells are non-viable, whereas *uvr8* plants can grow in the absence of UV-B light with no noticeable phenotype. In addition, further experiments show that UVR8 has a very low capacity for GEF activity, making it unlikely that UVR8 functions as a regulator through a similar mechanism to RCC1 (Brown, *et al*. 2005). Like RCC1, UVR8 is

localised to the nucleus and interacts with chromatin, including the promoter region of HY5 (Brown, *et al.* 2005, Cloix and Jenkins, 2008). Furthermore, UVR8 contains 14 tryptophans, 10 more than RCC1. These tryptophans are highly conserved throughout different UVR8s across the plant kingdom, including in the moss *Physcomitrella patens*.

The dimer interface of UVR8 is particularly interesting. Aside from the salt bridge network that holds the dimer together in darkness there are a large number of aromatic amino acids across the dimer interface. In total there are seven tryptophans, three phenylalanines and two tyrosines (Figure 1-11) (Christie, *et al.* 2012, Wu, *et al.* 2012).

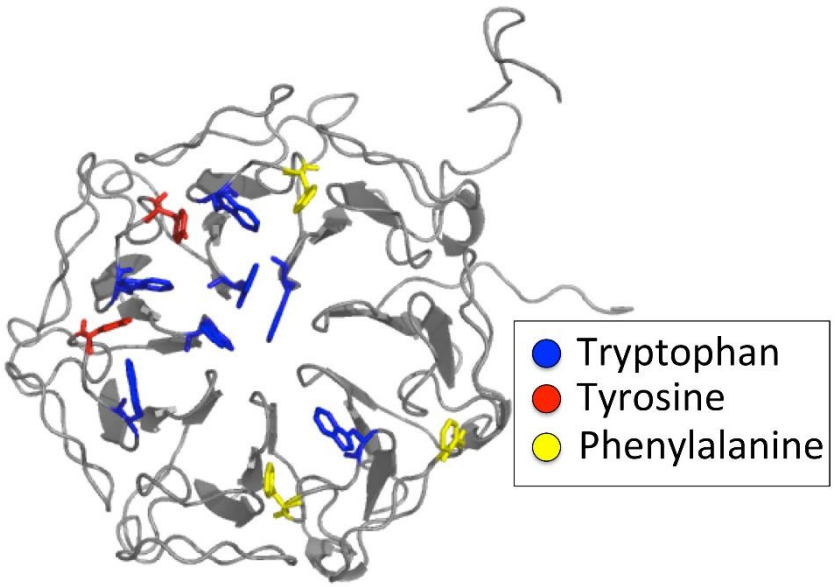

Figure 1-11: The dimer interface of UVR8. Dimer interface of UVR8 showing the twelve aromatic amino acids. Tryptophans are shown in blue, tyrosines in red and phyenylalanines in yellow.

Three of the tryptophans (W233, W285 and W337) from one side of the dimer form an exciton-coupled pyramid with a further tryptophan (W94) from the other side of the dimer (Christie, *et al.* 2012, Wu, *et al.* 2012). Through analysis of far UV Circular Dichroism (CD) -spectra it was found that after exposure to UV-B light exciton coupling was lost (Christie, *et al.* 2012). This suggested that the tryptophan pyramid is the internal chromophore of UVR8. Further experimentation has confirmed this. For example $UVR8^{W233F}$ and $UVR8^{W285F}$ have

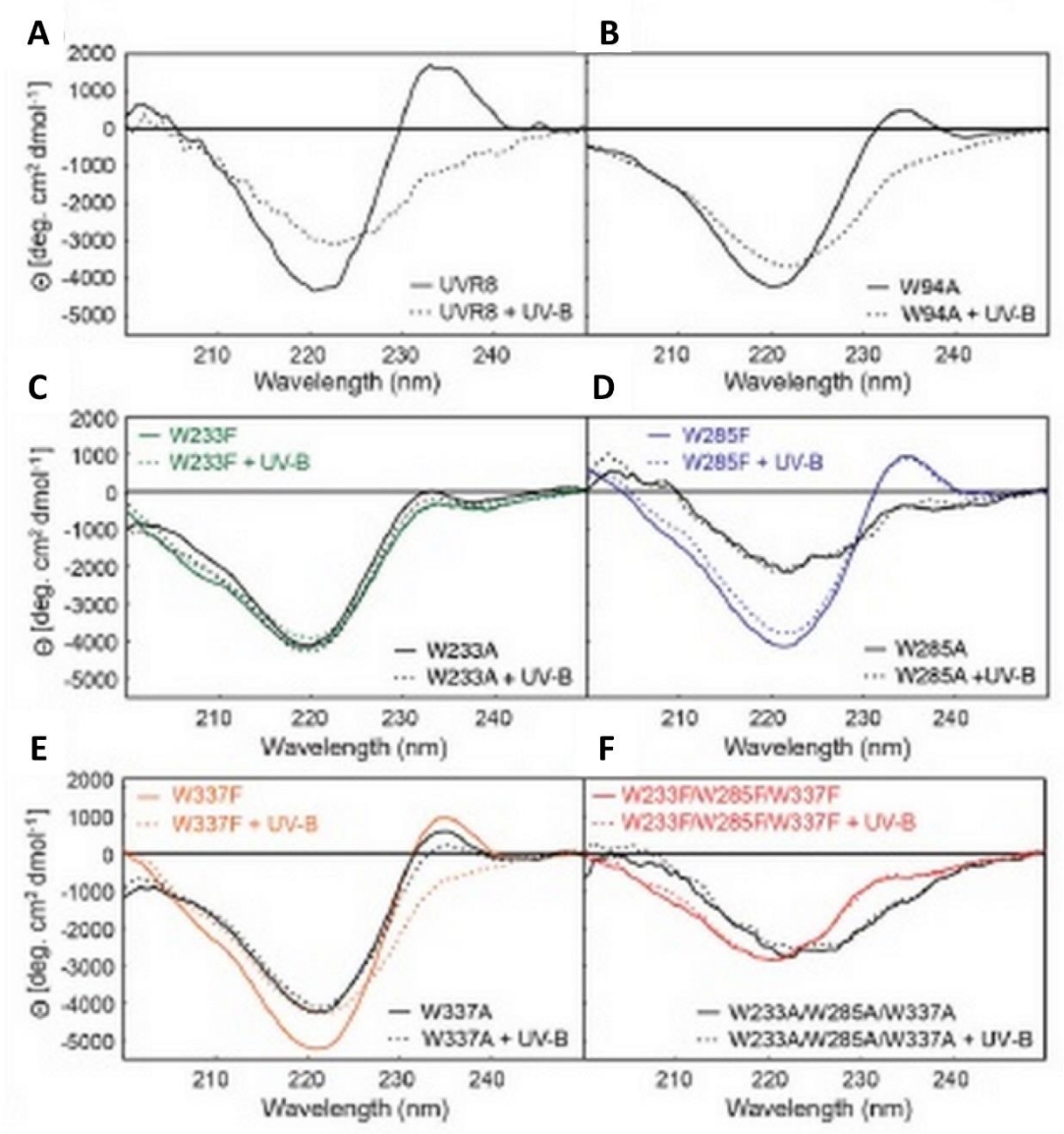

Figure 1-12: Circular Dichroism (CD) spectra showing presence or absence of exciton coupling between tryptophans in presence and absence of UV-B. Wild Type (WT) UVR8 (A) exhibits exciton coupling in the absence but not the presence of UV-B. W94A (B) shows both exciton coupling and response to UV-B, although to a lesser degree than WT. Exciton Coupling is reduced in the W233F, and W233A (C) W285F (D) and W337F and W337A(E) mutants. While W337F still shows a response to UV-B, none of the other single Tryptophan mutants shows a UV-B response. Exciton coupling is abolished in the W285A (D) and the triple tryptophan mutant (F) and neither show any response to UV-B (adapted from Christie *et al.*, 2012).

reduced exciton coupling and are constitutive dimers (Figure 1-12) (Christie, *et al*. 2012, Wu, *et al*. 2012).

It is therefore hypothesized that in darkness the tryptophan pyramid is exciton-coupled and the network of salt bridges holds the dimer together (Christie, *et al*. 2012, Wu, *et al*. 2012). Upon exposure to UV-B light, the tryptophan pyramid absorbs the UV-B and an electron becomes excited and is transferred from the pyramid into a nearby arginine/aspartate salt bridge, neutralising the charge and causing the dimer to separate (Christie, *et al*. 2012, Wu, *et al*. 2012, Mathes, *et al*. 2015). Further investigation into the photodynamics of UVR8 revealed that UVR8 has three stages of photodissociation: the initial absorption of a UV-B photon by the tryptophan pyramid; a conformational change that occurs over 50 ms and finally dimer dissociation that occurs over 200 ms (Miyamori, *et al*. 2015). Within the R146A/R286A and the R338A constitutive monomer mutants the second, conformational change step (which is likely to be the exposure of a hydrophilic region) occurs far more quickly than in wild type (WT) protein (3.4 ms and 5 ms respectively compared with 50 ms) (Miyamori, *et al*. 2015). It was hypothesised that this change in reaction rate is due to structural disruption of the tryptophan pyramid and this was confirmed by comparing with the D96N/D107N monomeric mutant which had an identical conformational change rate to the WT protein (Miyamori, *et al*. 2015).

1.6.2 The localisation of UVR8

Despite the absence of a Nuclear Localisation Signal (NLS), UVR8 localises to the nucleus after excitation with UV-B light (Figure 1-13) (Kaiserli and Jenkins 2007). Nuclear localisation is not enough to activate UVR8 and start the UV-B signalling pathway; exposure to UV-B light is also required (Kaiserli and Jenkins 2007). The exact mechanism of UVR8 nuclear localisation has not yet been determined although there is potential for UVR8 to associate with a protein that contains a NLS in order to gain access to the nucleus (Kaiserli and Jenkins 2007). An evaluation of the N-terminus of UVR8 across different plants showed a highly conserved region from 20-33 amino acids, a high degree of similarity from 12 to 20 amino acids and very little similarity before the twelfth residue. A deletion of

12 amino acids does not affect UVR8 function or localisation and a deletion of 23 amino acids stopped nuclear localisation (Kaiserli and Jenkins 2007).

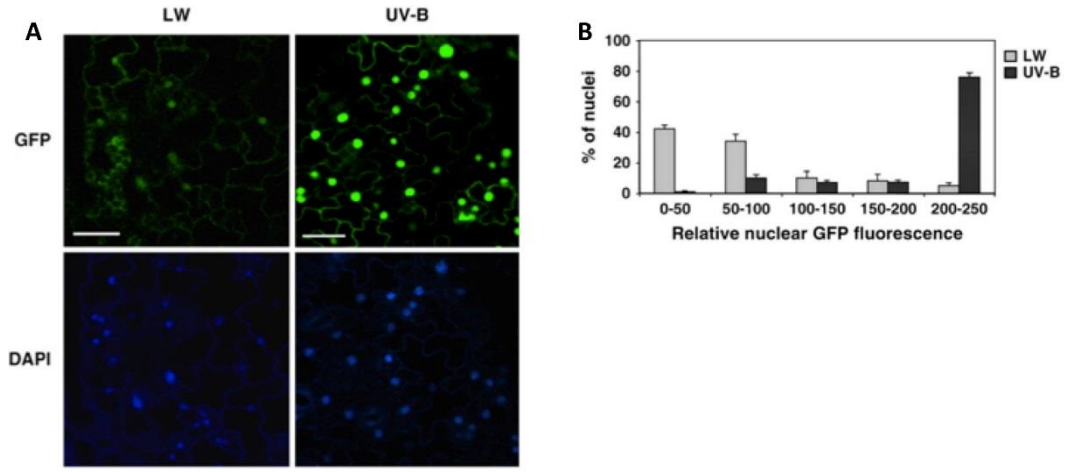

Figure 1-13: The localisation of UVR8. Confocal Images of *A. thaliana* containing the UVR8 protein tagged with Green Fluorescent Protein (GFP) construct (A). Relative nuclear GFP fluorescence in low white light (LWL) and UV-B as a percentage of nuclei is shown (B). After UV-B Illumination UVR8 accumulates in the nucleus. (adapted from Kaiserli and Jenkins (2007)).

Once in the nucleus, UVR8 binds to the chromatin (Cloix and Jenkins 2008). One area that UVR8 binds to is the *HY5* gene, including promoter and coding regions and just downstream of the coding region (Cloix and Jenkins 2008). There is no binding at further downstream or upstream areas, suggesting that UVR8 is quite localised. There were also several other genes that are regulated by UVR8 that the protein bound to, however not all of the DNA loci encoding proteins downstream of UVR8 in the UV-B signalling pathway were bound to by UVR8. Furthermore, UV-B light, although required for expression of the UV-B signalling pathway, is not required for UVR8 to bind to chromatin. UVR8 interacts with the chromatin at a histone level, in particular histone H2B (Cloix and Jenkins 2008). As UVR8 binds to histones, and the epigenetic modification of histones can affect gene transcription levels, it is hypothesised that UVR8 may regulate *HY5* and the other genes it binds to by histone modification. Methylation, phosphorylation, acetylation and ubiquitination of histones have been associated with the activation of genes. Levels of epigenetic acetylation of the genes in the UVR8 pathway were analysed and several, including *HY5* and *HYH*, showed some increase in levels of acetylation after UV-B exposure (Cloix and Jenkins, 2008).

1.6.3 UVR8 interactions

After UVR8 absorbs UV-B light and monomerises, it interacts with COP1 via its C-terminal region and accumulates in the nucleus (Cloix, *et al*. 2012, Heijge and Ulm 2012). It is not known whether UVR8 translocates to the nucleus or interacts with COP1 first. COP1 is an E3 ubiquitin ligase, but plays a different role in relation to UVR8. Despite COP1 interaction, exposure to UV-B light does not change the cellular abundance of UVR8, just the cellular distribution. Once in the nucleus, UVR8 associates with the promoter region of several UV-B regulated genes such as *HY5*. HY5 is a transcription factor for photomorphogenic responses, which up-regulates further genes involved in the UV-B response such as genes encoding Chalcone Synthase (CHS) and itself, the first dedicated enzyme in the flavonoid biosynthesis pathway, which protects against some damage from UV-B (Binkert, *et al*. 2014, Cloix, *et al*. 2012, Heijge and Ulm 2012). Other genes that are up regulated include the Repressor of UV-B Photomorphogenesis (RUP) proteins. These act as negative feedback for the UVR8 photomorphogenic pathway (Heijge and Ulm 2013, Heilmann and Jenkins 2013).

1.6.3.1 RUP activity and interaction with UVR8

RUP1 and RUP2 are 385 and 368 amino acids long respectively and share 63% of their identity, with a 349 amino acid overlap (Gruber, et al 2010, Wang, *et al*. 2011). Both proteins are composed of seven WD40 repeats (Gruber, et al 2010, Wang, *et al*. 2011). *RUP* expression is induced by UV-B, red, far-red and blue light (Gruber, *et al*. 2010). UVR8, COP1 and HY5 are required for induction by UV-B light (Gruber, *et al*. 2010). After expression, the RUP proteins localise to the cytoplasm and the nucleus and their localisation does not change in response to different light environments (Gruber, *et al*. 2010).

As previously mentioned the RUPs are negative regulators for the UVR8 photomorphogenic pathway (Heijge and Ulm, 2013, Heilmann and Jenkins, 2013). They interact with UVR8 (Heijge and Ulm, 2013, Heilmann, *et al*. 2013). While UVR8 will redimerise independently of any other protein in a purified protein solution it regenerates far quicker in the presence of the RUPs (Miyamori, *et al*. 2015, Heijge and Ulm 2013 and Heilmann, *et al*. 2013). The

RUP proteins influence UVR8 dimer regeneration independently of COP1 (Heijge and Ulm, 2013). Total levels of UVR8 protein did not change between a *rup1rup2* mutant plant, wild-type (WT) and a *rup1rup2*^{OX} (overexpressor) (Heijge and Ulm, 2013). While UVR8 regeneration does not require protein synthesis, it still occurs more rapidly when protein synthesis is possible (Heilmann and Jenkins, 2013). Optimal regeneration also requires the C27 region of UVR8 and the presence of COP1 (Heilmann and Jenkins, 2013).

When comparing the response of the *rup1rup2* mutant to WT plants it was found that when *rup1rup2* plants were given insufficient UV-B to cause a UVR8-COP1 interaction in WT plants, a UVR8-COP1 interaction was still observed (Heijge and Ulm, 2013). When the *rup1rup2* plants were given enough UV-B to cause a UVR8-COP1 interaction in WT plants, the amount of COP1 that could be co-IP'ed was increased (Heijge and Ulm, 2013). This would suggest that the RUP proteins compete with COP1 to interact with UVR8 and potentially impair UVR8-COP1 interaction. Furthermore, the UVR8-COP1 interaction in WT plants is not stable after 4 hours exposure to white light, however this interaction is stable in the *rup1rup2* mutant under the same conditions (Heijge and Ulm, 2013). A *rup1rup2* mutant plant is hypersensitive to UV-B and produces more anthocyanin, greater *HY5* and *CHS* expression and shortened hypocotyls (Gruber, *et al*. 2010). These plants also exhibit dwarfism and a dark green colour (Gruber, *et al*. 2010). These hypersensitive responses require UVR8 and HY5 (Gruber, *et al*. 2010). A overexpression of RUP1 and RUP2 has a different effect, blocking the UVR8 photomorphogenic pathway leading to reductions in *CHS* and *HY5* levels (Gruber, *et al*. 2010). As such plants without the RUP proteins acclimate to UV-B better than WT plants and overexpressors are more sensitive to UV-B damage and stress (Gruber, *et al*. 2010).

RUP1 and RUP2 are also known as Early Flowering by Overexpression 1 (EFO1) and EFO2 respectively as plants that overexpress the RUP proteins are also early flowering (Wang, *et al*. 2011). Interestingly when individual mutant lines were produced the *efo2-1/rup2* mutant was also early flowering in both short and long days compared to WT lines, while the *efo1-1/rup1* mutant showed no difference in flowering time compared to WT (Wang, *et al*. 2011). The *efo2-1/rup2* plant

also had changes in morphology including changed hypocotyl and stem elongation and leaf morphology as well as an increase in levels of Flowering Locus T (FT) (Wang, *et al*. 2011).

1.7 Variation within *A. thaliana*

A. thaliana is the plant species that is used throughout this study. *A. thaliana* has a truly impressive range from 68°N in Scandinavia to ~0° in Tanzania and Kenya and ranges in altitude from below sea level in the Netherlands to above 4000m in the Himalayas (Anwer and Davis, 2013, Koorneef *et al*. 2004). This incredible growth range means that *A. thaliana* can grow in a multitude of different environments, although it is frequently found within disrupted habitats (Horton, 2012, Koorneef *et al*. 2004). The natural range of *A. thaliana* is within Eurasia, although it has since been introduced and naturalised across the globe and is found in New Zealand and even remote Pacific Islands (Horton, *et al*. 2012, Koorneef, *et al*. 2004).

The primary limiting factor on *A. thaliana* growth range is the average temperatures in spring and autumn. If the average monthly temperatures are too low or exceed 22°C *A. thaliana* cannot grow (Koorneef, *et al*. 2004). Low precipitation is also a limiting factor (Koorneef, *et al*. 2004). Interestingly this makes the typical lab growing conditions extremely unnatural as 20°C is on the highest limit for *A. thaliana* growth.

The strains that are typically used are L*er*, Col and Ws, lines originally collected from Landsberg, Germany, Columbia, USA and Wassilewskija, Russia from the wild by Friedrich Leibach and since inbred within laboratories (Alonso-Blanco and Koorneef, 2000). While *A. thaliana* that grow wild are selfing and therefore inbred and almost entirely homozygous, variation does still occur between different 'ecotypes' (Alonso-Blanco and Koorneef, 2000). *A. thaliana* self-fertilises around 97% of the time, but this number does depend on which population of *A. thaliana* is being investigated (Abbot and Gomes, 1988, Platt, *et al*. 2010). Indeed, polymorhpisms found within the same geographical area are rare but present (Koorneef, *et al*. 2004). Platt (2010) undertook a study on 149 single nucleotide polymorphisms (SNPs) from 5707 *A. thaliana* plants from

around the globe; within these parameters 95% of plants studied had five or fewer heterozygous loci (Platt, *et al*. 2010). When *A. thaliana* that have been collected from different geographical and environmental locations are grown under identical conditions variation can be observed (Alonso-Blanco and Koorneef, 2000, Koorneef *et al*. 2004). Indeed differences have been seen in leaf production rate, colour, size and shape; trichome density; pathogen resistance; tolerance to abiotic stresses such as freezing or high temperature stress, drought, heavy metal tolerance, carbon dioxide abundance, ozone, light intensity; in circadian rhythm and in seed dormancy (Alonso-Blanco and Koorneef, 2000, Alonso-Blanco, *et al*. 2003, Anwer and Davis, 2013, Hilcher *et al*. 2009). However, despite this difference between ecotypes, there is no association between geographic location and genetic distance: a hallmark of a species that has recently dramatically expanded its range through human induced migration (Koorneef, *et al*. 2004).

The ecotypes that are used frequently are often not representative of the average *A. thaliana* ecotype. For example, when trichome density is measured, L*er* has a very low trichome density compared to the average *A. thaliana* plant, while Col has a high density in comparison (Hilscher *et al*. 2009). Futhermore, comparing just Col and L*er* shows that there is a great deal of difference even between these two ecotypes. There are 111 genes that are present in Col that are partially or completely deleted within L*er* (Koorneef, *et al*. 2004). These deletions are mainly found in transposon and R genes, areas of high genetic turnover, but also include some genes of unknown function (Koorneef, *et al*. 2004). Col/L*er* recombinant inbred lines had significant variation in circadian rhythm, which led to the identification of four putative Quantitative Trait Loci (QTLs) that control the period of the circadian clock (Swarup, *et al*. 1999). Indeed variation between *A. thaliana* accessions has been identified many times over. There is variation in traits from telomere length (Fulcher, *et al*. 2015), cold acclimation (Schulz, *et al.*, 2015) and circadian rhythms (Montaigu, *et al.*, 2015).

One of the variables that *A. thaliana* responds differently to, depending upon ecotype is UV light. Two studies investigated the response of seven ecotypes to

supplemental UV-A or UV-A and UV-B (Cooley *et al*. 2001, Torebinejad and Caldwell, 2000). This study found that under UV-A, some plants showed sensitivity to supplemental UV-A, while others showed no response or a positive response (Cooley *et al*. 2001). Under supplemental UV-A and UV-B, once again some plants were inhibited while others showed no difference to a negative control (Cooley *et al*. 2001). Furthermore, the degree to which the different ecotypes reacted to the light treatments varied (Cooley *et al*. 2001).

By investigating the natural variation in *A. thaliana* a later study found that PhyB varied between ecotypes in a way that affected the plant response to light (Filiault *et al*. 2008). This reinforced an earlier study that showed that different *A. thaliana* ecotypes responded significantly differently to all light wavelengths tested (white, blue, red and far-red light) as well as two different plant hormone treatments (Gibberellic Acid (GA) and Brassinosteroids (BRZ)) (Maloof, *et al*. 2001). It was found that hypocotyl length varied between the ecotypes regardless of treatment, and that those ecotypes with longer hypocotyls were collected closer to the equator where PAR is higher and were therefore likely adapted to a higher light environment (Maloof, *et al*. 2001). Supporting this theory, there was no correlation between dark grown hypocotyl length and latitude (Maloof, *et al*. 2001). Most interesting was that some of ecotypes studied behaved in ways similar to already documented genetic mutants while other exhibited entirely new patterns of behaviour: for example one ecotype had an extremely unusual response to far-red light, Lm-2 was 100 times less sensitive to far-red light than Col-0 (Maloof, *et al*. 2001). This difference in response was mapped to a single amino acid change within PhyA where Lm-2 differed from Col-0 at position 548 where a methionine had been changed to a threonine (Maloof, *et al*. 2001). This single change stabilised PhyA in far-red light, meaning that Lm-2 retained sensitivity to red light but was far less responsive to far-red light (Maloof, *et al*. 2001). This underlines how small a change is required to change protein function and the importance of investigating more than one ecotype.

While isolation by distance does not correlate to genetic distance in *A. thaliana*, as previously mentioned, latitude, altitude and climate does have an affect

(Méndez-Vigo, *et al*. 2011). Flowering time is strongly affected by temperature and so far two genes involved in flowering time, Flowering Locus C (FLC) and PhyC have been shown to follow latitudinal clines (Méndez-Vigo, *et al*. 2011).

1.8 The effect of UV-B on plants in a natural solar environment

While long-term effects of ecologically relevant UV-B on UVR8 have not been investigated there has been investigation into the effect of long term UV-B on plants in a natural solar environment. UV-B stress is not the default state of a plant in a natural solar environment (Hectors, *et al*. 2007, Hideg, *et al*. 2013). However, this does not mean that UV-B has no effect on plant morphology. Ecologically relevant UV-B in *A. thaliana* results in a redistribution of growth with a decreased rosette diameter, decreased inflorescence height but increased number of flowering stems (Hectors, *et al*. 2007). In *Lolium perenne*, ambient UV-B had no effect on the above ground biomass of the plant (Hideg, *et al*. 2013). Furthermore changes in gene expression can be seen with differences in auxin, brassinosteroids and gibberellins (Hectors, *et al*. 2007) and that the gene expression is different in different plant tissues (Casati, *et al*. 2004). Long term UV-B exposure also results in increased antioxidant levels with plants maintaining a pool of antioxidants such as ascorbate, xanthophyll and α-tocopherol (Hectors, *et al*. 2014). Exposure to UV-B radiation can also result in chromatin modifications that are frequently associated with epigenetic marks (Müller-Xing, *et al*. 2014).

There are both UVR8 dependent and UVR8 independent reactions to ecologically relevant UV-B radiation (Wargent, *et al*. 2009). For example, UVR8 has been shown to be involved in the shade avoidance response in plants, working antagonistically to the Phytochrome shade avoidance response (Hayes, *et al*. 2014, Mazza and Ballaré, 2015). A UV-B signal will inhibit the shade response through degradation of PIF4 and PIF5 and stabilisation of the DELLA proteins via UVR8 controlled increase in *Giberellin 2 Oxidase 1* (*GA2ox1*) transcript (Hayes, *et al*. 2014). Furthermore, UVR8 has been shown to be involved in the regulation of endopolyploidy in response to UV-B radiation (Gegas, *et al*. 2014, Wargent, *et al*. 2009).

Alternatively, plants that are observed in a natural solar environment tend to have increased herbivore and pathogen resistance than plants in an attenuated UV-B solar environment (Ballaré, *et al*. 2012, Ballaré, 2014, Ding, *et al*. 2012). When given low levels of supplementary UV-B, roses had increased resistance to *Podosphaera pannosa,* (powdery mildew) (Kobayashi, *et al*. 2013). This effect was caused by changes in secondary metabolites (Kobayashi, *et al*. 2013). Ecologically relevant UV-B radiation has been shown to provide resistance to the necrotrophic fungus *Cinerea botrytis* throught change in plant phenolics in a UVR8 dependent manner (Demkura and Ballaré, 2012, Hua, 2013). It has also been suggested that UV-B radiation may affect the composition of the plant cell wall, leading to increased deposition of syringyl-type lignins resulting in a far more robust cell wall that is more resistant to pathogen penetration (Hideg, *et al*. 2013, Hua, 2013). Moreover, four cultivars of soybean plants (*Glycine max*) that were exposed to solar UV-B radiation have increased resistance to two different species of stink bug, *Nezara viridula* and *Piezodorus guildinii* (Zavala, *et al*. 2014). The cultivars had different basal levels of phenolics, and while the stink bugs preferred plants grown in UV-B attenuated conditions to those that had been grown in natural solar UV-B conditions, plants which contained more of the isoflavonoids daidzin and genistin sustained less damage (Zavala, *et al*. 2014).

Plants that receive natural solar UV-B radiation both higher transcript levels of JA biosynthetic enzymes (Izaguirre, *et al*. 2006) and higher overall JA levels (Ding, *et al*. 2012) than those that were in an attenuated UV-B environment. However, this relationship has not been fully understood as contradictory evidence has been found which showed that greenhouse grown plants that were given supplementary UV-B did not have increased JA levels (Demkura, *et al*. 2010). This would suggest that the UV-B regulation of JA is complex and controlled by more than just the presence of ecologically relevant UV-B. Considering the antagonistic relationship seen between UVR8 and the Phytochromes for shade response (Hayes, *et al*. 2014, Mazza and Ballaré, 2015) this would not be surprising.

Of particular note is that the effect UV-B has on plants differs greatly depending on both the species of the plant, the growth form that the plant takes and the time of day (Barnes, *et al.* 2014, Sedej, 2014). Plants that were given supplementary UV-B in addition to natural solar UV-B radiation demonstrated a variety of responses over several time scales. *Fagus sylvatica* showed a decrease in photosynthetic capability after three years while similar declines in the rate of photosynthesis were only seen after five years in *Fraxinus excelsior, Betula pendula, Tilia cordata, Quercus robur and Acer pseudoplatanus* (Sedej, 2014). This reduction may be caused by direct damage to the photosynthetic apparatus and photosystem II in addition to Reactive Oxygen Species (ROS) damage; however reduced gas exchange due to UV-B induced stomatal closure may also be affecting the photosynthetic rate (Kataria, *et al.* 2014, Sedej, 2014, Tossi, *et al.* 2014). In contrast, an increase in photosynthetic rate was observed in *Acer rubrum* after three years of supplemental UV-B radiation (Sedej, 2014). This demonstrates the different resposnes of different species to the same stimuli.

When looking at the effect of UV-B of photosynthetic capability, it is important to note that pre-treatment with supplementary UV-B to plants grown in glasshouse conditions increases photosynthetic performance after transfer to a natural solar environment and that photosynthetic performance can be increased by UV-B (Davey, *et al.* 2012, Wargent, *et al.* 2014, Singh *et al.* 2014). *Lactuca sativa* that had been acclimated to UV-B in glasshouse conditions had increased photosynthetic capability once transferred to field conditions compared to plants that had not been acclimated to UV-B and plants that remained in glasshouse conditions (Wargent, *et al.* 2014). This demonstrates that acclimation to UV-B can also affect acclimation to high PAR environments, which considering that PAR and UV-A play a role in determining plant acclimation to UV-B, is not surprising (Krizek, 2004).

1.9 Conclusions

Since the confirmation of UVR8's role in UV-B perception and photomorphogenesis, fantastic progress has been made on characterising the molecular response of UVR8. The mechanism through which UVR8 perceives UV-B and the immediate response of the molecule have been documented. The role of

the RUP proteins and how they function to negatively regulate the UV-B photomorphogenic pathway and facilitate the regeneration of the UVR8 dimer has been elucidated. A shift has also occurred in how UV-B is considered in terms of plant growth. While UV-B can certainly be a stressor to a plant, it is recognised that long term, low UV-B exposure is how plants will grow in a wild environment. Adaptation and acclimation to UV-B and UV-B stress have been separated. Furthermore, the variation within *A. thaliana* is increasingly being seen as an excellent analytical tool for determining the effect of unknown genes, refining knowledge about the structure and function of already documented genes and interactions. The 1001 Genomes Project has also made this style of investigation possible on a previously impractical large scale.

1.10 Aims of this study

There were three main aims of this study. Firstly to test whether the UVR8 photoequilibrium acts a simple switch mechanism. Secondly to determine the factors that affect the photoequilibrium. Thirdly to investigate the diversity of *A. thaliana* UVR8 and associated genes and to evaluate adaptation.

Determining whether the UVR8 photoequilibrium acts as a switch was investigated in Chapter 3 via the effect of long term UV-B irradiation on the status of UVR8 in controlled growth room conditions. While UVR8 has been investigated *in planta* it was often under short, high intensity UV-B treatments in plants that had never been exposed to UV-B. Previous studies had also shown that the RUP proteins affected regeneration of dimeric UVR8 and had shown that ecotype had an effect on the response of plants to UV-B. The two most commonly used lab ecotypes, Col and L*er;* three ecotypes from different altitudes, Edi-0, Kas-1 and Shakdara; and the *rup1rup2* mutant line were exposed to varying fluence rates of UV-B over a long time period and the effect on UVR8 dimer/monomer status documented. The response to varying fluence rates of UV-B and how UVR8 influenced this was investigated by studying the growth patterns of Col-0 and L*er*, a constitutively monomeric mutant *uvr8*^{D96ND107N}, a 4 times overexpressor of UVR8, *uvr8*^{OX} and a UVR8 null mutant *uvr8-1*. The rate of monomerisation in UV-B naïve plants was also investigated in

L*er*, Col and *rup1rup2* to give further context with which to understand how UVR8 reacted to long term exposure to biologically relevant doses of UV-B.

The response of UVR8 under natural conditions affected by not only changes in UV-B fluence rate, but also PAR, temperature and day-length has not been studied previously. Chapter 4 investigates the response of UVR8 to natural daylight and determines how important each of the environmental factors mentioned is in establishing the UVR8 photoequilibrium. The effect of varying UV-B in a natural solar environment on UVR8 has not been studied in detail, and this was investigated by performing field studies across several different seasons in *A. thaliana*. The relationship between UVR8 configuration and different, recorded environmental conditions was investigated using Generalized Linear Modelling (GLM). Further examination was carried out on the relationship between temperature and UVR8 configuration by looking at the rate of regeneration in UV-B naïve plants that had been acclimated to a range of different temperatures.

The variety of growth response within *A. thaliana* combined with access to the exceptional 1001 Genomes Project made it possible to investigate both whether UV-B related genes were variable on an amino acid level between different ecotypes and whether these changes were correlated geographically, by UV-B environment or both. Chapter 5 addresses these concerns by looking at two sets of genes: those directly related to UV-B photoreception – *UVR8*, *RUP1* and *RUP2* – and those that are involved on a transcriptional level – *COP1*, *HY5* and *HYH*. All changes from the Col-0 WT amino acid sequence were documented for 855 ecotypes from across the globe. Individuals were clustered together by either geographical location (using latitude and longitude of origin) or altitude (using altitude of origin) and whether these individuals were more related to individuals within the same or different clusters was determined through the use of TCS networks and AMOVA. Col-0 was used as a WT sequence, not only because it is a very commonly used ecotype in laboratory environments and extremely well documented, but also because it is treated as the WT by the 1001 Genomes Project.

Chapter 2: Materials and Methods

2.1 Materials

2.1.1 Plant materials

2.1.1.1 Seed stocks

Wild-type *A. thaliana* cv. Landsberg *erecta* (L*er*), Columbia (Col-0), Shakdara (Sha), Edinburgh (Edi-0) and Kashmir (Kas-1) were obtained from The European Arabidopsis Stock Centre (NASC, Nottingham, UK). Prof. Daniel Kliebenstein (UC Davis, CA, USA) provided the *uvr8-1* mutant (L*er*). Dr Bobby Brown produced the *rup1rup2* double mutant (Col-0 background) by crossing the single mutants *rup1-1* and *rup2-1* obtained from NASC. Dr Monika Heilmann provided the Green Fluorescent Protein (GFP)-tagged UVR8 over expressor line coupled to the Cauliflower mosaic virus 35S promotor (35S) referred to as *35S-GFP-UVR8ox* (L*er*) and the *UVR8*^{D96ND107N} (L*er*) mutants.

2.1.1.2 Growth of A. thaliana on soil

2.1.1.2.1 Plants for controlled environment timecourses

A. thaliana seeds were sown on the surface of 7cm disposable pots containing compost soaked in insecticide solution (0.2 g/l Intercept® (Scotts, Ipswich, Suffolk, UK)). For each controlled growth room time course (2.3.5.1 and 2.3.5.3) three blocks of twelve pots each were prepared to determine if there were random effects based upon location in the growth room. The pots were kept under a humidifier and vernalised at 4˚C for 48 hours before being placed in growth rooms under 120 µmol m^{-2} s^{-1} white light in a 12h photoperiod with appropriate UV-B treatment (2.3.4). Plants were grown at 20˚C unless otherwise indicated.

2.1.1.2.2 Plants for field timecourses

A. thaliana seeds were sown on the surface of 7cm disposable pots containing compost soaked in insecticide solution (0.2 g/l Intercept® (Scotts, Ipswich, Suffolk, UK)). The pots were kept under a humidifier and vernalised at 4˚C for 48 hours before being placed in growth rooms under 120 µmol m^{-2} s^{-1} constant white light at 20˚C for 7 days before being transferred outside. Plants were then

grown outside on the roof of the Bower Building (Glasgow, UK: 55.872, -4.295) for a further 14 days in either a plus (no filter) or zero (Autostat CT5 filter) UV-B environment.

2.1.1.3 Surface Sterilisation of A. thaliana seeds

A. thaliana seeds were surface sterilised for growth on agar plates to prevent contaminating fungi by a five minute incubation in a sodium hypochlorite solution (50% (volume/volume(v/v))) followed by three one minute washes in sterile dH_2O.

2.1.1.4 Growth of A. thaliana on Agar Plates

Sterilised *A. thaliana* seeds were sown on 0.8% agar plates containing 2.15 g/l Murashige and Skoog salts (½ MS) with the pH adjusted to 5.7. Seeds were cold-treated on the plates in darkness at 4˚C for 48 hours before being placed in growth rooms under 120 µmol m^{-2} s^{-1} constant white light for 10 days. Plants were grown at 20˚C unless otherwise indicated.

2.1.2 Chemicals and reagents

The chemicals used for experiments described were obtained from ThermoFisher Scientific Ltd (Loughborough, Leicestershire, UK), Sigma Aldrich Ltd. (Poole, Dorset, UK) or Bio-Rad Laboratories (California, USA) unless stated otherwise.

2.1.2.1 Antibodies

Immunoblots were carried out with commercial and non-commercial antibodies kindly donated by other researchers. These, along with the working dilution, can be found in table 2-1.

Table 2-1: Antibodies used in this study, their application, working dilution and source.

Antibody	Application	Working Dilution	Source
anti-UVR8 (C-terminal)	Semi-native Western Blot	1/5000	Prof Gareth I Jenkins, MVLS, University of Glasgow, UK
Anti-GFP	Semi-native Western Blot	1/5000	Clontech, Living Colors® EGFP Monoclonal Antibody. Cat. # 632569.

2.1.2.2 Plasmid Vectors

The pHS vector was used for *Escherichia coli* protein expression and purification. It was kindly provided by Michael Hothorn (The Salk Institute for Biological Studies, California, USA).

2.1.2.3 Antibiotics

Kanamycin was obtained from Sigma-Aldrich and chloramphenicol from Duchefa Biochemie B.V. (Haarlem, The Netherlands). Working concentrations of antibiotics used are found in table 2-2.

Table 2-2: The antibiotics used in this study, the solvent used and the working concentration.

Antibiotic	Solvent	Working Concetration
Kanamycin	EtOH	50µg/ml
Chloramphenicol	H_20	34µg/ml

2.1.3 Bacterial strains

E. coli strains TOP10 (Agilent Technologies, California, USA) and Rosetta 2 (DE3) pLysS (Novagen, Merck KGaA, Darmstadt, Germany) were transformed with pHS plasmid vector containing UVR8 construct driven by the 35S promotor for protein expression.

2.2 General laboratory procedures

2.2.1 pH Measurements

pH measurements for solutions and media were done with a glass electrode attached to a Jenway 3320 pH meter (Jenway, Felsted, Essex, UK).

2.2.2 Centrifugations

An Eppendorf 5415D bench-top centrifuge, SORVALL LEGEND RT Centrifuge and SORVALL EVOLUTION RC Centrifuge were used for up to 2ml, 50ml and ≥50ml volumes respectively.

2.2.3 Sterlisations

Sterilisation of equipment, solutions and media was performed using a bench-top autoclave (Prestige Medical, Model 220140) for 15 min at 120°C and 1 atm. Filter

sterilisation was performed by filtration through a 0.2 µM pore diameter Nalgene filter.

2.3 Plant treatments

2.3.1 Light sources

White light treatments were performed in controlled growth room environments using warm white fluorescent tubes L36W/30 (Osram, Munich, Germany). For long term UV-B treatments narrowband UV-B tubes Philips TL20W/01RS (Philips, Aachen, Germany) were used. These lights have a maximal expression at 311nm and emit extremely low levels of emitted UV-A and blue light and as such do not induce UV-A/blue light regulated *CHS* expression (Brown *et al*. 2009). For UVR8 monomerisation and regeneration experiments broadband UVB-313 fluorescent tubes (Q-Panel Co., USA) were used covered by cellulose acetate filter (Cat No. FLM400110/2925, West Design Products, Nathan Way, London) to cut off any UV-C. The levels of blue and UV-A light emitted by broadband UV-B lights are not high enough to induce *CHS* expression (Christie and Jenkins, 1996). Detailed spectra of the lights used measured with a Macam Spectroradiometer Model SR9910 (Macam Photometrics Ltd., Livingston, UK) are included in Figure 2-1.

2.3.2 Light Fluence Rate Measurements

White light was measured using a LI-250A LI-COR meter with a LI190 quantum sensor (LI-COR, Lincoln, NE, USA). UV-B fluence rates were measured using a Skye Spectrosense 1 meter (Skye Instruments) with a SKU 430 sensor (Skye Instruments, Powys, UK). For field measurements a 30s average reading was recorded to take account of changing weather conditions.

2.3.3 Temperature Treatments

For the UVR8 regeneration experiments the *A. thaliana* seedlings were grown at 20°C for 10 days at 120 µmol m^{-2} s^{-1} white light before being transferred to 20 µmol m^{-2} s^{-1} white light environment at either 5°C, 10°C, 30°C or remaining at 20°C for 24 hours to allow adjustment to the temperature environment and to prevent artifacts based on the initial shock of temperature change. UV-B treatments were given (2.3.4) and the plants remained in the appropriate temperature treatment for the remainder of the timecourse.

2.3.4 UV-B Treatments

For controlled environment timecourses *A. thaliana* seedlings were grown in 120 µmol m^{-2} s^{-1} PAR plus either 3.0 µmol m^{-2} s^{-1}, 1.0 µmol m^{-2} s^{-1}, 0.3 µmol m^{-2} s^{-1} or 0 µmol m^{-2} s^{-1} supplemental narrowband UV-B for 21 days.

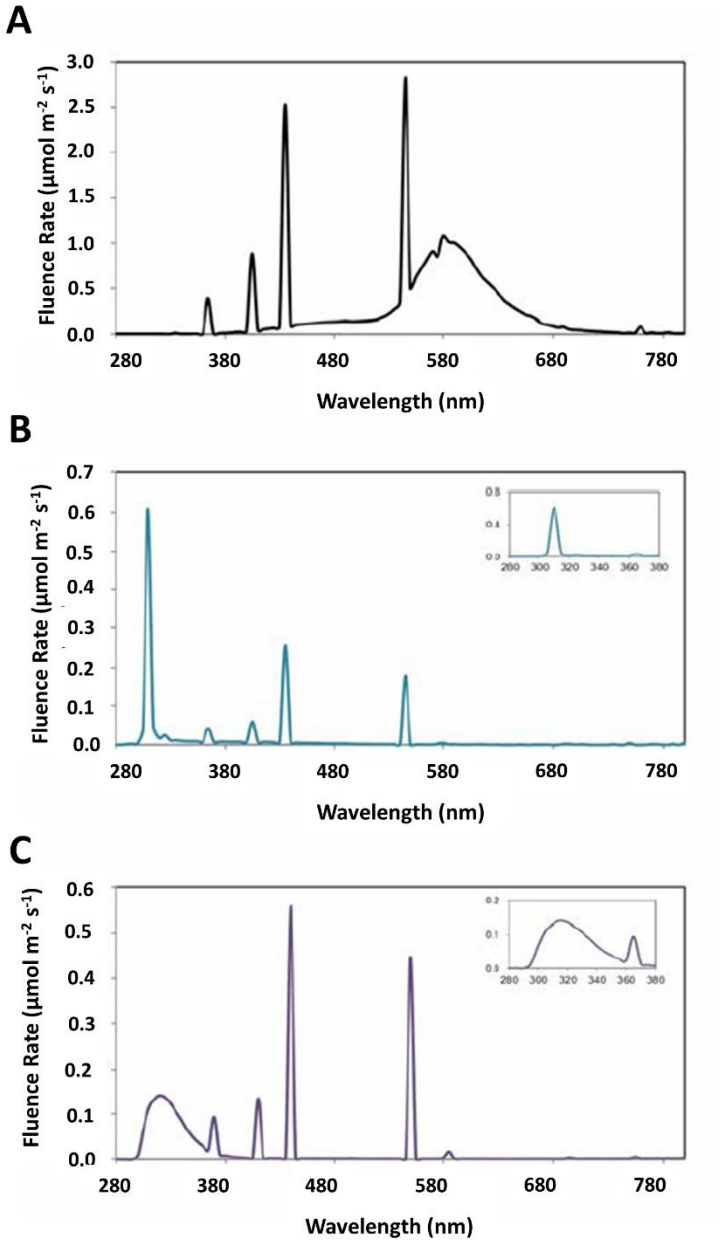

Figure 2-1: Detailed spectra of the light sources used. (A) Spectrum of warm white fluorescent tubes L36W/30. (B) Spectrum of narrowband UV-B tubes Philips TL20W/01RS (C) Spectrum of broadband UVB-313 fluorescent tubes (Q-Panel Co., USA). (Adapted from Heilmann, 2013).

For monomerisation experiments plants were grown at 120 µmol m^{-2} s^{-1} for 10 days and placed in darkness for 16 hours before being exposed to 3.0 µmol m^{-2} s^{-1} UV-B for 6 hours.

For regeneration experiments plants were grown as previously described (2.3.3) before being placed in 21 µmol m^{-2} s^{-1} broadband UV-B for 15 minutes. Plants were then kept in darkness for the remainder of the timecourse. See 2.3.5.3 for further details.

2.3.5 Timecourses

2.3.5.1 Controlled Environment

Samples were harvested at nine timepoints throughout the day: 30 mins before lights on, the mid-point of the light cycle, 30 mins after the end of the light cycle and a further six time points taken at equidistant points between these. Alternatively for dark-cycle timecourses the samples were taken 30 mins before lights off, the mid-point of the dark cycle, 30 mins after lights on and at 6 equidistant points throughout the dark cycle. Shoots were collected using scissors, packaged in aluminium foil and snap frozen in liquid nitrogen. Samples were processed as soon as possible but were stored at -80°C for up to a week.

2.3.5.2 Field Environment

Samples were harvested at nine timepoints throughout the day: 30 mins before sunrise, at three timepoints equally spaced between the first timepoint and solar noon, at solar noon, a further three equally spaced samples between solar noon and the final timepoint and 30 mins after sunset. Shoots were collected using scissors, patted dry with tissue if appropriate, packaged in aluminium foil and snap frozen in liquid nitrogen. Samples were processed as soon as possible but were stored at -80°C for up to a week.

2.3.5.3 Regeneration and Monomerisation Assays

For the regeneration assays samples were taken pre-UV-B treatment, immediately after UV-B treatment and at 15 min, 30 min, 60 min, 120 min, 240 min and 360 min after treatment. Monomerisation assay samples were taken immediately before UV-B treatment and at 15 min, 30 min, 45 min, 60 min, 75 min, 90 min, 105 min and 120 min during the UV-B treatment. Light treatement was performed as described in 2.3.2. Samples were harvested and stored as described in 2.3.5.1 and 2.3.5.2. After storage protein was extracted and run on

a semi-native Western Blot as described in 2.5.1. These results were then analysed in ImageJ as described in 2.5.1.10.

2.3.6 Morphology Analysis

A. thaliana plants were grown on soil as described for controlled timecourses in 2.3.4. For each repeat five separate plants were harvested using scissors and placed in a pre-weighed plastic measuring boat. Each boat was weighed to determine the fresh weight of the five plant shoots. The plants were then dried overnight at 50°C and weighed again to determine the dry weight of the plants. This was done eighteen times for each accession (eighteen weighing boats, each containing five whole plants).

In order to determine the leaf area of the rosette, individual *A. thaliana* plants were dissected and each leaf placed onto double sided tape on white A4 paper to ensure as high a contrast in the final image as possible. This was scanned at as high a resolution as possible with a ruler for scale and saved as a .tif image to ensure minimal data loss. ImageJ was used. The image was transformed to 8 bit and the threshold adjusted to remove the background. The scale was set using a scanned ruler and the Analyse Paricles command measured the area of the leaves. The area of the leaves were copied to Excel for further analysis.

2.4 Amplification of Plasmid DNA

2.4.1 Transformation of chemically competent *E. coli* cells

Strains of *E. coli* cells TOP10 and Rosetta 2 (DE3) pLysS (Novagen, Merck KGaA, Darmstadt, Germany) were used. All strains were transformed according to the manufacturer's instructions with a heat shock at 42°C and plated onto agar plates containing Luria Broth (LB) medium and the appropriate antibiotic for the selection of the plasmid. Plates were incubated at 37°C overnight.

2.4.2 Isolations of plasmid DNA

Small-scale plasmid DNA purifications from *E. coli* were performed using the Qiagen® Plasmid Mini Kit. A single bacterial colony was inoculated into 10 ml of LB medium containing the appropriate antibiotics for plasmid selection. The cultures were incubated overnight at 37°C with constant shaking (200 rpm). Cells were pelleted at 6000 g for 10 min and the supernatant was discarded. Cell

lysis and plasmid DNA purification was carried out according to the manufacturer's instructions. Plasmid DNA was stored at -20°C.

2.4.3 DNA sequencing

Sequencing of DNA was carried out by the Dundee Sequencing Service (University of Dundee, UK) or by GATC Biotech (Konstanz, Germany) according to the service's instructions using primers provided by the service (Table 2-3). Sequencing was performed to verify the sequence of the DNA insert for protein purification.

Table 2-3: The primers used for sequencing and their sequence.

Primer Name	Primer Sequence
T7	TAATACGACTCACTATAGGG
T7 terminal	GCTAGTTATTGCTCAGCGG

2.5 Protein Methods

2.5.1 Protein extraction and analysis from plants

2.5.1.1 Protein Isolation from A. thaliana plants

For protein extractions, *A. thaliana* plants were ground in liquid nitrogen using a mortar and pestle. The powder was transferred to a pre-cooled Eppendorf tube containing micro-extraction buffer (20 mM HEPES pH 7.8, 450 mM NaCl, 50 mM NaF, 0.2 mM theylenediaminetetraacetic acid (EDTA), 25% (v/v) glycerol, 0.5 mM phenylmethylsulphonylfluoride (PMSF), 1 mM 1,4-Dithiothreitol (DTT) and protease inhibitor mix (Complete Mini, EDTA-free, Roche)). The homogenate was then centrifuged at 16000 g for 10 min at 4°C and the supernatant was transferred to a fresh pre-chilled tube.

2.5.1.2 Quantification of protein concentration

The protein concentration of obtained samples was determined by the Bradford colorimetric method using bovine serum albumin (BSA) as a standard. Bradford assay solution (Bio-Rad, UK) was diluted five-fold with distilled water and filter sterilized to remove any particles. To each 1 ml of Bradford solution, 1 µl of protein extract was added and mixed well to obtain a homogenous colour. The absorbance at 595 nm was recorded with a spectrophotometer (Eppendorf,

Germany) against a blank sample (Bradford solution with 1 µl micro-extraction buffer). The concentration of each sample was calculated based on the equation of a standard curve that was generated using a serial dilution of BSA standards of known concentrations (1, 2, 4, 6, 8, 10 µg/µl).

2.5.1.3 Sodium Dodecyl Sulfate Polyacrylamide Gel Electrophoresis (SDS-PAGE)

Protein samples were denatured by adding required amounts of 4 x SDS protein sample buffer (250 mM Tris(hydroxymethyl)aminomethane (Tris)-HCl pH 6.8, 2% (weight/volume(w/v)) SDS, 20% (v/v) ß-mercaptoethanol, 40% (v/v) glycerol, 0.5% (w/v) bromophenol blue) and subsequent boiling of the samples for 5 min at 95°C. Depending on the size of the protein of interest either a 10% or a 12.5% polyacrylamide separating gel with a 4% polyacrylamide stacking gel was used (Separating: 10% or 12.5% (w/v) polyacrylamide, 0.38 M Tris-HCl pH 8.8, 0.1% (w/v) SDS, 0.05% (w/v) APS, 0.007% (v/v) N,N,N',N'-tetramethylethane-1,2-diamein (TEMED); Stacking: 4% (w/v) polyacrylamide, 132 mM Tris-HCl pH 6.8, 0.1% (w/v) SDS, 0.05% (w/v) APS, 0.15% (v/v) TEMED). Proteins were separated according to their size in SDS running buffer (25 mM Tris-HCl pH 8.5, 190 mM glycine and 0.1% (w/v) SDS) at 200 V for approximately 45 min. Protein molecular weights were determined using a pre-stained molecular weight marker (P7708, New England Biolabs).

2.5.1.4 Semi-native SDS-PAGE

To investigate the dimer to monomer ratio of UVR8 proteins semi-native SDS-PAGE gels were used. SDS-PAGE gels with the respective percentages were used as described in 2.5.1.3. 2x native sample buffer (Invitrogen, LC0725) was added to the samples and loaded on an SDS-PAGE gel without boiling. Protein separation was carried out as described in 2.5.1.3.

2.5.1.5 Coomassie Blue staining

Gels were stained for approximately 10 min at room temperature with shaking (100 rpm) in 0.1% Coomassie Brilliant Blue R250 (Bio-Rad), 45% methanol and 10% acetic acid and subsequently destained in 45% methanol and 10% acetic acid. To completely remove all background stain, gels were left in rehydration buffer (10% ethanol and 5% acetic acid) overnight before gels were scanned and dried under vacuum onto 3M paper.

2.5.1.6 Western Blot Transfer

Protein extracts separated by SDS-PAGE were transferred onto nitrocellulose membranes (Bio-Rad, UK) at 400 mA for 45 mins in transfer buffer (25 mM Tris-HCl pH 8.5, 190 mM glycine and 20% (v/v) methanol). Membranes were then stained with Ponceau solution (0.1% (w/v) Ponceau S, 1% (v/v) acetic acid) to reveal protein bands and thus determine if equal loading of protein samples had been achieved. The membranes were destained with Tris buffered Saline (TBS) (25 mM Tris-HCl pH 8, 150 mM NaCl, 2.7 mM KCl). Membranes were then blocked using 10% (w/v) non-fat dried milk in Tris buffered saline Triton-X (TBS-T) (25 mM Tris-HCl pH 8, 150 mM NaCl, 2.7 mM KCl, 0.1% (v/v) Triton-X) to prevent non-specific binding of the antibodies.

2.5.1.7 Immunolabelling

Primary antibodies were used in the concentration shown in Table 2-1 in TBS-T with 10% non-fat dried milk. Incubation was preferably done overnight at 4°C. If this was not practical the incubation time was shortened to 1 hour at room temperature. Between primary and secondary antibody incubations membranes were washed 3 times with Tris buffered saline Triton-X Tween (TBS-TT) (25 mM Tris-HCl pH 8, 150 mM NaCl, 2.7 mM KCl, 0.1% (v/v) Triton-X, 0.005% (v/v) Tween) and one time with TBS-T for a total of 20 mins. Depending upon the organism in which the primary antibody had been raised, secondary anti-rabbit (Promega, Cat # W401B) or anti mouse (Promega, Cat # W402B) horseradish peroxidase (HRP) conjugated antibodies were used in either 1/20000 or 1/10000 dilutions in TBS-T with 10% non-fat dried milk respectively. The membranes are incubated with shaking at room temperature for 1 hour followed by 5 washes with TBS-TT and 1 with TBS for a total of 30 mins.

2.5.1.8 Immunodetection

For detection of chemiluminescent signals, ECL Plus Western Blotting Detection Reagent (Amersham or Peirce Fisher) was used according to the manufacturer's instructions. The blots were imaged using the Fusion FX Vilberlourmat (Peqlab, Deutschland & Österreich, UK) fitted with the Fusion FX7 826. WL/Superbright WhiteLED bar Epi illumination; six 8W -213nm Tube and with the chemiluminesence filter installed.

2.5.1.9 Stripping of immunolabelled protein membrane

A stripping procedure is necessary for complete antibody removal from an already immunolabelled protein membrane in order to re-probe with different antibodies. Membranes developed by chemiluminescence were washed in TBS and then incubated in stripping buffer (100 mM β-mercaptoethanol, 2% (w/v) SDS, 62.5 mM Tris-HCl pH 6.8) at 50°C for 30 min with gentle agitation (30 rpm). Membranes were then washed at least three times with TBS-T for at least 15 min in total at room temperature followed by blocking with 10% non-fat dried milk in TBS-T for 1 hour. Immunolabelling and immunodetection were carried out as described in 2.5.1.7 and 2.5.1.8.

2.5.1.10 Semi-quantitative measurements of Western Blots

Images taken from the Fusion FX Vilberlourmat (Peqlab, Deutschland & Österreich, UK) were saved in .tif format and opened using as were scans of the corresponding Ponceau stains. For all Westerns protein loading was corrected using the Ponceau stain. Lanes were defined, background corrected and the density of the ribulose-1,5-bisphosphate carboxylase large subunit (rbcL) band measured. For controlled environment timecourses and field timecourses each lane was defined, background corrected and total protein corrected using the corresponding data from the Ponceau analysis. Then the density of the UVR8 dimer band and the UVR8 monomer band was measured within each lane. The sum of these two bands was considered to be the total UVR8. The percentage of either UVR8 dimer or UVR8 monomer can then be calculated.

For monomerisation and regeneration assays, data was corrected for background and normalised for protein loading as above. Lanes were defined and the density of each UVR8 dimer band was measured within each lane. The total UVR8 dimer in darkness was taken as 100%, and the rest of the data normalised to this.

2.5.2 Protein purification and analysis from *E. coli*

2.5.2.1 Culture growth

A starter culture of 100 ml of LB medium with appropriate anitbiotics was inoculated with a single colony of transformed Rosetta (DE3) pLysS cells and incubated overnight at 37°C with constant shaking (200 rpm). The next morning,

one litre of Terrific Broth medium (ForMedium™, Hunstanton, UK) with appropriate antibiotics was inoculated with 10 ml of the overnight culture. The culture was incubated on a shaking incubator (200 rpm) at 37°C until its density reached an Optical Density $(OD)_{600}$ of 1.0. Cultures were then transferred to a 16°C shaker (200rpm) and allowed time to adapt before protein expression was induced by adding isopropyl-beta-D-thiogalactopyranoside (IPTG) to a final concentration of 60 µM. The cultures were then incubated overnight at 16°C with constant shaking. Cells were pelleted the next morning by centrifugation at 4000 rpm at 4°C for 20 mins. Pellets were flash frozen in liquid nitrogen and stored at -80°C until proteins were purified.

2.5.2.2 Protein purification

Cells were resuspended in Wash Buffer I (50 mM Tris-HCl pH 8.0, 500 mM NaCl, 20 mM imidazole, 1 mM ß-mercaptoethanol, 10% glycerol, EDTA free protease inhibitor tablets (Roche)) at a 3:1 ratio of buffer to cells. Cells were lysed by sonication at 4°C until viscosity of the lysate decreased. To remove nucleic acids 2 µl Benzonase®Nuclease (Novagen) per 100 ml of lysate was added. Cell debris was pelleted by centrifugation at 16000 g at 4°C for 30 mins and the supernatant was collected.

All of the following steps were carried out in the cold room at 4°C. In order to form a resin bed, 0.8 ml nickel charged resin (Ni-NTA Super flow, 30401, Qiagen) per 1l TB culture was equilibrated by washing with 10 column volumes (CV) of Wash Buffer I. Equilibrated resin was transferred to a beaker and incubated with the supernatant previously collected for one hour with mixing. The mixture was then transferred back into the column and the supernatant allowed to flow through. The supernatant was collected and passed through the column twice more to ensure maximal binding to the column. This was followed by a wash step with 10 CV of Wash Buffer I. Subsequently, the ends of the column were capped and the resin with the bound proteins resuspended in 3 CV of Incubation Buffer (50 mM Tris-HCl pH 8.0, 500 mM NaCl, 10 mM Magnesium Adenosine Triphosphate (MgATP), 2.5 mM $MgCl_2$, 1 mM ß-mercaptoethanol) to remove bound chaperone proteins. After a 15 minute incubation period on a rolling shaker, the cap was removed and the buffer allowed to flow through followed by a final wash step

with 10 CV of Wash Buffer II (50 mM Tris-HCl pH 7.5, 150 mM NaCl, 1 mM ß-mercaptoethanol). To elute the His-tagged protein five one CV fractions were collected after addition of elution buffer (50 mM Tris-HCl pH 7.5, 150 mM NaCl, 250 mM imidazole, 1 mM ß-mercaptoethanol). Fractions two to four were pooled and used for the second purification step.

The resin bed was composed of 0.35 ml strep resin (*Strep*-Tactin® Superflow®, 2-1208-002, IBA, Goettingen, Germany) per 1l TB culture was equilibrated with 5 CV Wash Buffer II. Equilibrated resin was transferred to a beaker and incubated with the pooled elution fraction from the first purification step for one hour with mixing. The mixture was transferred back to the column, the supernatant allowed to flow through and the resin washed with 5 CV of Wash Buffer II. For the on-column cleavage of the tags to elute the protein, the ends of the column were capped, the resin resuspended in 2CV of Wash Buffer II and small ubiquitin-related modifier (SUMO) protease added. The mixture is incubated on a rolling shaker overnight. The next morning, the column is uncapped and the flow through collected. Subsequently the column is washed 3 times with 1 CV of Wash Buffer II. The three washes were pooled and passed through the column an additional time. Purified proteins were flash frozen in liquid nitrogen and stored at -80°C.

2.5.2.3 Purification of SUMO protease

Cleavage of the affinity tags of purified UVR8 was done via incubation with the SUMO protease. This was done to elute UVR8 from the column. SUMO protease is a highly active cysteinyl protease also known as Ulp which cleaves in a highly specific manner, recognising the tertiary structure of the ubiquitin-like protein, SUMO rather than an amino acid sequence. A recombinant fragment of Ulp1 (Ubl-specific protease 1) from *S. cervisiae* (ScUlp 1 residues 403-621) was cloned into a vector with a non-cleavable N-Terminal 6 x His and StrepII tag (construct obtained from Michael Hothron) and expressed in Rosetta (DE3) pLysS cells. Culture growth, induction of protein expression as well as harvesting of the culture was done as described under 2.5.2.1.

Thawed cell pellets were resuspended 3:1 ratio buffer:pellet in lysis and wash buffer (25 mM Tris-HCl pH 7.6, 1 M NaCl, 2 mM ß-mercaptoethanol, 10 mM imidazole) and sonicated as described under 2.5.2.2. The lysate was then centrifuged as described under 2.5.2.2. Cobalt resin (2 ml resin per 1 l TB medium used for culture growth) was equilibrated with lysis and wash buffer as described under 2.5.2.2, incubated with the clarified cell lysate, washed and incubated with Incubation Buffer containing Adenoside Triphostphate (ATP) to wash off chaperone proteins (50 mM Tris-HCl pH 7.6, 1 M NaCl, 10 mM MgATP, 2.5 mM $MgCl_2$, 1 mM ß-mercaptoethanol). After another wash step the SUMO protease was eluted from the column with 4 CV of elution buffer (25 mM Tris-HCl pH 7.6, 1 M NaCl, 2 mM ß-mercaptoethanol, 200 mM imidazole). The purified protease was then desalted with a Sephadex G-25 M column (GE-Healthcare) and concentrated to a final concentration of 3 mg/ml (final storage buffer: 25 mM Tris-HCl pH 8, 350 mM NaCl, 2 mM ß-mercaptoethanol). Aliquots of 100 µl were snap frozen in liquid nitrogen and stored at -80°C.

2.6 Data Analysis

2.6.1 Generalised Linear Modelling

Generalised Linear Modelling is a powerful statistical technique that underlies many individual tests such as the t-test and ANOVA. GLMs are particularly powerful as both continuous and factorial data can be interpreted using a single model. Furthermore, GLMs can be used to determine the importance of random factors and influence within a system. The power of this statistical analysis is particularly useful for field studies, this along with its versatility is the reason that they are the main statistical tool used within this thesis.

2.6.1.1 Development of custom scripts for GLM analysis

Custom scripts for testing GLMs were manually designed and written for use with R x64 3.2.0 (Fig 2-2). Initially, it was tested whether the block that the plants had been in resulted in a significant effect on the UVR8 photoequilibrium or plant leaf area/mass. After this had been determined, the effect of each factor was modelled both individually, additively and with interactions. Within the controlled environmental conditions, UV-B was treated as a categorical rather

than a continuous value as four set treatments rather than a continuous range of UV-B fluence rates were used.

```
#This command states that when the user refers to CompareWeight, R should read the .csv file
#that is named "LeafWeight.csv"
CompareWeight<-read.cvs("LeafWeight.csv")
#This command states that when the user types commands, R should look within CompareWeight
#for variables, etc.
attach(CompareWeight)
#This command asks R to summarise what is contained within CompareWeight. This allows the user
#to see what the variables are names, and that the correct data file has been attached
summary(CompareWeight)
#This creates a null model that only contains the intercept and calls it 'Intercept'.
Intercept<-glm(Fresh~1)
#This creates a model that states the fresh weight of the plants is only affected by the UV-B
#treatment and calls that model 'UVnull'.
UVnull<-glm(Fresh~UV)
#This creates a model that states the fresh weight of the plants is only affected by the
#ecotype of the plants and calls that model 'Ecotypenull'.
Ecotypenull<-(Fresh~Type)
#This compares the 'UVnull' model to the 'Intercept' model to determine which best explains the
#data.
anova(Intercept, UVnull, test="Chisq")
#This compares the 'Ecotypenull' model to the 'Intercept' model to determine which best explains
#the data.
anova(Intercept, Ecotypenull, test="Chisq")
#This compares the 'UVnull' model to the 'Ecotypenull' model to determine which should be the new
#null model.
anova(UVnull, Ecotypenull, test="Chisq")
#This defines a more complex model where fresh weight of the plants is affected by the UV-B
#treatment, the ecotype of the plants and the interaction between these two factors. The model
#is called 'Complex'.
Complex<-glm(Fresh<-UV*Ecotype)
#This takes a complex model and simplifies it one step at a time to a pre-determined stop point
#to determine what model is the best fit for the data.
drop1(Complex, scope=~UV, test="Chisq")
```

Figure 2-2: An example GLM script used for statistical analysis within R. Lines that begin with '#' are comments and are not read by the program.

2.6.2 Construction of Haplotypes

Six genes were chosen to construct the haplotype: UVR8 (At5G63860), COP1 (At2G32950), HY5 (At5G11260), HYH (At3G17609), RUP1 (At5G52250) and RUP2 (At5G23730). The default sequence was chosen to be the sequence found in the Columbia (Col-0) ecotype as this is the sequence used for the The *Arabidopsis* Information Resource (TAIR) database. As the accessions used within *A. thaliana* are lab lines, they have been inbred to the point of homozygosity. The sequences for each gene were obtained for all accessions from the 1001 Genomes Project database (2.6.2.1).

2.6.2.1 Databases

The 1001 Genomes database (http://1001genomes.org/) contains the sequences of 855 *A. thaliana* accessions at the time of writing. Each ecotype was recorded and the continent, country, latitude and longitude found using information from both The European Arabidopsis Stock Centre (NASC, Nottingham, UK) and The Arabidopsis Biological Resource Center (ABRC, Ohio State University, Ohia, USA). The altitude of each ecotype was found by using the latitude and longitude coordinates and Google Maps.

2.6.2.2 SNP designation

The amino acid sequence for each chosen gene from each accession was compared using the Genome Browser tool from 1001 Genomes. Only non-synonymous changes were recorded. Each different non-synonymous change was designated a haplotype number and the amino acid change and nucleic acid change recorded.

2.6.2.3 Development of custom scripts for analysis

2.6.2.3.1 Sorting Scripts

Custom scripts for sorting and analysing data were manually designed and written for use with Python 3.4 (https://www.python.org/) and edited with IDLE. The functionality of the scripts was verified using subsets of the available data with results checked by hand.

2.6.2.3.2 Individual genes

Alignments were created by creating a 'wild-type' sequence from each of the non-synonymous codons found in the population. The sequence for each haplotype differed according to the changes seen between that haplotype and the 'wild-type' sequence. The alignments were manually written into a .nexus file that could be accepted by PopART (Fig 2-3).

2.6.2.3.3 Alignment Scripts

Custom scripts for producing multi-gene alignments and outputting file-types that are compatible for other programs were manually designed for use with Python 3.4 and edited with IDLE. The functionality of the scripts was tested using a small subgroup of the available data and the results were checked by hand.

2.6.2.4 TCS networks

TCS networks and associated statistical analyses were performed using the open source software PopART to determine if individuals within specific groupings (such as geographical location of origin) were more related to individuals within the same group, suggesting population structure or to those within a different group, suggesting no population structure (http://popart.otago.ac.nz). Networks were laid out within the software. Pie charts showing the composition of each

haplotype within the network were created using the PopArt software and the image edited by adding labelling using Powerpoint 2013.

```
#NEXUS
BEGIN TAXA;
DIMENSIONS NTAX=22;
TAXLABELS
UVR8_1
UVR8_2
UVR8_3
UVR8_4
UVR8_5
UVR8_6
UVR8_7
UVR8_8
UVR8_9
UVR8_9
UVR8_10
UVR8_11
UVR8_12
UVR8_13
UVR8_14
UVR8_15
UVR8_16
UVR8_17
UVR8_18
UVR8_19
UVR8_20
UVR8_21
UVR8_22
;
END;
BEGIN CHARACTERS;
DIMENSIONS NCHAR=57;
FORMAT DATATYPE=DNA MISSING=? GAP=- MATCHCHAR=. ;
MATRIX
UVR8_1 GCCGACCTTCCTAATCACACCCACTCTGGTGAGCACGATGTATGTGTAGTTAATACG
UVR8_2 ...........................................................A.........
UVR8_3 .........T.....T......A.....................................
UVR8_4 .........T.....T............................................
UVR8_5 ..................T......A....................................
UVR8_6 .G..G..............................................................
UVR8_7 .......G...........................................A.........
UVR8_8 .........T.....T......A..........G...........................
UVR8_9 ..........................G.....................................
UVR8_10 ....................G..................G.....................
UVR8_11 ..........T.............A.....................................
UVR8_12 .G.....................................................................
UVR8_13 ................T......A........T.............................
UVR8_14 ............G...T......A.....................................
UVR8_15 .........T.....T......A.....................................A.....
UVR8_16 ..........................................................................T.
UVR8_17 ..........................................................T.........
UVR8_18 ..........................................................A.........
UVR8_19 ..........................................................T.....
UVR8_20 .G.....................................A.....................
UVR8_21 ................T......G.....................................
UVR8_22 ..........................C.....................................
;
END;
```

Figure 2-3: An example of the .nexus file manually coded for data input into PopART.

Chapter 3: The UVR8 Photoequilibrium

3.1 Introduction

Plants in their natural environments have to respond to a variety of signals in order to grow and compete. One of these signals is UV-B light. UV-B has long been thought of as a stressor to plants (Casati, *et al*. 2004, Cooley, *et al*. 2001, Frohnmeyer and Staiger, 2003, Jordan, 1996). However, recently a far more nuanced approach has been considered. Plants that have been given ecologically relevant doses of UV-B light in controlled conditions have been seen to better adapt to natural solar light after transplant to the field than those that were grown in zero UV-B through UV-B acclimation (Wargent, *et al*. 2014). Furthermore, in natural solar conditions there is evidence that plants that are stressed by UV-B are an exception to the rule: when the effect of ambient solar UV-B on *Lolium perenne* was investigated, no significant effect on biomass was observed (Hideg, *et al*. 2013); and within *A. thaliana* continuous exposure to ecologically relevant UV-B radiation did not affect photosynthetical capacity or express the UV-B stress genes (Hectors, *et al*. 2007). While *A. thaliana* that had been exposed to ecologically relevant doses of UV-B over a long period of time did not exhibit a stress response, a change in morphology was observed (Hectors, *et al*. 2007). A redistribution of growth with a decreased rosette diameter and decreased inflorescence height but an increase in number of flowering stems was observed as were changes in phytohormone expression (Hectors, *et al*. 2007). The existence of two distinct responses for UV-B suggests that there is a UV-B acclimation and photomorphogenic pathway and a UV-B stress pathway. With the discovery of the UV-B photoreceptor UVR8 (Christie, 2012, Rizzini, 2011 and Wu, 2011), further elucidation on this subject was achieved.

UVR8 has been categorised as the UV-B photoreceptor in plants (Christie, 2012, Rizzini, 2011 and Wu, 2011). It has been shown to be separate from the UV-B stress pathway: UV-B stress tolerance in *A. thaliana* has been shown to be dependent on Mitogen-Activated Protein Kinase (MAPK) Phosphatase 1 (MKP1) independent of UVR8 (González-Besteiro, *et al*. 2011). Nevertheless, UVR8 is

involved in the acclimation of plants to UV-B. It is involved in the production of flavonoids, shade avoidance and stomatal closure (Brown, *et al*. 2005, Hayes, *et al*. 2014, Tossi, *et al*. 2014). UVR8 exists in darkness as a homodimer and upon absorption of UV-B light monomerises (Miyamori, *et al*. 2015, Christie *et al*. 2012, Wu, *et al*. 2011). The regeneration of UVR8 from the active monomer state to the inactive dimer state has also been shown to be dependent upon whole plant cells as regeneration is far quicker than in plant extract or purified protein (Heijdge and Ulm, 2013 and Heilmann and Jenkins, 2013).

These studies are of great importance in understanding the molecular mechanisms of UV-B photoreception, however they do not address how long term, ecologically relevant UV-B light affects the composition of UVR8 or how this in turn affects the ability of the plant to acclimate to UV-B. The current model is that UVR8 exists as a dimer in darkness and rapidly or instantaneously dissociates to a monomer in plus UV-B conditions and requires zero UV-B conditions in order to regenerate dimeric UVR8 (Fig 3-1) (Heijdge and Ulm, 2013, Miyamori *et al*. 2015, Tilbrook, *et al*. 2013, Wu, *et al*. 2012). The aim of this chapter was to test the the model that UVR8 photoequilibrium acts as a simple switch mechanism under long-term UV-B light conditions. It was hypothesised that UVR8 does act as a switch as a simple switch but that complete monomerisation would occur more quickly in plants that were grown under higher UV-B fluence rates. This was done by monitoring the UVR8 photoequilibrium after plants had been grown in 12 hour day/night cycles under three separate UV-B fluence rates and a minus UV-B control. It is further hypothesised that *A. thaliana* accession will affect the $UVR8^{dimer}$ to $UVR8^{monomer}$ switch. Finally it is posited that long-term UV-B will affect the morphology of *A. thaliana*, dependent upon the fluence rate used.

In order to investigate the rate of monomerisation and regeneration of UVR8 in UV-B acclimated plants and the effect that this had on plant morphology, several experiments were undertaken. Plants were grown under four different UV-B conditions for three weeks before samples were taken over a timecourse. These were analysed on semi-native Westerns via immunoblotting to allow for quantification of the $UVR8^{dimer}$/$UVR8^{monomer}$ ratio. To ensure that UVR8 was not

monomerising before the start of the light cycle a dark timecourse was undertaken. Several *A. thaliana* accessions from different altitudes and therefore different UV-B environments were examined to determine the effect of ecotype on the $UVR8^{dimer}/UVR8^{monomer}$ ratio. Finally the effect that different levels of UVR8 protein and alterations in the $UVR8^{dimer}/UVR8^{monomer}$ ratio had on physiology were investigated.

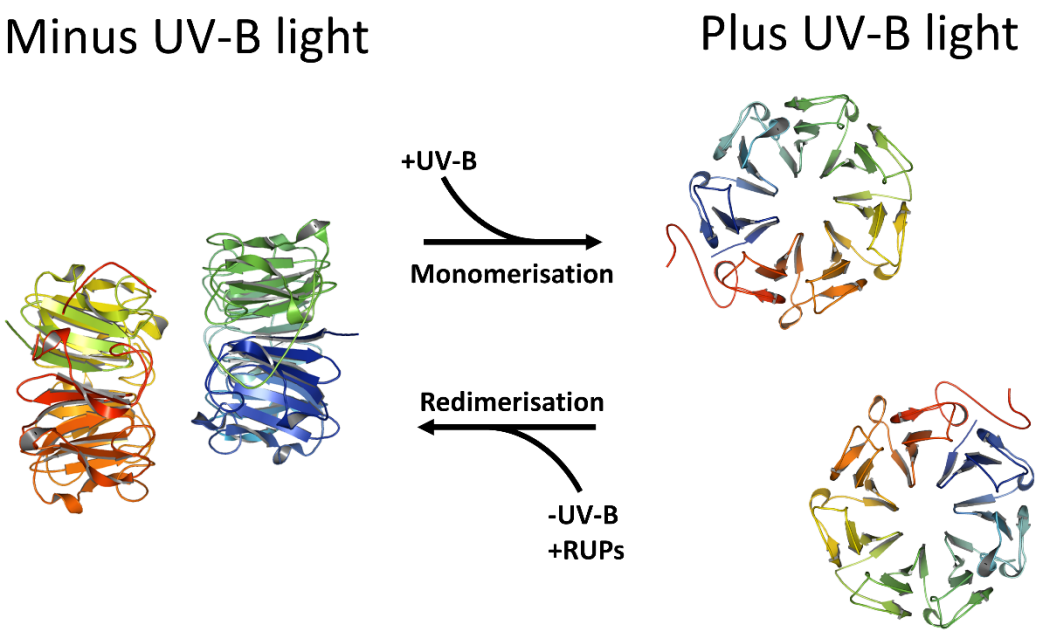

Figure 3-1: A current model of the monomerisation and redimerisation of UVR8 under plus and zero UV-B conditions. UVR8 is seen to be entirely dimeric in darkness or zero UV-B conditions. Following UV-B illumination UVR8 monomerises rapidly and stays monomeric while under plus UV-B conditions. Upon the exclusion of UV-B light and in the presence of the RUPs UVR8 will redimerise over the course of 3 hours and will remain dimeric until illumination with UV-B light.

3.2 UVR8 forms a photoequilibrium under long term, photoperiodic UV-B light conditions

The configuration of UVR8 in plants exposed to long term, ecologically relevant UV-B has not been investigated. To study this two ecotypes of *A. thaliana* - Col-0 and L*er* and one mutant - *rup1rup2* – were grown in a 12 hour light/dark cycle for 21 days under one of three UV-B treatments and a zero UV-B control. For each of the three biological repeats, three blocks of twelve pots of plants were grown to determine whether location within the growth room caused an effect. The lme4 package within R was used to determine whether growth room position had a siginificant effect (UVR8 Dimer % = Intercept + ε, where ε is the random

factor; UVR8 Dimer is only affected by the random position within the room). As no effect was found, each block could be considered a separate repeat (n=9).

During each biological repeat The UV-B treatments were grown under 120 µmol m^{-2} s^{-1} of white light with either 3.0 µmol m^{-2} s^{-1}, 1.0 µmol m^{-2} s^{-1} or 0.3 µmol m^{-2} s^{-1} supplementary UV-B. Zero UV-B growth conditions were used as a control. UV-B treatments were chosen to represent different natural solar conditions. Within this study it was determined that 3.0 µmol m^{-2} s^{-1} was equivalent to a sunny summer's day in Glasgow, UK and was 65% of the maximum UV-B fluence rate observed (Chapter 4); 1.0 µmol m^{-2} s^{-1} was equivalent to a cloudier, spring day which was also frequently observed (Chapter 4). The use of 0.3 µmol m^{-2} s^{-1} supplementary UV-B corresponded to a dark and rainy day or a darker winter's day (Chapter 4).

Samples were harvested 30 minutes before the start light period, 30 minutes after the start of the light period, at the mid point of the light period, 30 minutes before the dark period and 30 minutes after the dark period as well as at a further four equidistant time points. For each sample ten plants (minus roots) were harvested at random from each block of pots. Samples were snap frozen in liquid nitrogen and stored for a maximum of a week before processing via semi-native Western blot. Blots were analysed using ImageJ (Fig 3-2).

In the zero UV-B controls for each ecotype and mutant, there was never less than 95% dimer (Fig 3-2B-D) and there was frequently no monomerisation seen at all. This finding supports previous work which states that UVR8 requires UV-B to monomerise (Christie, *et al*. 2012, Miyamori *et al*. 2015, Rizzini, *et al*. 2011, Wu, *et al*. 2011). When examining the supplementary UV-B treatments it became clear that in UV-B acclimated plants, complete UVR8 monomerisation was neither instantaneous nor rapid. Instead there was a mix of both $UVR8^{monomer}$ and $UVR8^{dimer}$ found for all timepoints, UV-B treatments, ecotypes and mutant (Fig 3-2B-D).

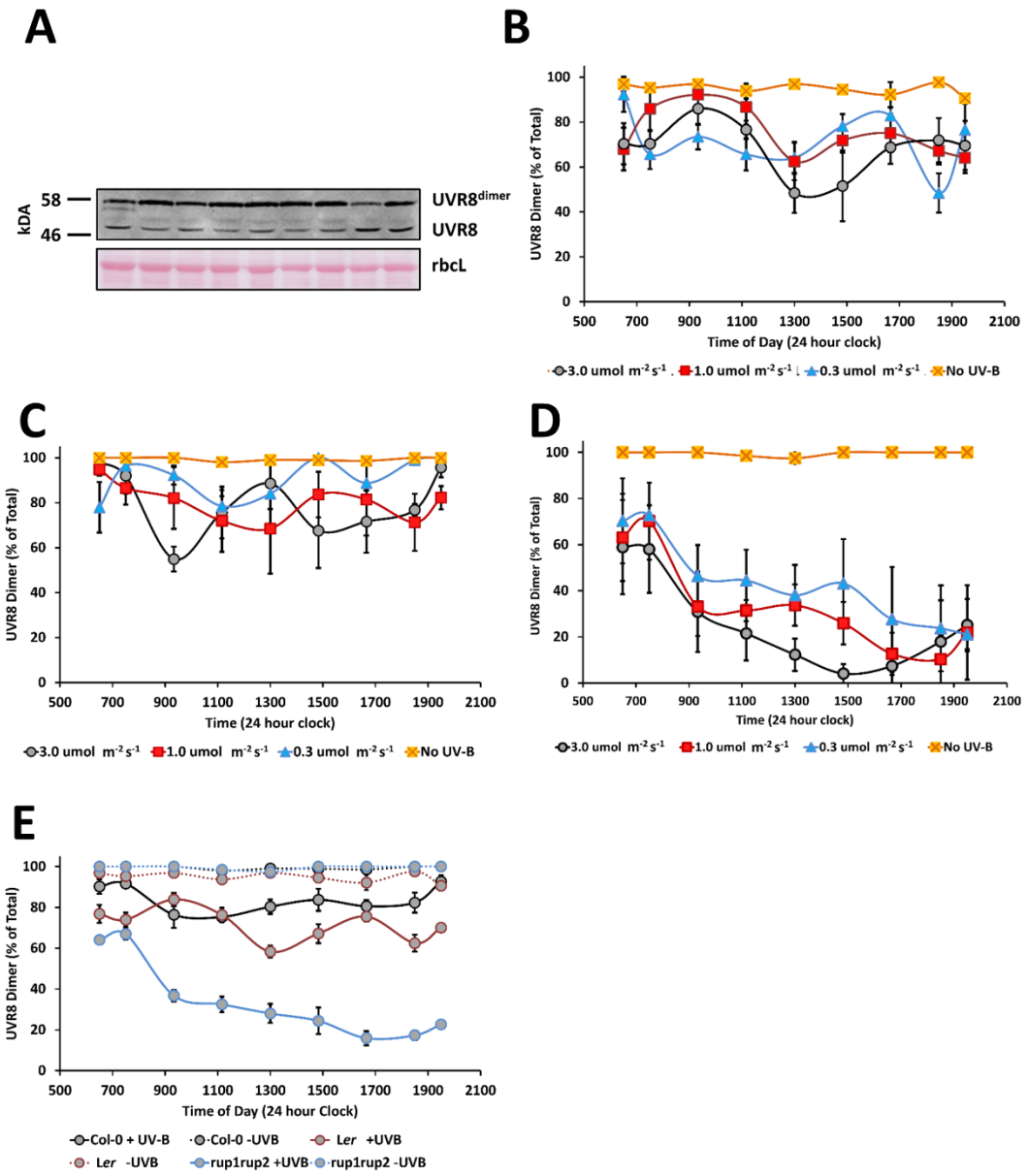

Figure 3-2: An analysis of the UVR8 photoequilibrium in controlled growth conditions. L*er* (B), Col-0 (C) and *rup1rup2* (D) plants were grown for three weeks under a 12 hour light/dark cycle with 120 µmol m^{-2} s^{-1} and either 0.3 µmol m^{-2} s^{-1}, 1.0 µmol m^{-2} s^{-1}, 3.0 µmol m^{-2} s^{-1} supplementary UV-B or a negative UV-B control. Samples were then harvested 30 minutes before the start of the light cycle, 30 minutes after the end of the light cycle and at 7 equally spaced timepoints throughout the light cycle. Samples were then analysed by unboiled, semi-native Western Blot via immunodetection. Protein loading was controlled and normalised using rbcL levels. The $UVR8^{dimer}/UVR8^{monomer}$ ratio was quantified using imageJ. (A) A representative unboiled semi-native Western Blot before quantification and rbcL loading control. Both $UVR8^{dimer}$ and $UVR8^{monomer}$ can be seen. Quantified Western Blot data showing the $UVR8^{dimer}/UVR8^{monomer}$ ratio at 0.3 µmol m^{-2} s^{-1}, 1.0 µmol m^{-2} s^{-1}, 3.0 µmol m^{-2} s^{-1} and in a negative UV-B control within (B) L*er*, (C) Col-0 and (D) *rup1rup2*. The data shown is the mean $UVR8^{dimer}/UVR8^{monomer}$ ratio $\pm$ S.E (n=9). (E) A comparison of the plus UV-B (0.3 µmol m^{-2} s^{-1}, 1.0 µmol m^{-2} s^{-1} and 3.0 µmol m^{-2} s^{-1}) averaged across the timecourses versus the negative UVB control for L*er*, Col-0 and *rup1rup2*. Data shown is the mean $UVR8^{dimer}/UVR8^{monomer}$ ratio $\pm$ S.E (n=9 for negative UV-B control, n=21 for plus UV-B treatment)

For L*er*, under the lowest supplementary UV-B treatment the $UVR8^{dimer}/UVR8^{monomer}$ ratio was initially very high before the onset of the light cycle, 92% of the total UVR8 protein is $UVR8^{dimer}$ and when compared to the other UV-B treatments via ANOVA, not significantly different to the zero UV-B control (p=0.298) (Fig 3-2B). Under the 0.3 μmol m^{-2} s^{-1} UV-B treatment, as would be expected if the UVR8 response to UV-B light was rapid, complete monomerisation, there was initially a sharp drop in $UVR8^{dimer}$. At 0730 hours, the $UVR8^{dimer}$ dropped to 66% and when compared to the other treatments via ANOVA, was significantly different to the zero UV-B treatment (p=0.016). However, after this point no further monomerisation was seen and complete monomerisation was absent. The balance between $UVR8^{dimer}/UVR8^{monomer}$ remained relatively stable throughout the day, with one further period of monomerisation at the end of the light period between 1700 and 1900 hours. Regeneration was seen after the onset of the dark cycle at 1930 hours, with 77% $UVR8^{dimer}$ observed.

Compared with the low 0.3 μmol m^{-2} s^{-1} supplementary UV-B treatment, the medium 1.0 μmol m^{-2} s^{-1} supplementary UV-B treatment began with a smaller pool of $UVR8^{dimer}$, 68%, at 0630 hours before the onset of the light treatment. This is significantly different from the zero UV-B and low UV-B treatments when compared via ANOVA (p=0.0125). However, in a reversal of the trend observed for the low UV-B light treatment, there was an increase in the $UVR8^{dimer}$ followed by a period of monomerisation. This pattern repeated, with a second period of regeneration followed by monomerisation. Regeneration was not seen immediately after the onset of the dark cycle.

The high UV-B treatment of 3.0 μmol m^{-2} s^{-1} supplementary UV-B followed a remarkably similar pattern to the medium UV-B treatment. The initial $UVR8^{dimer}$ level was 70% at 0630 hours – significantly different to the zero and low UV-B treatments when compared via ANOVA (p= 0.0163), followed by a sinusoidal pattern of $UVR8^{dimer}$ regeneration and monomerisation. Once again, no regeneration was seen immediately after the onset of the dark cycle.

In comparison, Col-0 showed a slightly different UVR8 photoequilibrium pattern (Fig 3-2C). As in L*er*, the zero UV-B treated plants were almost entirely dimeric UVR8 throughout the light cycle. The 0.3 µmol m^{-2} s^{-1} plants showed a different patter to the similarly treated L*er* plants. Before the light cycle begins there was 78% $UVR8^{dimer}$ within the lowest UV-B treatment, significantly less dimer than the zero UV-B treatment when compared via ANOVA (p=0.0338). Regeneration of the $UVR8^{dimer}$ was observed 30 minutes after the onset of the light cycle. Monomerisation was observed throughout the day, but a large pool of $UVR8^{dimer}$ was maintained throughout the light cycle and 100% $UVR8^{dimer}$ was seen twice throughout the timecourse; once at 1450 hours during the light cycle and once at 1930 hours, 30 minutes after the end of the light cycle.

When given the 1.0 µmol m^{-2} s^{-1} treatment of supplementary UV-B a different pattern was observed. $UVR8^{dimer}$ was seen to be at a high level before the onset of the light cycle: 95% of the total protein was $UVR8^{dimer}$. A steady reduction in the level of $UVR8^{dimer}$ was observed until the mid-point of the light cycle at 1300 hours. This was also the lowest level of $UVR8^{dimer}$ recorded for this light treatment. The balance of $UVR8^{dimer}$/$UVR8^{monomer}$ was maintained throughout the day with fluctuations between timepoints that are not significantly different to each other (the largest change was between 1300 hours and 1500 hours and had a p=0.1778). A small degree of regeneration was seen after the onset of the dark cycle.

Plants treated with 3.0 µmol m^{-2} s^{-1} display a different pattern of $UVR8^{dimer}$/$UVR8^{monomer}$ ratio throughout the timecourse. At the timepoint 30 minutes before the start of the light period $UVR8^{dimer}$ was observed to be 98%, not significantly different to the zero UV-B treatment (p=0.3183). The 3.0 µmol m^{-2} s^{-1} treated plants then showed a similar pattern of monomerisation and regeneration of the medium and high UV-B treated L*er* plants. A sinusoidal pattern of monomerisation and regeneration was observed. Nevertheless, the level of $UVR8^{dimer}$ never dropped below 50%. Regeneration after the onset of the dark cycle was observed.

As the RUP proteins are essential for efficient redimerisation of UVR8, it was to be expected that the UVR8 photoequilibrium in the *rup1rup2* mutant plants would be different to that of the Col-0 WT background of the mutants (Fig 3-2D). Interestingly, while different balances of $UVR8^{dimer}$/$UVR8^{monomer}$ and different patterns of monomerisation and regeneration were observed between different UV-B treatments for Col-0, the *rup1rup2* mutant plants had very similar patterns of $UVR8^{dimer}$/$UVR8^{monomer}$ ratio.

In the absence of UV-B, UVR8 did not monomerise in the *rup1rup2* mutant plants. For all three treatments the $UVR8^{dimer}$ level was similar at 0630 hours, 70% $UVR8^{dimer}$, 63% $UVR8^{dimer}$ and 58% $UVR8^{dimer}$ for 0.3 μmol m^{-2} s^{-1} supplementary UV-B, 1.0 μmol m^{-2} s^{-1} supplementary UV-B and 3.0 μmol m^{-2} s^{-1} supplementary UV-B respectively and not significantly different to each other ($p=0.508$). This initial timepoint was significantly different to the zero UV-B treatment ($p=0.00578$). While the $UVR8^{dimer}$/$UVR8^{monomer}$ ratio did not immediately change after the onset of the light cycle, all three treatments showed substanstial monomeriation between 0730 and 0900. After this point the balance of $UVR8^{dimer}$/$UVR8^{monomer}$ remained relatively stable in each different UV-B treatment. Regeneration was seen in both the medium 1.0 μmol m^{-2} s^{-1} and high 3.0 μmol m^{-2} s^{-1} UV-B treatments after the onset of the dark cycle and towards the end of the light cycle respectively. No regeneration was seen in the 0.3 μmol m^{-2} s^{-1} supplementary UV-B treatment.

In order to determine how the different factors involved in this experiment (time of harvest, UV-B fluence rate and accession) affected the $UVR8^{dimer}$/$UVR8^{monomer}$ ratio, GLM was performed using R. First, as UVR8 does not monomerise in the absence of UV-B a simple model was performed to determine whether UV-B fluence rate could explain the data: UVR8 % = UV-B Fluence Rate, where UVR8 Dimer % was treated as a continuous variable and UV-B Fluence Rate was treated as a factorial variable (zero, low, medium or high UV-B). This model was significant ($p=<2e^{-16}$) and was treated as the null model: to be replaced further models must better explain the data.

From these timecourses, the different ecotypes appear to have different UVR8 photoequilbria. By collating the data collected from plus UV-B treatments, the effect of ecotype or mutant can be more clearly seen (Fig 3-2E). The most complex model fitted was UVR8 Dimer % = UV-B Fluence Rate + Ecotype + Time + UV-B Fluence Rate*Ecotype*Time, where UVR8 Dimer % and Time were treated as continuous variables and UV-B Fluence Rate and Ecotype were treated as factorial variables (zero, low, medium and high UV-B Fluence Rate and Col-0, L*er*, and *rup1rup2* ecotypes). This complex model states that UVR8 Dimer is affected by the UV-B Fluence Rate, the ecotype of plant, the time of harvest and interaction between all three of these variables. To determine the model that provided a good fit to the data while also not over-fitting the data the drop1 command within R was used. This simplifies the model one interaction and term at a time, comparing the simpler model to the more complex model via a Chi-Squared test. More complex models are penalised and so must provide a larger increase in significance to be kept. The model that best explained the data was UVR8 Dimer % = UV-B Fluence Rate + Ecotype, where the $UVR8^{dimer}/UVR8^{monomer}$ ratio is affected by both the UV-B fluence rate and the ecotype of the plant ($p=<-2e^{-16}$).

When the effect of UV-B was investigated via ANOVA within each ecotype these differences became apparent. Within L*er* all three UV-B light treatments were significantly different to the zero UV-B control ($p=4.36e^{-08}$, $p=1.24e^{-06}$ and $p=5.57e^{-10}$ for the 0.3 µmol m^{-2} s^{-1}, 1.0 µmol m^{-2} s^{-1} and 3.0 µmol m^{-2} s^{-1}, respectively). However, there was no statistically significant difference between the low UV-B treatment and the other UV-B treatments (p=0.449 and p=0.354 for 1.0 µmol m^{-2} s^{-1} and 3.0 µmol m^{-2} s^{-1} respectively), or between the medium and high UV-B treatment (p=0.0939). This would suggest that while UVR8 forms a UV-B photoequilibrium in response to UV-B, the balance of photoequilibrium does not change significantly based on changes in the UV-B fluence rate or that changes occur at even smaller fluence rates. Alternatively, there may be a pattern, but as the data was so variable, the number of repeats was not high enough to expose that correlation.

Within Col-0 the $UVR8^{dimer}$ level was affected by which UV-B treatment was used. The zero UV-B control was significantly different to all three plus UV-B treatments ($p=0.049$, $p=1.53e^{-05}$ and $p=2.18e^{-07}$ for 0.3 µmol m^{-2} s^{-1}, 1.0 µmol m^{-2} s^{-1} and 3.0 µmol m^{-2} s^{-1} respectively). The $UVR8^{dimer}$/$UVR8^{monomer}$ ratio seen within the low UV-B treatment was significantly different from both the medium and high UVB treatments ($p=0.014411$ and $p=0.000683$ for 1.0 µmol m^{-2} s^{-1} and 3.0 µmol m^{-2} s^{-1} respectively). The medium and high UV-B treatments did not show a significant difference to one another ($p=0.313371$). Furthermore, that a difference was seen between the low, 0.3 µmol m^{-2} s^{-1} UV-B treatment and the higher treatments but not between the medium 1.0 µmol m^{-2} s^{-1} and high 3.0 µmol m^{-2} s^{-1} UV-B treatments would suggest that unlike L*er,* Col-0 exhibits a change in the balance of the UVR8 photoequilibrium based on UV-B fluence rate. It further suggested that the higher the fluence rate, the less dimer exists in the $UVR8^{dimer}$/$UVR8^{monomer}$ ratio up to a saturation point that occured between 0.3 µmol m^{-2} s^{-1} and 1.0 µmol m^{-2} s^{-1}.

Within the *rup1rup2* timecourses the zero UV-B control is significantly different to all three plus UV-B treatments ($p=1.77e^{-13}$, $p=<2e^{-16}$ and $p=<2e^{-16}$ for 0.3 µmol m^{-2} s^{-1}, 1.0 µmol m^{-2} s^{-1} and 3.0 µmol m^{-2} s^{-1} respectively). The low and high supplementary UV-B treatments did show significant difference to one another ($p=0.0132$). However, the medium UV-B treatment was not significantly different to either the low or the high UV-B treatment ($p=0.1595$ and $p=0.272$ for 0.3 µmol m^{-2} s^{-1} and 3.0 µmol m^{-2} s^{-1} respectively). Once again, because there was a pattern that was shared between the UV-B treatments, it was possible to predict that the level of $UVR8^{dimer}$ decreased as the light cycle continues. Unlike both L*er* and Col-0, it appeared that UV-B fluence rate did have an effect on the balance of the UVR8 photoequilibrium and that a saturation point was not reached in the *rup1rup2* mutant. However this effect was not linear, the 1.0 µmol m^{-2} s^{-1} treatment did not cause three times the monomerisation of the 0.3 µmol m^{-2} s^{-1}, nor did the 3.0 µmol m^{-2} s^{-1} cause three times the monomerisation of the 1.0 µmol m^{-2} s^{-1} treatment.

UVR8 did not function like a simple $UVR8^{dimer}$»$UVR8^{monomer}$ switch. However, it had also been demonstrated that the presence or absence of UV-B was not the

only determining factor in the $UVR8^{dimer}/UVR8^{monomer}$ ratio. The GLM showed that ecotype also played a role. While there was no evidence to suggest that the levels of UVR8 protein were altered in a circadian manner, the presence of $UVR8^{monomer}$ before the start of the light cycle could indicate that under long term UV-B treatments, UVR8 monomerisation occured pre-emptively to the light cycle.

3.3 UVR8 does not monomerise pre-emptively under long term, photoperiodic UV-B conditions

As statistical analysis showed that the variation in the $UVR8^{dimer}/UVR8^{monomer}$ ratio was not completely explained by only UV-B, it is worthwhile considering the idea that circadian regulation may moderate either monomerisation or redimerisation. The total amount of UVR8 is not affected by light treatments (Kaiserli and Jenkins, 2007) however, UVR8 was frequently seen as monomeric before the onset of the light treatment (Fig 3-2). The regeneration of UVR8 during the dark cycle is important, as it is possible that after long term treatment with UV-B, UVR8 begins to monomerise before the onset of the light cycle.

In order to determine whether this was the case Col-0, L*er* and *rup1rup2* mutants were grown in a 12 hour light/dark cycle for 21 days under one of three UV-B treatments and a zero UV-B control. For each of the three biological repeats, three blocks of twelve pots of plants were grown to determine whether location within the growth room caused an effect. The lme4 package within R was used to determine whether growth room position had a siginificant effect (UVR8 Dimer % = Intercept + ε, where ε is the random factor; UVR8 Dimer is only affected by the random position within the room). As no effect was found, each block could be considered a separate repeat (n=9).

The plants were grown for 21 days in a 12 hour light/dark cycle with 3.0 μmol m^{-2} s^{-1} supplementary UV-B. A 3.0 μmol m^{-2} s^{-1} s UV-B treatment was chosen as it produced the largest amount of monomerisation during the light cycle during the previous timecourses (Fig 3-2). Samples were harvested 30 minutes before the onset of the dark cycle, 30 minutes after the onset of the light cycle and at 6

equally spaced times throughout the dark cycle. For each sample ten plants (minus roots) were harvested at random from each block of pots. Samples were snap frozen in liquid nitrogen and stored for a maximum of a week before processing via semi-native Western blot. Blots were analysed using ImageJ (Fig 3-3).

There was a clear $UVR8^{dimer}/UVR8^{monomer}$ ratio seen at the end of the light cycle in all three plant types (Fig 3-3B-D). In L*er* the $UVR8^{dimer}/UVR8^{monomer}$ ratio can be seen 30 minutes prior to the start of the light cycle (Fig 3-3B). However, further monomerisation was seen after the onset of the dark cycle at 2000 hours. The $UVR8^{dimer}$ levels recovered slightly at 2206 hours before remaining stable until 0424 hours. A substantial amount of $UVR8^{dimer}$ regeneration was seen at 0630 hours, just before the onset of the light cycle. This was the highest level of dimer seen in the timecourse. UVR8 appeared to monomerise after the onset of the light cycle at 0730 hours.

Within the Col-0 timecourse the level of $UVR8^{dimer}$ remained stable until 2206 hours, after which a small amount of $UVR8^{dimer}$ regeneration was seen (Fig 3-3C). However, the $UVR8^{dimer}$ level then remained stable from 0012 hours to 0218 hours. After this point substantial $UVR8^{dimer}$ regeneration was seen and the $UVR8^{dimer}$ level reached its highest point 30 minutes before the end of the dark cycle. After the onset of the light cycle, a decrease in the total $UVR8^{dimer}$ level was seen.

The *rup1rup2* plants showed a different pattern of $UVR8^{dimer}/UVR8^{monomer}$ ratio (Fig3-3D). The level of $UVR8^{dimer}$ remained stable after the onset of the dark cycle at 2000 hours. From this point there was continuous redimerisation until 0012 hours. The $UVR8^{dimer}$ level remained steady until 0424 before a further slight increase in $UVR8^{dimer}$ regeneration at 0630 hours. The highest level of $UVR8^{dimer}$ was observed at the timepoint 30 minutes prior to the onset of the light cycle. After the onset of the light cycle there was an immediate decrease in the total $UVR8^{dimer}$ percentage.

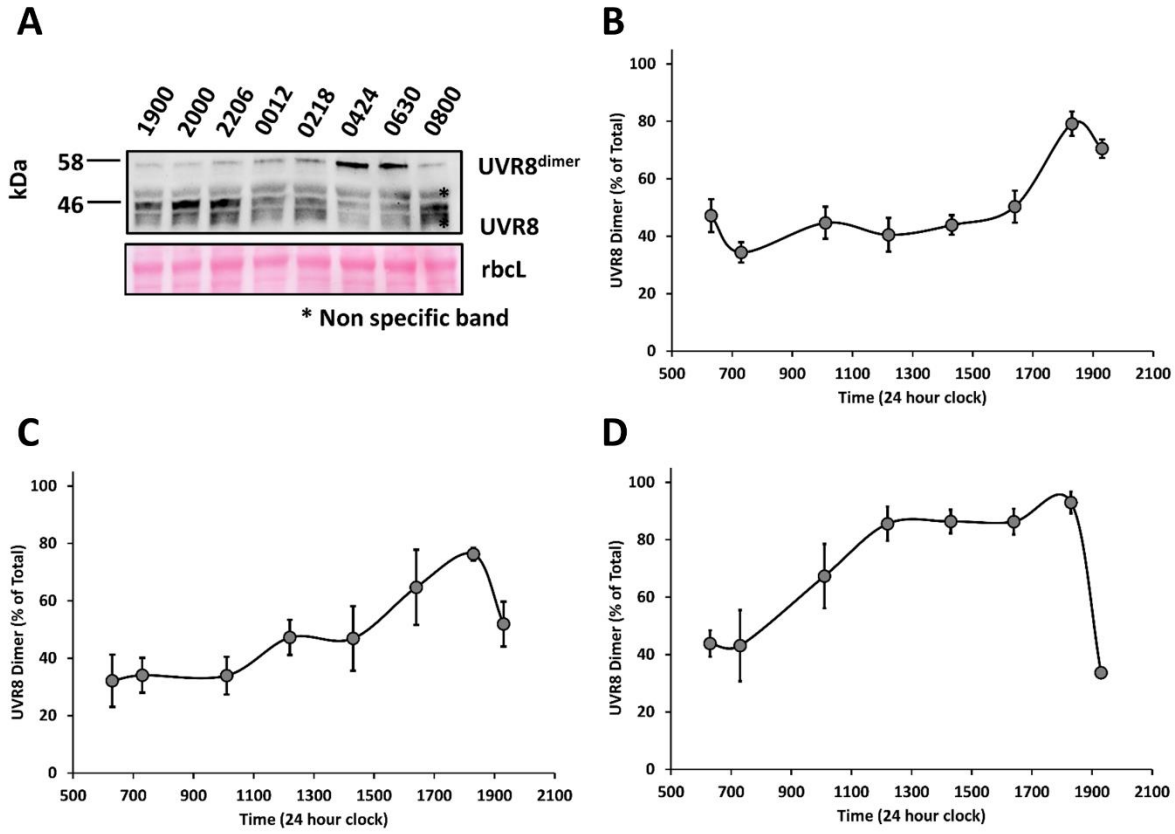

Figure 3-3: Quantification of the recovery of the UVR8^{dimer} during the dark cycle. (A) A representative unboiled Western used for quantification of the UVR8^{dimer}/UVR8^{monomer} ratio and a Ponceau stain showing levels of rbcL used for normalisation of protein loading. Both UVR8^{dimer} and UVR8^{monomer} can be seen. Quantified Western Blot showing the recovery of the UVR8^{monomer} to the UVR8^{dimer} over the dark cycle in L*er* (B), Col-0 (C) and *rup1rup2* (D). Data shown is the mean UVR8^{dimer}/UVR8^{monomer} ratio $\pm$ Standard Error (SE) (n=9). Plants were grown for 21 days in a 12 hour light dark cycle of 120 µmol m^{-2} s^{-1} plus supplementary UV-B (3.0 µmol m^{-1} s^{1}). Samples were then harvested 30 minutes before the dark cycle, 30 minutes after the onset of the light cycle and at equidistant points throughout the dark cycle. Samples were then analysed by non-boiled, semi-native Western Blot via immunodetection, Protein levels were controlled and normalised using both Bradford assay and rbcL levels. The UVR8^{dimer}/UVR8^{monomer} ratio was quantified using imageJ.

The timepoint immediately prior to the onset of the light period displayed the greatest amount of $UVR8^{dimer}$ in the case of all three plant types investigated. This would suggest that the existence of an $UVR8^{dimer}/UVR8^{monomer}$ ratio at this time point was not due to pre-emptive monomerisation of UVR8 regulated in a circadian manner. However, there are other factors that influence the $UVR8^{dimer}/UVR8^{monomer}$ ratio, such as ecotype. The difference displayed in $UVR8^{dimer}/UVR8^{monomer}$ ratio indicated different ecotypes of *A. thaliana* may respond differently to the same treatments of UV-B.

3.4 The UVR8 photoequilibrium varies with ecotype

While both Col-0 and L*er* plants that had been treated with long term, ecologically relevant fluence rates of UV-B had similar patterns of UVR8 photoequilibrium, the balance of this photoequilibrium was significantly different between the two ecotypes. As there are many different accessions of *A. thaliana* it is possible that the UVR8 photoequilibrium may differ in relation to the typical fluence rate of the environment from which the ecotype was origninally. UV-B fluence rate varies with many different factors, including altitude (Fioletov, *et al*. 2010). Therefore, to determine whether the UVR8 photoequilibrium is dependent upon the *A. thaliana* ecotype studied, three ecotypes that are found at varying altitudes were investigated: Edi-0 is found in Edinburgh, UK which grows at 42m above sea level; Kas-1 is found in Kashmir, India which grows at 1580m above sea level and Shakdara from Pamiro-Alay, Tajikistan which grows 3400m above sea level.

Once again the plants were grown with three blocks of twelve pots of plants per ecotype to determine whether where the trays were positioned within the growth room caused an effect. The lme4 package within R was used to determine whether growth room position had a siginificant effect (UVR8 Dimer % = Intercept + ε, where ε is the random factor; UVR8 Dimer is only affected by the random position within the room). As no effect was found, each block could be considered a separate repeat (n=9).

These plants were grown for 21 days under a 12 hour light/dark cycle with 120 μmol m^{-2} s^{-1} white light plus one of four light treatments: 3.0 μmol m^{-2} s^{-1}, 1.0 μmol m^{-2} s^{-1}, 0.3 μmol m^{-2} s^{-1} or no supplementary UV-B. Samples were harvested 30 minutes prior to the light cycle, at the midpoint of the light cycle, 30 minutes subsequent to the dark cycle and at six further equally spaced timepoints taken throughout the light cycle. For each sample ten plants (minus roots) were harvested at random from each block of pots. Samples were snap frozen in liquid nitrogen and stored for a maximum of a week before processing via semi-native Western blot. Quantification was performed using ImageJ (Fig 3-4).

As found previously, it is important to note that little to no monomerisation of UVR8 was seen in the zero UV-B control (Fig 3-4B-D). With the Edi-0 photoequilibrium there was a consistent pattern for all three UV-B treatments (Fig 3-4B). Prior to the beginning of the light cycle there was $UVR8^{monomer}$ present and the total $UVR8^{dimer}$ decreased following the onset of the light cycle. In the 0.3 μmol m^{-2} s^{-1} and 1.0 μmol m^{-2} s^{-1} supplementary UV-B timecourses there was a constant regeneration of the $UVR8^{dimer}$ until the midpoint of the light cycle followed by a decrease in the total $UVR8^{dimer}$ and a final increase in the $UVR8^{dimer}$ level after the start of the dark cycle. The 3.0 μmol m^{-2} s^{-1} supplementary UV-B timecourse was similar, but while the lower treatments showed two cycles of decrease and increase in $UVR8^{dimer}$ level, the higher treatment had three, with an additional decrease and increase in $UVR8^{dimer}$ level seen at the midpoint of the light cycle.

In comparison the Kas-1 ecotype showed a different pattern (Fig 3-4C). The lowest treatment of UV-B had a very high level of $UVR8^{dimer}$ before the onset of the light cycle. There was a small reduction in $UVR8^{dimer}$ after the light cycle begins which was maintained until the midpoint of the light cycle. After this there was complete regeneration of the $UVR8^{dimer}$ and no further change was seen. The 1.0 μmol m^{-2} s^{-1} supplementary UV-B timecourse was similar to the one seen in Edi-0. There was an initial reduction in $UVR8^{dimer}$ followed by gradual regeneration of the dimer until the midpoint of the light cycle when the reduction of $UVR8^{dimer}$ levels was repeated, showing regeneration of $UVR8^{dimer}$ after the end of the light cycle. The high treatment of UV-B showed a wider

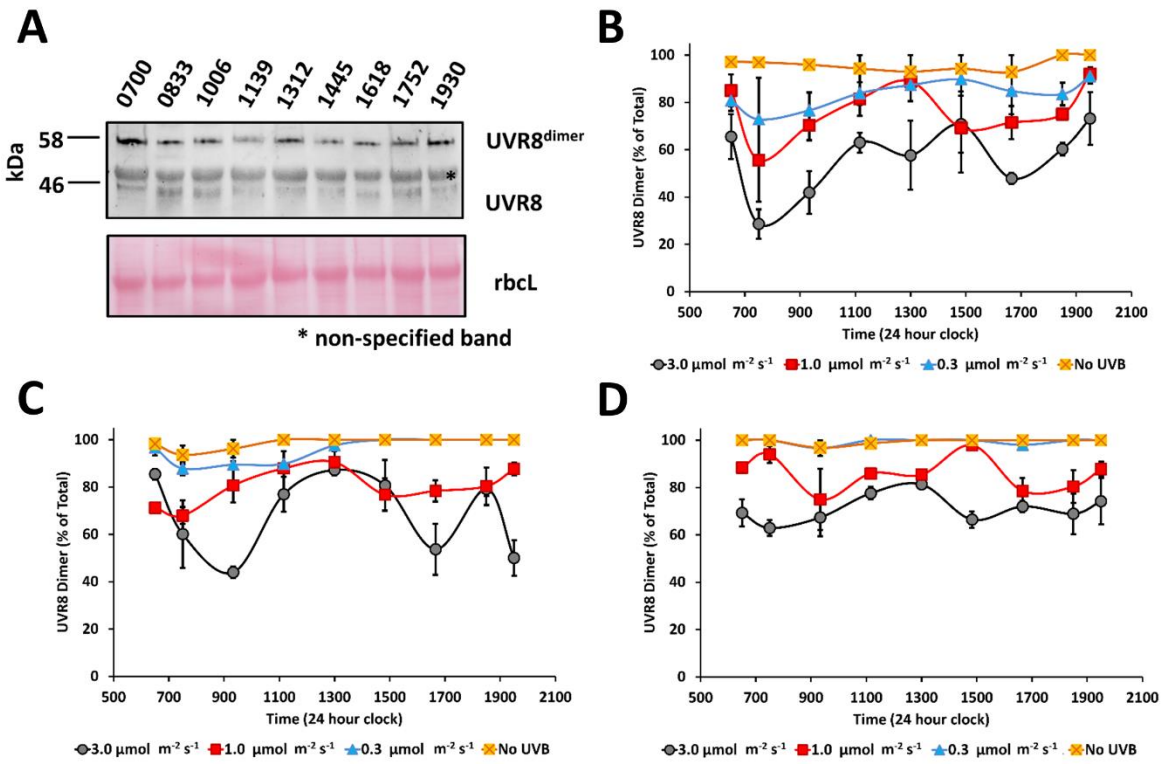

Figure 3-4: The effect of ecotype on the UVR8^{dimer}/UVR8^{monomer} ratio. Plants were grown for 21 days in a 12 hour light/dark cycle with 120 µmol m^{-2} s^{-1} white light and either 0.3 µmol m^{-2} s^{-1}, 1.0 µmol m^{-2} s^{-1}, 3.0 µmol m^{-2} s^{-1} supplementary UV-B or a negative UV-B control. Samples were harvested 30 minutes prior to the onset of the light cycle, 30 minutes after the onset of the dark cycle and at equally spaced timepoints throughout the light cycle. Samples were then analysed by unboiled, semi-native Western Blots via immunodetection. Protein levels were controlled and normalised using rbcL levels. The UVR8^{dimer}/UVR8^{monomer} ratio was quantified using imageJ. (A) A representative unboiled, semi-native Western Blot used for quantification and Ponceau stain used for quantification of the UVR8^{dimer}/UVR8^{monomer} ratio and normalisation of the total protein level respectively. Both UVR8^{dimer} and UVR8^{monomer} can be observed. Quantified semi-native Western Blot data showing the photoequilibrium of UVR8 at 0.3 µmol m^{-2} s^{-1}, 1.0 µmol m^{-2} s^{-1}, 3.0 µmol m^{-2} s^{-1} and in a negative UV-B control for (B) Edi-0, (C) Kas-1 and (D) Shakdara. The data shown is the mean UVR8^{dimer}/UVR8^{monomer} ratio $\pm$ S.E (n=9).

variation in the $UVR8^{dimer}/UVR8^{monomer}$ ratio. Monomerisation was seen between 0630 hours and 0920 hours; 1300 hours and 1640 hours; and 1920 and 2000 hours. Regeneration was seen between 0920 and 1300 hours and 1640 and 1920 hours.

Within the Shakdara timecourse there was no apparent difference between the zero UV-B control and the 0.3 µmol m^{-2} s^{-1} UV-B treatment (Fig 3-4D). The 1.0 µmol m^{-2} s^{-1} UV-B showed an initial increase in $UVR8^{dimer}$ after the onset of the light cycle. This was followed by two cycles of monomerisation and regeneration as seen previously. The 3.0 µmol m^{-2} s^{-1} UV-B had an initial decrease in $UVR8^{dimer}$ before a slow regeneration period reaching a peak at the midpoint of the light cycle.

The use of GLM can be used to determine how the variables interact to best describe the data. Again, as UV-B is required for UVR8 monomerisation, the first model fitted was UVR8 Dimer % = UV-B Fluence Rate (the $UVR8^{dimer}/UVR8^{monomer}$ ratio is affected by only the UV-B fluence rate), where UVR8 Dimer % was treated as a continuous variable and UV-B Fluence Rate was treated as a factorial variable (zero, low, medium or high UV-B). This model was extremely significant and was accepted as the null model ($p=<2e^{-16}$). Subsequently a complex model was defined and the drop1 function used to simplify the model one variable and interaction at a time: comparing the more complex model to the simpler model and keeping the model best fits the data. The most complex model fitted was UVR8 Dimer % = UV-B Fluence Rate + Ecotype + Time + UV-B-Fluence Rate*Ecotype*Time (the $UVR8^{dimer}/UVR8^{monomer}$ ratio is affected additively by UV-B fluence rate, the ecotype of the plant and the time of harvest as well as by interactions between these three factors), where UVR8 Dimer % and Time were treated as continuous variables and Ecotype and UV-B Fluence Rate were treated as factorial variables. The most parsimonious model was UVR8 Dimer % = UV-B Fluence Rate + Ecotype + UV-B Fluence Rate*Ecotype ($p=5.99e^{-06}$). Therefore the $UVR8^{dimer}/UVR8^{monomer}$ ratio was affected by the UV-B fluence rate and the ecotype of the plant investigated, but also by interactions between these two variables.

These data clearly demonstrate that different ecotypes have different $UVR8^{dimer}/UVR8^{monomer}$ ratio with respect to UV-B. There are many different abiotic factors that could potentially affect the $UVR8^{dimer}/UVR8^{monomer}$ ratio including total UVR8 production. The effect of a range of photoperiodic, long term UV-B treatments on plant morphology should also be investigated.

3.5 RUP1 and RUP2 affect the rate of monomerisation in UV-B naïve *A. thaliana* plants.

The rate of monomerisation of UVR8 is very clear in purified protein (Chapter 4). *In planta* it is extremely rare to see the 100% monomerisation that is seen *in vitro* or even in extract. For each of the three biological repeats three blocks of nine plates were sown to determine whether the position within the growth room affected the monomerisation. The lme4 package within R was used to determine whether growth room position had a siginificant effect (UVR8 Monomer % = Intercept + ε, where ε is the random factor; UVR8 Monomer is only affected by the random position within the room). As no effect was found, each block could be considered a separate repeat (n=9).

The rate of monomerisation and how the RUPs affect this rate was investigated in 10 day old, UV-B naïve plants in L*er*, Col-0 and *rup1rup2* mutants. Seeds were sterilised to ensure no contamination by competing fungi or bacteria and were grown on ½ MS plates for 10 days in 120 μmol m^{-2} s^{-1} white light. The lids of the plates were removed and the plants were exposed to 3.0 μmol m^{-2} s^{-1} UV-B for two hours. Plants were harvested randomly from within each block before the UV-B treatment, immediately after the UV-B treatment and then at 15 minute intervals for the duration of the timecourse. Samples were snap frozen in liquid nitrogen before being processed and stored for a maximum of seven days. The level of monomer was measured via semi-native Western blot and the blot quantified using ImageJ (Fig 3-5).

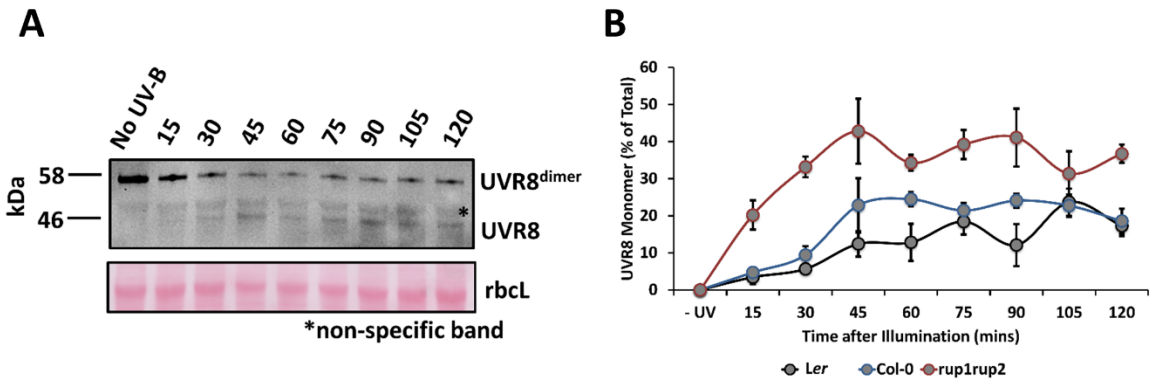

Fig 3-5: The rate of UVR8 monomerisation in L*er*, Col-0 and *rup1rup2* at a constant fluence rate of UV-B. 10 day old, UV-B naïve L*er*, Col-0 and *rup1rup2* plants were exposed to 3.0 µmol m^{-2} s^{-1} UV-B for two hours. Samples were harvested prior to UV-B exposure and then every 15 minutes following light switch on. Protein extract from the plants was run on a non-boiled SDS-PAGE and UVR8 was identified using immunoblotting. Dimer to monomer ratio was calculated using ImageJ. (**A**) A representative Western Blot showing both UVR8 dimer and UVR8 monomer. rbcL was used as a loading control. (**B**) A quantified graph of UVR8 monomerisation over time for L*er*, Col-0 and *rup1rup2* showing standard error (n=9).

The rate of monomerisation in L*er* varied throughout the first 45 minutes of exposure to UV-B (Fig 3-5B). After 45 minutes there was no increase in the overall amount of monomer, with monomer levels fluctuating between 12% and 23%. Complete monomerisation was never seen.

Col-0 had a similar pattern of monomerisation. From 45 minutes onwards the level of UVR8 monomer did not change and remained steady between 22% and 24%.

The *rup1rup2* mutants demonstrated a different result, although they too only showed an increase in UVR8 monomer levels during the first 45 minutes of UV-B exposure. After 45 minutes the level of monomer remained between 34% and 42%. The *rup1rup2* mutant plants showed a faster monomerisation rate and a higher stable level of monomer after exposure to UV-B than either L*er* or Col-0.

3.6 Long term, photoperiodic UV-B treatment causes changes to plant morphology

There is a clear difference in the UVR8 photoequilibrium based upon several different factors including the UV-B treatment given and the ecotype of *A. thaliana* studied. The RUP proteins have also been shown to affect the $UVR8^{dimer}/UVR8^{monomer}$ ratio. These results raise several questions. Firstly could the total amount of UVR8 explain the variability between ecotypes? Studies looking at variation within *A. thaliana* have found that variation between

ecotypes can be explained by differences in protein sequence (Maloof, *et al*. 2001), but that differences in total protein composition also exist, for example between Col-0 has 111 genes that are entirely deleted or truncated in L*er* (Koorneef, *et al*. 2004). Alternatively, what effect does UVR8 and RUP amount have on the physiology of UV-B acclimated plants and does the ability to form a dimer affect the growth of UV-B acclimated plants?

UVR8 protein levels are not affected by light treatments (Kaiserli and Jenkins, 2007). However, this does not mean that UVR8 protein levels do not vary between different ecotypes of *A. thaliana* (Koorneef, *et al*. 2004). Work investigating the regenerative capabilities of the $UVR8^{dimer}$ have shown that for the highest rate of regeneration *de novo* protein synthesis is required (Heijge and Ulm, 2013 and Heilmann and Jenkins, 2013). While Heijge and Ulm, (2013) showed that the increase in regeneration rate was most likely due to *de novo* production of RUP proteins, a difference in total UVR8 protein amount could lead to a difference in the $UVR8^{dimer}$/$UVR8^{monomer}$ ratio.

The levels of UVR8 within several accessions of *A. thaliana* (L*er*, Col-0, Edi-0, Kas-1 and Shakdara) were compared to *rup1rup2*, *uvr8-1* and $UVR8^{D96ND107N}$ mutants. The *rup1rup2* mutant was chosen as it is a null mutant for the RUPs which are involved in UVR8 dimer regeneration. The *uvr8-1* mutant was used as it is a null UVR8 mutant. The $UVR8^{D96ND107N}$ mutant is a constitutive monomer which was used to determine whether the dimer plays a role in function. The plants were grown for 21 days in a 12 hour light/dark cycle with 120 µmol m^{-2} s^{-1} and 3.0 µmol m^{-2} s^{-1} supplementary UV-B. Samples were harvested at the midpoint of the light cycle and immediately processed for protein extraction. The total UVR8 amount was analysed by Western Blot and immunodetection and quantified using ImageJ (Fig 3-6). L*er* samples were chosen to have a relative density of 1.0 (Fig 3-6B). The *uvr8-1* plants were a negative control as they do not contain UVR8 protein.

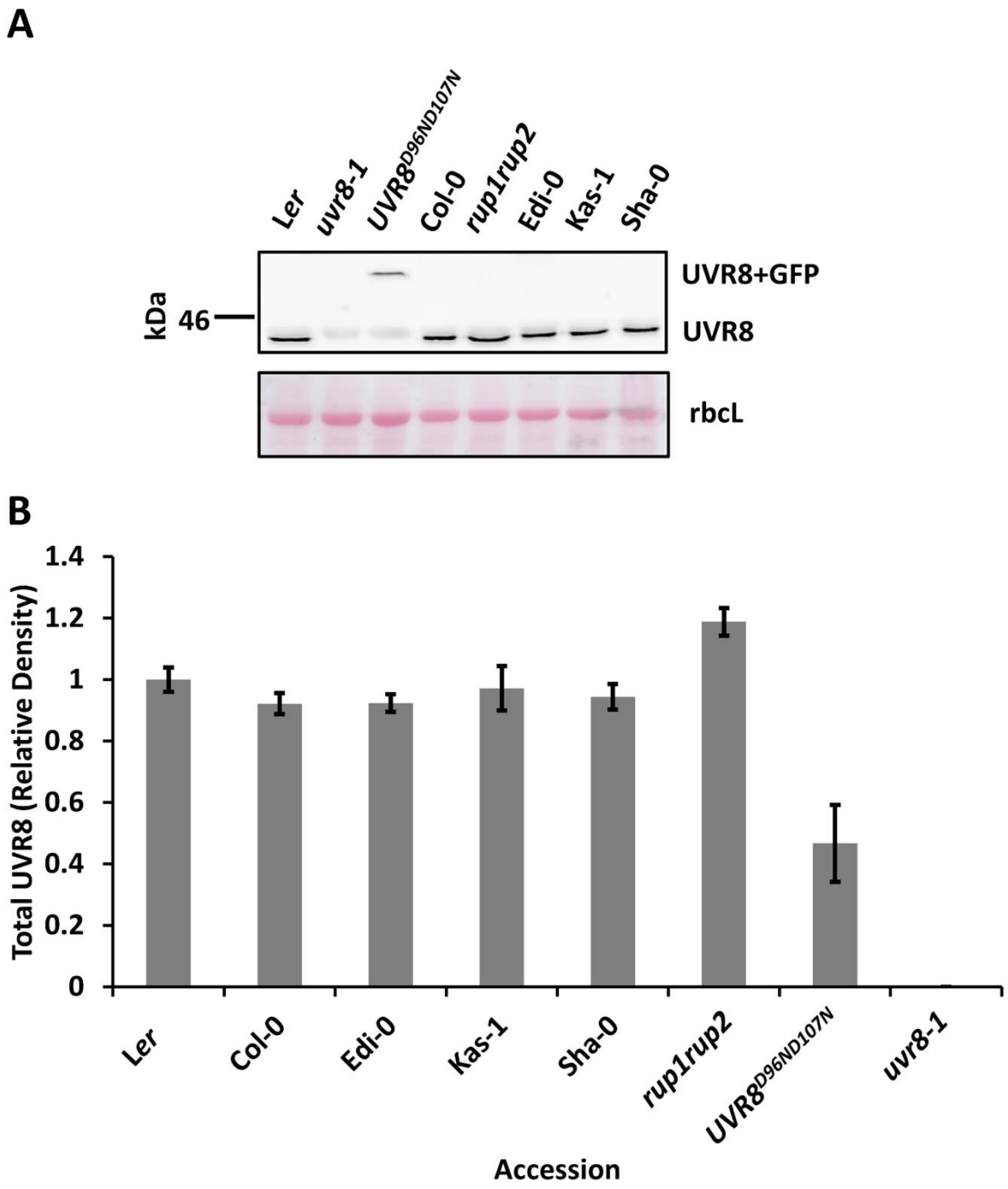

Figure 3-6: The total UVR8 amount in various *A. thaliana* ecotypes and mutants. L*er*, Col-0, Edi-0, Kas-1, Sha-0, *rup1upr2*, *uvr8-1* and UVR8^{D96ND107N} plants were grown for 21 days in a 12 hour light/dark cycle with 3.0 µmol m^{-2} s^{-1} supplementary UV-B. Samples were harvested at the midpoint of the light cycle. Samples were analysed by Western Blot via immunodetection and protein levels were controlled and normalised using rbcL levels. The total level of UVR8 was quantified using imageJ. (A) An example boiled Western Blot showing the total amount of UVR8 protein from the various ecotypes and mutants and Ponceau stain used to normalise protein levels. (B) Quantification of the total level of UVR8 in L*er*, Col-0, Edi-0, Kas-1, Sha-0, *rup1rup2* and *uvr8-1*; and the total UVR8-GFP levels in UVR8^{D96ND107N}. The L*er* samples were chosen to have a relative density of 1.0. The data shown is mean protein amount $\pm$ S.E (n=3).

ANOVA analysis determined that L*er* did not have a significantly different total amount of UVR8 to any of the wild-type accessions (p=0.0641, p=0.0677, p=0.1856, p=0.1043 for Col-0, Edi-0, Kas-1 and Shakdara respectively). The *rup1rup2* mutant also showed no significant difference in total UVR8 amount to L*er* (p=0.2512) while the UVR8^{D96ND107N} mutant has significantly less (p=1.52e^{-06}).

This pattern was similar for Col-0. There is no significant difference between Col-0 and any of the wild-type plants for total UVR8 amount (p=0.97733, p=0.55324 and p=0.79324 for Edi-0, Kas-1 and Shakdara respectively). Similarly, Col-0 had significantly more total UVR8 than the *UVR8^{D96ND107N}* mutant (p=5.84e^{-05}). On the other hand, Col-0 did show significantly less total UVR8 compared to the *rup1rup2* mutant (p=0.00582).

Edi-0 did not have a significantly different total UVR8 amount to either Kas-1 or Shakdara (p=0.5721 and p=0.8152 respectively). However, like Col-0 it did have significantly less UVR8 than the *rup1rup2* mutant (p=0.00619). Similarly the *UVR8^{D96ND107N}* mutant had less total UVR8 than Edi-0 (p=5.52e^{-05}).

Kas-1 and Shakdara were not significantly different it terms of total UVR8 (p=0.7389). Both had significantly less total UVR8 than the *rup1rup2* mutant (p=0.02040 and p=0.0102 for Kas-1 and Shakdara respectively) and more total UVR8 than the *UVR8^{D96ND107N}* mutant (p=1.82e^{-05} and p=3.47e^{-05} for Kas-1 and Shakdara respectively).

Comparing the mutant lines to one another showed that the *rup1rup2* mutant had significantly more total UVR8 than the *UVR8^{D96ND107N}* mutant (p=2.20e^{-07}). No UVR8 was observed for the *uvr8-1* mutant as expected. It was interesting to note that the *rup1rup2* mutant plants had more total UVR8 than was seem in their background line Col-0. The RUP proteins are involved in the negative regulation of the UV-B photomorphogenic pathway. While UVR8 was not drastically upregulated in the *rup1rup2* plants (1.2x upregulation), it was possible that lack of negative regulation has resulted in a slightly increased UVR8 amount.

In order to determine the effect that UVR8 and RUP amount have on the physiology of UV-B acclimated plants and how the ability to form a dimer affects the growth of UV-B acclimated plants two wild-type accessions (L*er* and Col-0);

two mutants that affect UVR8 amount (*uvr8-1* which is a null mutant and 35S GFP-UVR8OX in a WT background which overexpresses UVR8 to 4x the WT level (Heilmann, communication); a constitutively monomeric UVR8 mutant (*UVR8^{D96ND107N}*); and a mutant with hindered UVR8^{dimer} regenerative capabilities (*rup1rup2* which lacks both RUP proteins) were grown under photoperiodic long term UV-B conditions for 21 days.

For each of the six biological repeats three blocks of twelve pots of plants were sown to determine if position within the growth room affected the morphology of the plants. The fresh and dry weight as well as the rosette area was calculated for plants within each block and each repeat. The lme4 package within R was used to determine the significance of growth room position on all three of these traits (Fresh Weight/Dry Weight/Leaf Area = Intercept + ε, where ε is the random effect of placement within the room and either fresh weight, dry weight or leaf area was only affected by that random factor). Placement within the room was not found to effect any of the three measurements therefore each block could be considered a separate repeat (n=18).

The six different ecotypes and mutants were sown on soil, saturated with intercept to stop insect herbivory and grown under a 12 hour light/dark cycle with either zero, 0.3 μmol m^{-2} s^{-1}, 1.0 μmol m^{-2} s^{-1} or 3.0 μmol m^{-2} s^{-1} supplementary UV-B for 21 days. Samples were harvested at the light cycle midpoint and treated in one of two ways. The first set of samples (five plants without roots in each sample) were weighed in a boat of known weight immediately before being dried overnight at 50°C and weighed a second time in the same boat in order to measure fresh and dry weight of the plants. The second set of samples (one rosette per sample) were dissected, scanned and the total leaf rosette area was quantified using Image J.

Generally the zero UV-B grown plants had the highest fresh weight (Fig 3-7). The fresh weight was lower in 0.3 μmol m^{-2} s^{-1} UV-B grown plants but showed no further drop or only a slight decrease in fresh weight with the increase to 1.0 μmol m^{-2} s^{-1} UV-B. There was then a further dramatic drop in fresh weight, with

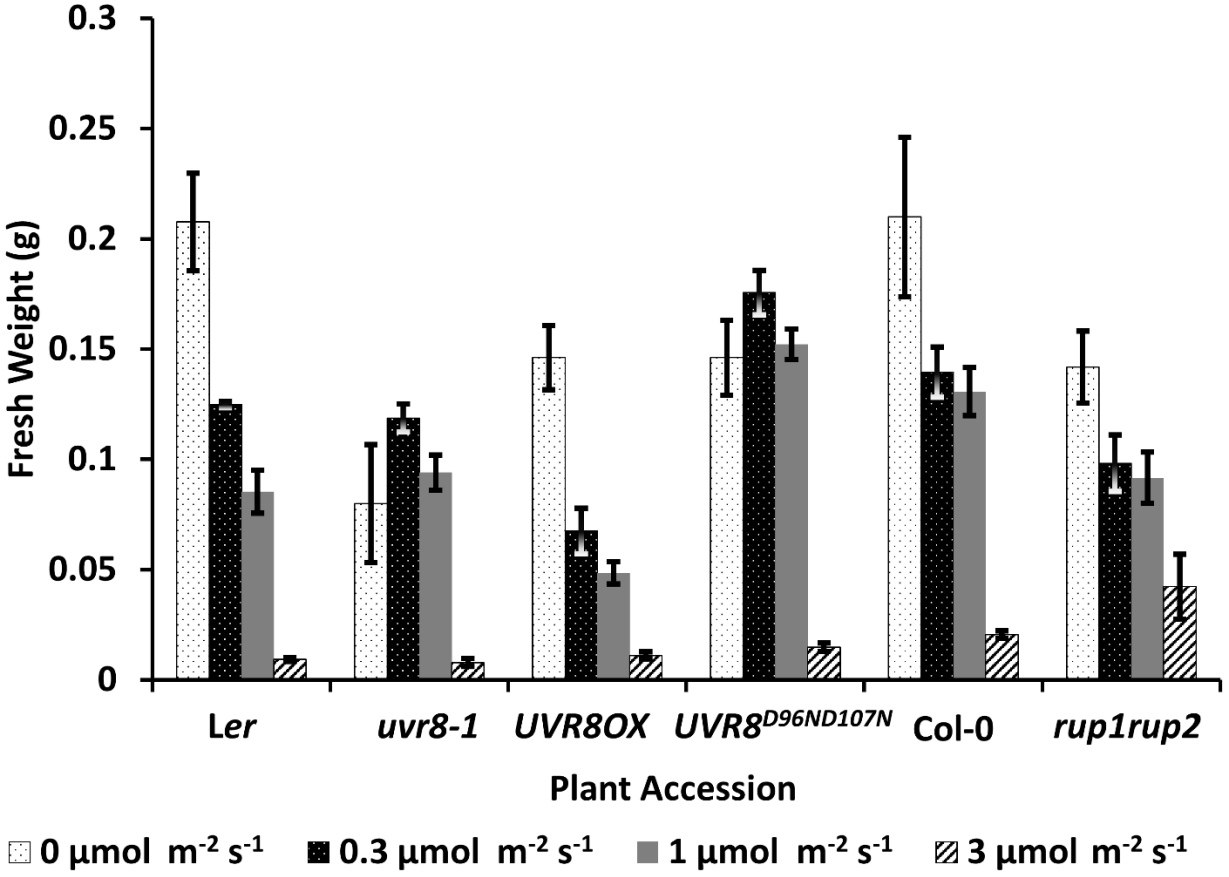

Figure 3-7: A comparison of the effect that various *A. thaliana* ecotypes, mutants and UV-B treatments have on the fresh weight of the plants. L*er*, *uvr8-1*, UVR8OX, UVR8^{D96ND107N}, Col-0 and *rup1rup2* plants were grown for 21 days in a 12 hour light/dark cycle with either 3.0 µmol m^{-2} s^{-1} 1.0 µmol m^{-2} s^{-1}, 0.3 µmol m^{-2} s^{-1} supplementary UV-B or with no supplementary UV-B. Plants were harvested at solar noon, five plant shoots were weighed together and the mean taken for each sample. A comparison of the effect of UV-B treatment on the fresh weight of L*er*, *uvr8-1*, UVR8OX, UVR8^{D96ND107N}, Col-0 and *rup1rup2* plants grown with 120 µmol m^{-2} s^{-1} white light and either 3.0 µmol m^{-2} s^{-1}, 1.0 µmol m^{-2} s^{-1}, 0.3 µmol m^{-2} s^{-1} supplementary UV-B or with no supplementary UV-B. The data shown is the mean weight $\pm$ S.E (n=18).

the 3.0 µmol m^{-2} s^{-1} grown plants having the lowest fresh weight of all the growth conditions. The exceptions to this pattern were the *uvr8-1* and *UVR8*^{D96ND107N} plants. Within these plants a slight increase in fresh weight was seen between the zero UV-B and 0.3 µmol m^{-2} s^{-1} UV-B growth conditions. The fresh weight of the 1.0 µmol m^{-2} s^{-1} UV-B plants was similar to that of the zero UV-B grown plants in both of these mutants. However, the dramatic drop in fresh weight under 3.0 µmol m^{-2} s^{-1} UV-B was still observed.

To determine whether the fresh weight of the plant was better described by UV-B or ecotype, GLM was performed. The first model hypothesised that fresh weight was only affected by UV-B: Fresh Weight = UV-B Fluence Rate, where Fresh Weight was treated as a continuous variable and UV-B Fluence Rate as a factorial variable (zero, low, medium and high UV-B fluence rate). This model was significant ($p=<2e^{-16}$). The second model posited that the fresh weight was only affected by ecotype: Fresh Weight = Ecotype, where Fresh Weight was treated as a continuous variable and Ecotype as a factorial variable. This model was also highly significant ($p=<2e^{-}16$). Therefore to determine which model should be the null model, AIC was compared. The model that stated that fresh weight was affected by only UV-B was a better fit by this criteria and was therefore chosen as the null hypothesis.

As can be seen both UV-B fluence rate and accession had an effect on the fresh weight of the plant. GLM was used to determine whether these factors may be interacting. To determine which model had the best fit the drop1 function in R was used. This compares more complex models with simpler models by dropping one interaction or variable at a time to a predetermined limit. The most complex model used was that Fresh Weight = UV Fluence Rate + Accession + UV-B Fluence Rate*Ecotype, where Fresh Weight was treated as a continuous variable and both UV-B Fluence rate and Ecotype were treated as factorial variables. This model was indeed the best fit for the data, indicating that fresh weight was affected by both UV-B fluence rate, the plant accession and the interaction between these two factors.

Once again, the plants grown under zero UV-B have the highest dry weight (Fig 3-8). There was a small decrease in dry weight under 0.3 µmol m^{-2} s^{-1} UV-B conditions and no change between 0.3 µmol m^{-2} s^{-1} UV-B and 1.0 µmol m^{-2} s^{-1} UV-B. There was a final drop in dry weight under 3.0 µmol m^{-2} s^{-1} UV-B. There were two ecotypes that do not follow this general pattern. The first was the *UVR8*^{D96ND107N} mutant. The dry weight under zero UV-B and 1.0 µmol m^{-2} s^{-1} UV-B conditions were comparable. However, under 0.3 µmol m^{-2} s^{-1} UV-B growth conditions, the mean dry weight was higher and far more variability was observed. As with the majority of the other ecotypes, there was a drop in dry weight under the 3.0 µmol m^{-2} s^{-1} UV-B growth conditions. The other ecotype that does not follow the general pattern was the *rup1rup2* mutant. Within these plants there was no change in dry weight between the zero, 0.3 or 1.0 µmol m^{-2} s^{-1} UV-B grown plants. While there was a drop in dry weight under 3.0 µmol m^{-2} s^{-1} UV-B, these plants had a far larger dry weight than the other ecotypes.

Again, when determining what variable should be used for the basis of the null model for dry weight two different models were fitted to the data using R. The first hypothesised that dry weight was only affected by UV-B: Dry Weight = UV-B Fluence Rate, where Dry Weight was treated as a continuous variable and UV-B Fluence Rate as a factorial variable. This model was significant when compared to the intercept via a Chi-Squared test ($p=<2e^{-16}$). The second model fitted was that dry weight was only affected by ecotype: Dry Weight = Ecotype, where Dry Weight was treated as a continuous variable and Ecotype as a factorial variable. This was also a significant model when compared to the intercept by Chi-Squared test ($p=<2e^{-16}$). Therefore the AIC value was used to determine which model had the best fit. The model that best described the data, and was therefore chosen as the null model was that the dry weight was only affected by the UV-B fluence rate.

To determine whether an additive or interactive effect between the UV-B fluence rate and ecotype would better fit the data the drop1 command within R was used. This compares simpler and more complex models via the Chi-Squared test to find the best fit, more complex models are penalised to avoid over-fitting the model as generally the more complex the model, the better the fit of data.

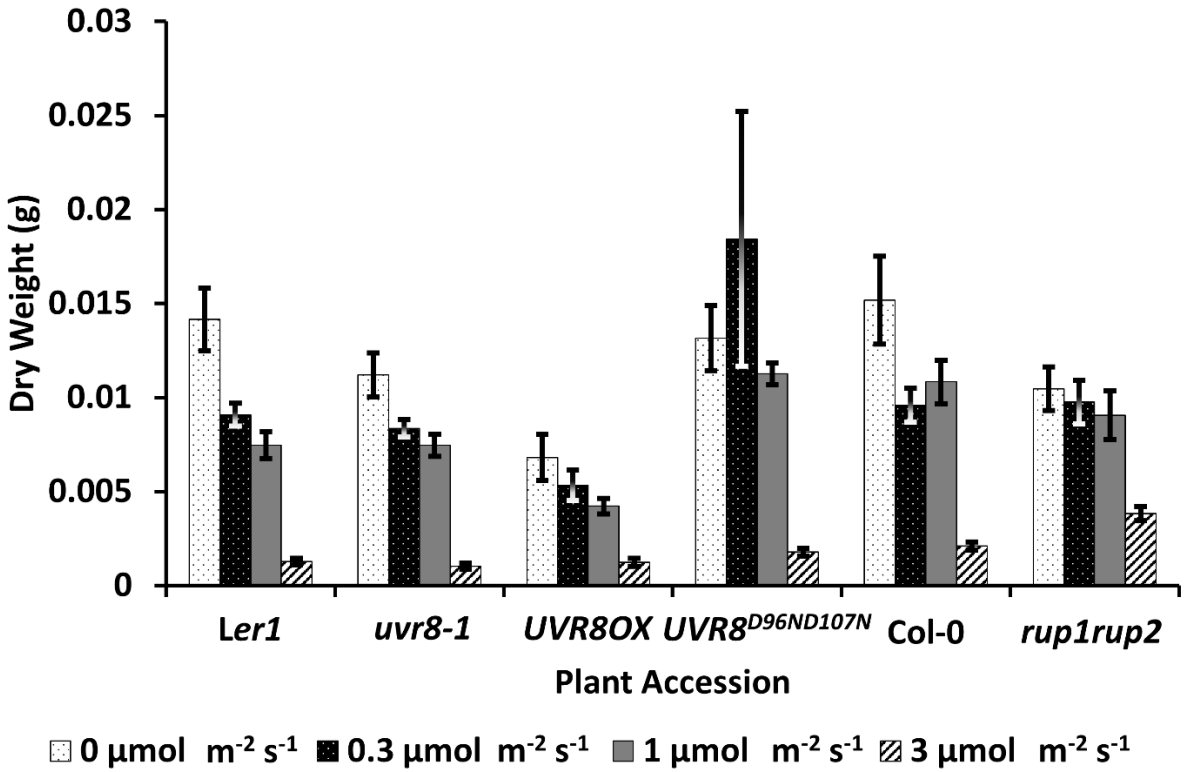

Figure 3-8: : A comparison of the effect that various *A. thaliana* ecotypes, mutants and UV-B treatments have on the dry weight of the plants. L*er*, *uvr8-1*, UVR8OX, UVR8^{D96ND107N}, Col-0 and *rup1rup2* plants were grown for 21 days in a 12 hour light/dark cycle with 120 µmol m^{-2} s^{-1} white light and either 3.0 µmol m^{-2} s^{-1} 1.0 µmol m^{-2} s^{-1}, 0.3 µmol m^{-2} s^{-1} supplementary UV-B or with no supplementary UV-B. Plants were harvested at solar noon, before being dried overnight at 50°C. Five plant shoots were weighed together and the mean taken for each sample. A comparison of the effect of UV-B treatment on the dry weight of L*er*, *uvr8-1*, UVR8OX, UVR8^{D96ND107N}, Col-0 and *rup1rup2* plants grown with 120 µmol m^{-2} s^{-1} white light and either 3.0 µmol m^{-2} s^{-1}, 1.0 µmol m^{-2} s^{-1}, 0.3 µmol m^{-2} s^{-1} supplementary UV-B or with no supplementary UV-B. The data shown is the mean weight $\pm$ S.E. (n=18).

The most complex model was defined as Dry Weight = UV-B Fluence Rate + Ecotype + UV-B Fluence Rate*Ecotype, where Dry Weight was treated as a continuous variable and both UV-B Fluence rate and Ecotype were treated as factorial variables. This model was the best fit for the data therefore the dry weight was affected by both UV-B fluence rate, the ecotype of the plant and the interaction between these two factors.

There was a different pattern for leaf area than either fresh or dry weight (Fig 3-9). There was an increase in total leaf area from zero UV-B to 0.3 UV-B μmol m^{-2} s^{-1} UV-B treated plants. There was then a decrease and the 1.0 μmol m^{-2} s^{-1} UV-B treated plants were similar in area to the zero UV-B treated plants. As with the fresh and dry weight, leaf area was reduced under 3.0 μmol m^{-2} s^{-1} UV-B conditions. There were two ecotypes that did not follow this pattern, the *UVR8*^{D96ND107N} and the *rup1rup2* mutanst. Both of these types had relatively high leaf area that did not change between the zero, 0.3 μmol m^{-2} s^{-1} UV-B or the 1.0 μmol m^{-2} s^{-1} UV-B treated plants. While there was a decrease in leaf area for both these ecotypes under μmol m^{-2} s^{-1} UV-B conditions, this reduction was smaller than the other ecotypes.

As with the fresh and dry weight data, a null model was required. The first model fitted was that total leaf area was only affected by UV-B: Leaf Area = UV-B, where Leaf Area was treated as a continuous variable and UV-B was treated as factorial variable. This model was significant ($P=<2e^{-16}$). The second model was fitted so that total leaf area was only affected by ecotype: Leaf Area = UV-B, where Leaf Area was treated as a continuous variable and Ecotype was treated as a factorial variable. This model was also significant ($p=2.885e^{-07}$). Therefore the model that fitted leaf area as only affected by UV-B was chosen as the null model.

To determine whether there was additive or interactive effects between UV-B fluence rate and ecotype on leaf area, further modelling was performed. The drop1 function was used to quickly define and compare models from more to less complex. The most complex model defined was that the leaf area was affected by the UV-B fluence rate, the ecotype of the plant and the interaction between

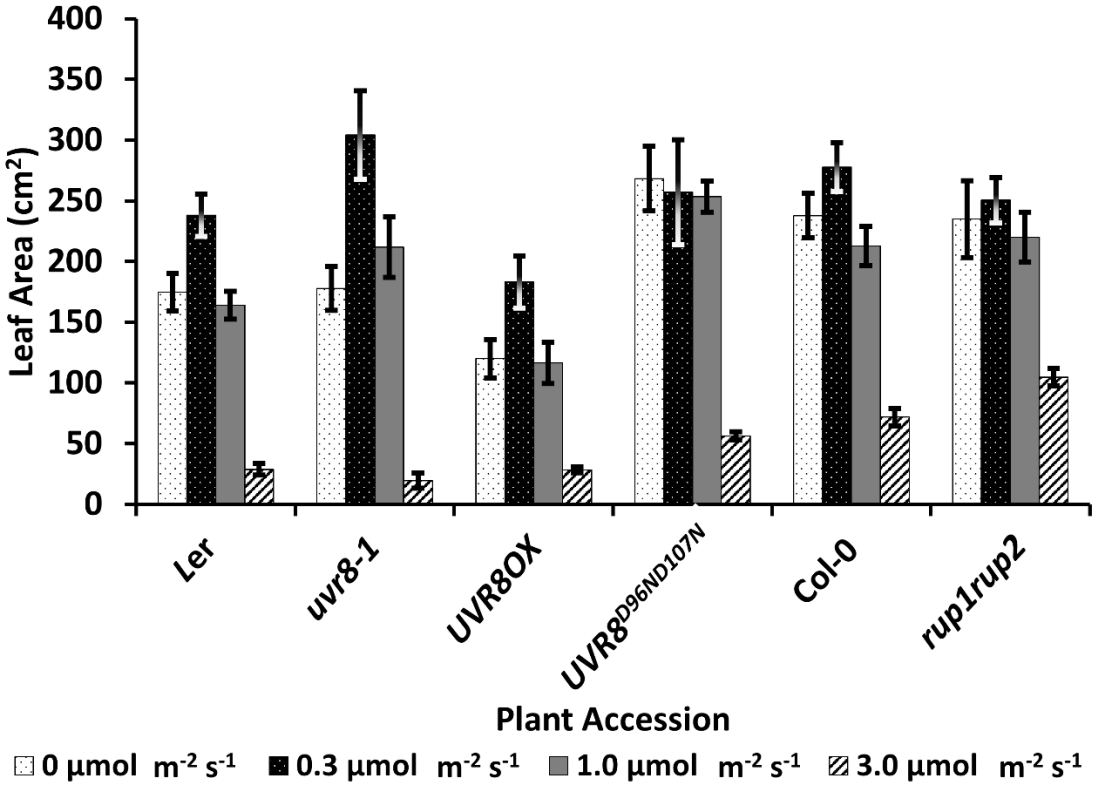

Figure 3-9: A comparison of the effect that various *A. thaliana* ecotypes, mutants and UV-B treatments have on the leaf area of the plants. L*er*, *uvr8-1*, UVR8OX, UVR8^{D96ND107N}, Col-0 and *rup1rup2* plants were grown for 21 days in a 12 hour light/dark cycle with 120 µmol m^{-2} s^{-1} white light and either 3.0 µmol m^{-2} s^{-1} 1.0 µmol m^{-2} s^{-1}, 0.3 µmol m^{-2} s^{-1} supplementary UV-B or with no supplementary UV-B. Plants were harvested at solar noon, each plant was dissected and the leaves affixed to a white background for measurement. Leaf area measurement was completed through imageJ. A comparison of the effect of UV-B treatment on the leaf area of L*er*, *uvr8-1*, UVR8OX, UVR8^{D96ND107N}, Col-0 and *rup1rup2* plants grown with 120 µmol m^{-2} s^{-1} white light and either 3.0 µmol m^{-2} s^{-1}, 1.0 µmol m^{-2} s^{-1}, 0.3 µmol m^{-2} s^{-1} supplementary UV-B or with no supplementary UV-B. The data shown is the leaf area $\pm$ S.E. (n=18).

these two factors: Leaf Area = UV-B Fluence Rate + Ecotype + UV-B Fluence Rate*Ecotype, where the Leaf Area was treated as a continuous variable and the Ecotype and UV-B Fluence Rate were threated as factorial variables. This model best fitted the data, therefore the leaf area was affected by both the UV-B fluence rate, the ecotype and the interaction between these factors.

3.7 Discussion

The current model of UVR8 monomerisation and regeneration (Fig 3-1) is too simplistic to describe the kinetics of the UV-B photoreceptor within plants that have been exposed to photoperiodic, long term UV-B. In leaf extract, yeast and protein purification systems UVR8 exists as a dimer in zero UV-B conditions and rapidly monomerises in response to UV-B (Christie, *et al*. 2012, Huang, *et al*. 2014, Rizzini, *et al*. 2011 and Wu, *et al*. 2012). Regeneration of the $UVR8^{dimer}$ in these conditions requires both the RUP proteins and the exclusion of UV-B light (Heijge and Ulm, 2013, Heilmann and Jenkins, 2013). These data clearly show that the model has to be updated.

3.7.1 UVR8 does not act as a simple UV-B switch

When plants were acclimated to an ecologically relevant dose of UV-B light their photoreception of UV-B light changes. UVR8, rather than acting as a simple $UVR8^{dimer}$ to $UVR8^{monomer}$ on/off switch, formed a mix of both $UVR8^{dimer}$ and $UVR8^{monomer}$ establishing a photoequilibrium (Fig 3-2 and Fig 3-4). It can be clearly seen that plants grown in a zero UV-B environment did not show a substantial degree of UVR8 monomerisation, in keeping with the current model that under zero UV-B conditions UVR8 forms a dimer and no UV-B protective signalling occurs (Christie, *et al.*, 2012, Rizzini, *et al*. 2011, Wu *et al.*, 2012, Miyamori, *et al*. 2015). However under long term UV-B treatments, while UVR8 monomerisation does occur, there was also $UVR8^{dimer}$ present. Frequently, $UVR8^{monomer}$ was seen before the light cycle begins and therefore before exposure to UV-B has occurred. Furthermore, regeneration of the $UVR8^{dimer}$ was observed in the presence of UV-B. This would suggest that UVR8 behaves differently in UV-B naïve plants and UV-B acclimated plants.

3.7.2 Several factors affect the UVR8 photoequilibrium

In order to determine which elements of the growth conditions were affecting the UVR8 photoequilibrium, generalised linear modelling was used for statistical analyses. There are several clear advantages to using this system. These include the ability of generalised linear modelling to cope with a conjunction of numeric and factorial influences and to model the interaction of multiple influences. Generalised linear modelling also allows for random factors to be built into a model, which can account for truly random differences in sample collection. There are drawbacks to any statistical system used and in the case of generalised linear modelling there is an overall trend for more complex models having better fit, to the detriment of predictive powers. This can be addressed with the use of log likelihood ratio tests and AIC tests which can be used to assess which model balances both predictive power and descriptive power.

There was clear statistical evidence that the UVR8 photoequilibrium was affected by several factors. In the absence of UV-B no photoequilibrium was formed (Fig 3-2 and Fig 3-4). This was to be expected. As indicated by previous studies (Brown and Jenkins, 2008) UVR8 was responsive at extremely low fluence rates, with the majority of 0.3 μmol m^{-2} s^{-1} timecourses having more $UVR8^{monomer}$ throughout the day than a zero UV-B control.

When larger fluence rates of UV-B were given, the change in UVR8 photoequilibrium was not consistent between ecotypes. Although as UV-B fluence rate increased $UVR8^{dimer}$ levels decreased, the different ecotypes showed different UV-B saturation points, after which further increases in UV-B fluence rate did not result in further monomerisation. This lead to the second observation that *A. thaliana* accession has a significant effect on the final balance of the UVR8 photoequilibrium which interacted with the UV-B level. This is especially clear when looking at the ecotypes found at high altitudes (Fig 3-4). The UVR8 photoequilibrium observed at 0.3 μmol m^{-2} s^{-1} UV-B for both Kas-1 and Shakdara was not significantly different to the zero UV-B control, while the medium and high UV-B treatments showed significant reductions in $UVR8^{dimer}$. This lead to the conclusion that the accessions found at higher altitudes required

a higher UV-B fluence rate to see the same degree of monomerisation seen in accessions from lower altitudes.

As would be expected the presence of the RUP proteins affects the $UVR8^{dimer}$/$UVR8^{monomer}$ ratio. It has been previously reported that the RUP proteins are essential for optimal $UVR8^{dimer}$ regeneration rate (Heidge and Ulm, 2013, Heilmann and Jenkins, 2013). As can be seen from Fig 3-2D and Fig 3-2E the *rup1rup2* mutants have a significantly lower proportion of $UVR8^{dimer}$, although a $UVR8^{dimer}$/$UVR8^{monomer}$ ratio was still apparent. This would suggest that regeneration is a key factor in maintaining the UVR8 photoequilibrium, but that even the absence of the RUP proteins in UV-B acclimated plants was not sufficient to force a complete $UVR8^{dimer}$»$UVR8^{monomer}$ rapid switch to occur.

3.7.3 The photoequilibrium of UVR8 is not circadian regulated

It was observed that $UVR8^{monomer}$ was present before the onset of the light cycle in almost all of the plus UV-B timecourses (Fig 3-3, Fig 3-3 and Fig 3-4). While this trend is not seen in the zero UV-B control, there is the potential that after being initially primed with UV-B light the photoequilibrium of UVR8 could be directly regulated by the circadian clock. However, time of sample collection did not appear to be a determining factor in $UVR8^{dimer}$/$UVR8^{monomer}$ photoequilibrium. In order to address this issue a timecourse that covered the dark cycle for UV-B acclimated plants was performed. If the $UVR8^{dimer}$/$UVR8^{monomer}$ was regulated in a circadian manner it was expected that UVR8 would regenerate to 100% dimer over the course of the night and pre-emptively begin monomerisation before the onset of the light cycle. It became clear from Fig 3-3 that this was not the case. UVR8 was slow to regenerate to dimer during the dark cycle and never regenerated completely to 100% dimer. In all cases the highest level of $UVR8^{dimer}$ was seen at the time point immediately prior to the light cycle. These data combined with the lack of correlation between time and UVR8 photoequilibrium demonstrated that the UVR8 photoequilibrium was not circadian regulated.

3.7.4 The RUP proteins affect the accumulation of $UVR8^{monomer}$ in UV-B naïve plants

As it had been shown that the $UVR8^{dimer}$/$UVR8^{monomer}$ ratio was affected by several factors including the RUP proteins, the effect of the RUP proteins on

monomerisation in UV-B naïve plants was also measured. While there was no appreciable difference in the monomerisation rate between Col-0 and L*er*, there was difference between either of the two wild-type ecotypes and the *rup1rup2* mutant line.

The *rup1rup2* mutant line maintained a higher level of monomer than either of the two WT plants. This was likely not due to any differences in basal monomerisation rate, but rather that the amount of $UVR8^{monomer}$ that accumulates in the *rup1rup2* mutant was higher due to the slower regeneration rate caused by lack of RUP proteins. Interestingly, even in UV-B naïve plants complete monomerisation of UVR8 was not seen. Indeed, all three lines of *A. thaliana* maintained appreciable dimer pools. This would suggest that even in naïve conditions, the fluence rate of UV-B needed to completely monomerise UVR8 is extremely high. For example, in order to completely monomerise UVR8 to measure the rate of regeneration, 21 μmol m^{-2} s^{-1} UV-B is required, 7 times the fluence rate of the high UV-B treatments used in controlled growth conditions (Heijdge and Ulm, 2013, Heilmann and Jenkins, 2013).

3.7.5 Plant morphology is affected by both the total UVR8 amount and the conformation of available UVR8

It has already been shown that UV-B treatment affects plant morphology and physiology (Carbonell-Bejerano, *et al.*, 2014, Wargent, *et al.*, 2014, Ballaré, *et al.*, 2012, Hectors, *et al.*, 2007, Morales, *et al.* 2013). While studies investigating the effect of the presence or absence of UVR8 and the RUPs on plant photomorphogenesis and UV-B stress tolerance (Hayes, *et al.* 2014, Favory, *et al.*, 2009, Gruber, *et al.* 2010, Kliebenstein, *et al.*, 2002, Robson, *et al.* 2015, Tilbrook, *et al.*, 2013, Tossi, *et al.*, 2014, Vandenbussche, *et al.*, 2014, Wang, *et al.*, 2011) or whether UVR8 monomerisation alone is sufficient for UV-B photomorphogenesis (Huang, *et al.*, 2014, O'Hara and Jenkins, 2012); the effect of total UVR8 amount and the effect of the conformation of available UVR8 upon plant growth has not been investigated.

As can be seen in Fig 3-6, total UVR8 amount did not change significantly between ecotypes. This would suggest that the differences in UVR8 photoequilibrium were not due to differences in the total available UVR8. There

were several other factors that could cause the differences between the ecotypes. The role a genetic component could play is investigated within Chapter 5 of this thesis.

Both the *rup1rup2*, *uvr8-1* and UVR8^{D96NS107N} mutants displayed a significant different in total UVR8 amount. The *uvr8-1* mutant is a UVR8 null mutant and no UVR8 was detected as expected. The UVR8^{D96ND107N} mutant is a constitutive monomer and had significantly less UVR8 present than wild-type plants. These plants are not expressing UVR8 under a native promotor, instead utilising the 35s promotor. However, while a change in UVR8 levels was expected here, it was expected that the levels of UVR8 would be higher rather than lower due to the promotor used. It could be that genetic silencing has played a role. Furthermore, only one UVR8^{D96ND107N} line was used in this study, this is a transgenic line so the levels of GFP-UVR8 is determined by the 35S promotor and will vary between lines. The *rup1rup2* mutant plants on the other hand had significantly more UVR8 available than wild-type plants. As the RUPs are negative regulators of UVR8, it could be that they are also involved in regulating the total protein amount as well as the regeneration to dimer.

When investigating the role of UV-B on plant growth there was a general reduction in both fresh and dry weight with an increase in UV-B. However, leaf area saw an initial increase in size with increases in UV-B followed by a reduction in size as UV-B continued to increase.

In comparison, ecotype had a more complex effect. While the two wild-type accessions studied had no significant difference in fresh weight or dry weight, L*er* plants had a smaller leaf area than Col-0. This would suggest that these plants distribute resources in a differential manner. The *uvr8-1* mutant did not show a significant difference in size, fresh or dry weight compared to the L*er* mutant, however the *UVR8OX* was significantly smaller and lighter in both fresh and dry weight to L*er*. The *rup1rup2* mutant had a lower fresh weight than Col-0, but did not differ for either dry weight or leaf area. The UVR8^{D96ND107N} mutant was only larger in leaf area to L*er*, otherwise it showed no difference to the wild-type. These data suggest that there was not a simple linear correlation

between growth and UVR8 amount, nor between degree of monomerisation and growth. While an increase in UVR8 amount resulted in a significant decrease in fresh and dry matter accumulation and leaf area, the UVR8 null mutant was not different to the wild-type plants. Furthermore, both plant types with a higher proportion of $UVR8^{monomer}$ do not share growth traits. The constitutively monomeric mutant was larger than the wild-type, but the mutant hindered in $UVR8^{dimer}$ regeneration was smaller. This would suggest that it was not purely UVR8 amount or degree of monomerisation that was important to plant morphology but that the $UVR8^{dimer}$ also plays an as yet undefined role.

3.8 Conclusions

UVR8 is not a simple photoreceptor switch. Instead it forms a photoequilibrium with a ratio of $UVR8^{dimer}/UVR8^{monomer}$. This ratio is affected by several factors including the fluence rate of UV-B, the plant ecotype and the presence of the RUP proteins. The UVR8 photoequilibrium is not affected by the time of day and does not begin to monomerise before the onset of the light cycle. However, these results were all gained in extremely strict growth conditions. In a field environment, a plant would not only be exposed to one consistent UV-B treatment. Instead a variety of UV-B, PAR and temperatures would be experienced. In order to determine whether the UVR8 photoequilibrium is an artefact created by artificial growth conditions, Chapter 4 of this thesis investigates the UVR8 photoequilibrium in a natural solar environment.

Chapter 4: UVR8 in a Natural Solar Environment

4.1 Introduction

While UVR8 has been researched extensively, studies have focused primarily on acute UV-B conditions in either purified protein, in a yeast model or in leaf protein extract (Christie, *et al.*, 2012, Huang, *et al.*, 2014, Rizzini, *et al.*, 2011, Wu, *et al.*, 2012). Those that have focused on the effects of UV-B on UVR8 *in planta* have principally focused on the localisation of UVR8 (Cloix, *et al.*, 2012, Kaiserli and Jenkins, 2007), the regeneration of the dimer in darkness after extreme UV-B treatments (Heijge and Ulm, 2013, Heilmann and Jenkins, 2013) or the effect of mutations within the UVR8 structure on its ability to rescue *uvr8* mutants (O'Hara and Jenkins, 2012). While the effects of natural solar radiation on UVR8 itself have not been studied in depth, the effects on plants as an entire organism have.

UV-B stress is highly species dependent and varies depending upon the exposure time and fluence rate, rather than the dose of UV-B given to plants (Jordan, 1996, Casati, *et al.*, 2004). The UV-B stress pathway has been studied in depth and has been shown to induce genes involved in other stress pathways such as drought and cold stress (Kilian, *et al.*, 2007). Exposure to stressful levels of UV-B induce ROS and MAPK signalling cascades within plants (Robson, *et al.*, 2015, Besteiro, *et al.*, 2011). Plant responses to UV-B stress include DNA, ribonucleic acid (RNA) and lipid damage, reduction of photosynthetic potential, leaf curling and reduced fertility and viability (Frohnmeyer and Steiger, 2003). Nevertheless, plants exist in an environment with highly variable and constant UV-B and are able to acclimate and responsd appropriately to UV-B in a photomorphogenic fashion.

UVR8 is a photoreceptor that is responsive at very low and ambient amounts of UV-B, down to 0.1 μmol m^{-2} s^{-1} (Brown and Jenkins, 2008). Indeed, when investigating the effects of long term, ecologically relevant UV-B treatments, plants did not show the typical symptoms of UV-B stress such as reduced photosynthetic capacity or the induction of stress genes (Hectors, *et al.*, 2007).

Further investigation has shown that although plants show a distinct UV-B response, for example, in *A. thaliana* changes include a smaller rosette size, decreased hypocotyl and stem height, redistribution of growth and changes in the chemical composition of cell walls: the stress response is different and not related to the UVR8 driven photomorphogenic response (Hectors, *et al.*, 2007).

The effect that UV-B has on plants in a natural solar environment has been studied in several species. In many cases, the separation of stress and photomorphogenesis has been reinforced. In *Vinis vitifera* UV-B exposure is vital to secondary metabolism within the grape berry skin, altering phenylpropanoid, flavonol and monoterpenoid biosynthesis while not affecting either ripening or berry to skin ratio (Martínez-Lüscher, *et al.* 2014, Carbonell-Bejerano, *et al.*, 2014). Furthermore, when investigating *Lactuca sativa,* photosynthetic capacity was increased in pre-UV-B-treated plants after transplantation to field environments compared to zero UV-B-treated plants and glasshouse grown plants (Wargent, *et al.*, 2014).

The effect of UV-B is not just limited to plant morphology, but also to disease and herbivore resistance. When plants that have been exposed to UV-B are compared to those that are UV-B naïve; UV-B naïve plants show less resistance to herbivory and this correlation becomes stronger when only studies investigating the effects of natural solar light are taken into account (Ballaré, *et al.*, 2012). Furthermore, if plants in the field receive attenuated UV-B, they show an increased number of insects (Ballaré, *et al.*, 2012). Finally, UV-B has also been seen to be effective at increasing resistance to pathogens, such as *Botrytis cinerea*. *uvr8* mutant plants have an increased susceptibility to *B. cinerea* and wild-type plants show an increased resistance to the pathogen after exposure to UV-B (Ballaré, *et al.*, 2012).

The level of UV-B that reaches plants on Earth varies depending on several factors. The lower range of the UV-B spectrum does not reach the Earth's surface as it is attenuated by the ozone layer (Jordan, 1996). UV-B level increases with altitude and decreases with latitude (Beckmann, *et al.* 2014). Other factors such as rainfall, cloud cover, pollution and the stratospheric ozone

levels also affect the UV-B fluence rate (Jordan, 1996, Tilbrook, *et al.*, 2013). It must also be considered that in a natural environment many plants will experience canopy shading. How UV-B penetrates the canopy is dependent upon many factors such as the species composition and the physical structure of the canopy (Jordan, 1996, Robson, *et al.*, 2015). In addition, in a natural environment the UV-B fluence rate will alter with the time of day and time of year as the sun rises and sets at different times, making the conditions markedly different to a controlled growth room environment. Finally, the ratio of PAR to UV-B will also change as UV-B light is scattered by the ozone layer. An area of ground that is shaded and has a low PAR fluence rate does not necessarily have a correspondingly low UV-B fluence rate (Robson, *et al.*, 2015).

Chapter 3 of this thesis focuses on chronic UV-B treatment and its affect upon UVR8 *in planta*, however, little has been done to investigate the effect of natural solar conditions on UVR8. Studies employing long term natural solar radiation have not looked at UVR8 and have instead focused upon whole plant morphology (Hectors, *et al.*, 2007), changes in gene expression (Robson, *et al.*, 2015) or changes in cell metabolite composition (Morales, *et al.*, 2013, Ballaré, *et al.*, 2012). When considering the behaviour of UVR8 it has been assumed that UVR8 exhibits an instantaneous shift from being fully dimeric in darkness to being fully monomeric after absorption of UV-B (Wu, *et al.*, 2012, Rizzini, *et al.*, 2011). However, this work has made it clear that while this may be true of UV-B naïve plants, it is not the case for plants that have been exposed to long term ecologically relevant UV-B which instead form a dimer/monomer photoequilibrium.

The UV-B photoreceptor UVR8 has been shown to monomerise in a controlled environment and the dynamics of monomerisation have been thoroughly investigated in purified protein. Chapter 3 of this thesis demonstrated that the simple $UVR8^{dimer}$ » $UVR8^{monomer}$ switch was not sufficient to describe the dynamics of UVR8 in a chronic UV-B environment. In a natural field environment, the plants will experience a range of light fluence rates, temperatures and day lengths and it is unknown how these various factors will influence the photoequilibrium of the protein. Therefore the aim of this chapter was to

determine the factors that are important for the photoequilibrium of UVR8. It is hypothesised that while the UVR8 photoequilbrium will differ throughout both the individual timecourses and the year, this will be due to changes in UV-B fluence rate. Other factors will be measured and investigated as appropriate including time of harvest, PAR and temperature. It is further hypothesised that the rate of regeneration of the dimer rather than the rate of monomerisation will be a deciding factor in the final balance of the UVR8 photoequilibrium.

4.2 Purified UVR8 protein will monomerise in natural solar light

Previous studies looking at the monomerisation dynamics of UVR8 within many different systems - *in planta*, *in vivo* and *in vitro* - have investigated the effects of UV-B light in controlled growth room experiments.

The ability of purified protein to monomerise under natural solar conditions was investigated by placing UVR8 purified via *E. coli* outdoors onto the roof of the Bower Building (Glasgow University, Glasgow, UK). Samples were retrieved shortly before dawn, at solar noon, shortly after sunset and at a further six equidistant time points throughout the day (three between dawn and solar noon and three between solar noon and sunset). These samples were snap frozen in liquid nitrogen before being analysed via a Coomassie stained, semi-native SDS-PAGE (Fig 4-1).

UVR8 protein purified from *E. coli* will monomerise when exposed to natural UV-B light. Figure 4-1**A** shows dimeric, purified UVR8 placed outside pre-dawn, and tracks the monomerisation of UVR8 as the sun rises. UVR8 had begun to monomerise by 0820 hours, 83 minutes after sunrise, despite a very low UV-B fluence rate. The purified UVR8 had completely monomerised by solar noon at 1321 hours. The highest level of UV-B was recorded at 1140 hours, 0.62 μmol m^{-2} s^{-1}. UVR8 did not regenerate into a dimer throughout the remainder of the day, despite the low overall UV-B fluence rate. The sun sets at 1953 and by 2000 hours UVR8 was still completely monomeric.

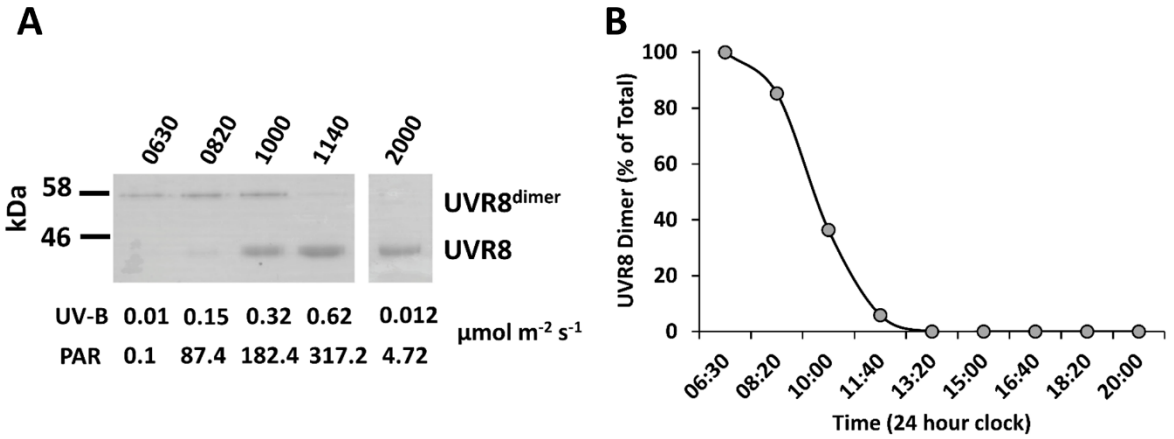

Figure 4-1: Monomerisation of purified UVR8 protein in natural solar light. Purified UVR8 protein was exposed to natural solar light on the 31st of March 2013, where dawn occurred at 0650 hours, solar noon at 1321 hours and sunset at 1953 hours. UVR8 monomerisation is shown over time with associated UV-B and PAR fluence rates shown in (**A**) Coomassie Blue stained semi-native SDS-PAGE and (**B**) Quantified UVR8 dimer shown as a percentage of the total UVR8 protein.

The rate of monomerisation varied throughout the day, as would be expected due to the extremely low light levels observed in the hours just post-dawn and due to the differing UVR8 dimer levels. A constant decrease in dimer at a rate of 14.6% per hour is achieved, with a peak rate of 29.34% per hour and a trough rate of 3.54% per hour during active monomerisation. Purified UVR8 was able to monomerise in extremely low levels of natural solar UV-B light, and was unable to regenerate into a dimer while even low levels of UV-B are present. Once there was no UV-B present, regeneration was slow, supporting the findings of Heilmann and Jenkins (2013).

The monomerisation of UVR8 that has been purified from *E. coli* demonstrates the sensitivity of the UVR8 photoreceptor as previously stated by Brown (2008) and its activity in natural solar conditions. The lack of re-dimerisation reinforces the findings of Heidge and Ulm (2013) and Heilmann and Jenkins (2013) that the RUP1 and RUP2 proteins are required for efficient dimer regeneration.

4.3 The UVR8 photoequilibrium in plants acclimated to natural solar light is highly variable

In accordance with work shown previously (Chapter 3), in acclimated plants UVR8 demonstrates a photoequilibrium between the dimeric and monomeric forms after chronic UV-B exposure in controlled growth conditions. Over the course of a year, L*er* ecotype *A. thaliana* were germinated and grown for seven

days in 120 μmol m^{-2} s^{-1} in 12 hour light/dark cycles before being transferred outdoors onto the roof of the Bower Building (Glasgow University, Glasgow, UK) where they were grown for a further 14 days. Sowing of plants was staggered in order to achieve three non-consequtive timecourses a week. The plants were then harvested at set time points relating to the position of the sun in the sky in order to ensure that samples taken on different days could be compared to each other. Samples were taken shortly before sunrise, at solar noon, shortly after sunset and at a further six timepoints equally spaced in time (three between the first time point and solar noon and three between solar noon and the last time point). After samples had been harvested they were snap frozen in liquid nitrogen and the protein extracted using the method described in Kaiserli and Jenkins (2007). The relative ratio of UVR8 dimer to UVR8 monomer was determined through quantitative semi-native Western Blots using imageJ. UV-B and PAR fluence rates were measured at the time of sampling along with an ambient temperature reading (Fig 4-2). For each day only one timecourse was undertaken due to space constrictions. Furthermore each timecourse is undertaken with new plants as measuring the UVR8 equilibrium is a destructive process.

The relationship between the UVR8 photoequilibrium and environmental factors such as UV-B fluence rate, temperature and PAR fluence rate was examined through GLM. The data from all of the outdoor timecourses was pooled and sorted under appropriate headings: the factor that was affected (UVR8 Dimer %) and the factors that were causing the change (time of harvest, UV-B fluence rate, PAR fluence rate, temperature). As UVR8 does not monomerise without the presence of UV-B the simplest model was defined as UVR8 Dimer % = UV-B fluence rate, meaning that the UVR8 Dimer % is affected by only the UV-B fluence rate. The add1 function in R was used to quickly assess multiple models using Chi Squared to determine the difference between the models and whether to reject the null hypothesis. This function adds factors one at a time and compares them to the null hypothesis (in this case that only UV-B fluence rate determines the UVR8 Dimer %). The null hypothesis is rejected if the new model explains the data more accurately.

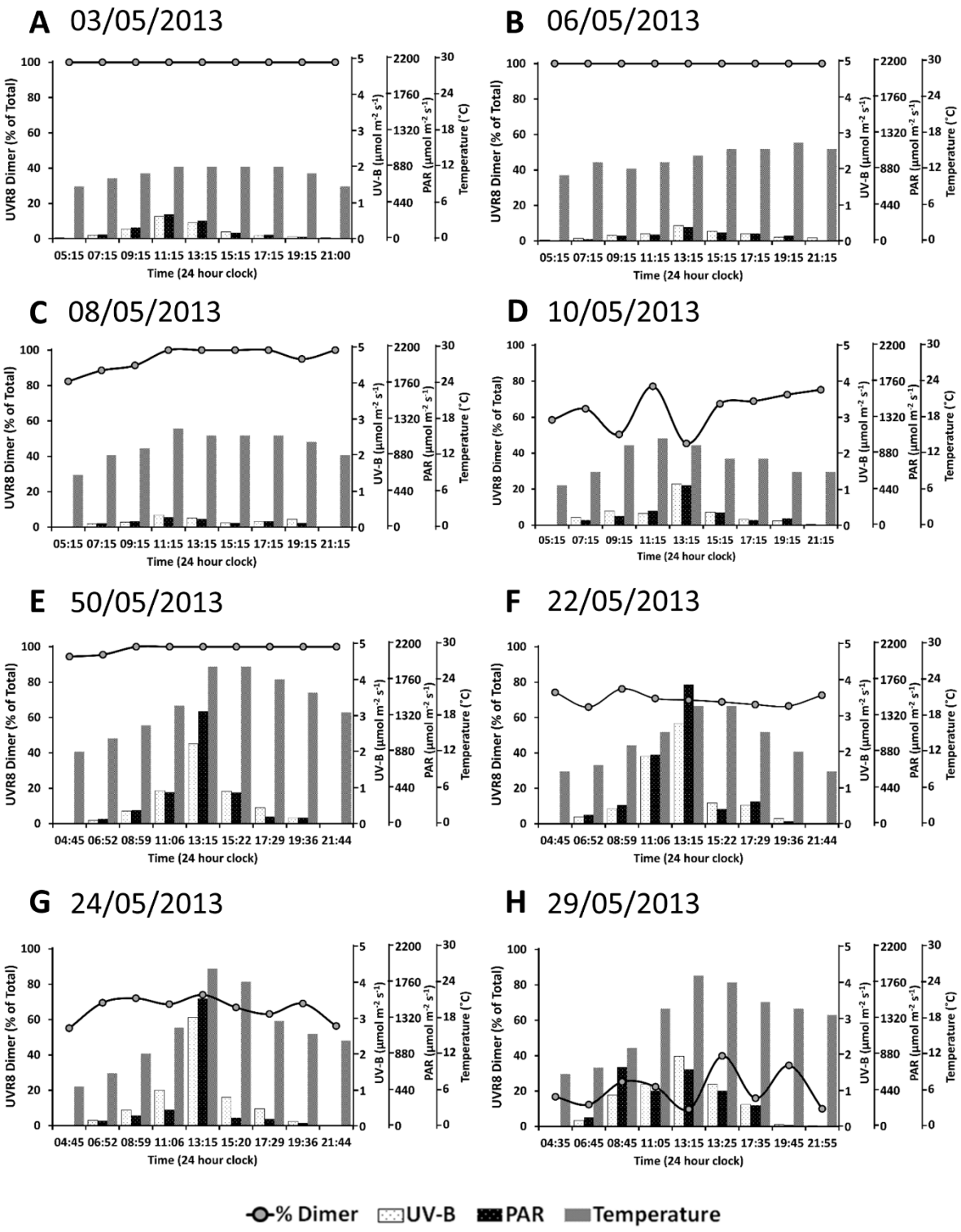
A 03/05/2013
B 06/05/2013
C 08/05/2013
D 10/05/2013
E 50/05/2013
F 22/05/2013
G 24/05/2013
H 29/05/2013
UVR8 Dimer (% of Total)
UV-B (µmol m-2 s-1)
PAR (µmol m-2 s-1)
Temperature (°C)
Time (24 hour clock)
% Dimer
UV-B
PAR
Temperature

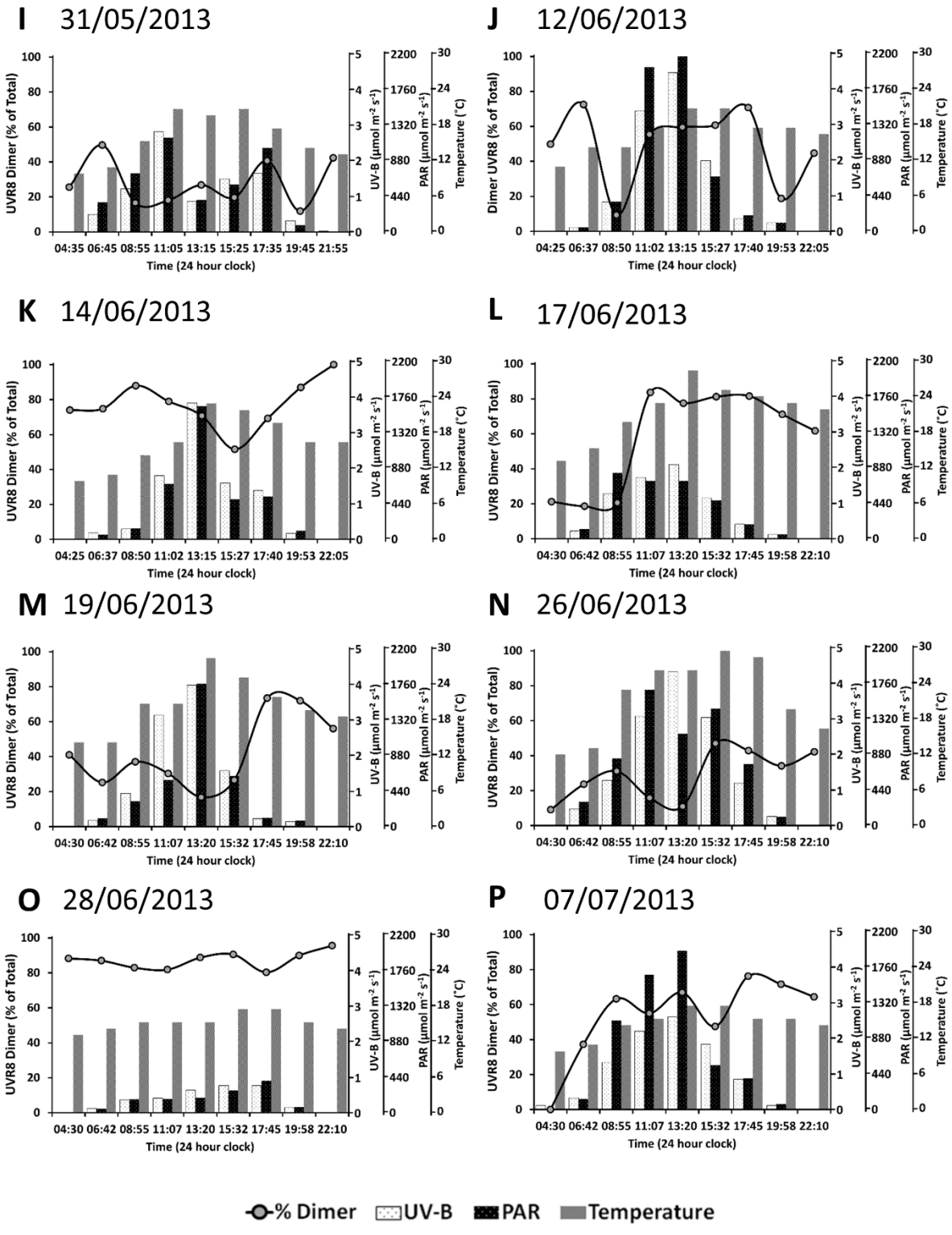
I 31/05/2013
J 12/06/2013
K 14/06/2013
L 17/06/2013
M 19/06/2013
N 26/06/2013
O 28/06/2013
P 07/07/2013
UVR8 Dimer (% of Total)
Dimer UVR8 (% of Total)
UV-B (µmol m-2 s-1)
PAR (µmol m-2 s-1)
Temperature (°C)
Time (24 hour clock)
% Dimer
UV-B
PAR
Temperature

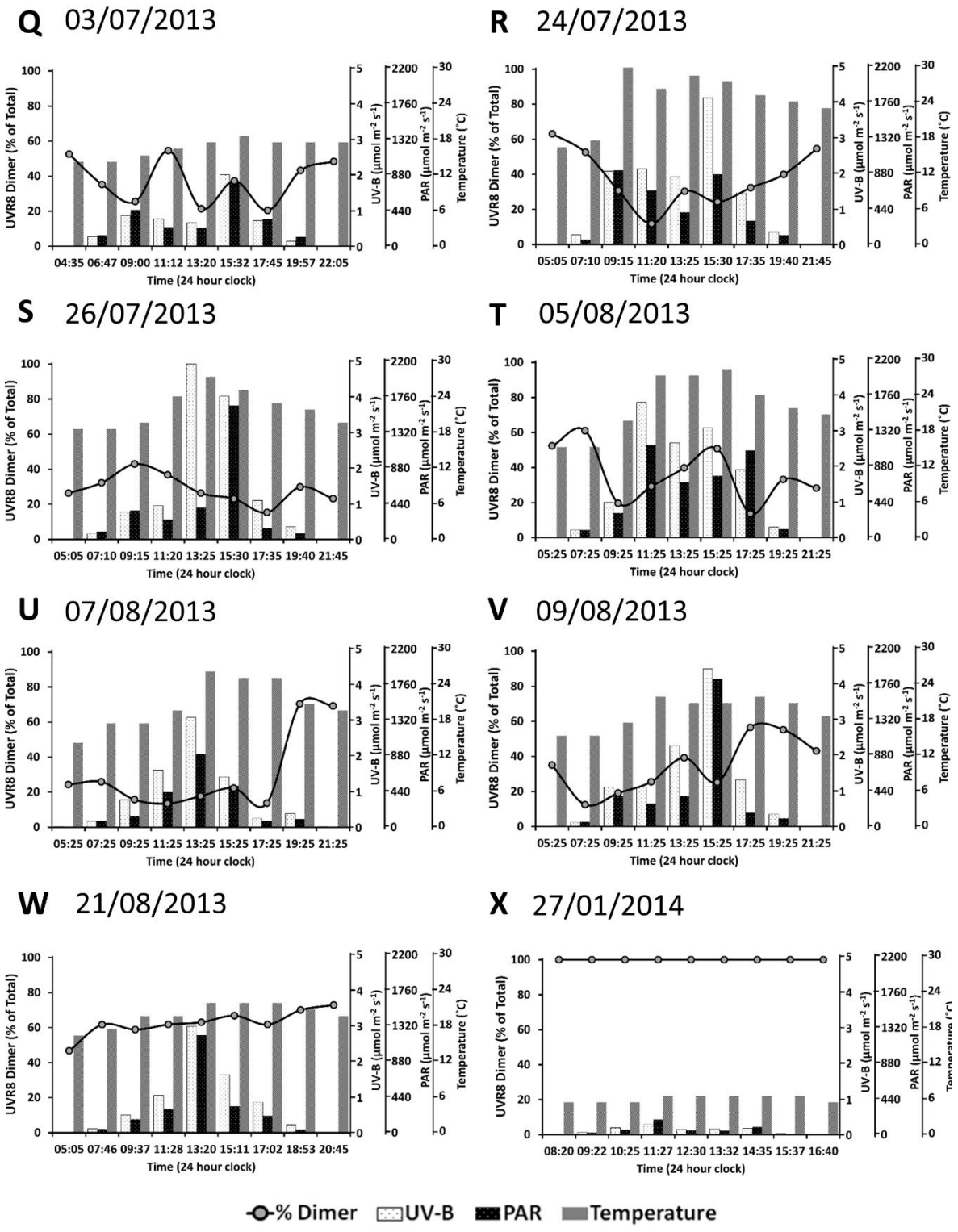
Q 03/07/2013
R 24/07/2013
S 26/07/2013
T 05/08/2013
U 07/08/2013
V 09/08/2013
W 21/08/2013
X 27/01/2014
UVR8 Dimer (% of Total)
UV-B (µmol m-2 s-1)
PAR (µmol m-2 s-1)
Temperature (°C)
Time (24 hour clock)
% Dimer
UV-B
PAR
Temperature

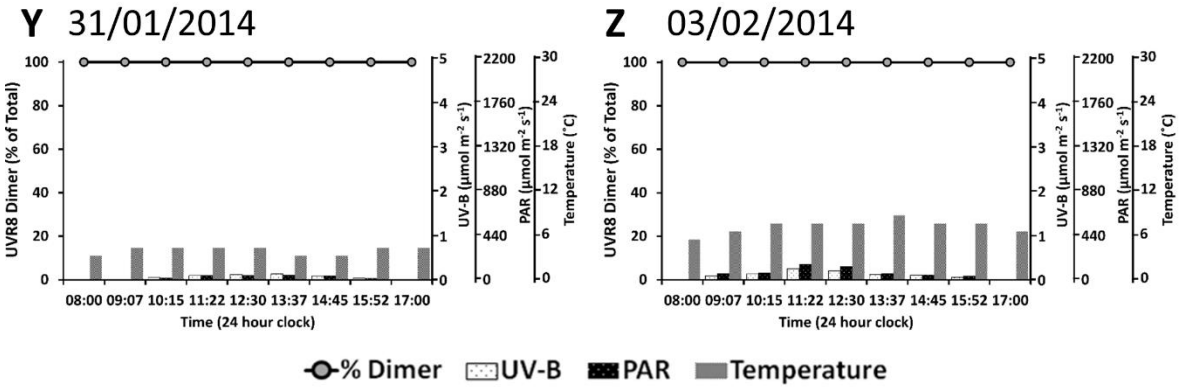

Fig 4-2: A series of outside timecourses measuring UVR8 dimer to monomer ratio, UV-B fluence rate, PAR fluence rate and ambient temperature. Acclimated L*er* plants were sampled across 26 days of 2013 and 2014. The first sample is pre-dawn, the fifth sample occurs at solar noon and the last sample is post-sunset. Other samples are taken at equidistant times between sunrise and solar noon; and solar noon and sunset. The time at which each sample was harvested is shown in 24 hour clock. UV-B and PAR fluence rates were measured as a 30s average at each of the harvest times. Ambient soil surface temperature was also recorded. The level of UVR8 dimer is calculated in ImageJ using a Western Blot image and is expressed as the percentage of UVR8 dimer compared to the total UVR8 seen. (A) 03/05/2013: Sunrise began at 0529, solar noon occurs at 1313, sunset ends at 2100. (B) 06/05/2013: Sunrise began at 0523, solar noon occurs at 1314, sunset ends at 2106. (C) 08/05/2013: Sunrise begins at 0518, solar noon occurs at 1314, sunset ends at 2110. (D) 10/05/2013: Sunrise began at 0514, solar noon occurs at1313, sunset finishes at 2114. (E) 20/05/2013 Sunrise begins at 0456, solar noon occurs at 1314 and sunset ends at 2132. (F) 22/05/2013 Sunrise begins at 0450, solar noon occurs at 1314, sunset ends 2139. (G) 24/05/2013 Sunrise begins at 0450, solar noon occurs at 1314, sunset ends 2139. (H) 29/05/2013 Sunrise begins at 0443, solar noon occurs at 1314, sunset ends 2147. (I) 31/05/2013 Sunrise begins at 0441, solar noon occurs at 1315, sunset ends 2149. (J) 12/06/2013 Sunrise begins at 0432, solar noon occurs at 1317, sunset ends 2202. (K) 14/06/2013 Sunrise begins at 0431, solar noon occurs at 1317, sunset ends 2204. (L) 17/06/2013 Sunrise begins at 0431, solar noon occurs at 1318, sunset ends 2205. (M) 19/06/2013 Sunrise begins at 0431, solar noon occurs at 1318, sunset ends 2206. (N) 26/06/2013 Sunrise begins at 0433, solar noon occurs at 1320, sunset ends 2207. (O) 28/06/2013 Sunrise begins at 0434, solar noon occurs at 1320, sunset ends 2206. (P) 01/07/2013 Sunrise begins at 0436, solar noon occurs at 1321, sunset ends 2205. (Q) 03/07/2013 Sunrise begins at 0438, solar noon occurs at 1321, sunset ends 2204. (R) 24/07/2013 Sunrise begins at 0507, solar noon occurs at 1324, sunset ends 2138. (S) 26/07/2013 Sunrise begins at 0511, solar noon occurs at 1324, sunset ends 2135. (T) 05/08/2013 Sunrise begins at 0529, solar noon occurs at 1323, sunset ends 2115. (U) 07/08/2013 Sunrise begins at 0533, solar noon occurs at 1323, sunset ends 2111. (V) 09/08/2013 Sunrise begins at 0537, solar noon occurs at 1323, sunset ends 2107. (W) 21/08/13 Sunrise begins at 0600, solar noon occurs at 1320, sunset ends 2039. (X) 27/01/14 Sunrise begins at 0820, solar noon occurs at 1230, sunset ends 1640. (Y) 31/01/14 Sunrise begins at 0813, solar noon occurs at 1230, sunset ends 1648. (Z) 03/02/14 Sunrise begins at 0811, solar noon occurs at 1231, sunset ends 1650.

While UV-B fluence rates were frequently above the fluence rate required to completely monomerise *in vitro* purified UVR8, there was only a single timepoint where no dimer is present (Fig 4-2P). There were more frequent occurrences of 100% UVR8 dimer when the UV-B fluence rate was high (Fig 4-2E), than the reverse.

The first timepoint taken always occurs pre-dawn. Notably, despite the length of the night varying throughout the year, this timepoint generally demonstrates a dimer:monomer ratio (Figs 4-2D-O and Figs 4-2Q-W). An increase in UVR8 dimer % between the pre-dawn sample and the first post-dawn sample was seen in just under half of the timecourses (Figs 4-2C-E, Figs 4-2I-J, Fig 4-2N, Fig 4-2P and Figs 4-2S-U). This supports the previous data that demonstrated the lag response of UVR8 dimer regeneration during the controlled dark timecourses.

There were several days where no UVR8 monomerisation is observed (Figs 4-2A-B, and Figs 4-2X-Z). These days were characterised by low UV-B fluence rates. The UV-B fluence rate was never recorded above 1.0 μmol $m^{-2}s^{-1}$ and only recorded above 0.5 μmol $m^{-2}s^{-1}$ on one of these days (Fig 4-2A). However, there were other days recorded with similar UV-B fluence rate measurements where UVR8 was seen to monomerise (Fig 4-2C and Fig 4-2O) suggesting that the photoequilibrium of UVR8 was dependent on more than just UV-B fluence rate. One of the most compelling features of this data series was the variety of photoequilibrium patterns. Days with similar UV-B fluence rates (Fig 4-2H and Fig 4-2I) can have similar levels of UVR8 dimer present. These can be compared with other recorded days (Fig 4-2J, Fig4-2K and Fig4-2P) which show significantly different patterns of photoequilibrium. If UV-B fluence rate was the only factor involved in establishing the UVR8 photoequilibrium, it should be expected that these timecourses would not have different patterns of dimer:monomer ratio nor different average levels of UVR8 dimer.

Fluctuations were also seen between timepoints. These fluctuations - when they occur - form a sinusoidal pattern, indicating a continuous adjustment to the UVR8 photoequilibrium based on the plant's environment. In a natural solar environment, the UV-B fluence rate can change rapidly. UV-B fluence rate

measurements form a bell curve, starting low before reaching their peak at solar noon before decreasing again towards sunset. Weather conditions, such as heavy clouds and rain will affect UV-B fluence rate, disrupting the typical light patterns (Fig 4-2I). Patchy clouds were less likely to cause a similar effect due to the difference in light distribution between UV-B and PAR, UV-B levels in shadow are often higher than the corresponding PAR measurements would suggest, due to the scattering effects of the atmosphere. As the $UVR8^{dimer}/UVR8^{monomer}$ ratio was more complex than the inverse curve of the UV-B fluence rate it was likely that there are other factors in a field environment that affect $UVR8^{dimer}/UVR8^{monomer}$ ratio.

Other timecourses demonstrate a far more stable dimer to monomer ratio (Fig 4-2F and Fig 4-2W) despite what appears to be significant differences in UV-B fluence rate. The same level of UVR8 dimer was seen when the UV-B fluence rate was at 3.0 µmol $m^{-2}s^{-1}$ as when the UV-B fluence rate was below 0.5 µmol $m^{-2}s^{-1}$ later the same day. This reinforces that while UV-B was essential for UVR8 monomerisation it was not the only factor involved in determining overall photoequilibrium of UVR8.

4.4 Total UVR8 protein level does not vary significantly in plants acclimated to natural solar light

It is possible that the UVR8 photoequilibrium could be affected by a difference in the overall total protein levels of UVR8; if more UVR8 is available overall, more monomerisation is required to reach the same total $UVR8^{monomer}$ compared a plant with less UVR8. To ensure that any change in equilibrium was due to changes in dimer to monomer ratio and not due to changes in protein level, total UVR8 protein level was investigated. Six of the timecourses shown in Fig 2 were run alongside a second block of plants that were identically grown but also had a zero UV-B shield (Autostat CT5). Samples were harvested at pre-dawn, solar noon, post sunset and three other times equidistant between sunrise and solar noon and solar noon and sunset. As samples were harvested based upon the sun's position in the sky, the time of harvest varied dramatically. To be able to compare the timecourses each harvest sample was given a timepoint number from 1-9. Therefore the pre-dawn harvest sample is always timepoint number 1,

each solar noon sample is always timepoint number 5 and each post-sunset sample is always timepoint number 9. After protein was extracted it was denatured to ensure that UVR8 became entirely monomeric and a Western Blot was performed. Protein loading was controlled using rbcL levels determined via Ponceau staining. The total amount of UVR8 was ascertained using ImageJ. The solar noon samples were chosen to be the timepoint to have a relative density of 1.0 (Fig 4-3). By measuring the total amount of UVR8 protein normalised against rbcL in both plus and zero UV-B conditions it is possible to determine how the protein levels change across the course of a day.

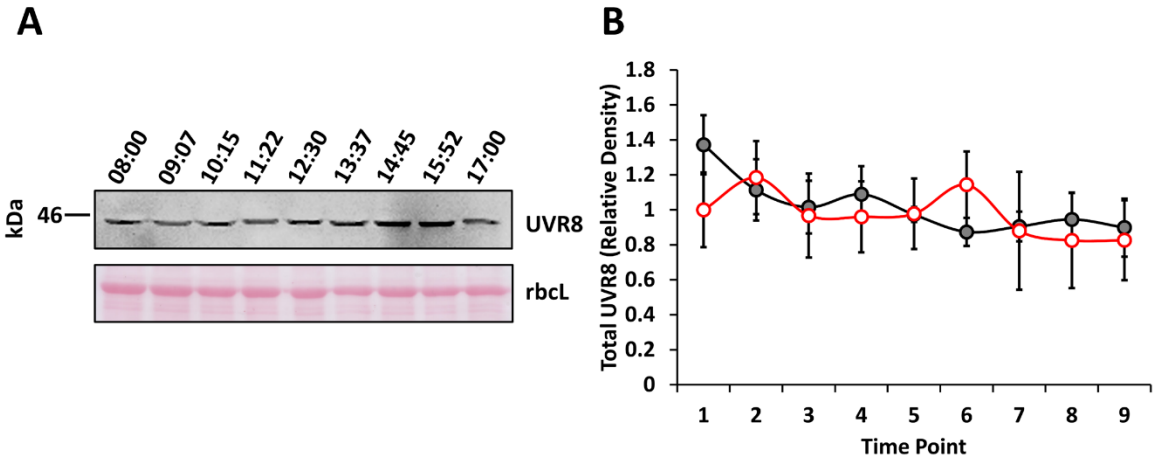

Fig 4-3: Quantification of the total UVR8 protein *in planta* in natural solar conditions with a negative UV-B control. L*er* plants were grown outside in either plus (black) or zero (red) UV-B conditions. Samples were harvested nine times throughout the day. Harvest times were chosen according to the sunrise, sunset and solar noon times. Samples were then analysed by Western Blot via immunodetection and protein levels were normalised using rbcL levels. (A) Boiled Western Blot showing total amount of UVR8 protein harvested across nine timepoints during the day. (B) Quantified Western Blot showing average UVR8 relative density with standard error (n=6).

An ANOVA analysis showed that there was no significant change in UVR8 levels at any point during the day, with a relative density range of 0.3. The levels of UVR8 in the zero UV-B control were slightly more variable, having a relative density range of 0.45. Nevertheless, there was no statistically significant difference between the samples during the day or between plants grown in plus or zero UV-B conditions. Therefore, UVR8 does not vary significantly in response to time of day or chronic UV-B treatment.

4.5 Both UV-B fluence rate and temperature affect the UVR8 photoequilibrium while PAR and time of day do not.

While UVR8 total protein amount does not change significantly to affect the photoequilibrium, the field study data provides a range of conditions that are potential contributing factors to the final balance of dimer to monomer ratio. The timecourses undertaken during 2013 and 2014 provided 234 samples with recorded time of day, UV-B fluence rate, PAR fluence rate and ambient temperature. While, as previously shown in chapter 3, UVR8 dimer to monomer relationship is not circadian, it is worthwhile reinforcing this with a larger and more varied data set.

For analysis of time of day, each individual timecourse is treated as a repeat (n=26). From the collected data, it was possible to see that UVR8 dimer to monomer levels remain steady throughout the day (Fig 4-4). Furthermore, there was a large dimer pool. It is important to note that the initial time point, which was always taken before sunrise and therefore in an absence of UV-B and in the dark, contains a substantial percentage of monomer. An ANOVA performed shows that time of day does not affect the UVR8 photoequilibrium (p=0.175). This indicates that there was no circadian effect on either the total UVR8 protein amount or the UVR8 dimer to monomer ratio.

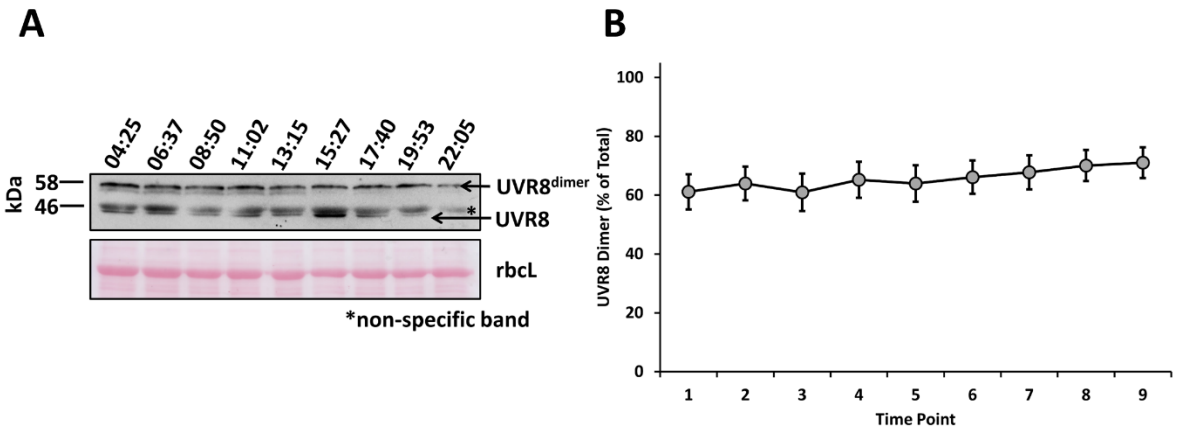

Fig 4-4: The average UVR8 photoequilibrium. An average photoequilibrium timecourse was constructed from the 26 timecourses performed throughout 2013 and 2014. (A) An example non-boiled Western Blot demonstrating the appearance of both monomer and dimer across the day. Samples were taken prior to dawn, at solar noon, post sunset and at six other time points equidistant between sunrise and solar noon and solar noon and sunset. rbcL was used as a loading control. (B) The average quantified level of UVR8 dimer measured as a percentage of the total UVR8 shown with standard error (n=26). Due to difference in day length, the timepoint number was used instead of time of day.

By breaking the data down in different ways it was possible to investigate the relationship between the other parameters of the study. The average dimer percentage was calculated for each parameter, with the measurements broken down into several groups tracking the moving average of UVR8 dimer % (for example, each degree of temperature is grouped). UV-B levels were broken down into different 12 different ranges; PAR levels into 13 different ranges; and temperature was calculated by ˚C (Fig 4-5).

UVR8 photoequilibrium was most affected by UV-B fluence rates under the 1.0-1.499 µmol m^{-2} s^{-1} bracket (Fig 4-5A). While UV-B was extremely low, below 0.05 µmol m^{-2} s^{-1}, UVR8 has an average dimer level of 65%. The next bracket was particularly interesting as the dimer percentage increases to nearly 100%. After this point there was a steady decrease of dimer level until the 1.0 µmol m^{-2} s^{-1} bracket was reached, with around 40% dimer. After this point there was no significant change in UVR8 dimer level. This is important for several reasons. Firstly, while the extremely low to no UV-B bracket (0-0.0499 µmol m^{-2} s^{-1}) had a lower percentage of dimer present than would be expected based on zero UV-B controls, this was due to the circumstances in which this data was collected.

Samples where the UV-B fluence rate was below 0.05 µmol m^{-2} s^{-1} were typically taken in pre-dawn and post-sunset condition. From both the individual timecourse data and the amalgamated graph it is possible to see that in these conditions there was frequently a substantial level of monomer present. UVR8 does not fully recover to 100% dimer after a night period in acclimated plants; therefore it would be expected that the extremely low UV-B samples have a relatively high monomer to dimer ratio.

In comparison, the next bracket, 0.5-0.99 µmol m^{-2} s^{-1} demonstrates a far higher level of dimer. The majority of these data points come from plants where there was a low level of UV-B across the entire day and where UVR8 appeared as primarily or entirely dimeric at the start of the day. This suggests that UV-B has a cumulative effect on the photoequilibrium of UVR8. For example, a plant that has been acclimated to low levels of UV-B will have a higher percentage of dimer

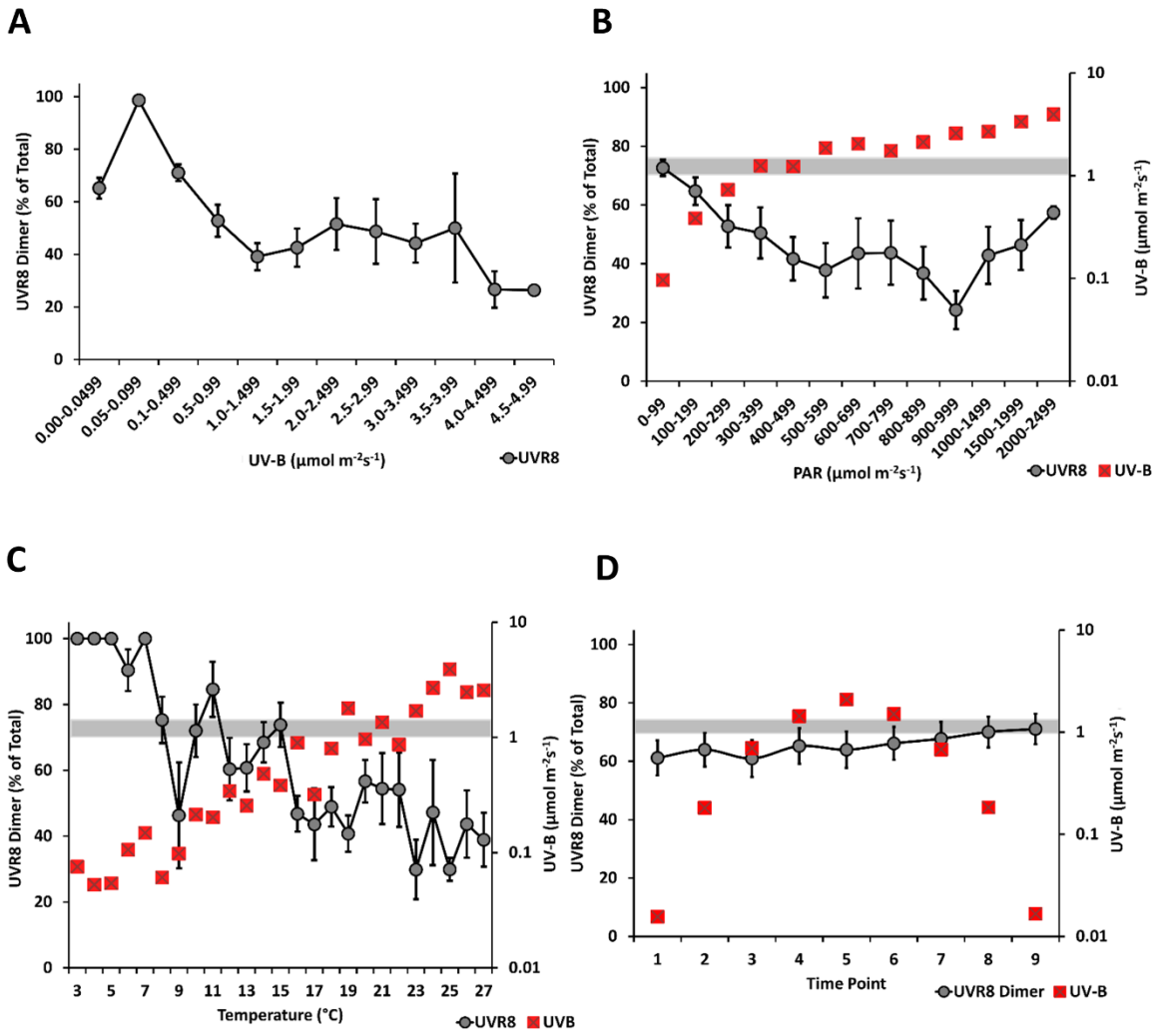

Figure 4-5: Relationships between UVR8 Dimer percentage and UV-B fluence rate, PAR fluence rate and ambient temperature. The average UVR8 dimer levels as a percentage of the total UVR8 amount are calculated within specified ranges for UV-B, PAR and temperature. This provides a visualisation of the relationship between the UVR8 photoequilibrium and several different factors. (**A**) The moving average of UVR8 dimer percentage as UV-B fluence rate increases. The UV-B saturation point is where as the UV-B fluence rate increases no further decrease in UVR8 dimer percentage is seen. This is marked by a grey box in (**B**), (**C**) and (**D**). (**B**) The moving average of UVR8 dimer percentage as PAR fluence rate increases with an overlay showing the realtionship between PAR and the UV-B fluence rate. (**C**) The moving average of UVR8 dimer as ambient temperature increases with an overlay showing the relationship between ambient temperature and the average UVR8 dimer percentage and UV-B fluence rate for each °C. (**D**) The average UVR8 photoequilibrium in outdoor grown UV-B acclimated plants shown relative to the time of day and the average UV-B fluence rate at each time box.

present at the start of a day than a plant that has been acclimated to higher levels of UV-B.

The dimer percentage levels associated with the UV-B fluence rate brackets decreased at a rate of 1% per increase of 0.01 µmol m^{-2} s^{-1} from 0.1-0.499 µmol m^{-2} s^{-1}; slowing to a decrease of 0.5% per increase in UV-B of 0.01 µmol m^{-2} s^{-1} from 0.5-0.99 µmol m^{-2} s^{-1}; and finally a decrease of 0.2% dimer per increase in 0.01 µmol m^{-2} s^{-1} from 1.0-1.499 µmol m^{-2} s^{-1}. After this point, no further increase in UV-B fluence rate provided a statistically significant decrease in dimer percentage. This would suggest that the saturation point for UV-B effect on the UVR8 photoequillibrium was within the 1.0-1.499 µmol m^{-2} s^{-1} bracket. This was reinforced by statistical analysis which shows a statistically significant association between UV-B and overall dimer percentage ($p=5.02e^{-09}$). This model was the null hypothesis for the data, that UVR8 Dimer % is affected by UV-B fluence rate. As this has shown to be a model that significantly explains the data, more complex models will have to outperform this null model to be accepted.

The effect of PAR on the UVR8 photoequilibrium was investigated in the same way (Fig 4-5B). The initial bracket for PAR was very similar to the initial bracket for UV-B. Dimer percentage was around 70%. Again, this data point correlates to those samples which were taken in the early hours of the morning or late hours of the evening. In the case of the PAR measurements, these samples are not just the pre-dawn and post-sunset samples. PAR levels were frequently below 99 µmol m^{-2} s^{-1} for a few hours after sunrise and before sunset depending on weather conditions. Again, the acclimation of the plants plays into the overall UVR8 photoequilibrium. Where plants were exposed to low levels of UV-B for an extended period of time they have a higher initial UVR8 dimer pool when a day begins.

As PAR increases there was initially a decrease in dimer levels, similar to that shown by an increase in UV-B. A decrease of 0.1% in UVR8 dimer levels per 1 µmol m^{-2} s^{-1} increase in PAR for 0-99 µmol m^{-2} s^{-1}; followed by a decrease of 0.15% dimer per 1 µmol m^{-2} s^{-1} increase in PAR for 100-199 µmol m^{-2} s^{-1}. However

after this point there was no significant decrease in UVR8 dimer percentage as PAR increases. While the relationship between PAR and the $UVR8^{dimer}/UVR8^{monomer}$ ratio is significant ($p=5.12e^{-06}$) controls show that UVR8 does not monomerise at any PAR level during outside timecourses however this does not rule out an additive effect. A model was tested to determine whether an additive effect between UV-B and PAR existed (UVR8 Dimer % = UV-B Fluence Rate + PAR Fluence Rate). This model did not explain the data more accurately than the null hypothesis that the UVR8 Dimer % is affected by only the UV-B fluence rate and so was rejected. To visualise this, the average UV-B fluence rate for each PAR bracket was calculated and a UV-B saturation box representing the saturation bracket of 1.0-1.499 µmol m^{-2} s^{-1} was added (Fig 4-5B). When UV-B fluence rate breaches this saturation box, any further increase in UV-B will not cause an additional increase in monomerisation. Therefore any further change in the photoequilibrium was likely to be caused by another parameter.

In this way it was possible to see that the initial decrease in dimer levels occurs below the UV-B saturation line and was therefore likely to be caused by increases in UV-B fluence rate rather than increases in PAR. Furthermore, after the UV-B levels have crossed the saturation line there is no further change in photoequilibrium.

While the trends for both UV-B and PAR fluence rates had saturation points, after which no further decrease in dimer levels was seen, the trend for temperature is far more linear (Fig 4-5C). The initial lower temperatures have a very high level of dimer and this decreases as the temperature increases. This translates to a decrease of 2.5% per 1˚C increase in ambient temperature. This relationship was extremely strong ($p=2.74e^{-16}$), however the null hypothesis was not rejected as UVR8 requires UV-B to monomerise and therefore UV-B Fluence Rate must be a factor in the final model. A model was performed to determine whether there was an additive effect between temperature and UV-B fluence rate (UVR8 Dimer = UV-B Fluence Rate + Temperature). This model was highly significant and replaced the null model as a better fit to the data. This would suggest that temperature could have an effect on the $UVR8^{dimer}/UVR8^{monomer}$

ratio, however more directed experiments are required in order to isolate this effect.

Using GLM it was possible to determine not only whether there was an additive effect between factors, but also an interactive effect. The drop1 function in R was used to define the most complex model and drop one factor to achieve the most parsimonious model. The most complex model used was %Dimer = UV-B Fluence Rate + PAR Fluence Rate + Temperature + UVB-Fluence Rate*PAR Fluence Rate*Temperature. It was determined that the data is best described as %Dimer = UV-B Fluence Rate + Temperature. While interactions between these factors improved the fit of the model, it was not improved enough to discard the null model. This means that the UVR8 photoequilibrium is affected by both UV-B fluence rate and Temperature working additively.

4.6 Regeneration of the UVR8 dimer varies according to temperature

To determine if temperature affected the UVR8 photoequilibrium in controlled conditions a minus UV-B experiment was performed. UVR8 purified from *E. coli* were either kept on ice or incubated at a range of temperatures (from 4°C to 46°C) for an hour. This range of temperatures was chosen as it both covers the optimal range of growth for *A. thaliana* and goes beyond it to a temperature where *A. thaliana* could not survive (Koorneef, *et al.* 2004). After incubation samples were run on a semi-native SDS-PAGE and analysed using ImageJ (Fig 4-6).

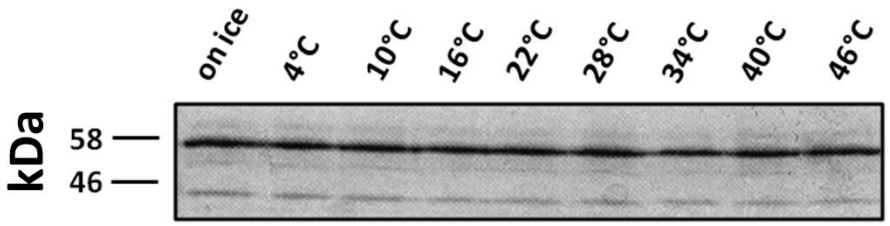

Fig 4-6: UVR8 dimer stability by temperature. Purified UVR8 protein was incubated at a series of temperatures without UV-B for 1 hour. Samples were analysed by non-boiled SDS-PAGE.

By incubating purified UVR8 at 6°C intervals in zero UV-B conditions for 1 hour it is possible to determine the stability of the UVR8 dimer. Previous experiments with purified protein have shown that UVR8 will monomerise on ice, but only in the presence of UV-B. Regeneration of the dimer has also been shown at room

temperature over a period of 48 hours (Heijge and Ulm, 2013 and Heilmann and Jenkins, 2013).

In zero UV-B conditions, the UVR8 dimer was temperature stable up to 46˚C, confirming that monomerisation was not induced by temperature. Therefore, as temperature had an effect on the photoequilibrium of UVR8 it was more likely to affect the rate of regeneration rather than the rate of monomerisation.

Further investigation into the role temperature had to play in maintaining the photoequilibrium was performed through regeneration assays. For each repeat of the experiment three blocks of *A. thaliana* plants were grown at different positions in the growth room to determine if position was affecting the experiment to determine whether position within the treatment room affected the UVR8 photoequilibrium using the lme4 package within R (UVR8 Dimer % = Intercept + ε, where ε is the random factor; UVR8 Dimer is affected only by the random position within the room). No effect was found so room position was discarded as a factor and the each block was considered a separate repeat (n=9). To determine whether temperature was affecting UVR8 itself, the RUP proteins or another factor, WT and *rup1rup2* mutant plants were used.

Plants were grown in constant 120 μmol m^{-2} s^{-1} white light for 10 days before being moved to the temperatures studied. Four temperatures were chosen to represent the range of temperatures seen during the outdoor experiments: 5°C for colder winter days, 10°C for spring days, 20°C both as a control (this is the temperature that *A. thaliana* is typically grown at for controlled growth room experiments) and to represent summer days and 30°C to represent the warmest temperatures seen. The plants were allowed to adapt to these temperatures for 24 hours to ensure that any differences in regeneration were due to the temperature chosen and not the shock of changing temperature. The plants were kept at these temperatures for the rest of the experiment. They were given an short, extremely high dose of UV-B (15 minutes at 21 μmol m^{-2} s^{-1} as seen in both Heijdge and Ulm (2013) and Heilmann and Jenkins (2013)) before being allowed to recover in the dark. Samples were taken before UV-B treatment to establish that UVR8 was entirely dimeric, immediately after UV-B treatment

to ensure that UVR8 had completely monomerised and then at a further six timepoints over six hours. Samples were frozen in liquid nitrogen before protein was extracted. The dimer/monomer ratio was determined via semi-native Western blot and analysed using ImageJ (Fig 4-7).

In these experiments the total $UVR8^{dimer}$ in darkness before the UV-B treatment was used as the 100% $UVR8^{dimer}$ baseline. Using this number it was possible to determine both that UVR8 had completely monomerised – there was no dimer visible – how quickly UVR8 returned to the initial base level and whether more UVR8 was produced.

In L*er* plants complete recovery of the UVR8 dimer occured at 240 minutes. However, the overall level of UVR8 rose to an average of 133% by 360 minutes. The overall rate of regeneration for L*er* at 30°C was not significantly different, as complete recovery of the UVR8 dimer also occured at 240 minutes. The increase in total protein was also extremely similar, with the 30°C treated plants showing an average of 127% total protein by 360 minutes. In comparison both mid and cold treated plants showed a much slower recovery and neither produced more UVR8 protein. The 5°C plants reached complete $UVR8^{dimer}$ regeneration by 360 minutes. However the 10°C did not completely recover the UVR8 dimer in the time given. This was interesting as if the internal environment and composition of the plant remained the same in regards to UV-B photoreception and signalling, it would be expected that the colder the temperature the slower the regeneration and that as temperature increased so would regeneration rate as the optimal temperature for protein activity was approached and reached. Clearly, these plants do not show this pattern, suggesting that the activity of the proteins involved in the UVR8 photoequilibrium are modified in colder temperatures either by total protein amount or post-translational modification.

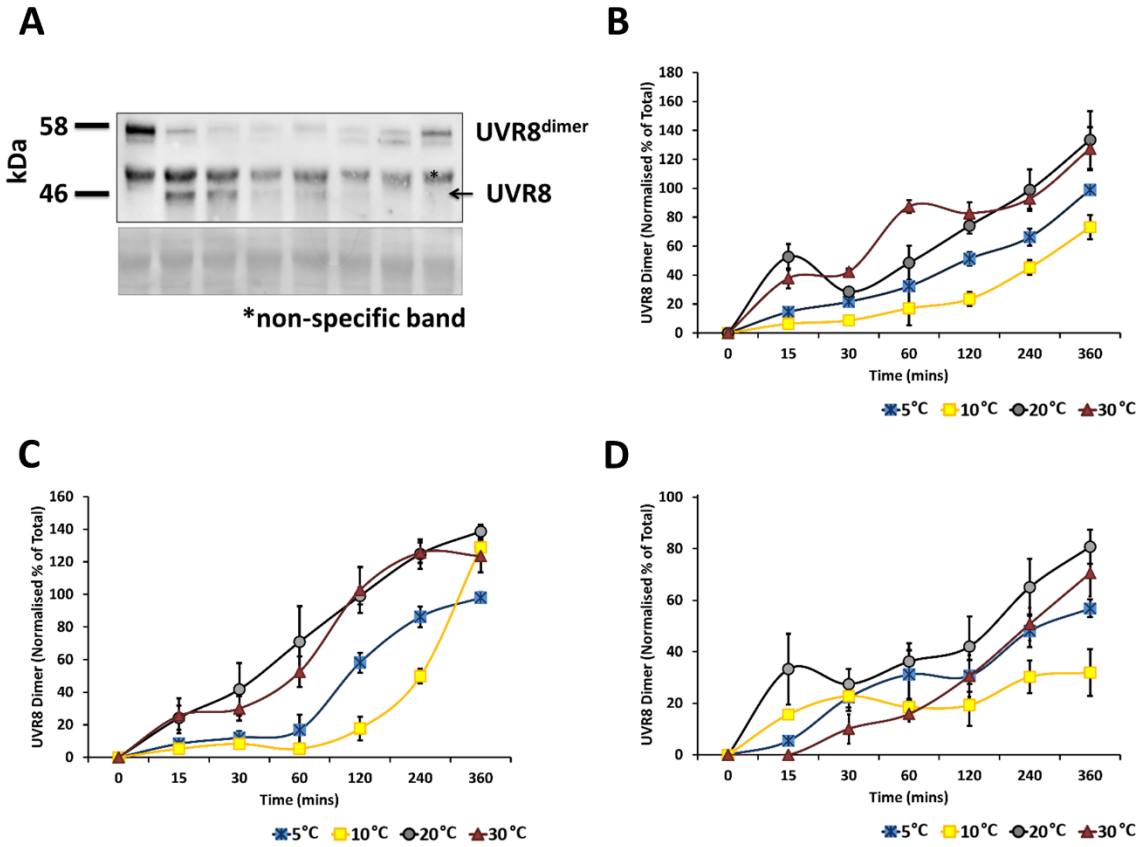

Fig 4-7: The effect of temperature on regeneration of the UVR8 dimer in Col-0, L*er* and *rup1rup2* plants. 10 day old UV-B naïve plants were transferred to four temperatures of interest for 24 hours in 20 µmol $m^{-2}s^{-1}$ white light. These plants were then given a brief, high intensity UV-B dose of 21 µmol m^{-2} s^{-1} for 15 minutes before being allowed to recover in darkness for 6 hours in the investigated temperature. UVR8 dimer percentage was measured through semi-native immunoblotting and quantified using ImageJ. (**A**) A representative Western Blot showing UVR8 dimer and monomer. rbcL was used as a loading control. Samples were taken prior to UV-B treatment, immediately post-UV-B treatment and then 15, 30, 60, 120, 240 and 360 minutes post-UV-B treatment. A quantified graph of UVR8 dimer regeneration at 5°C, 10°C, 20°C and 30°C showing standard error (n=9) for (B) L*er*, (C) Col-0 and (D) *rup1rup2*.

This pattern was repeated to some extent by the Col-0 plants. The control 20°C plants showed a faster regeneration of UVR8 to 100% dimer, this being achieved by 120 minutes. By 360 minutes, the total protein level had increased to 138%, very similar to the protein levels reached by L*er*. The 30°C treated plants had a lower increase in the amount of total protein, reaching the peak level at 240 minutes with 125%. The regeneration rate to 100% was similar than the 20°C plants, reaching a return to the $UVR8^{dimer}$ baseline at 120 minutes.

The 10°C treated plants appeared to regenerate far slower during the first 120 minutes of recovery, with less than 20% of the original $UVR8^{dimer}$ baseline recovered. If the regeneration of UVR8 had continued at a linear rate past this point it would have taken 10 hours for UVR8 to reach the prior dimer baseline. However within the next two hours to 240 minutes the dimer recovery more than doubled to 50% followed by an incredible rate of recovery to 128% between 240 and 360 minutes. Therefore, complete recovery was achieved between 240 and 360 minutes. The 5°C treated plants show a similar pattern to the 10°C treated plants during the first hour of recovery. Between 60 minutes and 240 minutes the 5°C treated plants recovered quicker than the 10°C treated plants, with 85% of the baseline recovered. However, while in the 10°C plants an extremely fast regeneration was seen in addition to more protein than was present in the baseline, the 5°C treated plants dimer recovery slowed. While the UVR8 dimer was able to recover to 100% at 5°C in Col-0 by 360 minutes, it did not show additional protein production in the recovery period allowed.

The rate of regeneration in the *rup1rup2* mutant plants was far more variable than in either the Col-0 or *Ler* plants. Total regeneration to 100% dimer was not seen at any temperature, nor was production of extra UVR8 protein. The overall regeneration rate at 20°C was 0.20%, compared to 0.19% at 30°C. At lower temperatures less UVR8 recovery was seen; the UVR8 dimer had only recovered to 31% in 10°C at a rate of 0.09% per minute and to 56% in 5°C at a rate of 0.15% per minute.

A comparison of the different lines showed that L*er* and Col-0 display a similar pattern of recovery, overall rate of dimer regeneration and extra UVR8 protein

production at 5°C, 20°C and 30°C. However at 10°C, although the initial recovery rate and pattern of regeneration was similar, Col-0 plants regenerated dimer at a faster rate and appeared to produce more UVR8 protein between 240 and 360 minutes, whereas in L*er* no UVR8 amount exceeding the baseline is produced at this temperature at all.

As a contrast, the *rup1rup2* plants are most similar to the WT plants at 10°C, showing a very slow rate of recovery. The rate of regeneration of the UVR8 dimer in the *rup1rup2* plants was most similar to Col-0 and *Ler* plants within the first hour following UV-B treatment for the cold 5°C and control 20°C treatment. After this point, at both temperatures, the regeneration rate and production of UVR8 in the *rup1rup2* plants was far slower. At 30°C there was very little similarity at all, with production of UVR8 and rate of regeneration of the dimer slower at every time interval.

4.7 Discussion

As shown previously in this thesis (Chapter 3) the simple model that UVR8 exists as a dimer in zero UV-B conditions which rapidly dissociates to a monomer in plus UV-B conditions does not describe the behaviour of UVR8 under continuous UV-B illumination. Although a great deal has been done to investigate the function of UVR8 in a controlled growth environment and the effect that natural solar UV-B has on plants, the function of UVR8 within plants in a natural solar environment has not been investigated. Additionally, the role that other factors may have on the balance of the photoequilibrium of UVR8, such as PAR to UV-B ratio and temperature has not been examined. This chapter showed that UV-B and temperature were important factors in determining the UVR8 photoequilibrium.

4.7.1 UV-B acclimated *in planta* conditions are key to the UVR8 photoequilibrium

UVR8 does not act as a simple $UVR8^{dimer} \rightleftharpoons UVR8^{monomer}$ switch in natural solar light. However, it is important to note that it is not a difference between controlled UV-B conditions and the natural solar spectrum that causes UVR8 to hold a photoequilibrium. Firstly, a photoequilibrium showing a balance between $UVR8^{dimer}$ and $UVR8^{monomer}$ had already been demonstrated in Chapter 3 of this

thesis. Furthermore, as shown in Fig 4.1, purified UVR8 protein did rapidly monomerise in very low fluence rates of UV-B and remains in the monomeric form throughout the day, despite the UV-B fluence rates remaining low. In addition, as seen previously (Heilmann and Jenkins, 2013) purified UVR8 was very slow to regenerate into the dimeric form. Ten minutes after sunset there was no visible $UVR8^{dimer}$. *In planta,* Heilmann and Jenkins (2013) begin to observe regeneration of the dimer after only five minutes and substantial regeneration after ten minutes compared to purified protein, where regeneration is only seen to begin around three hours after UV-B treatment. This supports previous discoveries regarding the importance of the intact cell in the regeneration of UVR8.

4.7.2 The UVR8 photoequilibrium is highly variable under natural solar conditions

While it has been made clear that UVR8 requires UV-B to monomerise (Miyamori, *et al*. 2015, Rizzini, *et al*. 2011, Wu, *et al*. 2011) the timecourses performed under natural solar conditions demonstrated that UV-B is not the only factor affecting the photoequilibrium. There was an extremely high level of variability shown between the different field condition timecourses (Fig 4-2). High variability in itself does not indicate that factors other than UV-B fluence rate effect the UVR8 photoequilibrium. Especially as there was a high variation of UV-B fluence rate recorded. However, there were days when very similar fluence rates of UV-B were measured that showed vastly different patterns of $UVR8^{dimer}/UVR8^{monomer}$ ratio. On some days, no monomerisation was seen, even though the UV-B fluence rate was well above what was required for purified UVR8 monomerisation or even the monomerisation of UVR8 in a controlled environment (Fig 4-2B and Fig 4-2E). On other days that were similiar with respect to UV-B fluence rate measurements, a far lower $UVR8^{dimer}/UVR8^{monomer}$ ratio was observed (Fig 4-2A and Fig 4-2H). This would suggest that factors other than UV-B fluence rate are involved.

Another interesting observation from this data was that while UVR8 was frequently observed as being completely dimeric in low UV-B conditions, it was very rarely seen to be completely monomeric in high UV-B conditions. Indeed, there was only one instance of 100% monomerisation throughout all 26

timecourses (Fig 4-2P); which occurred before sunrise when UV-B fluence rates were generally ~0.01 – 0.04 µmol m^{-2} s^{-1}. This would indicate that in natural solar conditions, in UV-B acclimated plants, UVR8 was very resistant to complete monomerisation.

It is important to note that while the length of night that UVR8 has had to recover varies with the time of year, from 15.5 hours (for Fig 4-2X) to 6.33 hours (for Fig 4-2K). Only five of the recorded timecourses (Fig 4-2B-C and Fig 4-2X-Z) had 100% $UVR8^{dimer}$ recorded at the first, pre-dawn timepoint. All five of these timecourses exhibited very low fluence rates of UV-B throughout the day. However, comparison with another timecourse that had comparable UV-B fluence rate readings (Fig 4-2D) which recovered to 100% dimer as the day progressed again suggests that it was not only the UV-B recorded on the day of the timecourse that was responsible for the dynamics of the UVR8 photoequilibrium, but that other factors were involved. It was possible that the previous day's UV-B fluence rate could affect the initial $UVR8^{dimer}/UVR8^{monomer}$ ratio. However, after the first timepoint post dawn, the UVR8 photoequilbrium demonstrates a significant degree of variability that cannot be said to be affected by the previous day's fluence rate.

A common pattern within the timecourses is a sinusoidal wave pattern of increase and decrease of the $UVR8^{dimer}/UVR8^{monomer}$ ratio. Excluding those timecourses that exhibit 100% dimer throughout the day, the sinusoidal trend was seen to a greater or lesser degree throughout the timecourses. This would suggest that the $UVR8^{dimer}/UVR8^{monomer}$ ratio is being affected by inputs other than UV-B fluence rate.

4.7.3 The UVR8 photoequilibrium is unlikely to be affected by total UVR8 protein levels

It has previously been reported that UVR8 total protein levels are unaffected by UV-B treatment (Kaiserli and Jenkins, 2007). However, it has been shown that for the most efficient rate of $UVR8^{dimer}$ regeneration, *de novo* protein synthesis is required (Heijge and Ulm, 2013, Heilmann and Jenkins, 2013). Therefore, it seemed wise to determine that chronic UV-B treatment did not change the production of UVR8 protein. If the total amount of UVR8 protein within the cell

changed depending on the presence of UV-B in a UV-B acclimated plant, it is likely that the $UVR8^{dimer}/UVR8^{monomer}$ ratio would also be affected.

As Fig 4-3 demonstrated, not only was there no significant difference in total UVR8 levels between UV-B acclimated plants and UV-B naïve plants, but no significant difference in total UVR8 levels throughout the day regardless of UV-B treatment. This showed that while the *de novo* protein synthesis affects the rate of regeneration to the dimeric form, possibly through *de novo* synthesis of RUP proteins (Heijdge and Ulm, 2013, Heilmann and Jenkins, 2013), a change in $UVR8^{dimer}/UVR8^{monomer}$ ratio was not seen due to changes in protein level of UVR8.

4.7.4 The photoequilibrium of UVR8 is affected by abiotic environmental factors

In order to determine the importance of different factors upon the photoequilibrium of UVR8, further analysis of the 26 timecourses was required. By pooling the information, the $UVR8^{dimer}/UVR8^{monomer}$ ratio was able to be directly compared to each of the key factors involved: UV-B fluence rate, PAR fluence rate, temperature and time of day.

UVR8 is not regulated by the circadian clock and the levels of UVR8 have been shown to be steady regardless of light treatment; however RUP expression is gated by the circadian clock (Tilbrook, *et al.*, 2013, Wang, *et al.*, 2011). The RUP proteins are key to maintaining the UVR8 photoequilbrium (Chapter 3). Therefore, the effect that time of day had upon UVR8 was investigated (Fig 4-4B and Fig 4-5F). Statistical analysis determined that time of day did not affect the $UVR8^{dimer}/UVR8^{monomer}$ ratio ($p=0.175$).

While it has already been extensively demonstrated that UVR8 does not respond in the absence of UV-B light (Brown, *et al.*, 2005, Brown and Jenkins, 2008, Christie, *et al.*, 2012, Cloix, *et al.*, 2012, Favory, *et al.*, 2009, Hayes, *et al.*, 2014, Huang, *et al.*, 2014, Kaiserli and Jenkins 2007, O'Hara and Jenkins 2012, Rizzini, *et al.*, 2011, Vandenbussche, *et al.*, 2014, Wargent, *et al.*, 2009 and Wu, *et al.*, 2012), these studies focused primarily either on how UVR8 affected morphology, photomorphogensis or gene expression *in planta* or on the molecular structure function of purified UVR8. None of these papers has looked

at the $UVR8^{dimer}/UVR8^{monomer}$ ratio and how it changes with the UV-B fluence rate. It is important to investigate this relationship. It has been shown that PAR does not affect UVR8 (Cloix, *et al.*, 2012 and Kaiserli and Jenkins, 2007). However, that does not mean that an interactive effect between UV-B and PAR upon regulation of the UVR8 photoequilibrium doe not exist. Indeed, evidence shows that UV-B naïve plants can be primed for a UV-B response using blue light (Wade, *et al.*, 2001). In the case of PAR, it was important that while an association was seen between the UVR8 Dimer % and PAR and this association increased when the additive effect of UV-B fluence rate and PAR was investigated, it did not fit the data better than the null hypothesis that only UV-B affects UVR8 Dimer % and so was rejected (Fig 4-5D).

The final factor that was measured was the ambient temperature. Temperature was strongly correlated with UV-B fluence rates (Fig 4-5E). The same conditions that were applied to the PAR dataset were also applied to determine if temperature affected the $UVR8^{dimer}/UVR8^{monomer}$ ratio. There was an extremely strong association between the $UVR8^{dimer}/UVR8^{monomer}$ ratio and temperature, a stronger statistical correlation than between the $UVR8^{dimer}/UVR8^{monomer}$ ratio and the UV-B fluence rate. However, further investigation showed that in the absence of UV-B, monomerisation did not occur even at quite high temperatures (Fig 4-6). Therefore it was the additive and interactive effects of Temperature and UV-B Fluence rate that were important. The model that best fit the outside data was confirmed to be %Dimer = UV-B Fluence Rate + Temperature. The UVR8 photoequilibrium was affected by the UV-B fluence rate and the temperature. This would suggest that temperature may help to describe some of the variation seen within the timecourses that is not explained by the UV-B fluence rate.

4.7.5 The $UVR8^{dimer}/UVR8^{monomer}$ ratio is affected by temperature via the rate of reversion from monomer to dimer.

By measuring the regeneration rate of the $UVR8^{dimer}$ in UV-B naïve plants at a series of varying temperatures in two ecotypes and the *rup1rup2* mutant, the effect of temperature and the role the RUPs play in the regeneration rate was investigated (Fig 4-7). For both Col-0 and L*er* plants at 20°C, regeneration rate was rapid; conversely regeneration in the *rup1rup2* mutant was reduced and

slow, although faster than seen in purified protein, supporting results from Heidge and Ulm (2013) and Heilmann and Jenkins (2013). There did not appear to be much difference in regeneration rate at the higher temperature of 30°C from the baseline control from any of the three plant lines. The lower temperatures showed differentiation, in that for both Col-0 and L*er* slower regeneration of the dimer was seen compared to a similar rate of regeneration for the *rup1rup2* plants. Furthermore, for both the Col-0 and L*er* lines, the regeneration rate at 5°C was quicker than at 10°C. This correlates with the outside data, where samples taken between 7-10°C showed a lower level of dimer.

The lack of difference in rate of regeneration in the *rup1rup2* mutants suggested that the difference seen through temperature was not due to the kinetics of the $UVR8^{dimer}$ or $UVR8^{monomer}$. Instead the differential in regeneration, and therefore in $UVR8^{dimer}/UVR8^{monomer}$ ratio and UVR8 photoequilibrium, was due to the RUP proteins.

There are several possibilities for how temperature may be affecting the RUP proteins. The RUP proteins are expressed not only in response to UV-B, but also in response to red, far-red and blue light (Gruber, *et al.*, 2012); the expression of the RUPs is under circadian control (Tilbrook, *et al.*, 2013, Wang, *et al.*, 2011). It was possible that the RUPs experience differential expression under different temperature conditions, for example at low temperatures like 5°C expression may be higher. The expression level may decrease as temperatures increase. This differential in expression level could lead to a difference in protein level, partially compensating for reduction in protein activity at lower temperatures. However, measurements of RUP protein levels have not been reported, so differences in expression level do not necessarily correlate to differences in protein level.

Alternatively, the changes in regeneration rate could just be due to differences in protein activity. The optimal growth temperature for *A. thaliana* is 22-23°C (ABRC Seed handling guidelines). It is not unreasonable to assume that at lower temperatures proteins will have a lower activity. The slower regeneration rate

seen at 5°C and 10°C compared to 20°C and 30°C could be explained by differences in protein activity due cold. While plants had been grown at both 5°C and 10°C in this study, they were not germinated at these temperatures and the plants had established true leaves before being transferred to these conditions. Furthermore it was possible that a combination of change in protein expression and protein activity resulted in the difference between regeneration rates at varying temperatures. While both 5°C and 10°C are cold temperatures for *A. thaliana,* the difference in regeneration rate between 5°C and 10 °C may be explained by a stress response. An *A. thaliana* plant that is experiencing 5°C over a sustained period of time is likely to be experiencing cold stress. One of the responses to stress can be a change in flowering time, a response that the RUP proteins are involved in, where they are known as EFO (Wang, *et al*. 2011). If cold temperatures cause an increase in RUP protein expression, this could have a knock on effect causing an earlier flowering time (Wang, *et al*. 2011). This could be particularly useful for winter annual *A. thaliana*, which germinate in autumn, survive the winter as rosettes and flower in spring and early summer (Koorneef, *et al*. 2004). These ecotypes frequently need to be vernalised as rosettes in order to flower. However this does not mean that an ecotype that is a summer rather than winter annual would not also respond to 'vernalisation' through the upregulation of flowering genes.

4.7.6 Relating controlled growth room experiments to field conditions

This study has combined statistical conclusions drawn from both controlled growth room conditions and field conditions. While a controlled growth room environment allows for manipulation of specific conditions, meticulous controls and a very stable environment; field conditions are by definition more variable. It is impossible to repeat exact days. However, just as controlled growth conditions allow for elucidation into the reaction of plants grown in identical conditions with one changing variable, field experiments are also incredibly important for understanding how plants actually grow in their natural environment. The environment that a plant is growing in changes on many different timescales, from extremely small and transitory changes – for example, the shadow of an animal passing over the plant; to short term changes, changes

in weather; to long term, the changing average temperature as seasons pass. Plants must not only decide whether or not to react to such stimuli, but also interpret potentially conflicting signals. By combining controlled growth room experiments with field experiments it was possible to determine how UVR8 and the RUP proteins act in an ideal environment; but also to see whether this did translate to the mechanics and kinetics of these proteins in plants growing in a natural environment.

4.7.7 The limitations of semi-quantitative work

The analysis performed in Chapters 3 and 4 of this study relies heavily on semi-quantitative Western Blot analysis. This method has been utilised, accepted and widely-published both within and without the UV-B field. The use of two separate controls to ensure equal protein loading reduces the risk of artificial changes between timepoints for total protein amount, which in turn lowers the chance of artificial changes being found in the photoequilibrium. By measuring the proportion of UVR8 dimer to UVR8 monomer within one lane, artifacts caused by differing protein amounts between blots and timepoints were once again minimised. Use of the Fusion Imager allows for saturation in the images being analysed to be noticed and re-exposed to remove saturation and allow for differences in protein level to be analysed. Biological replicates not only showed the variability of biological systems within one set of conditions, but also between separate Western Blots. Nevertheless, with all of these precautions Western Blot analysis is still semi-quantitative. Furthermore, while it has been shown that UVR8 can be completely dimeric on a non-boiled SDS-PAGE Western Blot, it is possible that some monomerisation could occur post-harvest of a sample, leading to an artificial change in the UVR8 photoequilibrium.

Real time measures of protein-protein interaction have been developed. For example use of bioluminescence resonance energy transfer (BRET) to examine nuclear localisation of COP1 and its ability to form a homodimer have been investigated (Subramanian, *et al.* 2004). This technique involves using two differentially tagged proteins that emit one frequency of luminescence when interacting with each other and only one of the proteins emits a different wavelength of luminescence when protein cleavage occurs. There are several

reasons why this technique has not been utilised in this study. Firstly, while interactions between homodimers have been published (Subramanian, *et al*. 2004) and proteins have to be within range of dimerisation for the wavelength of luminescence to change (Bücherl, *et al*. 2010, Bücherl, *et al*. 2014) there is an issue in measuring homodimers compared to heterodimers. Aside from the time consuming nature of creating stable lines that produce two differently labelled versions of the same protein, there is no guarantee that each labelled protein will dimerise with a protein of the reciprocal label. Therefore, while this technique would address some of the issues with semi-quantative Western Blot analysis, it too would result in a UVR8 photoequilibrium that was artificial.

4.8 Conclusions

The UVR8 photoequilibrium in a natural solar environment is extremely complex. While the photoequilibrium requires UV-B to develop, it has been shown that other factors are involved which regulate the overall $UVR8^{dimer}/UVR8^{monomer}$ ratio. Temperature, in particular, plays a key role through interaction with the RUP proteins. This would suggest that the primary deciding factor in balancing the UVR8 photoequilibrium are the RUPs, a conclusion that is supported by the inability of purified UVR8 to form a photoequilibrium in natural solar light and the requirement of the RUPs for efficient dimer regeneration shown by Heidge and Ulm (2013) and Heilmann and Jenkins (2013). This would suggest that if plants have evolved to acclimate to different levels of UV-B as suggested by previous results in Chapter 3 of this thesis, changes would occur with the RUP proteins rather than within UVR8. Chapter 5 of this thesis posits that those *A. thaliana* plants that have evolved within a high UV-B environment (for example, high altitude or low latitude) will have common mutations in a UV-B acclimation haplotype.

Chapter 5: Global Distribution and Population Genetics of the UV-B Haplotype in *A. thaliana.*

5.1 Introduction

Studies on UVR8 and the UV-B response have primarily focused on *A. thaliana*, and indeed even more narrowly on the Col-0 and L*er* ecotypes (Cloix, *et al*. 2012, Heijdge and Ulm, 2013, Heilmann and Jenkins, 2013, Kaiserli and Jenkins, 2007, O'Hara and Jenkins, 2012). The effect of protein structure on UVR8 *in planta* has also been studied previously. For example, through mutagenesis studies the 27 amino acids found at the C terminal of UVR8 have been found to be required for interaction with COP1, although UV-B exposure is required for the interaction (Cloix, *et al*. 2012). Moreover this region is necessary for gene expression and has been tied to UV-B hypocotyl repression in *A. thaliana* (Cloix, *et al*. 2012) and partially to UV-B mediated shade avoidance (Hayes, *et al*. 2014). However, the C27 region is not required for UVR8 photoreception (Christie, *et al*, 2012, Wu *et al*. 2012). UVR8 without the C27 region can still monomerise, accumulate in the nucleus and interact with chromatin (Cloix, *et al*. 2012). Finally, this region of the protein is also the area of interaction for the RUP proteins, but unlike the UVR8-COP1 interaction, UVR8-RUP interaction does not require UV-B exposure (Cloix, *et al*. 2012).

Other mutagenesis studies have shown how different point mutations affect the interaction and function of the UV-B photomorphogenic pathway proteins. For example $UVR8^{G145S}$ and $UVR8^{G202R}$ result in non-functional mutants - in that CHS is not upregulated - that are unable to interact with COP1 (Favory, *et al*. 2009). Mutational studies performed on COP1 determined which region is important for interaction with UVR8 (Favory, *et al*. 2009). The effect of point mutations on whether UVR8 exists primarily as a dimer or as a monomer have also been performed and how this affects interaction with COP1, RUP1 and RUP2 has been reported (O'Hara and Jenkins, 2012, Huang, *et al*. 2014). These studies also

linked gauges of UV-B photomorphogenesis such as gene expression, anthocyanin levels or hypocotyl length to different point mutations (Huang, *et al*. 2014).

These studies have pushed understanding of how the structure of UVR8 and COP1 affect UV-B photomorphogenesis and plant response, revealing that UVR8 is the UV-B plant photoreceptor. However, it is possible that there are mutations that would not cause a strong phenotype in a lab environment that would still affect how a plant would respond to long term UV-B exposure. There is a huge natural variation present in *A. thaliana*, it exists over a truly impressive naturalised range found in North America, Europe, Africa and Asia from below sea level in the Netherlands to above 4000m (Anwer and Davis, 2013, Koorneef *et al*. 2004). This habitat span encompasses a wide range of different environmental conditions, which makes *A. thaliana* an ideal organism for studying environmental adaptation. The appropriateness of using *A. thaliana* has only increased with the 1001 Genomes Project, which has sequenced and put online the entire genome sequences of 855 different ecotypes collected from across the naturalised range of the plant (Table 5-1). Through the use of the 1001 Genomes Project it has been possible to document not only what polymorphisms are naturally occurring in the global *A. thaliana* population, but whether these changes are synonymous – resulting in no amino acid change – or non-synonymous – resulting in a change in protein sequence. Furthermore it was also possible to correlate what type of environments these changes occur in and whether this is different for different genes.

This study has shown that the ecotype of *A. thaliana* used has an effect on the UVR8 photoequilibrium and plant morphology under UV-B light (Chapter 3 and Chatper 4). Previous studies on the variability between different ecotypes of *A. thaliana* have shown that photoreceptors are targets for diversifying selection and that lab created 'mutants' are found within the natural population of *A. thaliana* (Filiault *et al.*, 2008, Maloof, *et al*. 2001). Indeed, it has already been found that different ecotypes vary in their response to UV-A and UV-B light (Cooley, *et al*. 2001, Torebinejad and Caldwell, 2000). When these studies were done, UVR8 had not yet been identified as the UV-B photoreceptor (Rizzini, *et al*. 2011, Christie, *et al*. 2012, Wu, *et al*. 2012). Therefore it was not possible to

Table 5-1: The countries where samples originated from and the number of ecotypes sampled from each country.

Country	Sample Number	Country	Sample Number
Armenia	7	*Libya*	1
Austria	8	*Lithuania*	4
Azerbaijan	3	*Mongolia*	1
Belgium	3	*Morocco*	3
Bulgaria	16	*Netherlands*	14
Canada	3	*Norway*	2
Canary Islands	1	*Poland*	3
Cape Verde Islands	2	*Portugal*	10
Croatia	2	*Romania*	8
Czech Republic	38	*Russia*	52
Denmark	4	*Serbia*	8
Finland	4	*Slovakia*	3
France	51	*Spain*	104
Georgia	7	*Sweden*	181
Germany	121	*Switzerland*	5
Greece	3	*Tajikistan*	5
India	2	*Tanzania*	2
Ireland	2	*Turkey*	2
Italy	56	*UK*	54
Japan	5	*Ukraine*	4
Kazakhstan	1	*USA*	40
Kyrgyzstan	5	*Uzbekistan*	3
Lebanon	2		

determine whether these changes were due to differences in the protein structure of UVR8, its interacting proteins or another factor such as anthocyanin accumulation. Now it is not only possible to compare the sequences of UV-B responsive proteins in the relatively small number of ecotypes that have been studied, but also a far larger number from across the naturalised range of the plant. This has allowed an initial study to be performed that compares the variation of these sequences when individual ecotypes are grouped geographically or altitudinally. In turn, this study can inform future experimentation, such as which ecotypes contain sequences that are found more frequently at higher altitudes than lower altitudes and therefore are more likely to have a different UV-B response.

In this study, only non-synonymous changes compared to the selected wild-type will be investigated to determine whether changes in protein sequence are correlated to a specific environment. Six genes were chosen for the analysis and were split into two different groups: genes that are directly involved in UV-B photoreception – UVR8, RUP1 and RUP2 - and those which are involved in the transcriptional response to UV-B – COP1, HY5 and HYH. UVR8 was chosen as the UV-B photoreceptor. Changes in UVR8 that correlate to high UV-B environments are likely to be indicators of adaptation. RUP1 and RUP2 have been shown to be the negative regulators of the UV-B photomorphogenic pathway, acting to redimerise UVR8 (Heijge and Ulm, 2013, Heilmann and Jenkins, 2013). Changes in these proteins could affect the efficiency with which they are able to interact with UVR8, changing the UVR8 photoequilibrium and resulting gene expression.

COP1 was chosen as while it is required for UVR8 mediated UV-B gene expression and photomorphogenesis (Favory, *et al.*, 2009) it also plays a major role in the other photoreception pathways. COP1 is a protein that interacts with a large number of proteins. It has been cited as interacting with COP1 Interacting Protein 8 (CIP8), SPA1, SPA2, SPA3, SPA4, B-box Zinc Finger Protein 24/Salt Tolerance (BBX24/STO), BBX25/Salt Tolerance Homolog (STH), PHYA, as well as with UVR8 (Torii, *et al.* 1999, Hoecker and Quail, 2001, Holm, *et al.* 2001, Laubinger and Hoecker, 2003, Laubinger, *et al.* 2004, Saijo, *et al.* 2008, Favory, *et al* 2009). It would therefore be expected that COP1 is under a lot of conserving selection pressure. Single amino acid changes have been shown to have a huge effect in COP1's ability to interact with UVR8 and therefore the UV-B photomorphogenic pathway (Favory, *et al.*, 2009). Changes within COP1 may be a response to differing UV-B environments, but could just as easily be due to changing PAR environments. This has to be taken into consideration when analysing the results. The same is true for HY5 and HYH. These genes are transcription factors that are redundant in function with HY5 playing the dominant role in the UV-B photomorphogenic pathway (Brown and Jenkins, 2008). Changes in these genes could relate to changes in gene specificity. However, these genes are involved in many different signalling pathways including flowering time, ethylene signalling and anthocyanin accumulation at

cold temperatures (Sibout, *et al*. 2006, Jonassen, *et al*. 2008, Nemhauser, 2008, Zhang, *et al.*, 2011). As has been shown in Chapter 4 of this work (Fig 4-5), as PAR rises, UV-B fluence rate also rises. Therefore it is possible that higher PAR fluence rates could be used as a shorthand for higher UV-B fluence rates.

In this study Col-0 has been chosen as the 'wild-type' ecotype, which was originally found in the USA at 38.5, -92.5, 264m above sea level. There are several reasons that Col-0 was chosen to be the wild-type. The first is that it is one of the key mutant plants used within this thesis and in studies of the RUP proteins, *rup1rup2*, is in a Col-0 background. Therefore, understanding of how the structure function of RUP proteins affects UV-B photomorphogenesis must be done with this in mind. Furthermore, Col-0 is a frequently used ecotype throughout many labs.

Therefore the aim of this chapter is to investigate the diversity of *A. thaliana* UVR8 and related UV-B response genes and to evaluate the variation of these different genes under different groupings. It is hypothesised that UVR8 in particular will vary in response to different light environments as other photoreceptors such as phytochrome have also been shown to be targets for diversifying selection (Filiault *et al.*, 2008). In contrast it is posited that the proteins that are involved in multiple pathways, such as COP1 and HY5, will be conserved through purifying selection. As HYH is a redundant protein to HY5, it is theorized that it will be less conserved that HY5. The RUP proteins are redundant to each other and involved in flowering as well as regulation of the UV-B photomorphogenic pathway (Wang, *et al.* 2011). Therefore, it is hypothesised that both will be conserved with RUP2 being more conserved as it plays a larger role in both UV-B regulation (Gruber, *et al*. 2010).

5.2 The variability of UVR8 protein sequence

In order to determine whether there were natural genetic differences between *A. thaliana* ecotypes that may affect the function of UVR8 and related proteins, the 1001 Genomes Project was used to determine the different natural haplotypes. The 1001 Genomes Project Browser was used to compare all UVR8 sequences found within the included ecotypes to Col-0. Only non-synonymous,

coding region sequences were documented. The residue position of the change was determined using an alignment Basic Local Alignment Tool (BLAST) from the National Center for Biotechnology Invformation (NCBI), the bl2seq. The sequence from Col-0 was designated haplotype number 1 as were all all ecotypes that did not contain any non-synonymous changes from the Col-0 sequence. Further haplotypes were documented using a list of the residues within Col-0 that changed within the new haplotype, the residue number and the residue within that haplotype. For example, for a P13L change Col-0 that contained a Proline at position 13, which had been changed to a Leucine at position 13 in a different ecotype.

As ecotype names were given, it was possible to use the NASC and ABRC to determine the latitude and longitude of origin of each ecotype: and then the altitude was determined through Google Maps or Google Earth, (Google Maps, 2015, Google Earth 2015). In order to analyse the large volume of data harvested from the 1001 Genomes Project, a series of scripts written in Python were created to sort and categorise the individuals according to geographical location or altitude (Appendix A). A further script, also constructed in Python, was created to output a file type for use in the PopArt statistical analysis program (Appendix B). These scripts can be adapted for any gene with any number of haplotypes for use with a Microsoft Excel input for future work and analysis. Further work is required to allow this script to automatically adapt to new categories and to create an easy to use GUI, but this is certainly achievable although outside the scope of this project.

The predicted protein structure as solved by both Christie *et al*. 2012 and Wu *et al*. 2012 was used to determine where the mutations fell in the 3D structure. This information in conjunction with current studies that document the effect of lab created mutations was used to inform whether a change would be likely to cause a complete knock-out of the protein or rather a partial loss of structure or function.

There were 22 different protein sequences found for UVR8 within the 855 *A. thaliana* sequences (Table 5-2). Within these 22 haplotypes there were 19

segregating sites: sites at which a polymorphism - or change in amino acid - was present. Five of these changes were parsimony informative sites: V308I, H67L, H118Q, P13L and A7G (Table 5-2). Of the 22 haplotypes observed, 10 were seen only once. However many of these haplotypes contained mutations that were also found elsewhere, for example haplotype 7 contained V308I, a mutation that was seen in 138 other individuals in haplotype 2. This would indicate that the haplotype 7 individual had experienced one more mutation event than the individuals within haplotype 2. Therefore when considering the implications of the location or environment in which haplotype 7 is found it was important to also consider whether or not it is grouped with the haplotype 2 individuals.

Table 5-2: Documentation of the shared mutations, unique muations, the haplotype they occur in, the frequency of the haplotype and the number of changes in comparison to the Col-0 UVR8 sequence. Haplotypes are displayed using the designated number, presence of a change is represented with a '+' and absence of a change with a '–'. Haploytpes are arranged to best show the relationship between the different shared mutations.

Haplotype	V3081	H67L	H118Q	P13L	A7G	Unique	Changes	Number
1	-	-	-	-	-	-	0	553
9	-	-	-	-	-	+	1	3
22	-	-	-	-	-	+	1	2
16	-	-	-	-	-	+	1	1
17	-	-	-	-	-	+	1	1
18	-	-	-	-	-	+	1	1
19	-	-	-	-	-	+	1	1
12	-	-	-	-	+	-	1	2
6	-	-	-	-	+	+	2	1
20	-	-	-	-	+	+	2	1
2	+	-	-	-	-	-	1	138
7	+	-	-	-	-	+	2	1
10	-	-	+	-	-	+	2	2
5	-	+	+	-	-	-	2	8
21	-	+	+	-	-	-	2	1
13	-	+	+	-	-	+	3	1
14	-	+	+	-	-	+	3	1
3	-	+	+	+	-	-	3	119
8	-	+	+	+	-	+	4	8
15	-	+	+	+	-	+	4	5
11	-	-	+	+	-	-	2	3
4	-	+	-	+	-	-	2	2

Three of the parsimony informative sites were frequently grouped together in various combinations. The P13L change was only observed without the co-

occurring H118Q change or the H67L change in one example each. Ten of the haplotypes contain some combination of these three amino acid changes. Haplotype 1 was by far the most common haplotype, suggesting that Col-0 does indeed contain the "wild-type" or ancestral UVR8 protein sequence.

5.2.1 UVR8 protein sequence variation differs by geographical location

A TCS network was constructed using the PopART tool (http://popart.otago.ac.nz, Clement, *et al.* 2002). This required that the aligned nucleotide sequence, the frequency of haplotype as well as the latitudes and longitudes that each was found in was provided. The number of geographical clusters to be used was also required. PopART clustered the sequences of the individuals into ten groups centered in Sweden, Tanzania, the Western USA, Spain, Greece, France, the Eastern USA, Kazakhstan, Japan and South West Russia (Fig 5-1). Each circle represented a different haplotype. The circles were sized based on the number of samples each represents. Furthermore they contained pie charts representing the proportion of each haplotype that can be found in each geographical cluster. Haplotypes were connected by edges to other haplotypes that they are related to. Each hatch mark on an edge documented how many changes were required to move from one haplotype to another. For example, there was one change between haplotype 1 and haplotype 2 and they were connected by an edge with one hatch mark. The black circular marks represented potential haplotypes that were not found within the sample population. It can be clearly seen that haplotype 1 was the most common haplotype followed by haplotypes 2 and 3. There were also several haplotypes that contain only one sample, represented by the smallest circle and documented in Table 5-2 (Fig 5-1).

There were two 'branches' of the network that were of particular interest. These branches showed that particular changes were common to particular geographical regions. Haplotypes 12, 20 and 6 were all found within the Swedish group of accessions and all contained the A7G change from Col-0. Indeed this change was only found within Sweden. This would suggest that either the A7G

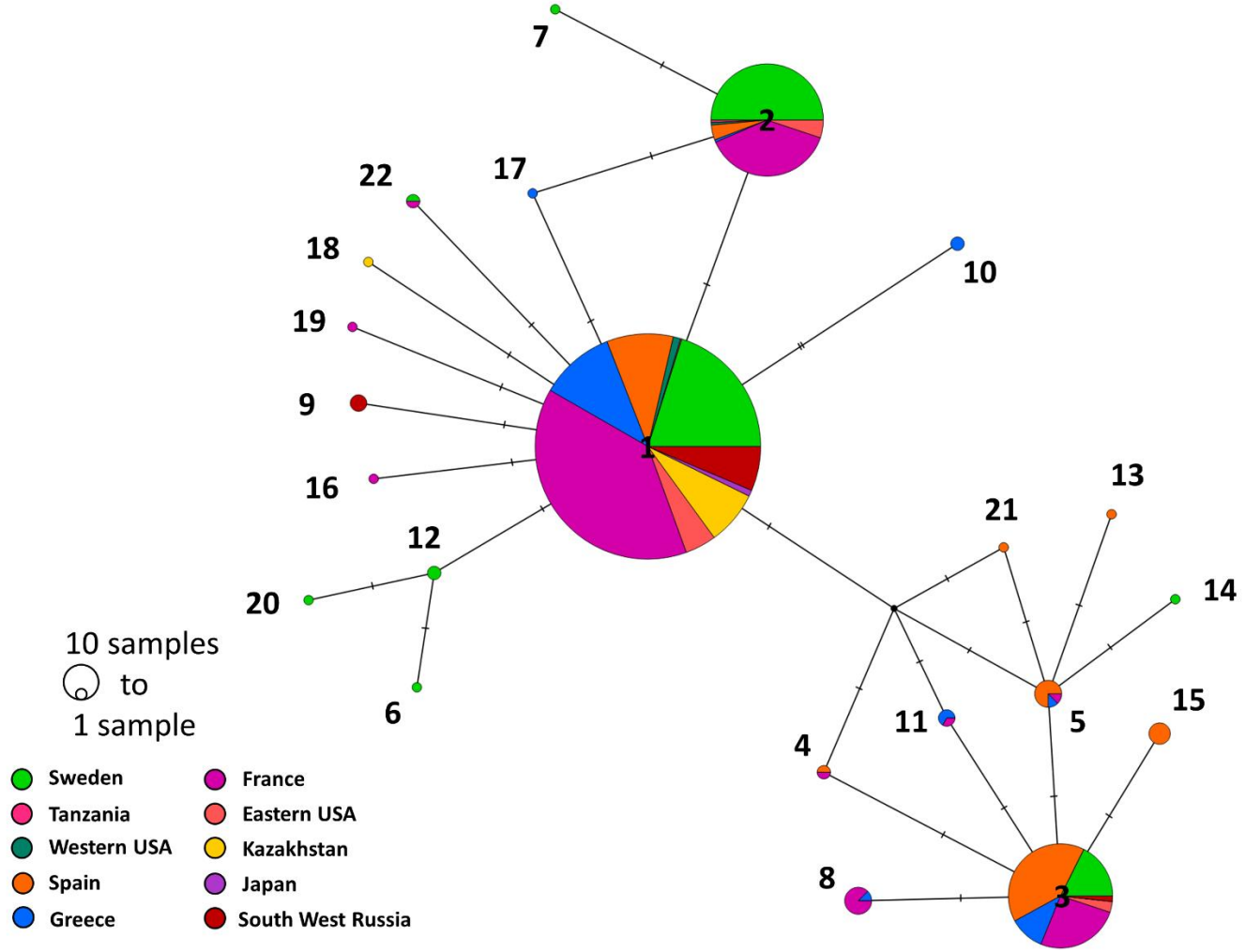
7
2
22
17
18
10
19
9
1
16
13
21
12
14
20
10 samples
to
1 sample
6
4
11
5
15
8
3
Sweden
France
Tanzania
Eastern USA
Western USA
Kazakhstan
Spain
Japan
Greece
South West Russia

Figure 5-1: A TCS network of UVR8 diversity grouped by geographical location. Circle size represents the number of samples within each haplotype with the location that each haplotype is found indicated by colour.

change was beneficial for the Swedish environment or that these haplotypes all had a common ancestor. The other branch was far more diverse both in the number of changes seen and the geographical locations these were found in. These haplotypes all contained a combination of the P13L, H67L and H118Q mutations (occasionally including a further unique mutation). These haplotypes were found primarily in the Spanish, French and Greek groups, which could be considered a Mediterranean supergroup. However, they were also observed in the Swedish, South West Russian and Eastern USA groups. An AMOVA test was used to determine whether the UVR8 haplotype varied based on geographical separation. Within the UVR8 haplotypes grouped by geographical location 13.27% of the variation occured among populations ($p<0.001$).

5.2.2 UVR8 sequence varies according to altitude

When altitude was used to group the individuals instead of geographical location the colouring of the TCS network changes dramatically. Seven different altitudinal groupings were used. Haplotypes were listed and the frequency within each altitude range (below 500m, between 500 and 1000m, between 1000 and 1500m, between 1500 and 2000m, between 2000 and 2500m, between 2500 and 3000m and above 3000m) was included for PopART to construct the TCS network (Fig 5-2). It becomes clear that although *A. thaliana* has a remarkable altitude range, the majority of individuals used within the 1001 Genomes Project were found below 500m. Of those that were found above 500m, a good proportion of them had the same sequence as Col-0. However there were still some interesting patterns that were worth considering. Haplotypes 3, 4, 5, 8, 11, 13 and 15 all contain individuals that were found above 500m and all of them contained at least two of the P13L, H67L and H118Q changes. Indeed haplotype 4 was found up to 1500m, haplotype 5 was found up to 2000m and haplotype 3 was found up to 2500m with all of these haplotypes including the H67L change. Haplotype 10 was relatively similar. It was found exclusively between 500 and 1000m and contains the H118Q mutation. There were two further haplotypes that were found above 500m, haplotype 2 which had a V308I change and haplotype 9 which contained a S160A change. The majority of these changes

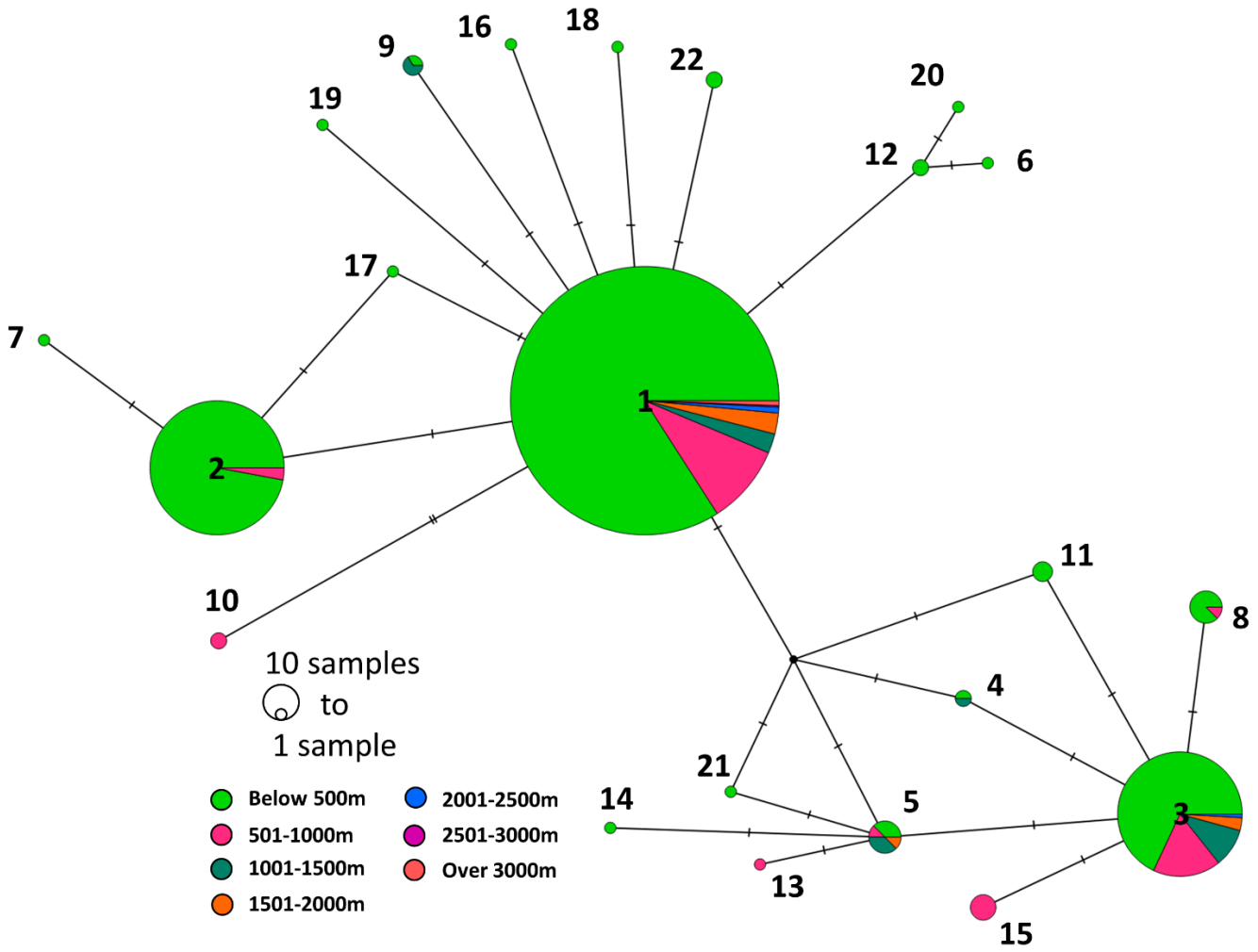
9
16
18
22
20
19
12
6
17
7
1
2
10
11
8
4
21
14
5
3
13
15
10 samples
to
1 sample
Below 500m
501-1000m
1001-1500m
1501-2000m
2001-2500m
2501-3000m
Over 3000m

Figure 5-2: A TCS network of UVR8 diversity grouped by altitude. Circle size represents the number of samples within each haplotype with the altitude that each haplotype is found indicated by colour.

were found on the outside of the UVR8 barrel, with P13L being the exception and found in the N-terminus. It was determined that grouping the UVR8 haplotypes by altitude resulted in significant differences between groups ($p<0.001$). However the amount of variation that was seen among populations is a lot smaller than was seen for geographical grouping at 5.17%. However, considering the degree of geographic separation this was not entirely surprising and would suggest that some of these changes were adaptive to higher altitude and therefore UV-B fluence rate.

5.3 The variability of the COP1 protein sequence

COP1 had 18 segregating sites. It also had three parsimony informative sites: P17L, Q256P and D579H. The remaining 15 sites were unique and the haplotypes frequently consisted of only one individual. The majority of the individuals sequenced (92%) had the same COP1 sequence (Table 5-3). There was only one other haplotype that contained more than one individual, haplotype 3. Indeed, COP1 contained more segregating sites than haplotypes.

Table 5-3: Documentation of the shared mutations, unique muations, the haplotype they occur in, the frequency of the haplotype and the number of changes compared to the Col-0 sequence of COP1. Haplotypes are displayed using the designated number, presence of a change is represented with a '+' and absence of a change with a '–'. Haploytpes are arranged to best show the relationship between the different shared mutations.

Haplotypes	P17L	Q256P	D479H	Unique	Changes	Number
1	-	-	-	-	0	788
3	+	-	-	-	1	38
5	+	-	-	+	2	1
14	-	+	-	-	1	1
15	-	+	+	-	2	2
17	-	-	+	-	1	1
2	-	-	-	+	1	3
4	-	-	-	+	1	5
6	-	-	-	+	1	2
7	-	-	-	+	1	1
8	-	-	-	+	1	1
9	-	-	-	+	1	1
10	-	-	-	+	1	1
11	-	-	-	+	1	2
12	-	-	-	+	1	1
13	-	-	-	+	3	5
16	-	-	-	+	2	2

5.3.1 The sequence of COP1 varies according to geographic location

When the haplotypes of COP1 were plotted as a TCS network using geographical clustering through PopART (http://popart.otago.ac.nz, Clement, *et al*. 2002) it became clear that there was not as much diversity found within the sequence as was seen within UVR8 (Fig 5-3). The geographical groups were centered around Russia, Tanzania, Kazakhstan, Spain, Finland, Greece, France, Japan, the USA and Sweden. The vast majority (92%) of the individuals were haplotype 1, which was found universally throughout all of the geographical groupings. The other haplotypes generally contained only one change from the Col-0 sequence, were found infrequently and did not contain many lineages. There were two small branches found within the network. Haplotypes 14, 15 and 17 were found in the Greek group, the Russian Group and the Japanese group respectively and contained either a Q256P change, a D579H change or both. The second small lineage was composed of haplotypes 3 and 5 which both contained a P17L change (haplotype 5 contained a further unique change). These haplotypes were both found in the French region, although haplotype 3 was further found in the Spanish, Swedish and USA groups.

While an AMOVA performed using geographical groupings gave a statistically significant p-value (p=0.005) there was far less variation than was seen for UVR8. Only 1.74% of the variation within COP1 was found among geographical groupings. These results would suggest that the COP1 sequence does vary according to geographical location, but that it was still conserved.

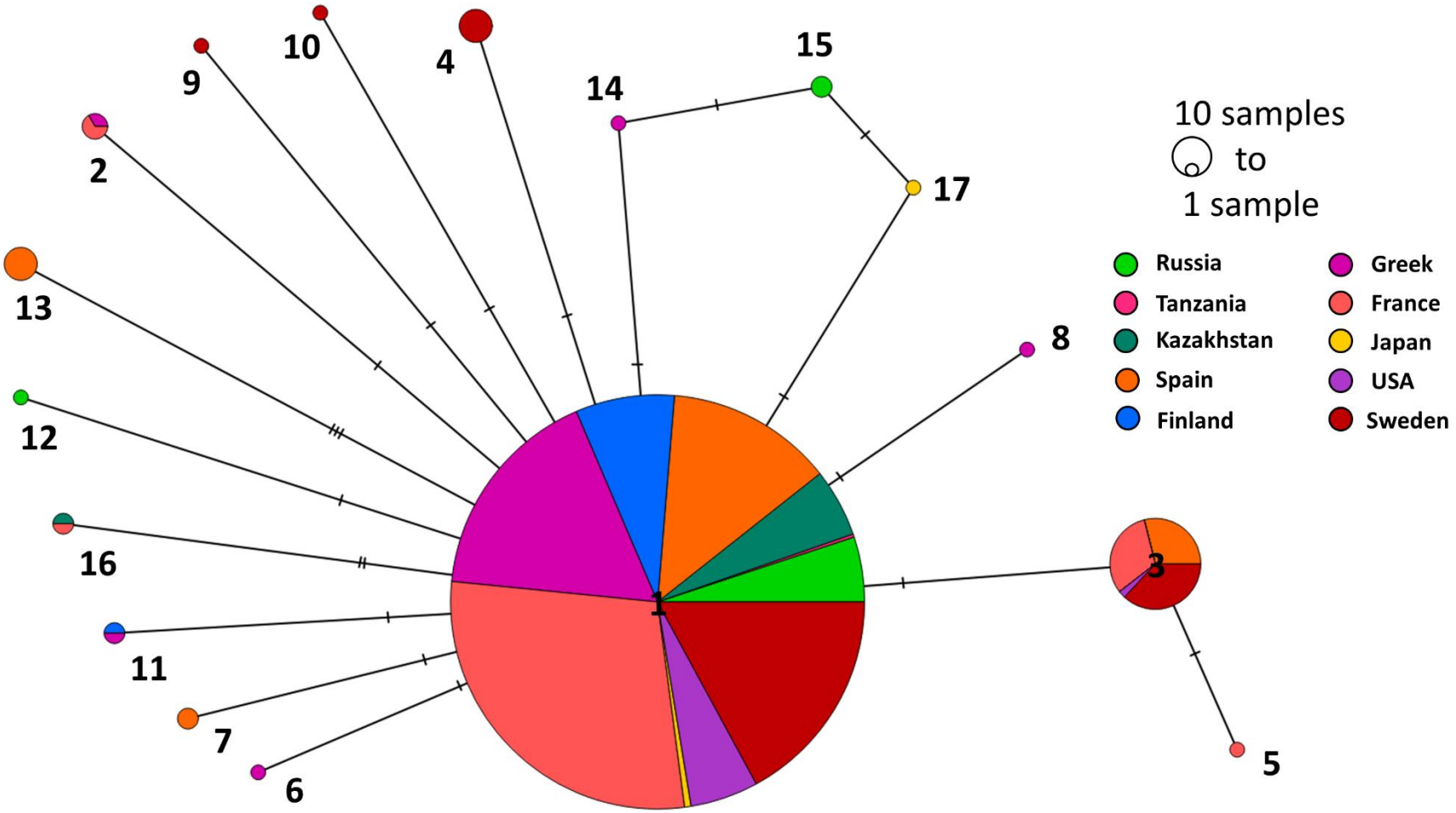
10
4
15
9
14
2
17
13
8
12
16
3
1
11
7
5
6
10 samples
to
1 sample
Russia
Greek
Tanzania
France
Kazakhstan
Japan
Spain
USA
Finland
Sweden

Figure 5-3: A TCS network of COP1 diversity grouped by geographic location using latitude and longitude. Circle size represents the number of samples within each haplotype with the cluster that each haplotype is found indicated by colour

5.3.2 COP1 does not show variation when individuals are grouped according to their altitudinal location

To create a TCS network the COP1 sequences were split into the same altitudinal groupings as UVR8. The haplotype frequencies within these groups is fed into PopART to create the network. Using altitude as a grouping for COP1 gave no clear indication that particular haplotypes or changes may be adaptive. While there were two haplotypes that were only found at high altitudes the most common haplotypes are also the haplotypes that occur in the widest range of altitudes. Haplotype 7 is found only between 1000-1500m and contains a unique G365A change. The second is haplotype 13 which is found between 500m and 2500m. Haplotype 13 contains a series of unique change: V9L, V252L and A317V. Of the two lineages of COP1 neither has multiple haplotypes that are found above 500m. Haplotype 3 is found above 500m up to 2500m and as previously mentioned contains a P17L change.

As expected from the TCS network, the AMOVA suggests that grouping the COP1 *A. thaliana* sequences by altitude does not result in significant differences in group compilation (p=0.176). While 1.67% variation is seen within the COP1 sequence explained by this grouping, the non-significant p-value suggests that this variation has occurred by chance.

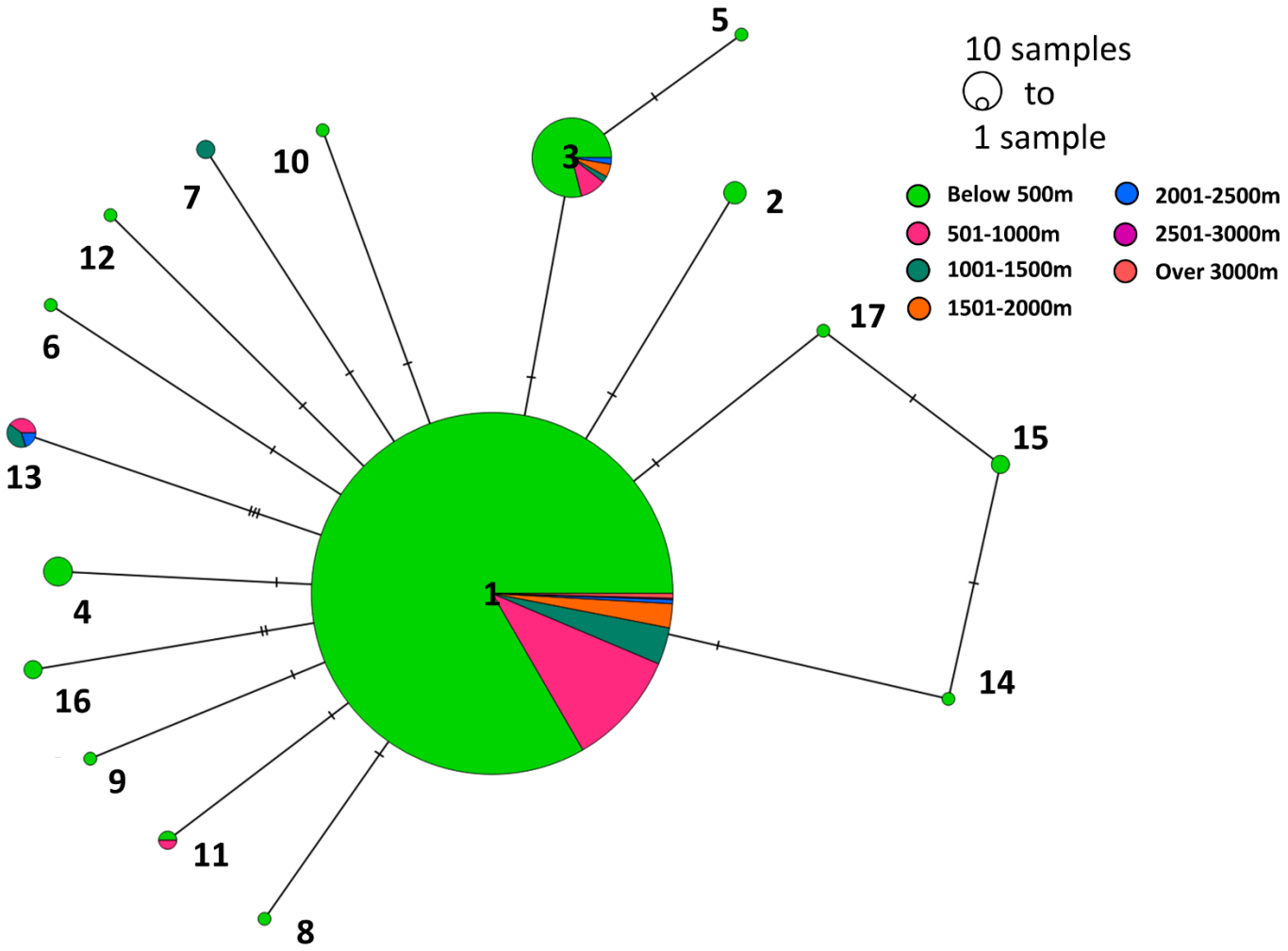
5
10
3
7
2
12
17
6
15
13
1
4
14
16
9
11
8
10 samples
to
1 sample
Below 500m
501-1000m
1001-1500m
1501-2000m
2001-2500m
2501-3000m
Over 3000m

Figure 5-4: A TCS network of COP1 diversity grouped by altitude of origin. Circle size represents the number of samples within each haplotype with the altitude that each haplotype is found indicated by colour.

5.4 The variability of the HY5 protein sequence

The HY5 protein is a transcription factor that is regulated by and interacts with the WD40 region of COP1 (Holm, *et al.*, 2001). Within the indivduals sequenced by the 1001 Genomes Project, eleven separate haplotypes have been identified (Table 5-4).

HY5 had 10 segregating sites, only one of which was parsimony informative. However, the mutation that was parsimony informative – S76N – was found in a large number of individuals. HY5 was unusual compared to both UVR8 and COP1 in that the individuals studied were relatively equally split between haplotype 1, the sequence identical to Col-0 and haplotype 2, which contains this frequently observed change S76N (Table 5-4).

Table 5-4: Documentation of the shared mutations, unique muations, the haplotype they occur in, the frequency of the haplotypes and the number of changes compared to the Col-0 sequence of HY5. Haplotypes are displayed using the designated number, presence of a change is represented with a '+' and absence of a change with a '–'. Haploytpes are arranged to best show the relationship between the different shared mutations.

Haplotypes	S76N	Unique	Changes	Number
1	-	-	0	444
2	+	-	1	379
3	+	+	2	1
7	+	+	2	3
9	+	+	2	1
11	+	+	2	2
10	+	+	3	3
4	-	+	1	16
5	-	+	1	3
6	-	+	1	6
8	-	-	1	2

5.4.1 HY5 does not exhibits significant variability between individuals that are observed in different geographical locations

A TCS network was created for the HY5 sequences using PopARt (http://popart.otago.ac.nz, Clement, *et al*. 2002) using geographical clustering via latitiude and longitude data. The ten clusters produced centered on North America, Kazakhstan, Greece, Tanzania, Japan, Finland, France, Denmark, Spain and Russia. The HY5 network was substantially different to both the UVR8 and COP1 networks. The majority of individuals were split between two haplotypes, haplotype 1 (identical to the Col-0 sequence) and haplotype 2 which contained an S76N change (Fig 5-5). There were five other haplotypes that incorporated both the S76N change and further unique changes. Similarly there were a further four changes that did not contain the S76N change but did contain entirely unique mutations from the Col-0 sequence. Both haplotypes 1 and 2 were found globally although in slightly different proportions. For example, more examples of haplotype 2 than haplotype 1 were found in the Greek, Finnish and Danish groups whereas more examples of haplotype 1 than haplotype 2 were found in the French and Russia groups. This global representation and lack of extended branches make it difficult to determine if certain haplotypes are found within specific geographic regions.

An AMOVA using these groupings shows that there is a significant difference between the composition of the ten groups ($p<0.001$). This is supported by the percentage of variation that is explained by differences seen among groups: 11.21%.

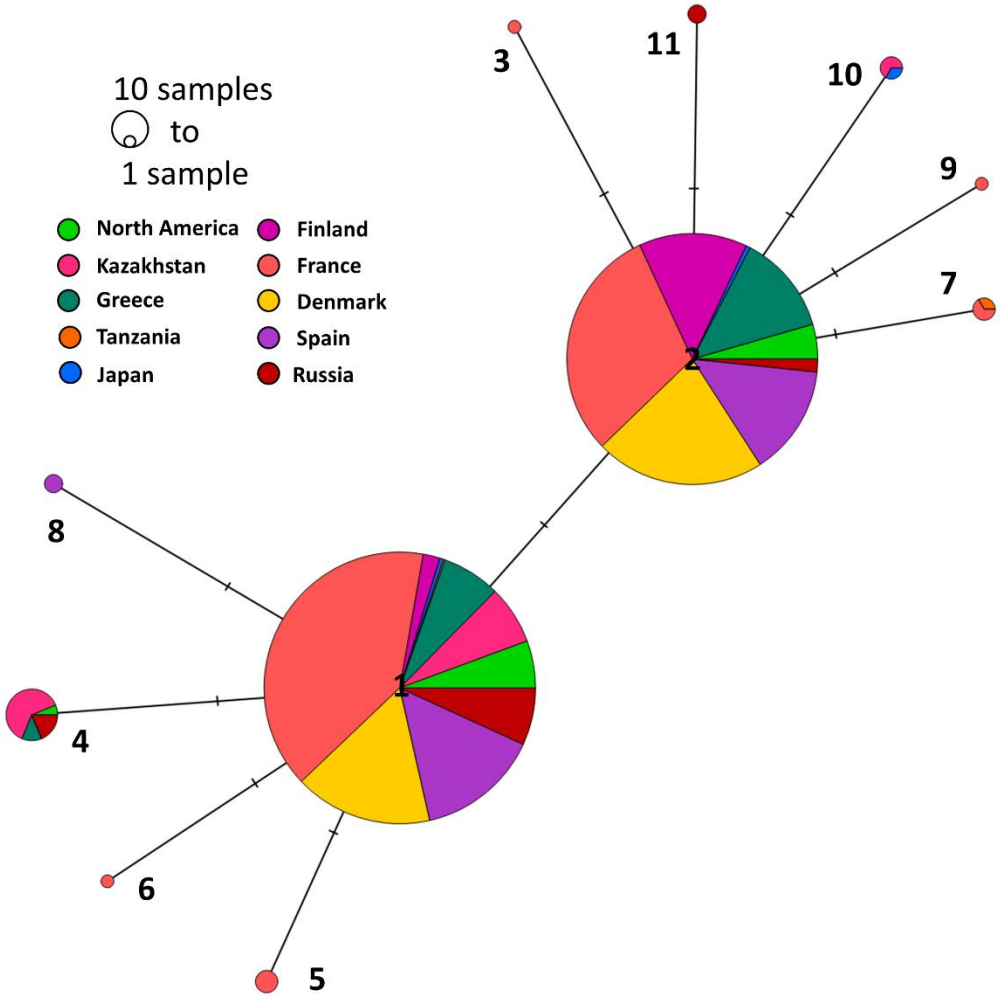
10 samples
to
1 sample
North America
Kazakhstan
Greece
Tanzania
Japan
Finland
France
Denmark
Spain
Russia
1
2
3
4
5
6
7
8
9
10
11

Figure 5-5: A TCS network of HY5 diversity grouped by geographic location using latitude and longitude. Circle size represents the number of samples within each haplotype with the cluster that each haplotype is found indicated by colour.

5.4.2 The sequence of HY5 does not vary in response to altitude

A second TCS network was constructed where the haplotypes were split into altitudinal groupings of 500m brackets as with the previous genes. The haplotype number and the frequency of this haplotype occurring in each altitudinal group was used by PopART to create the network (http://popart.otago.ac.nz, Clement, *et al.* 2002). Haplotype 1 and 2 were both found over a variety of altitudinal groups, however haplotype 1 was found more often at high altitude and at higher altitudes than haplotype 2 as it was found in every altitudinal group (Fig 5-6). There were three further haplotypes that were found above 500m. Haplotypes 7 contained the S76N and G159A changes and there was one instance of it being found between 500-1000m. Haplotype 8 contained an A50P change. Again there was only one instance of this being found above 500m, in this case between 1000-1500m. Haplotype 10 was slightly different in that the majority of the examples occur above 500m between 1500-2000m. It contains a Q70L and a S76N change.

The AMOVA analysis of the altitude grouping demonstrated that altitude did not explain any of the variation seen within HY5 (p=0.996). The groupings chosen explained 0% of the variation, which would suggest that the individuals are more related to individuals within other groupings than within their own.

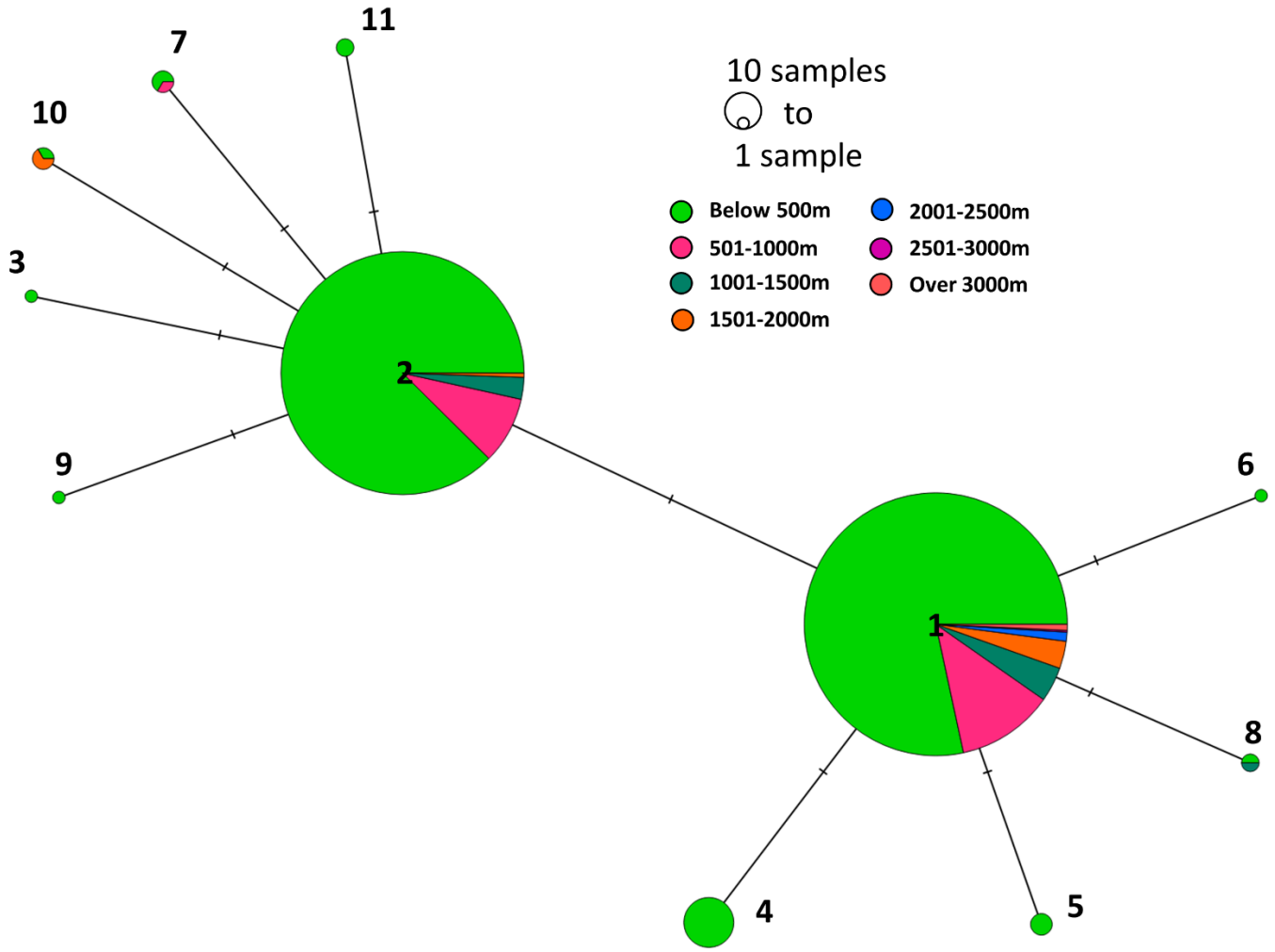
11
7
10
3
2
9
6
1
8
4
5
10 samples
to
1 sample
Below 500m
501-1000m
1001-1500m
1501-2000m
2001-2500m
2501-3000m
Over 3000m

Figure 5-6: A TCS network of HY5 diversity grouped by altitude of origin. Circle size represents the number of samples within each haplotype with the altitude that each haplotype is found indicated by colour.

5.5 The Global Distribution of HYH

The TCS network for the geographical grouping of the HYH sequences was created by reporting the haplotypes of HYH, the latitudes and longitude combinations these haplotypes were found in and the frequency of each haplotype at each coordinate. Ten geographical clusters were created centered on Spain, Finland, Tanzania, Greece, the USA, Kazakhstan, Russia, Sweden, Germany and Japan. HYH was unusual compared to the rest of the genes studied. It was extremely conserved and there were only 7 haplotypes observed (Table 5-5). Haplotype 1 was by far the most common haplotype seen and made up 96% of the total sequences found. There were only 7 segregating sites within HYH and only one of these was parsimony informative: amino acid 34 (Table 5-5).

Table 5-5: Documentation of the shared mutations, unique muations, the haplotype they occur in, the frequency of each haplotype and the number of changes compared to the Col-0 sequence. Haplotypes are displayed using the designated number, presence of a change is represented with a '+' and absence of a change with a '–'. Haploytpes are arranged to best show the relationship between the different shared mutations.

Haplotypes	M34L	Unique	Changes	Number
1	-	-	0	820
2	+	-	1	21
4	+	+	2	7
3	-	+	1	1
5	-	+	1	4
6	-	+	2	1
7	-	+	1	1

5.5.1 HYH does not vary significantly by geographical group

HYH was far more conserved than any of the other genes investigated in this work. Many of the geographical groups contained only haplotype 1, the most common haplotype by far which contained 820 of the 855 individuals that had been sequenced (Fig 5-7). Haplotypes 2 and 4 did seem to form a lineage within the Swedish grouping, both contained the M24L change and haplotype 4 containing an additional A57V change. Haplotype 2 was also found outwith the Swedish group in the Spanish, Russian, Greek and Kazakhstani groupings.

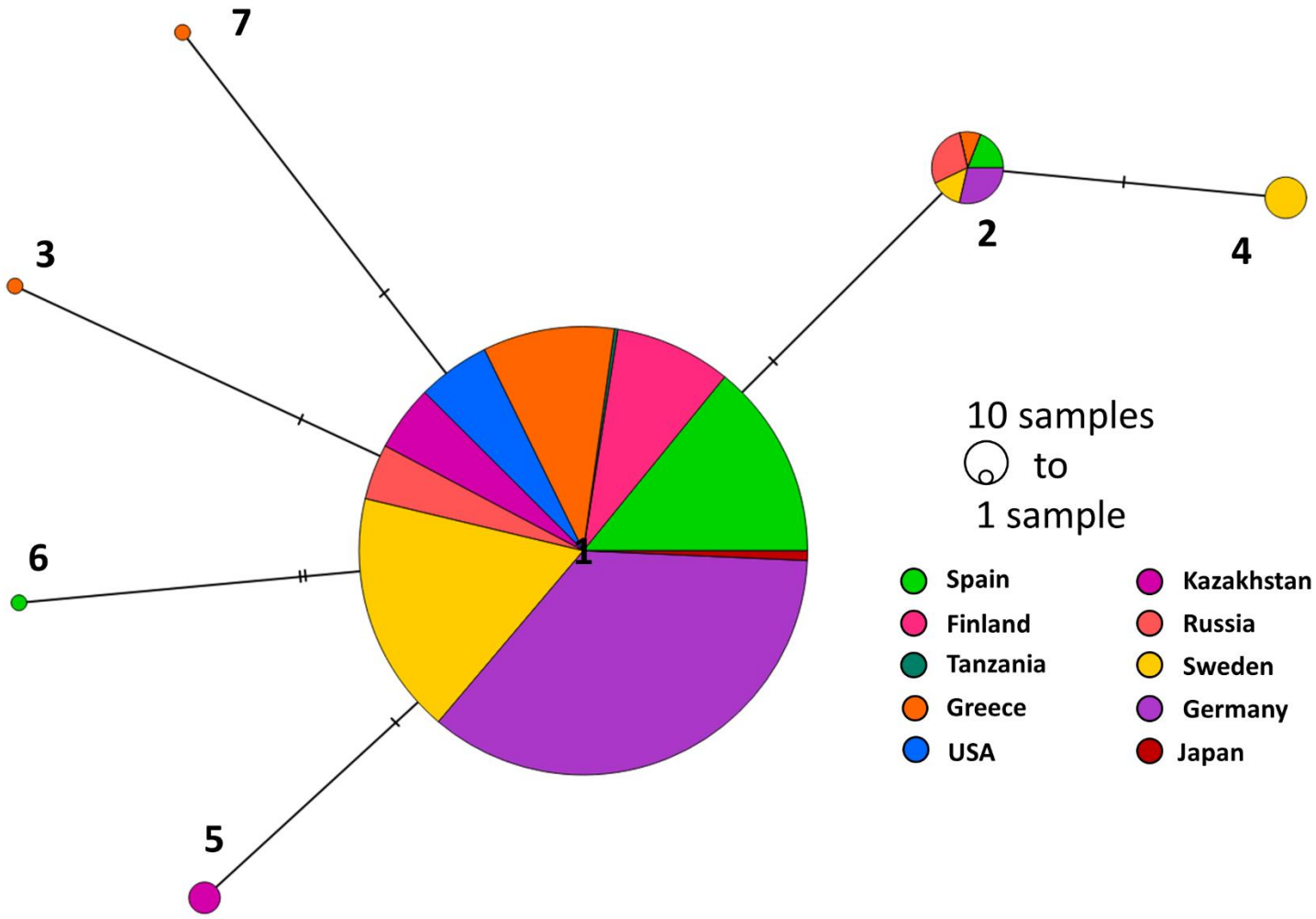
7
3
6
5
1
2
4
10 samples
to
1 sample
Spain
Finland
Tanzania
Greece
USA
Kazakhstan
Russia
Sweden
Germany
Japan

Figure 5-7: A TCS network of HYH diversity grouped by geographic location using latitude and longitude. Circle size represents the number of samples within each haplotype with the cluster that each haplotype is found indicated by colour.

Using AMOVA shows that the individuals within geographic groups were not more similar to those within their own groups compared to those without (p=0.074). Indeed, only 3.31% of the variation seen within HYH was explained by geographic separation. It is possible that a different way of grouping the haplotypes would explain a significant amount of the variation seen.

5.5.2 The sequence of HYH does not vary significantly according to the altitude of origin

The frequencies of each haplotype within seven 500m altitude groupings were used to build the TCS network using PopART. Haplotype 1 was found universally in every altitude grouping investigated (Fig 5-8). Haplotype 2 was primarily found below 500m, but also contained individuals that were found between 500-1000m and 1000-1500m. Haplotype 2 was the second most common haplotype, containing a M34L change, but it was still rare, composed of only 21 individuals. Haplotype 6 was the only haplotype that was not found below 500m, it was found exclusively between 500-1000m. However, there was only one example of haplotype six, which contained two unique changes: V61F and D76H. This would suggest that while it may be adaptive to a higher altitude it was not representative of widespread adaptation.

The AMOVA supported this hypothesis as groupings based on the altitude in which individuals were found do not return a significant p-value (p=0.996). Furthermore 0% of the variation that occured in HYH was explained by this grouping.

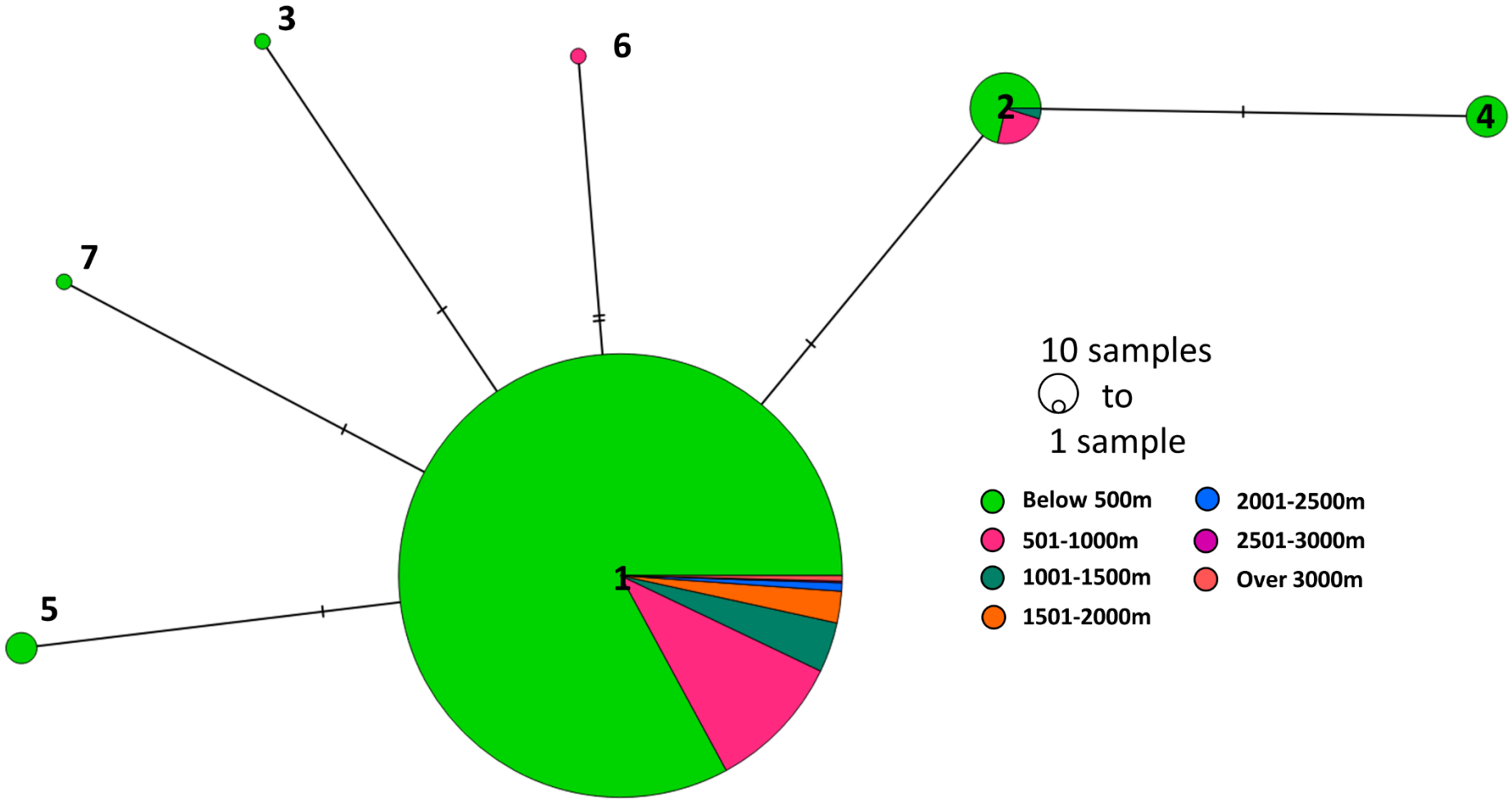

Figure 5-8: A TCS network of HYH diversity grouped by altitude of origin. Circle size represents the number of samples within each haplotype with the altitude that each haplotype is found indicated by colour.

5.6 The Global Distribution of RUP1

RUP1 had 57 haplotypes, making it far more diverse than the previous genes studied (Table 5-6). Within these haplotypes there were 46 segregating sites and 19 parsimony informative sites.

The Y117C change indicated that in the case of RUP1, Col-0 did not have the ancestral sequence or alternatively that the mutation was being heavily selected for. This change was seen in 53 of the 57 haplotypes. Furthermore, the haplotype that only contained this change, haplotype 2, was the most common haplotype by a large margin.

5.6.1 RUP1 has varies based on geographic location

A TCS network for RUP1 was created using the original latitude and longitude coordinates for each of the ecotypes and the frequencies of each haplotype at each unique coordinate. The individuals were clustered into ten geographical groups centered on Germany, Japan, the USA, Russia, Sweden, Kazakhstan, Tanzania, Morocco, Greece and Spain. The TCS network for RUP1 was far more complicated than any of the other genes investigated so far (Fig 5-9). Furthermore, RUP1 was the first gene that had been looked at that the most common haplotype was not found within Col-0. Haplotype 2 was the most frequently observed haplotype with an Y117C change and was seen universally throughout all the geographic groups. There were only four haplotypes this change was not seen in, haplotypes 1, 11, 14 and 25. Haplotype 1, haplotype 11 and haplotype 25 formed a lineage. Haplotype 14 contained many other changes and was more closely related to another lineage, suggesting that it may have lost the Y117C change separately. Haplotypes 11 and 25 contained two different unique changes, S7Y and T69I respectively. Haplotypes 1, 11 and 25 formed the smallest separate lineage. All three were observed in the German group which was where the majority of these haplotypes were seen. Haplotype 1 and 25 were also seen in Swedish and Greek groups. Finally haplotype 1 was also observed in the USA, Tanzanian and Spanish groupings.

Table 5-6: Documentation of the shared mutations, unique muations, the haplotype they occur in, the frequency of each of the haplotypes and the number of changes compared to the Col-0 sequence. Haplotypes are displayed using the designated number, presence of a change is represented with a '+' and absence of a change with a '–'. A '*' indicates an alternative change at the same residue number. Haploytpes are arranged to best show the relationship between the different shared mutations.

Haplotype	Y117C	R350Q	T343P	L340M	N344D	H34Q	G210A	R235Q	I18T/*S	D108G	D247E	F133L	T34A	L182L	R136Q	S61T	E115V	A229V	Unique	Changes	Number
1	-	-	-	-	-	-	-	-	-	-	-	-	-	-	-	-	-	-	-	1	73
11	-	-	-	-	-	-	-	-	-	-	-	-	-	-	-	-	-	-	+	1	1
25	-	-	-	-	-	-	-	-	-	-	-	-	-	-	-	-	-	-	-	1	3
14	-	+	+	+	+	-	+	-	-	+	+	+	-	-	-	-	-	-	+	9	1
2	+	-	-	-	-	-	-	-	-	-	-	-	-	-	-	-	-	-	-	0	443
3	+	-	-	-	-	-	-	-	-	-	-	-	-	-	-	-	-	-	+	2	38
7	+	-	-	-	-	-	-	-	-	-	-	-	-	-	-	-	-	-	-	1	9
9	+	-	-	-	-	-	-	+	-	-	-	-	-	+	-	-	-	-	-	2	62
10	+	-	-	-	-	-	-	-	-	-	-	-	-	-	-	+	-	-	-	1	11
13	+	-	-	-	-	-	-	+	-	-	-	-	-	-	-	-	-	-	-	1	5
15	+	-	-	-	-	-	-	-	-	-	-	-	-	-	-	-	-	-	+	1	6
16	+	-	-	-	-	-	-	-	-	-	-	-	-	-	-	+	-	-	+	2	14
17	+	-	-	-	-	-	-	-	-	-	-	-	-	-	+	-	-	-	-	1	2
20	+	-	-	-	-	-	+	-	-	+	+	-	+	-	-	-	-	-	+	5	1
21	+	-	-	-	-	-	-	-	-	-	-	-	-	-	-	-	-	-	+	1	6
23	+	-	-	-	-	-	-	-	-	-	-	-	-	-	-	-	-	-	+	1	12
26	+	-	-	-	-	-	-	-	-	-	-	-	-	-	-	-	-	-	+	1	8
28	+	-	-	-	-	-	-	-	*+	-	-	-	-	-	-	-	-	-	+	3	1
29	+	-	-	-	-	-	-	-	*+	-	-	-	-	-	-	-	-	-	-	1	1
34	+	-	-	-	-	-	-	+	-	-	-	-	-	+	-	-	-	-	+	3	4
39	+	-	-	-	-	-	-	-	-	-	-	-	-	-	-	-	-	-	+	1	1
40	+	-	-	-	-	-	-	-	+	-	-	-	-	-	-	-	-	-	-	1	1
41	+	-	-	-	-	-	-	-	-	-	-	-	-	+	-	-	-	-	-	1	1
43	+	-	-	-	-	-	-	-	-	-	-	-	-	-	-	-	-	+	-	1	1
46	+	-	-	-	-	-	-	-	-	-	-	-	-	-	-	+	-	-	-	1	2

Haplotype	Y117C	R350Q	T343P	L340M	N344D	H34Q	G210A	R235Q	I18T/*S	D108G	D247E	F133L	T34A	L182L	R136Q	S61T	E115V	A229V	Unique	Changes	Number
47	+	-	-	-	-	-	-	+	-	-	-	-	-	-	-	-	-	-	+	3	1
48	+	-	-	-	-	-	-	-	-	-	-	-	-	-	-	-	-	-	+	2	4
51	+	-	-	-	-	-	-	-	-	-	-	-	-	-	-	-	-	-	+	1	1
53	+	-	-	-	-	-	-	-	-	-	-	-	-	-	-	-	-	-	+	1	1
55	+	-	-	-	-	-	-	-	-	-	-	-	-	-	-	-	-	-	+	1	1
56	+	-	-	-	-	-	-	-	-	-	-	-	-	-	-	+	-	-	+	2	2
57	+	-	-	-	-	-	-	-	-	-	-	-	-	-	-	-	-	-	+	1	1
18	+	-	-	+	-	-	-	-	-	-	-	-	-	-	-	-	-	-	-	1	2
54	+	+	-	+	-	-	-	-	-	-	-	-	-	-	+	-	-	-	-	3	1
12	+	-	+	+	-	-	-	-	+	-	-	-	-	-	-	-	+	-	-	4	2
4	+	+	-	-	-	-	-	-	-	-	-	-	-	-	-	-	-	-	-	1	54
6	+	+	-	-	+	-	+	-	-	-	-	-	-	-	-	-	-	-	-	3	1
8	+	+	-	-	-	-	-	-	-	-	-	-	-	-	+	-	-	-	-	2	3
27	+	+	-	+	-	-	-	-	+	-	-	-	-	-	-	-	-	-	-	3	1
49	+	+	-	-	-	-	+	-	-	+	+	+	-	-	-	-	-	-	+	6	1
52	+	+	-	-	-	-	-	-	-	-	-	-	-	-	-	-	-	-	+	2	2
30	+	+	-	+	-	+	-	-	-	-	-	-	-	-	-	-	-	-	-	2	7
32	+	+	-	+	-	+	-	-	-	-	-	-	-	-	-	-	-	-	-	3	1
45	+	+	-	+	+	+	-	-	+	-	-	-	-	-	-	-	-	-	-	6	1
50	+	+	+	-	+	+	-	-	-	-	-	-	-	-	+	-	-	-	-	5	2
5	+	+	+	+	+	+	-	-	-	-	-	-	-	-	-	-	-	-	-	5	40
19	+	+	+	+	+	+	+	-	-	+	+	-	+	-	-	-	-	-	+	10	1
22	+	+	+	+	+	+	-	-	-	-	-	-	-	-	+	-	-	-	-	6	1
24	+	+	+	+	-	+	-	-	-	-	-	-	-	-	+	-	-	-	+	6	5
31	+	+	+	+	-	+	-	-	-	-	-	-	-	-	-	-	-	-	-	4	1
33	+	+	+	+	+	+	+	-	-	+	+	+	-	-	-	-	-	-	+	10	1
35	+	+	+	+	+	+	+	-	-	+	+	+	-	-	-	-	-	-	-	9	2
36	+	+	+	+	+	+	+	-	-	+	+	+	-	-	-	-	-	-	-	9	1

Haplotype	Y117C	R350Q	T343P	L340M	N344D	H34Q	G210A	R235Q	I18T/*S	D108G	D247E	F133L	T34A	L182L	R136Q	S61T	E115V	A229V	Unique	Changes	Number
37	+	+	+	+	+	+	-	-	-	-	-	-	-	-	+	-	-	-	+	7	1
38	+	+	+	+	+	+	-	-	-	-	-	-	-	-	-	-	-	-	+	7	1
42	+	+	+	+	+	+	-	-	-	-	-	-	-	-	-	-	-	+	-	6	3
44	+	+	+	+	+	+	-	-	+	-	-	-	-	-	-	-	+	-	-	7	2

The next largest lineage was composed of four haplotypes: 10, 16, 46 and 56. This was a particularly interesting lineage as haplotype 10 and 46 both contained S61T and Y117C mutations through different codons for position 61. Similarly haplotypes 16 and 56 both contained the S39F, S61T and Y117C changes but differed in the mutation that resulted in S39F. This lineage was also split geographically. Haplotypes 10 and 46 were primarily and exclusively found in the German grouping whereas the majority of individuals found within haplotypes 16 and 56 were found in the USA.

The third lineage was composed of five haplotypes: 9, 13, 34, 41 and 47. Furthermore, haplotypes within this lineage either contained an I182L change, a R235Q change or both as well as further unique mutations. The most commonly observed haplotype within this part of the TCS network was haplotype 9 which contains both the I182L and R235Q mutations. The majority of the individuals that fall into these five different haplotypes – indeed all of the individuals for haplotypes 13, 34, 41 and 47 – were found in three geographic groups, the Kazakhstani, the Russian and the Greek. Haplotype 9 was found in a further three regions: the Spanish, German and Swedish groups.

The final lineage seen was very large and is composed of 29 haplotypes. As a whole this lineage was very diverse, found in all but two of the geographical groups: Japan and Tanzania. There were two haplotypes that are frequently found within this part of the network. Haplotype 4 contained an Y117C and a R350Q change and haplotype 5 which contained the Y117C change and five further changes that occur within a ten amino acid span: L340M, H243Q, T323P, N344D and R350Q. Haplotype 4 was primarily observed in the Swedish group whereas the most examples of haplotype 5 were seen in the Spanish group. Haplotypes that occurred one or two changes away from haplotype 4 such as haplotype 8, 26, 52 and 54 were also found exclusively in Sweden. All of these haplotypes contained a combination of the Y117C, R136 and R350Q changes. The haplotypes surrounding haplotype 5 were more diverse in their locations. There was a series of four haplotypes – 12, 42, 44 and 45 that were either found exclusively in the Russian group or were seen in both the Kazakhstani and Russian groups. These haplotypes contained various combinations of eight

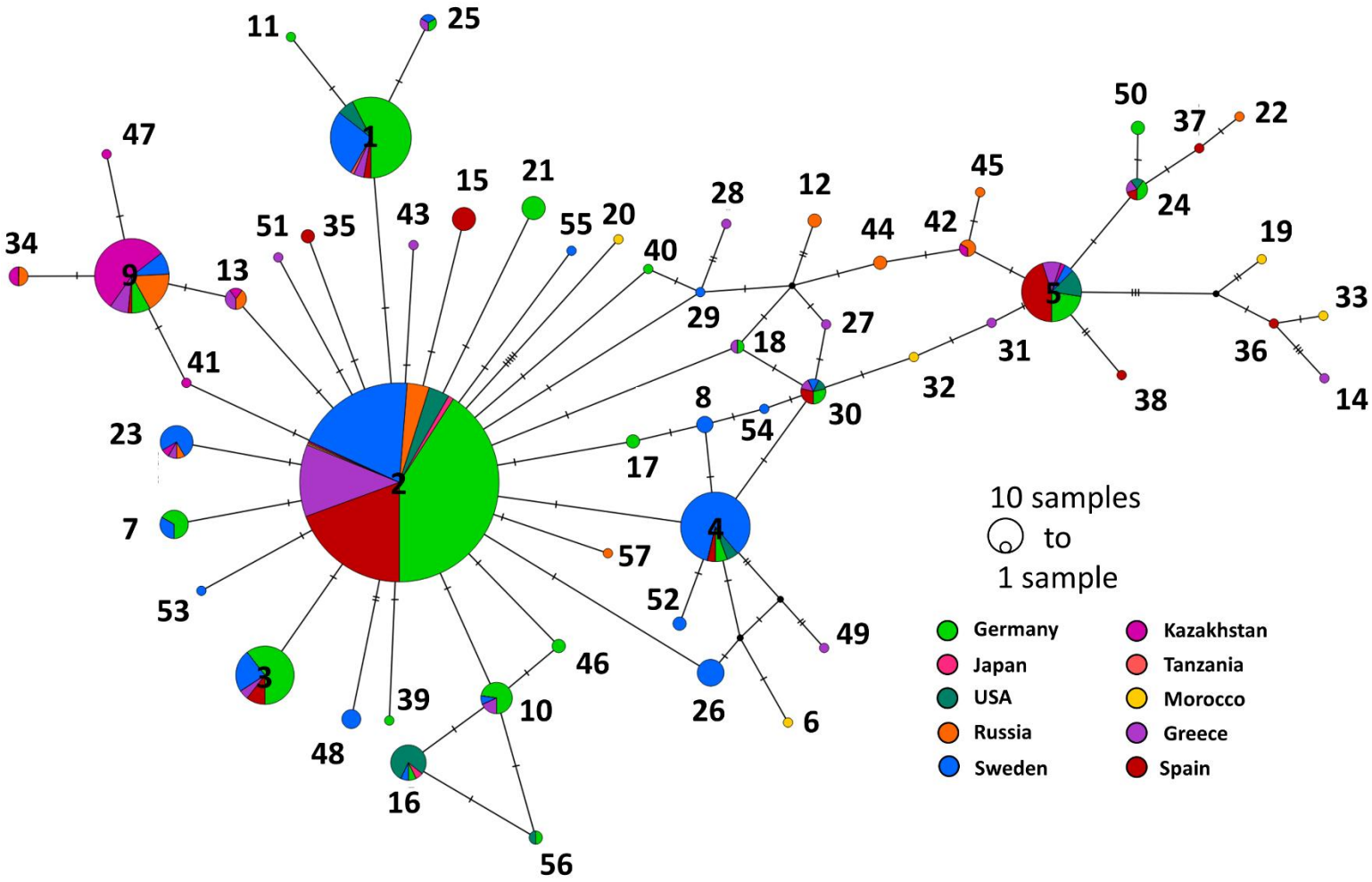

Figure 5-9: A TCS network of RUP1 diversity grouped by geographic location using latitude and longitude. Circle size represents the number of samples within each haplotype with the cluster that each haplotype is found indicated by colour.

different changes: I18T, E115K, Y117C, H242Q, T232P, N344D and R350Q. Finally within this large lineage there was a group that was substantially different to their nearest neighbour haplotype, with a minimum of four changes without an intermediate haplotype required to reach them. Haplotypes 14, 19, 33 and 36 were found in the Moroccan, Spanish and Greek groups. There were seven changes that occurred in all four of these haplotypes: G210A, D247E, L340M, T343P, N344D and R350Q. There were a further three changes that occurred in three of the four haplotypes: F133L, H342Q and Y117C which was not found in haplotype 14.

An AMOVA performed on these groupings has a significant p-value ($p<0.001$). The variation that was explained by differences among the geographic groups was 13.88%. This indicates that the changes found in RUP were in part influenced by geographic separation.

5.7.2 The RUP1 sequence varies based on the altitude of origin

When the haplotypes were sorted into altitudinal groups a very different pattern emerged compared to the geographic groupings. While the most common haplotype was found in several of the groups, it was not observed universally throughout all of the altitudinal groupings and did not contain any individuals from the highest altitudinal bracket. Similarly, the haplotype 1 lineage was primarily found below 500m, with only three individuals found at a higher altitude. The second lineage was found in the lowest altitudinal grouping, with only two individuals – one from haplotype 10 and one from haplotype 16 – appearing in the higher groups. The third lineage was far more interesting. Approximately a third of the individuals found within this lineage were found above 500m, which was a higher amount than the overall proportion of individuals found above this altitude. It was also of importance as haplotype 9 contained individuals that were found in six of the seven groups including the highest grouping, over 3000m. As previously noted, the haplotypes found within this lineage contain the Y117C change and a combination of the I182L and R235Q changes.

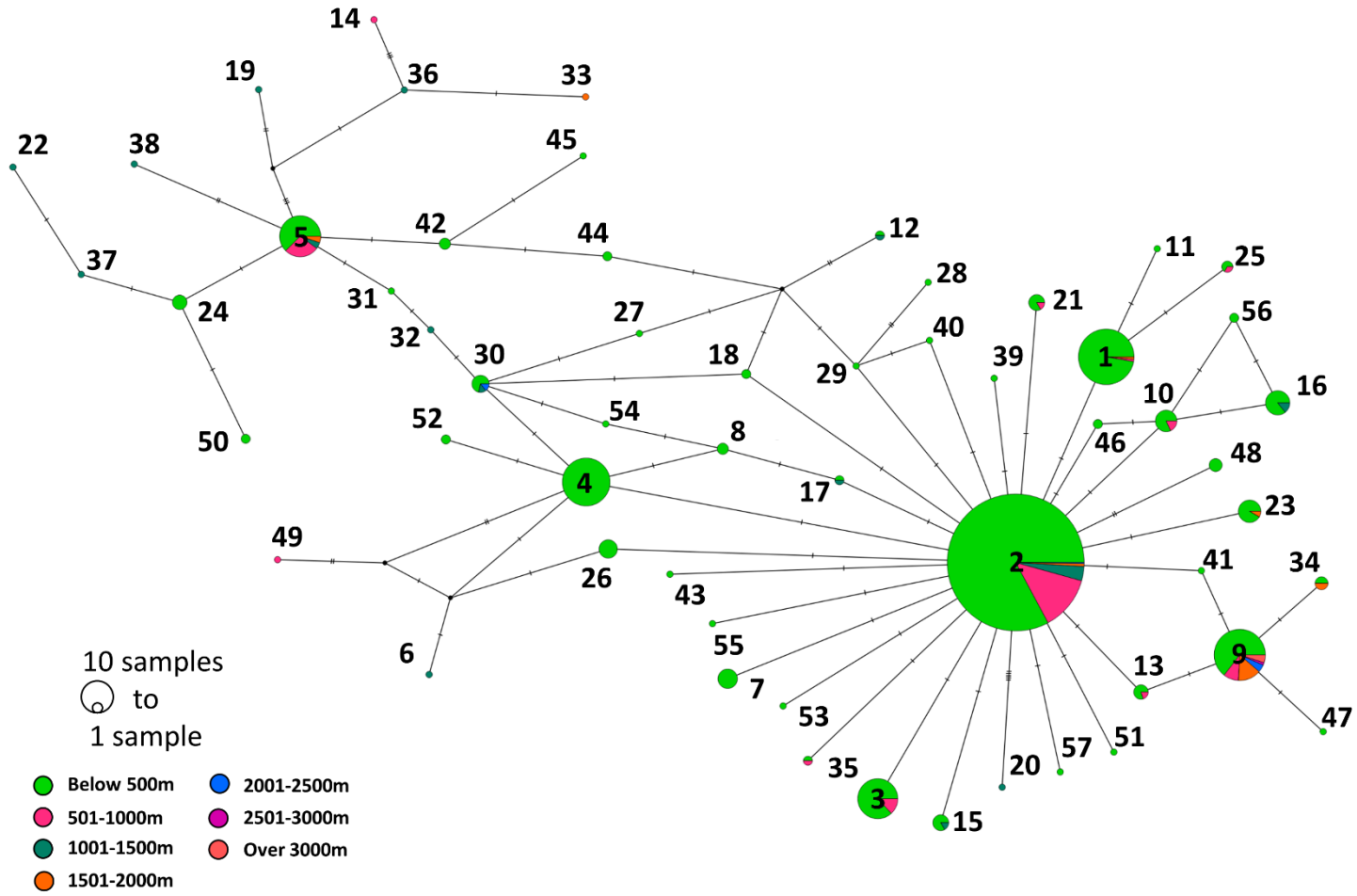

Figure 5-10: A TCS network of RUP1 diversity grouped by altitude of origin. Circle size represents the number of samples within each haplotype with the altitude that each haplotype is found indicated by colour.

In the largest lineage there were fourteen haplotypes that were observed above 500m: haplotypes 5, 6, 12, 14, 17, 19, 22, 30, 32, 33, 36, 37, 38 and 49. When looking at the similarities between these haplotypes only haplotype 14 did not contain the Y117C change. However there were a further five changes that occurred in over half the haplotypes: L340M, H342Q, T343P, N344D and R350Q. These changes were found in various combinations in all of the haplotypes except 17.

Within the large interconnected group of haplotypes, there were several regions that seemed to be found more frequently at high altitude than other altitudes. The region of the network containing haplotypes 14, 19, 33 and 36 was one of these. These were all found exclusively above 500m, and the majority were found above 1000m. Interestingly a further two haplotypes – 49 and 6 – contained some of these changes, in particular the D108G, G210A and R350Q changes.

While an AMOVA for this style of grouping was statistically significant (p=0.001), very little (3.70%) of the variation that occurs within the gene was explained by altitudinal groupings.

5.7 The Global Distribution of RUP2

RUP2 contained 53 segregating sites and 20 parsimony informative sites within 64 haplotypes and was the most diverse of the genes investigated within this study (Table 5-7). While there was a great deal of diversity, the majority of individuals were found within four different haplotypes. Over half of the haplotypes – 36 – only contained one individual. Of these there were only two that did not contain a change to a parsimony informative site: haplotypes 30 and 59. While the rest did contain a parsimony informative site, for 12 of the haplotypes this is the M126T change.

Table 5-7: Documentation of the shared mutations, unique muations, the haplotype they occur in, the frequency of each of the haplotypes and the number of changes compared to the Col-0 sequence. Haplotypes are displayed using the designated number, presence of a change is represented with a '+' and absence of a change with a '–'. A '*' represents a second independent change at the same residue as the first change. Haploytpes are arranged to best show the relationship between the different shared mutations.

Haplotype	M126T	I224V	ins16L	Q17E	ins17E	Q18E	ins18E	ins18G	R270C	G297S	H155N	L232W	T160A	C260F	C193S/ *C193F	C97S	T153S/ *T153A	Unique	Frequency	Changes
1	-	-	-	-	-	-	-	-	-	-	-	-	-	-	-	-	-	-	48	0
21	-	-	-	-	-	-	-	-	+	-	-	-	-	-	-	-	-	+	1	3
30	-	-	-	-	-	-	-	-	-	-	-	-	-	-	-	-	-	+	1	2
57	-	-	-	+	-	-	-	+	-	-	-	+	-	-	-	-	-	-	1	3
58	-	-	-	-	-	-	-	-	-	-	-	-	-	-	-	-	-	+	1	2
59	-	-	-	-	-	-	-	-	-	-	-	-	-	-	-	-	-	+	1	1
12	-	+	-	-	-	-	-	-	-	-	-	-	-	-	-	-	-	-	2	1
2	+	-	-	-	-	-	-	-	-	-	-	-	-	-	-	-	-	-	415	1
5	+	-	-	-	-	-	-	-	-	-	-	-	-	-	-	-	-	+	3	2
6	+	-	-	-	-	-	-	-	+	-	-	-	-	-	-	-	-	+	62	2
7	+	-	-	-	-	-	+	-	+	-	-	-	-	-	-	-	-	+	7	3
13	+	-	-	-	-	-	-	-	-	-	-	-	-	-	-	-	-	-	1	2
14	+	-	-	-	-	-	-	-	-	-	-	-	-	-	-	-	-	+	1	2
15	+	-	-	+	-	-	+	-	-	-	-	-	-	-	-	-	-	-	1	3
16	+	-	-	-	-	-	-	-	-	-	-	-	-	-	-	-	-	+	1	2
17	+	-	-	+	-	-	-	-	-	-	-	-	-	-	+	-	-	-	1	3
18	+	-	-	-	-	-	-	-	-	-	-	-	-	-	-	-	-	+	1	2
20	+	-	-	-	-	-	-	-	-	-	-	-	-	-	-	-	-	+	15	2
22	+	-	-	+	-	-	-	-	-	-	-	-	-	-	-	-	-	-	2	2
23	+	-	-	-	-	-	-	-	-	-	-	-	-	-	-	-	-	+	2	2
29	+	-	-	+	-	-	-	-	-	-	-	+	-	-	-	-	-	-	4	3
32	+	-	-	-	-	-	-	-	-	-	-	-	-	-	-	-	-	+	2	2
33	+	-	-	+	-	-	-	-	+	-	-	-	-	-	-	-	-	-	4	3

Haplotype	M126T	I224V	ins16L	Q17E	ins17E	Q18E	ins18E	ins18G	R270C	G297S	H155N	L232W	T160A	C260F	C193S/ *C193F	C97S	T153S/ *T153A	Unique	Frequency	Changes
35	+	-	-	+	-	-	-	-	-	-	-	+	+	-	-	-	-	-	2	4
36	+	-	-	-	-	-	-	-	-	-	-	-	-	-	-	-	-	+	1	2
39	+	-	-	+	-	-	-	-	-	-	-	-	+	-	-	-	-	+	1	3
40	+	-	-	-	-	+	-	-	-	-	-	-	-	-	-	-	-	-	3	2
42	+	-	-	-	-	-	-	-	-	-	-	-	-	-	-	-	-	+	1	2
43	+	-	-	-	-	-	-	-	-	-	-	-	-	-	-	-	-	+	1	3
46	+	-	-	-	-	-	-	-	-	-	-	-	-	-	-	-	-	+	1	2
50	+	-	-	+	-	-	-	-	-	-	-	-	-	+	-	+	-	-	1	4
51	+	-	-	-	-	-	-	-	+	-	-	-	-	-	-	-	*+	+	1	4
53	+	-	-	-	-	-	-	-	-	-	-	-	-	-	-	-	-	+	1	2
54	+	-	-	-	-	-	-	-	-	-	-	-	-	-	-	-	-	+	2	2
55	+	-	-	-	-	+	-	+	-	-	-	-	-	-	-	-	-	+	1	4
56	+	-	-	-	-	+	-	+	-	-	-	+	-	-	-	-	-	-	2	4
60	+	-	-	-	-	-	-	-	-	-	-	-	-	-	-	-	-	+	1	2
61	+	-	-	-	-	-	-	-	-	-	-	-	-	-	-	-	-	+	1	2
62	+	-	-	+	-	-	-	+	-	-	-	-	-	-	-	-	-	+	1	4
63	+	-	-	-	-	-	-	-	-	-	-	-	-	-	-	-	-	+	1	2
64	+	-	-	-	-	-	-	-	-	-	-	-	-	-	-	-	-	+	3	2
4	+	-	-	+	-	-	-	-	-	-	+	+	+	-	-	-	-	-	8	5
28	+	-	-	+	-	-	-	-	-	-	+	+	-	-	-	-	-	-	1	4
34	+	-	-	+	-	-	-	-	-	-	+	-	+	-	-	-	-	-	3	4
41	+	-	-	+	-	-	-	-	-	-	+	-	+	-	-	-	-	+	1	5
52	+	-	-	-	-	-	-	-	-	-	+	+	+	-	-	-	-	-	1	4
27	+	+	-	+	-	-	-	-	-	-	-	-	-	+	-	-	-	-	1	4
3	+	+	-	-	-	-	-	-	-	-	-	-	-	-	-	-	-	-	185	2
8	+	+	+	-	-	+	-	-	-	-	-	-	-	-	-	-	-	-	3	4
9	+	+	-	-	-	+	-	-	-	-	-	-	-	-	-	-	-	-	7	3

Haplotype	M126T	I224V	ins16L	Q17E	ins17E	Q18E	ins18E	ins18G	R270C	G297S	H155N	L232W	T160A	C260F	C193S/ *C193F	C97S	T153S/ *T153A	Unique	Frequency	Changes
10	+	+	-	-	-	-	-	-	-	+	-	-	-	-	-	-	-	-	1	3
11	+	+	-	+	-	-	-	-	-	-	-	-	-	-	-	-	-	-	21	3
19	+	+	-	+	-	-	-	+	-	+	-	-	-	-	-	-	-	-	3	5
24	+	+	-	-	-	-	-	-	-	-	-	-	-	-	-	-	-	-	1	2
25	+	+	+	+	-	-	-	-	-	-	-	-	-	-	-	-	-	+	1	5
26	+	+	-	-	-	-	-	-	-	-	-	-	-	-	-	-	-	+	1	4
31	+	+	-	+	-	-	-	-	-	-	-	-	-	+	-	-	-	+	3	5
37	+	+	-	-	-	-	-	-	-	-	-	-	-	-	-	-	+	-	2	3
38	+	+	-	-	-	-	-	-	-	-	-	-	-	-	*+	-	-	-	1	3
44	+	+	-	+	-	-	-	-	-	-	-	-	-	-	-	-	-	+	2	4
45	+	+	-	-	-	-	-	-	-	-	-	-	-	-	-	-	-	-	1	3
47	+	+	-	+	+	-	-	-	-	-	-	-	-	+	-	+	-	-	5	6
48	+	+	-	+	+	-	-	-	-	-	-	-	-	+	-	+	-	+	1	8
49	+	+	-	-	-	-	-	-	-	-	-	-	-	-	-	-	-	+	1	3

5.7.1 RUP2 varies by geographical location

As with RUP1 the most common haplotype was not found in Col-0 (Fig 5-11). Instead haplotype 2 – which contained a M126T change – was more prominent and was found in every geographic grouping. Once again this change was found in the majority of haplotypes. Only haplotypes 1, 12, 57, 58 and 59 did not contain this change. Furthermore, there did not seem to be any geographic similarity between haplotype 1 and the haplotypes that surrounded it. Haplotype 1 was primarily found in the French geographic group, although it was also found in the Spanish, Greek, Swedish, German and USA groups.

Haplotype 3 was the next most numerous haplotype observed after haplotype 2 and it occurred in every geographic group apart from Tanzania. It contained the M126T change that was almost universal as well as an I224V change which occurred in another 17 haplotypes including the haplotypes which were most closely related to haplotype 3: haplotypes 10, 12, 24, 25, 26, 29, 37 and 38. However, while all of these haplotypes contained this common change they were not found within close geographic regions and were instead spread out geographically, occurring within seven of the ten geographic clusters.

Another haplotype that contained a large number of individuals was haplotype six which had the M126T change and a further R270C change. The only groups it was not observed in were the Tanzanian and the Japanese groupings. The haplotypes that were connected to it were primarily observed in the German, Greek and Russian groups: haplotypes 21, 33 and 51. They also contained the R270C change and while there was no other change that could be seen in all of these haplotypes, the changes they contained were found within other haplotypes such as the Q17E mutation.

There were a few areas of the TCS network that were worth focusing on. There were five haplotypes that branch off from the main interconnected network: haplotypes 27, 30, 47, 48 and 50. While all contained a M126T change there were two other changes that were also universally found within these haplotypes: Q17E and C260F. Furthermore there were a further two changes that were found within four out of five of the haplotypes: C97S and I224V. Finally

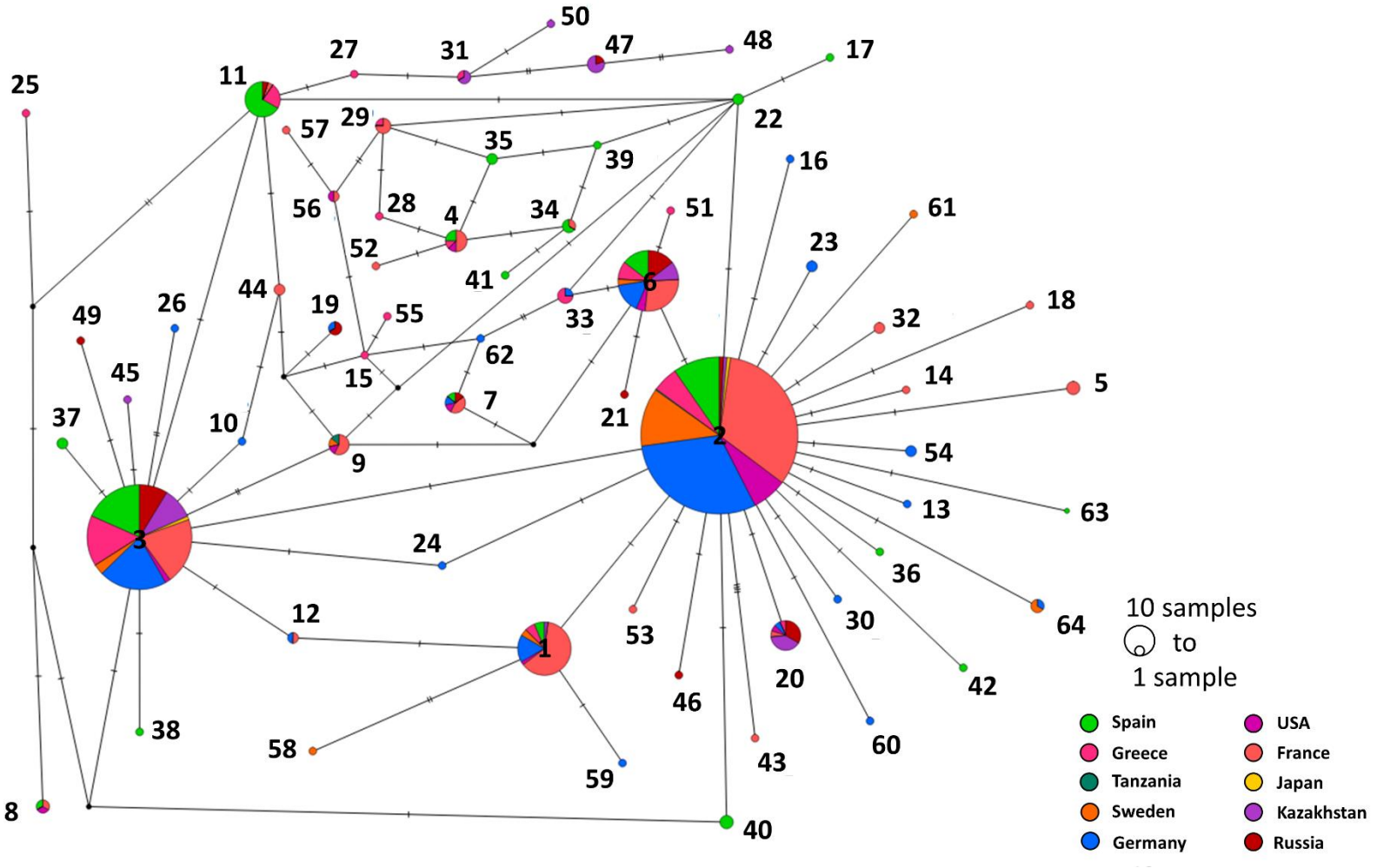

Figure 5-11: A TCS network of RUP2 diversity grouped by geographic location using latitude and longitude. Circle size represents the number of samples within each haplotype with the cluster that each haplotype is found indicated by colour.

there was a very severe change found within two of these haplotypes. At position 17 for both haplotype 47 and 48 there had been an insertion of a glutamic acid. These haplotypes were also grouped geographically, being found in either Greece, Kazakhstan or Russia.

The second area that was of interest was a group of six haplotypes that were primarily observed in the Spanish geographic grouping but were also found in the French, Greek and Kazakhstani groupings: haplotypes 4, 22, 34, 35 and 39. These haplotypes all contained both the M126T change and a Q17E change. Furthermore they all contained a combination of a H155N, T160A and L232S changes.

The AMOVA of these groupings showed that there was a statistically significant structure to the changes seen in RUP2 when using geographic groupings ($p<0.001$). However this method of grouping the sequences explained less of the variation than for other genes that were also found to be significant as only 5.06% of the variation was seen among populations

5.7.4 RUP2 varies significantly between altitudes

Using altitudinal groupings illustrated a very different pattern (Fig 5-12). Haplotype 2, which was found over the widest geographical area, was far less widespread in the altitudinal groups that it was found in. Over 75% of the individuals that haplotype 2 was comprised of were found below 500m, with the majority of the rest found between 500-1500m. A far higher proportion of individuals were found above 500m in haplotype 3, which contained individuals found in six of the seven groups, including over 3000m. However there were two haplotypes that both contained more than one individual and that contained a higher proportion of high altitude compared to low altitude individuals. The first was haplotype 20, which contained the M126T change a further unique change: V271M. It was found primarily between 1500-2000m, but was also present up to 3000m. The second was haplotype 47. Only one instance of haplotype 47 was found below 500m and indeed it was observed above 3000m. Haplotype 47 contained many changes: an insertion of a glutamic acid at position 17, Q17E, C87S, M126T, I224V and C260F.

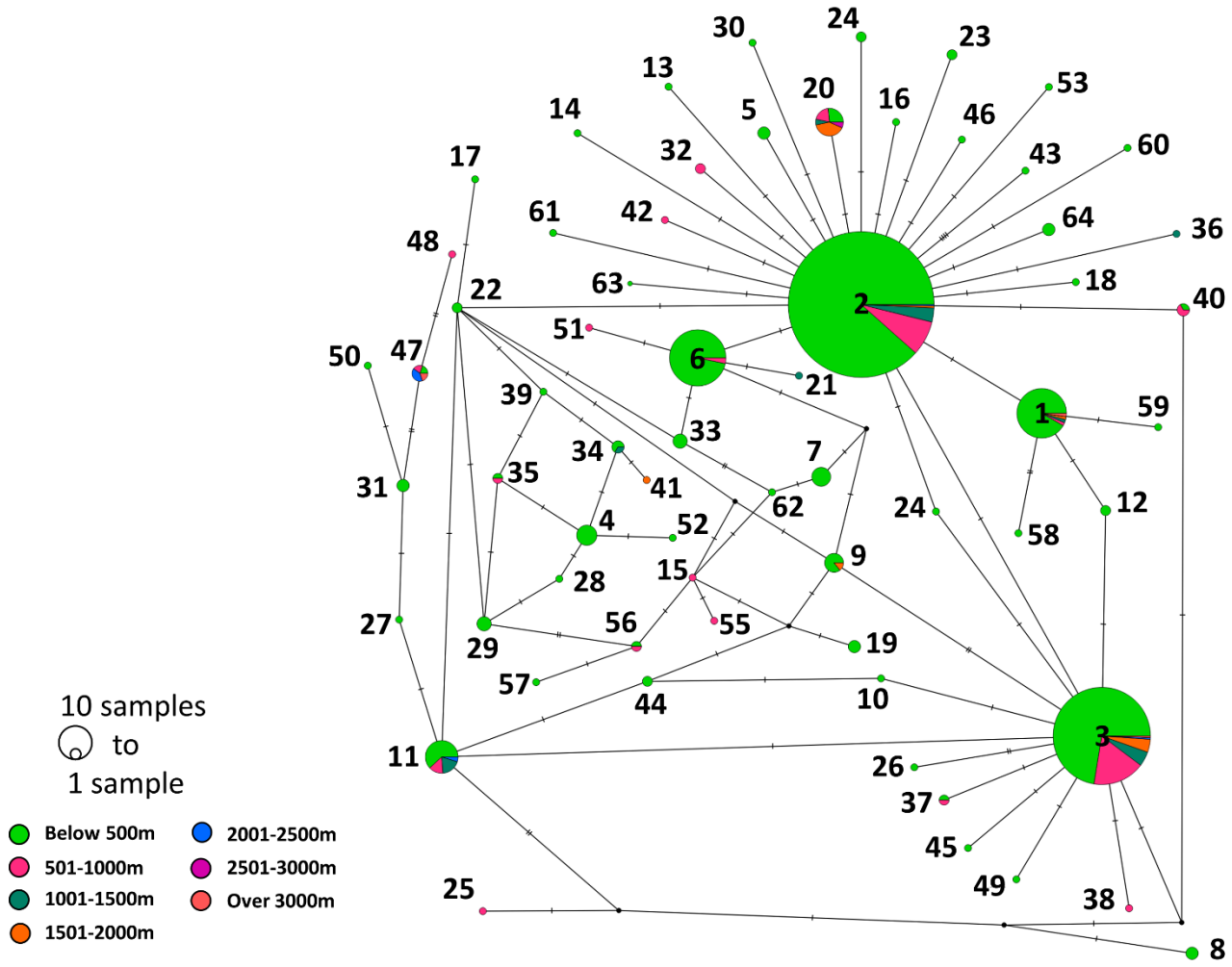

Figure 5-12: A TCS network of RUP1 diversity grouped by altitude of origin. Circle size represents the number of samples within each haplotype with the altitude that each haplotype is found indicated by colour.

An AMOVA performed using altitude as a grouping system for the RUP2 sequences returns significant ($p<0.001$). Interestingly, the values are similar to those when using geographical location as a grouping factor.

5.9 Discussion

As discussed previously in this thesis (Chapter 3), the accession of *A. thaliana* was a determining factor in the photoequilibrium of UVR8. In the case of this work the different accessions were taken from three very different altitudes, 42m above sea level in the case of Edi-0, 1580m above sea level for Kas-1 and 3387m above sea level for Shakdara (Chapter 3). While the differences in photoequilibrium suggested that accessions at different altitudes were adapted to different levels of UV-B, these accessions also came from three different countries: the UK, India and Tajikistan respectively. The difference in photoequilibrium could just as easily be due to geographical separation and localised populations that did not follow a trend across the entire *A. thaliana* range. By using the 1001 Genomes database it was possible to take 855 accessions from the entire natural range of *A. thaliana* and determine whether there was variation in the protein sequence of UV-B related genes when clustered by geographical location or altitude of origin.

5.9.1 Genes involved in the initial UV-B photoreception vary significantly according to both geographical location of origin and altitude of origin.

Three of the genes investigated – UVR8, RUP1 and RUP2 – are directly involved in the photoreception of UV-B light. UVR8 absorbs UV-B light and RUP1 and RUP2 are involved in regenerating the UVR8 dimer. These three genes showed significant variation between both geographical and altitudinal clusters.

The crystal structure of *A. thaliana* UVR8 based on the Col-0 sequence has been confirmed by two independent studies (Christie, *et al.* 2012 and Wu, *et al.* 2012). These studies made it possible to determine where within the UVR8 protien the changes from Col-0 occurred and what kind of effect these changes may have had.

Four of these changes at positions 7, 8, 10 and 13 were found within the N-terminal. The N-terminal was not part of the crystal structure due to its

disordered nature (Christie, *et al*. 2012, Wu, *et al*. 2012). However, this region of the protein is key to nuclear localisation as it is known that UVR8 that does not have the first 23 amino acids of the N-terminal is impaired in nuclear translocation (Kaiserli and Jenkins, 2007). Therefore it is possible that mutations within this region could result in a differed pattern of cellular distribution for UVR8.

There were also changes found within the disordered C-terminal region at positions 391 and 417. Again, this part of the protein was not included in the crystal structure (Christie, J.M., *et al*. 2012, Wu, D., *et al*. 2012). It is required for COP1 binding and therefore UVR8 function (Favory, *et al*. 2009, Cloix, *et al*. 2012). However recent research suggests that the RUP proteins also bind to this region and UVR8 may be regulated by competitive binding between COP1 and the RUPs (Cloix, *et al*. 2012). Therefore changes to this region may result in differences in affinity to either COP1 or the RUPs, resulting in a different balance of regulation.

The third grouping of changes were found on the dimer interface. Directed mutations here have a variety of effects including constitutive monomerisation, constitutive dimerisation or a weakened dimer (Christie, *et al*. 2012, O'Hara and Jenkins, 2012, Rizzini, *et al*. 2011, Wu, *et al*. 2012). The changes observed are different to the site directed mutagenesis that has been performed, however that does not rule out that these mutations could result in a weaker dimer, changing the overall UVR8 photoequilibrium.

The grouping with the largest number of changes was those that occur on the outside of the protein opposite the dimer interface. These included changes at positions 35, 67, 118, 222, 224 and 294. Changes here may be involved in protein-protein interaction as although the C-terminal is required for initial interaction with COP1 and the RUPs, it is unknown whether these proteins bind only to the C-terminal or if they dock onto the main barrel of the protein (Cloix, *et al*. 2012, Favory, *et al*. 2009, Gruber, *et al*. 2010) Therefore, these mutations could be important in the turnover in binding between COP1 and the RUPs. There are a further three mutations seen on the outside of the barrel of UVR8 at

positions 308, 160 and 268. Again, it is possible that these mutations are involved in protein-protein interaction.

There was one change that is found within the water filled core of UVR8 at position 73 (Christie, *et al*. 2012, Wu, *et al*. 2012). This could results in structural changes if it were a strong mutation. However, the T73S mutation is a relatively mild mutation; both amino acids are hydrogen bonding, hydrophilic and have no charge. Finally there was one change that would result in a non-functional UVR8. Haplotype 18 contained a change at position 317 from a Cysteine residue to a stop codon. UVR8 is a seven-bladed ß-propeller protein and this stop codon would truncate the final one and half 'blades' of the propeller as well as the C-terminal region that is required for UVR8 function (Christie, *et al*. 2012, Wu, *et al*. 2012).

The five changes that were parsimony informative - A7G, P13L, H67L, H118Q and V308I – all occurred within the N-terminal or on the outside of the protein barrel (Christie, *et al*. 2012, Wu, *et al*. 2012).

Within UVR8 there were six haplotypes that are seen more frequently at high and medium altitude than they are at low altitudes (haplotypes 3, 4, 5, 8, 11, 13 and 15). Interestingly all of these haplotypes contained a combination of two or more of the following mutations from Col-0: P13L, H67L and H118Q. Furthermore these amino acids all occur in unstructured regions of the protein (Christie, *et al*. 2012, Wu, *et al*. 2012). It is possible that these three changes are key in regulating not the sensitivity of UVR8 to UV-B, but its interaction with other proteins that lead to differences in the regulation of the UVR8 photoreception pathway as all three of these changes are present on the outside of the protein, in regions that may be key to protein-protein interaction.

RUP1 is composed of seven WD40 domains and a single serine rich region. While there is no crystal structure for RUP1, it has been demonstrated that WD40 domains usually form ß-propellor structures and are highly interactable with both DNA and other proteins (Xu and Min, 2001). Many of the changes that are seen within the individuals sequenced for the 1001 Genomes Project occur within one of these WD40 repeats (Magrane and Uniprot Consortium, 2011).

Within the first repeat there were two changes: R99L and D108G. The second repeat contained a further five changes: F123L, F133L, G135V, R136Q and P141T. Both the third and fourth WD-40 repeats contained six changes. Within the third repeat I182L, N178S, R198L, G179D, G165R and M194I were observed and within the fourth repeat G210A, R235Q, D247E, A229V, R243G and P222L were seen. A further two changes were found within WD-40 repeat five: T269A and S278N. There were two changes within the sixth repeat: V337F and S319P. Finally there were four changes within the seventh repeat: R350Q, S354I, G283S and D349del. The WD40 repeats themselves are important for the structure of the protein, resulting in a 7-bladed ß-propellor structure (Xu and Min, 2011). It is possible that changes within these regions may change the flexibility or strucutural integrity of the protein, but mutagenesis studies would be required to confirm these hypotheses.

Serine-rich regions are not well documented. However, crystal structures of other proteins that contain serine-rich regions suggest that they fold as a helix bundle indicative of a protein interaction region (Briknarová, *et al*. 2005). The serine rich region of RUP1 also contained a further eight changes, two of which are mutations from serine – S61T and S39F – while a further one change was to a serine: I18S. Position 18 was of particular interest because another separate change was seen to appear here: I18T. Of the remaining four changes one was severe – a L21 deletion. The other three are T34A, D57Y and T69I. Due to the limited mutagenesis studies available on RUP1 it is difficult to determine what kind of effect these changes may have on protein function; but it would not be unreasonable to suggest that as they occur within a region that is known for protein-protein interaction that they may alter the specificity or strength of binding between RUP1 and another protein.

There were a further 10 changes observed. One of these occurs in the N-terminal of the protein, S7Y. The remaining 9 occur between the WD-40 regions, which are know for determining interaction specificity (Xu and Min, 2011). Interestingly six of these changes are found within a seven amino acid region just prior to the start of the seventh WD-40 repeat: L340M, G341S, H342Q, T343P, N344D and G347E. Often these changes co-occur (Table 5-11). Of the three changes

remaining one occurs between the third and fourth WD-40 domain, T206M, and two occur between the first and second, E115K and Y117C.

RUP1 has a much greater diversity with 56 total haplotypes. There are several haplotypes that occur more frequently at higher than lower altitudes. While all of these haplotypes contain the Y117C change they also contain a combination of the following changes: L340M, H342Q, N344D and R350Q. It is possible that these changes alter the binding potential of RUP1 to UVR8 or alter other inter-protein dynamics that in turn leads to a change in the response to UV-B as they occur between two WD-40 repeats which are regions key to protein protein interactions in WD-40 proteins (Xu and Min, 2011). Of course the region of RUP1 that interacts with UVR8 has not yet been determined. It would be interesting to test these possibilities by assaying different ecotypes with different RUP-UVR8 combinations or creating new combinations via transgenic lines.

As expected, RUP2 has a very similar predicted structure to RUP1. It is a WD-40 protein with seven WD-40 repeats (Magrane and Uniprot Consortium, 2011). The changes that are seen can be classified as either occurring within a WD-40 repeat, within the N-terminal region or between WD-40 repeats. The majority of mutations that are observed occur within the WD-40 repeats, 34 of 53. Within the first WD-40 repeat, one of the mutations that is observed is an extremely severe mutation that would result in a non-funtional RUP2: $E47^{STOP}$. This change would truncate the protein mid way through the first WD-40 repeat which is found at positions 38-77 resulting in a protein fragment that would likely be degraded (Magrane and Uniprot Consortium, 2011). RUP2 mutants have been investigated and it has been shown that a lack of RUP2 results in early flowering, dwarfism and increased UV-B resilience (Wang, *et al*. 2011, Gruber, *et al*. 2010). Therefore it is likely that haplotype the ecotype with haplotype 59 would be phenotypically similar to these previously described mutants. There were three other changes that were observed within the WD-40 domain, but none were as severe: G43V, T57S and N76Y.

The second WD-40 domain contained six changes. Four of these were unique changes: R108G, S118A, R133R and F137L. A further one change was found in

three haplotypes: C97S. However one of the changes was extremely common: M126T. As was seen in the RUP1 sequences, haplotype 1 which was based on the Col-0 sequence was not the most common sequence in RUP2, indeed it was not even the second most common sequence. Haplotype 2 which contains this M126T change within the second WD-40 repeat was the most numerous haplotype and contained 49% of the individuals sequenced. This change was also extremely widespread throughout the rest of the haplotypes. There were only five haplotypes, including haplotype 1, that did not contain this change (Table 5-13). This would suggest that it is unlikely that for RUP2 the Col-0 sequence is the ancestral sequence or that alternatively the M126T is a change that is highly selected for.

The third WD-40 repeat contained a large number of changes for such a small region. Even though it is a span of 43 amino acids from position 141-184 it contained nine observed mutations: G143R, T153S/A, H155N, T160A, T170A, V173L, R177K, C178L and P179M. There were several interesting things to notice about these changes. The first ws that at position 153, there appear to be at least two separate mutation events to either a serine or an alanine from a threonine. This would suggest that either this region was unimportant to the structure and function of the protein or that changes here result in differences to function that were adaptive. Secondly, while these changes were happening within a relatively small region, a subset of them are further concentrated within the nine amino acid smap of 170-179, where five of these changes fall. Again this would suggest that this was a key region of variation.

There were fewer mutations observed within the fourth repeat, however once again one of these was an amino acid where there have been at least two separate mutation events: C193S/F. There were six further changes: I192V, S195G, V212I, I224V, D229N and L232W. Of these, the I224V was a common change seen. It was observed within haplotype three, the second most common haplotype that also contained a M126T change. Haplotype 3 contained 22% of the individuals sequenced. In addition, there were 17 of the 64 haplotypes that contained this change.

There were fewer changes in the fifth WD-40 repeat. Two of these were seen in more than one haplotype: C260F and R270C. The further three were unique changes: T238I, F247Y and V271M. Within the sixth and seventh repeats there were three changes in total. The two within the sixth repeat are G297S, which occurs in multiple haplotypes and F306S which is unique. There was only one change within the seventh repeat: V351I.

Within the N-terminal region of the protein there were seven different changes: K8Q, a leucine insertion at position 16, Q17E, Q18E, a glutamic acid insertion at position 18, V31G and S34P. This was particularly interesting due to the high density of changes at residues 16-18, including insertions. It is possible that RUP1 interacts with a protein via its N-terminal, although this has not yet been determined. The remaining changes occur between the WD-40 repeats, which is an area that dictates protein-protein interaction and specificity (Xu and Min, 2011). There were four changes observed here: A91V, G185D, Q235P and C329G.

Within RUP2 there were three haplotypes that occur more frequently at higher altitudes that contained similar changes: 3, 20 and 47. There were few similarities between these haplotypes other than the relatively ubiquitous M126T change, although I224V was found in both haplotypes 3 and 47, both of which occur above 3000m. The I224V change is not seen between two WD40 regions, however without a crystal structure and the limited mutagenesis studies that have been performed on RUP2 it is difficult to tell what effect this change may have on the protein. However it is possible that it facilitates protein docking. Further experimentation is required to determine whether this mutation causes structural or functional changes to the protein.

Interestingly, there were also similarities between geographically very disparate countries, for example Gemany and Tanzania both contained the shared haplotype 98. This was of particular note as Tanzania was part of the German East African Empire from 1880 to 1919, suggesting that the *A. thaliana* found within Tanzania was brought by colonial Germans (Austen, 1968).

5.9.2 The majority of the genes involved in early transcriptional response to UV-B varied significantly when grouped by geographical location, but not when grouped by altitude

The further three genes that were examined varied according to geographical location to different degrees. Both HY5 and COP1 showed variation according to geographical location, however geographical origin explained far more of the variability found within the sequence of HY5 than COP1. Neither of these genes showed variation based upon altitude. These genes are both involved in multiple light perception pathways and it is unsurprising that they are very conserved. However, changes are still clearly happening in a geographical manner suggesting that geographical separation is a factor for these genes, even if altitude is not.

There has been no crystal structure determined for COP1. However there are still regions of the protein that have predicted functions (Magrane and Uniprot Consortium, 2011). COP1 contains a cytoplasmic localization signal (CLS) from amino acids 67-177 within which three of the segregating sites fall: H83M, H92P and A149V (Stacey, *et al*. 1999). There is also within this region a subnuclear localization signal (SNLS) from position 120-177 which the A149V change is also within. Indeed this change is also part of a third region, a coiled coil from positions 124-201 which is often indicative of a role in gene expression but in COP1 is required for SPA1, SPA3 or SPA4 binding (Hoecker and Quail, 2011, Laubinger and Hoecker, 2003, Saijo, *et al*. 2003, Saijo, *et al*. 2008). There is one other change that falls within this region, Q190H. One of the changes occurs within a Damaged DNA Binding (DDB1) binding WD40 (DWD) domain, DWD box 2 from position 563-578: D579H. COP1 also contains a Really Interesting New Gene (RING) type Zinc finger within which one change falls: K83M.

HY5 contains two major regions: a basic Leucine Zipper (bZIP) and a site required for interaction with COP1 (Holm, *et al*. 2000). The bZIP region is particularly important as HY5 will interact both with itself forming a homodimer and with HYH forming a heterodimer using this region (Yoon, *et al*. 2007, Holm, *et al*. 2002). However none of the changes observed within the individuals

sequenced in the 1001 Genomes Project occur in these regions. That would suggest that there is a high degree of conservation of these regions.

HYH is different. It is extremely conserved and shows very little variation between populations groups. Neither grouping by geographical nor by alititudinal origin explained a significant degree of variation within the HYH sequence. This was a surprising result as HYH works redundantly with HY5 and is seen as the gene with less influence on phenotype (Brown and Jenkins, 2008). However HYH is well documented as playing a far lesser role than HY5 while regulating many of the same genes (Briggs, *et al*. 2006). Knockout mutations to only HYH cause a very subtle phenotype that is not as strong as the HY5 knockout phenotype; when HY5 is also knocked out the double *hy5hyh* mutant plants demonstrate a stronger phenotype than for either single mutant (Zhang, *et al*. 2011).

As with HY5, HYH contains two major regions, a bZIP domain and a region required for COP1 interaction (Holm, *et al*. 2002, Jakoby *et al* 2002). Unlike HY5, three of the seven segregating sites were found within these regions including the parsimony informative M34L. The M34L change was found within the COP1 interaction region as identified by Holm *et al*. in 2002. A further unique change was seen within this region, S24R. Neither of these changes was identical to previously documented mutagenesis studies, but it possible that they could affect the interaction of COP1 and HYH. There was one change observed within the bZIP domain: N116K. As a key motif within the bZIP domain is N-X7-K/R – where X is any amino acid – and that this motif is required for DNA interaction it is likely that this change, occurring at the start of such a motif, would result in a non-functional protein or a protein with reduced functionality (Jakoby, *et al*. 2002).

There are explanations as to why HYH is so conserved: it could be that changes to the sequence are far more deleterious in HYH than in HY5. Furthermore, although a weak phenotype is seen under UV-B when HYH is knocked out, that does not mean that a plant containing both HY5 and HYH does not have finer transcriptional control and therefore an advantage in a natural competitive environment (Zhang, *et al*. 2011, Nemhauser, 2008, Gangappa, 2013). Moreover,

it is important to remember that HYH is involved in multiple other signalling pathways. Although HYH only plays a redundant role in UV-B photomorphogenesis, where HY5 is the dominant partner, this does not mean that in some other pathways that relationship is reversed. It could be that while HYH is not required for optimal UV-B tolerance and acclimation, it is required for the plant to be competitive in another area, for example anthocyanin accumulation, ethylene signalling, auxin signalling, flowering time or nitrogen reductase activity, all of which both HYH and HY5 are involved in (Sibout, *et al*. 2006, Jonassen, *et al*. 2006, Nemhauser, 2008, Zhang, 2011).

5.10 Conclusions

The accession of *A. thaliana* that is studied will likely have an effect on protein structure and function. The ecotype that is most commonly used in studies, Col-0, has a sequence that is representative only 2.3% of the 855 ecotypes that were sequenced by the 1001 Genomes Project when only three genes are taken into account. It is important that this variation is taken into account when investigating the structure and function of a protein. This study has shown that there are ecotypes for UV-B responsive genes that contain non-functional proteins. There are several regions within the different UV-B responsive proteins that vary naturally within *A. thaliana* and would be good targets for further study on the structure/function relationship with regard to UV-B acclimation.

Chapter 6: Final Discussion

6.1 Introduction

UV-B light is a factor that most plants have to deal with on a day to day basis. In a natural solar environment plants are either adapted to an environment with UV-B or they acclimate through continuous exposure (Favory, et al, 2009, González Besteiro, *et al*. 2011, Hectors, *et al*. 2007, Hideg, *et al*. 2013, Jansen and Bornman, 2012). With the discovery of the UV-B photoreceptor UVR8, a significant breakthrough was made in understanding how plants respond to this important light signal (Christie *et al*. 2012, Rizzini *et al*. 2011, Wu *et al*. 2011). However, studies of UVR8 were performed in very artificial UV-B environments. UVR8 was either studied as a purified protein or in UV-B naïve plants (Christie, *et al.*, 2012, Huang, *et al.*, 2014, Rizzini, *et al*. 2011, Wu, *et al.*, 2012, Cloix, *et al.*, 2012, Kaiserli and Jenkins, 2007, Heijge and Ulm, 2013, Heilmann and Jenkins, 2013, O'Hara and Jenkins, 2012). The configuration of UVR8 was determined to be like a switch in these situations: in darkness and zero UV-B conditions UVR8 was expected to be entirely dimeric and in light and the presence of UV-B, UVR8 was expected to quickly switch to the monomeric form to initiate signalling. In order to determine whether this was the case in plants that were exposed to more long term UV-B a series of timecourses were constructed to test the monomerisation rate when moving from a dark to a light cycle. Further work was done by repeating these experiments in field conditions across the course of a year to obtain different light and temperature environments that would be experienced by non-laboratory grown plants. It was found that this model was not sufficient to describe the ratio of $UVR8^{dimer}$ to $UVR8^{monomer}$. Instead of acting like a on/off switch, UVR8 formed a photoequilibrium where even in the presence of UV-B a substantial pool of $UVR8^{dimer}$ was present. This indicated that UVR8 could regenerate in the presence of UV-B, and therefore that regeneration would play an important role in establishing the UVR8 photoequilibrium.

The RUP proteins have been characterised as negative regulators of the UV-B photomorphogenic pathway (Gruber, *et al*. 2010, Heijge and Ulm, 2013,

Heilmann and Jenkins, 2013). By interacting with UVR8, they facilitate the regeneration of the UVR8 dimer. This study found that a lack of RUPs did have an effect on the UVR8 photoequilibrium in that the *rup1rup2* plants had a smaller pool of $UVR8^{dimer}$ in the photoequilibrium. Furthermore, it was shown that temperature played a role in the RUPs capacity for $UVR8^{dimer}$ regeneration. While in WT plants temperature affected the rate of $UVR8^{dimer}$ regeneration, in the *rup1rup2* mutant there was no difference in regeneration rate of the $UVR8^{dimer}$ regardless of temperature. However, temperature was not the only factor that was found to affect the UVR8 phototequilibrium. Temperature, UV-B fluence rate and the accession of the plant studied were all found to act additively on both the UVR8 photoequilibrium and plant morphology, with the UV-B fluence rate and the accession also forming an interactive effect. To determine what might be influencing this difference between ecotypes the variability of UV-B related genes within *A. thaliana* ecotypes was investigated.

The 1001 Genome Project is currently in progress, with the sequences of 855 *A. thaliana* ecotypes published at the time of writing. Previous studies have already shown the great degree of variability between *A. thaliana* ecotypes; that while *A. thaliana* does not show a great deal of variation based upon geographical distance between individuals it does show environmental and altitudinal clines (Alonso-Blanco and Koorneef, 2000, Koorneef, *et al*. 2004, Platt, *et al*. 2010). Furthermore it has been shown that photoreceptors are a likely source of variation within the plant (Filiault *et al*. 2008). This study looked at the variation of six different genes involved in UV-B photomorphogenesis. Three of these genes are involved in the immediate photoreception of UV-B, UVR8, RUP1 and RUP2: three are involved in the transcription of UVR8 controlled genes as well as other light pathways, COP1, HY5 and HYH. It was found that the genes that are involved in transcriptional regulation were far less variable than those involved in UV-B photoreception. The RUPs in particular were extremely variable. The variability within UVR8, RUP1 and RUP2 was frequently seen in areas of the protein that are involved in protein-protein interaction. Furthermore, when individuals were clustered by altitude, they were more related to individuals within these clusters than without despite geographic separation.

6.2 UVR8 forms a photoequilibrium in both lab grown and field grown UV-B acclimated plants

This work now shows that UVR8 forms a photoequilibrium under long-term natural solar conditions rather than the simple $UVR8^{dimer}$ » $UVR8^{monomer}$ switch seen when using UV-B naïve plants, cell extract or purified protein. Under both strictly controlled laboratory growth conditions where plants were given four varying UV-B treatments and in highly variable field conditions UVR8 did not switch from the dimeric form in darkness/zero UV-B to entirely monomeric in light/plus UV-B. In plants that had never been exposed to UV-B, UV-B naïve plants, UVR8 was almost entirely dimeric in line with the studies in purified protein (Christie, *et al*. 2012, Miyamori, *et al*. 2015, Rizzini, *et al*. 2011, Wu *et al*. 2012) and regeneration *in planta* (Heijge and Ulm, 2013, Heilmann and Jenkins, 2013) (Fig 3-2 and Fig 3-4). However, unlike in the UV-B naïve plants, plants that had been acclimated to UV-B through exposure to either light/dark cycles with supplementary UV-B or natural solar light over a period of three weeks formed a photoequilibrium (Fig 3-2, Fig 3-4 and Fig 4-2). In these plants monomeric UVR8 was present before the start of the light cycle or dawn and a pool of dimeric UVR8 was present throughout the light cycle or the day. These results make it clear that in UV-B acclimated plants UVR8 does not require the absence of UV-B to redimerise.

There are several potential reasons that a UVR8 photoequilibrium exists in UV-B acclimated plants but not UV-B naïve plants. UVR8 is responsible for UV-B acclimation including the upregulation of CHS, flavonoids, genes that are protective of photosynthesis, phenolics and DNA repair (Brown *et al*. 2005, Ballaré *et al*. 2012, Robson, *et al*. 2014, Wargent *et al*. 2014). It is possible that through exposure to UV-B the chemical composition of the leaf changes so that UV-B penetration is reduced. This is especially appealing as UVR8 also affects leaf development, morphology and hypocotyl and stem length and the chemical and structural composition of leaves as well as overall plant growth patterns have been shown to affect UV-B penetration into leaves and overall UV-B stress (Sedeg, 2014). Furthermore, investigation into plant morphology between UV-B acclimated plants and UV-B naïve plants has shown that UV-B acclimated plants

have differences in chemical composition and photosynthetic competency (Carbonell-Bejerano, *et al*. 2014, Wargent, *et al*. 2014). Clearly UV-B acclimation through production of flavonoids and phenolics and modification of growth is useful to the plant only under UV-B conditions. However, different conditions demonstrate different UVR8 photoequilibriums, which further suggests that this response is fine tuned to the environment of the plant.

Other possibilities include changes in gene expression. UVR8 does affect gene expression, including stimulating the production of the negative regulator of the UV-B photomorphogenic pathway and the key factor in rapid UVR8 dimer regeneration, the RUP proteins. By changing the UV-B environment of the plant it is possible that the change in gene expression, in particular its increase in *RUP* expression, feeds back into the UVR8 photoequilibrium changing the balance between monomer and dimer.

Finally, UV-B is an entrainment signal for the circadian clock (Hua, *et al*. 2013, Tilbrook, *et al*. 2013). It is possible that after the initial exposure to UV-B, UVR8 monomerisation and redimerisation is partially controlled by the circadian clock. In this way UVR8 may begin to redimerise prior to the light cycle/dawn as a protective mechanism, explaining the presence of monomer that is present in zero UV-B conditions in the UV-B acclimated plants. This is supported by the fact that the RUP proteins are circadian regulated (Wang, *et al*. 2011). These hypotheses will be discussed in the following sections.

6.3 Abiotic factors influence the UVR8 photoequilibrium

UVR8 monomerises in response to UV-B (Christie, *et al*. 2012, Miyamori, *et al*. 2015, Rizzini, *et al*. 2011, Wu *et al*. 2012). However, this does not address how different factors affect the balance of the UVR8 photoequilibrium. Through the use of GLM, it was determined that UV-B was a determining factor in the extent of UVR8 monomerisation (Chapter 3 and Chapter 4). It is important to note that a difference did arise between the plants grown in controlled conditions and those grown in field conditions.

Within a controlled environment, a clear difference was seen between the zero UV-B treatment and each of the different UV-B fluence rates; even at the lowest

fluence rate used, 0.3 µmol m^{-2} s^{-1}. This supports data which shows UVR8 is a very sensitive photoreceptor. The UVR8 dependent pathway can be activated by only 0.1 µmol m^{-2} s^{-1} of UV-B and it is likely that multi-photon excitation is not required for UVR8 to monomerise (Brown, *et al.* 2009, Miyamori, *et al.* 2015). While significant differences in photoequilibrium were seen between the different UV-B treatments, this depended upon which ecotype was observed. With L*er* none of the UV-B treatments were significantly different to each other (Chapter 3). However, with Col-0 the low 0.3 µmol m^{-2} s^{-1} treatment was significantly different to the medium, 1.0 µmol m^{-2} s^{-1} treatment (Chapter 3). There was no difference observed between the medium and high, 3.0 µmol m^{-2} s^{-1} UV-B treatments within Col-0 (Chapter 3). This would suggest that while UV-B is the determining factor in whether a photoequilibrium is formed – as UVR8 is entirely dimeric in the absence of UV-B – factors other than the fluence rate of UV-B affect the balance of the photoequilibrium. Within the controlled experiments, the only variable other than UV-B fluence rate that was manipulated was *A. thaliana* ecotype used.

Within field conditions the UVR8 photoequilibrium was extremely variable (Chapter 4). This is to be expected as timecourses were performed throughout the course of a year and conditions changed on both a small – hourly and daily – and a large – weekly, monthly and seasonally – timescale. Not only did the temperature fluctuate, the length of day also changed as did the intensity of both UV-B and PAR light (Fig 4-2). This further supports the hypothesis that factors other than total UV-B dose and fluence rate affect the UV-B photoequilibrium. By using GLM it is possible to determine which recorded factors are affecting the UVR8 photoequilibrium and how they are interacting with each other. Once again, UV-B is shown to be a significant factor in beginning and establishing the photoequilibrium (Fig 4-5). It is interesting to note that as UV-B fluence rate increases so does the percentage of monomeric UVR8 until 1.0 µmol m^{-2} s^{-1} is reached. After that point, no further monomerisation is seen with a corresponding increase in UV-B fluence rate. Once again, this supports the data that UVR8 is a sensitive photoreceptor (Brown, *et al.* 2009, Miyamori, *et al.* 2015). This saturation also makes it possible to see

when a second factor is causing an increase in monomerisation beyond that caused by UV-B. By correlating the average UV-B fluence with UVR8 photoequilibrium and the other recorded factors it is possible to see whether further monomerisation occurs after the saturation point of UV-B has been reached, which would indicate that the second factor was influencing the UVR8 photoequilibrium in addition to UV-B.

It can clearly be seen from the field data that PAR and time of day do not affect the UVR8 photoequilibrium, either by themselves or in a UV-B synergistic way (Fig 4-5). Temperature does affect the UV-B photoequilibrium. While temperature is not in itself enough to cause monomerisation (Fig 4-6), in addition to UV-B it is statistically significant. Furthermore, although no additional increase in monomerisation is seen after the UV-B saturation point has been reached, at low temperatures the UVR8 photoequilibrium varies without a corresponding fluctuation in UV-B (Fig 4-5). In conjunction with this, in naïve plants that have been treated with a short term, high dose of UV-B, UVR8 regenerates to a dimer slower at 10°C than at 5°C. Both are slower than at 20°C and 30°C (Fig 4-7). There are several reasons why this might occur. Different *A. thaliana* ecotypes are either summer annuals which germinate in spring and flower in autumn or winter annuals which germinate in autumn, survive the winter as rosettes and flower in spring and early summer (Koorneef, *et al*. 2004). Those which are winter annuals may experience cold days that are nonetheless sunny, with high UV-B fluence rates. The increase in monomerisation between 7-10°C and decrease in regeneration rate at 10°C compared to 5°C may be a response that provides protection on cold but sunny winter days. The RUP protein level may also be affected by cold. This could lead to a change in the overall dimer photoequilibrium.

6.4 The photoequilibrium is affected by the RUP proteins

In addition to the abiotic factors, it is likely that the RUP proteins play a role in determining the balance of the UVR8 photoequilibrium. The RUP proteins have been clearly implicated in the regeneration of the UVR8 dimer (Heijge and Ulm, 2013, Heilmann and Jenkins, 2013). In controlled growth conditions the *rup1rup2* mutant plants show a significantly different photoequilibrium to the WT plants

(Fig 3-2). Furthermore the photoequilibrium of the *rup1rup2* mutant has a far higher proportion of monomer than the WT and there is no statistical difference between the three plus UV-B treatments (Fig 3-2). This would suggest that the RUPs do play a vital role in maintaining the UVR8 photoequilbrium as the *rup1rup2* plants seem unable to sustain the same pool of dimer as the WT plants. Furthermore, it appears that the temperature effect on the UVR8 photoequilibrium is in part regulated by the RUP proteins. When regeneration is assayed in UV-B naïve plants across a range of temperatures, the *rup1rup2* plants show no significant difference in regeneration rate. Once again this suggests that the presence of the RUP proteins affects the balance of the UVR8 photoequilibrium through the regeneration rate of the dimer (Fig 4-7).

6.5 The affect of *A. thaliana* ecotype of the UVR8 photoequilibrium

There was a difference in UVR8 photoequilibrium between Col-0 and L*er*. Col-0 and L*er* were originally collected in North America at 264m above sea level and Germany at 619m above sea level respectively (NASC). These results would suggest that ecotype and original location and environment of the ecotype could be affecting the UVR8 photoequilibrium. Three other ecotypes from different altitudes from geographically different locations were studied to determine whether ecotype has an effect (Chapter 3). Ecotypes from higher altitudes seemed to be less responsive to UV-B than ecotypes from lower altitudes. This result could indeed confirm that these plants maintain different UVR8 equilibria due to differences in UVR8, the RUPs or some other genes directly involved in the UV-B photomorphogenic pathway. However, it is well noted that the different *A. thaliana* ecotypes contain a high degree of variability both in genotype and phenotype (Alonso-Blanco and Koorneef, 2000, Koorneef *et al.* 2004). It is possible that these ecotypes have naturally different base levels of UV-B absorbing or reflecting compounds within their leaves regardless of UV-B. While this would still mean that some are more or less sensitive to UV-B, it does not necessarily translate that those from a high light or UV-B environment (for example from a low latitude or high altitude) were the ones that were least sensitive to UV-B.

6.6 The global variation of the UVR8 haplotype in *A. thaliana*

The controlled growth room timecourses demonstrated that there was variability between the different *A. thaliana* ecotypes in relation to UVR8 photoequilibrium. This was not unexpected. *A. thaliana* has a huge naturalised growth range, far outside of its original Eurasian range (Horton, *et al.* 2012) and has been found far outside of its accepted range in New Zealand and the Pacific Islands. While *A. thaliana* is a self-fertiliser 97% of the time and almost entirely homozygous naturally – there is very little heterozygosity and outcrossing observed in natural populations – the plants are adapted to their vastly different environments (Abbott and Gomes, 1988, Platt, *et al.* 2010, Alonso-Blanco and Koorneef, 2000). Variation can be seen between different ecotypes when they are grown in identical conditions, revealing differences in basic morphology such as leaf production rate, leaf colour, leaf size and shape, flowering time, seed dormancy, trichome density and even UV-B sensitivity (Alonso-Blanco and Koorneef, 2000, Alonso-Blanco, *et al.* 2003, Anwer and Davis, 2013, Hilscher, *et al.* 2009, Torabinejad and Caldwell, 2000). In addition to this, photoreceptors are hypothesised to be a common target of natural selection; both PhyA and PhyB have been characterised as having different structures that affect plant responses to light in different *A. thaliana* ecotypes (Filiault, *et al.* 2008, Maloof, *et al.* 2001). When the cross talk between different photoreceptors is taken into account, for example the antagonistic relationship between UVR8 and PhyB to optimise shade response, it is clear that very few changes could result in highly different plant responses (Mazza and Ballaré, 2015). Through use of the 1001 Genomes Project it was possible to document all non-synonymous sequence changes within chosen genes and relate these to different environmental clines such as latitude and longitude.

6.6.1 HYH is extremely conserved within *A. thaliana*

While *A. thaliana* does not have a heavily structured geographic population (Platt, *et al.* 2010), it was surprising that HYH varied so little between all 855 ecotypes that had been sequenced. Only seven different haplotypes were identified and of these the most common haplotype was found in 96% of the ecotypes surveyed (Chapter 5.5). No significant population structure was seen

using any of the groupings. HYH may be under extremely strong selection pressure and any changes to the sequence affect the plant so adversely it does not survive to produce offspring. As *hyh* null mutant plants exist and are able to survive and produce viable seed in a lab environment, it would be surprising if this was the case. Especially as it is extremely difficult to grow to seed the *cop1-4* mutant which has a GLN283-STOP mutation in COP1 - another gene studied here - that shows far greater variation than HYH.

6.6.2 COP1 and HY5 vary significantly according to geographical location, but not altitudinal location

COP1 is composed of seventeen different haplotypes, with the most common haplotype accounting for 92% of the sequences seen. HY5 has fewer haplotypes with only eleven different haplotypes observed, but far greater diversity as the most common haplotype accounts for 51% of the ecotypes surveyed. Neither HY5 nor COP1 vary based on altitudinal clines. Both show statistically significant variation between geographically distinct clusters based on the latitude and longitude of the origin of the ecotype (Chapter 5.3 and 5.4).

These results would suggest that while COP1 and HY5 do show variation based on geographical location of origin, it is not changing in response to a high light or UV-B environment. This is potentially due to the large degree of crosstalk between these proteins and other proteins as both are involved in multiple pathways. Furthermore, although COP1 inhibits photomorphogenesis in white light, it promotes UV-B photomorphogenesis (Favory, *et al.*, 2009). This antagonistic role could limit the potential variability and adaptability of COP1.

6.6.3 UVR8, RUP1 and RUP2 vary based on geography and altitudinal cline

UVR8, RUP1 and RUP2 are more variable than the other genes investigated, with 22, 57 and 64 haplotypes respectively. Within the UVR8 haplotypes the most common sequence composes 65% of the total ecotypes. Within 52% of the ecotypes studied contain the most common RUP1 sequence and 49% contain the most common RUP2 sequences. All three of these genes vary significantly when grouped by geographical or altitudinal location.

These three genes are the most directly involved in UV-B photoreception. UVR8 is the UV-B photoreceptor and RUP1 and RUP2 are directly involved in negative regulation of the pathway through UVR8 dimer regeneration. As such, it is unsurprising that these genes show different populations in high light and UV-B environments. These results would suggest that the amino acid sequence and structure of UVR8, RUP1 and RUP2 affects plant response to UV-B in an adaptive manner.

Furthermore, there are several changes that are seen proportionally more in high UV-B environments. Within UVR8, amino acid 13 and 67 are observed as Leucine rather than the more common Proline and Histidine respectively and at position 118 the more common Histidine is replaced with Glutamine. These changes frequently occur together or in different combinations and are seen at high altitudes. All three of these mutations occur in unstructured areas of the protein on the base of the monomer opposite the dimer interface. It is likely that these changes are not affecting how UVR8 perceives UV-B but rather how it interacts with other proteins, affecting regulation of the UVR8 photoreception pathway (Chapter 5.1). At high altitudes the RUP1 amino acid sequence has changes L340M, H342Q, T343P, N344D and R350Q. These changes are found between the sixth and seventh WD40 repeats, apart from R350Q which occurs at the very beginning of the seventh WD40 repeat. As the protein sequence between WD40 repeats is involved in protein interaction specificity, it is possible that these mutations can change how RUP1 interacts with other proteins. This would be of particular interest in regulating the redimerisation of UVR8 which requires RUP-UVR8 interaction. RUP2 contains one mutation that commonly occur at high altitudes: I224V. I224V occurs inside the fourth WD40 domain. Both Isoleucine and Valine are hydrophobic amino acids with neutral charge so it is unlikely that this mutation would affect the WD40 structure drastically however, further study would be required to determine if this change affected function.

6.7 Limitations of the study

There were several practical limitations found within this study. The first was determining the UVR8 photoequilibrium using semi-quantitative Western Blot analysis. While semi-quantitative Western Blot analysis, especially as performed

in this thesis is an accepted and published method it is true that it is not a truly quantitative method. This may lead to artefacts in the balance of the UVR8 photoequilibrium. However, at the time of writing, there was not a superior way to perform the Western Blot analysis. While fluorescent techniques for determining the respective proportions of two different interacting proteins have been developed through BRET or Förster resonance energy transfer (FRET), comparing the proportion of homodimer/monomer in a fully quantitative manner has not been solved using these methods (Bücherl, *et al*. 2010, Bücherl, *et al*. 2014). The LiCor Odyssey system is another potential option for performing fully quantitative Western Blots and provides a wider range for both sensitivity and saturation. Furthermore, this is a better system for comparison between two separate proteins than the one used within this study. However, the method of quantification is similar to that used in this thesis, and there was no easy access to a LiCor Odyssey system. Therefore, use of semi-quantitative Western Blot analysis was used as the best solution at the time of research.

Secondly, the sampling within the 1001 Genomes Project is not equal across all countries and environment types. There are some countries where only two ecotypes have been provided, and some altitudes where a population group will contain only one ecotype. While it has been shown that *A. thaliana* does not exhibit much polymorphism within local populations that does not mean that polymorphisms are absent (Koorneef, *et al*. 2004). This means that generally, each individual ecotype is likely to be representative of the local population, but not in all cases. The only solution to this is further sampling and sequencing.

6.8 Conclusions

The following conclusions can be drawn from this work:

1. UVR8 will monomerise in natural solar light over a wide range of UV-B fluence rates.
2. UVR8 does not exist as a simple $UVR8^{dimer}$ » $UVR8^{monomer}$ switch, instead a dynamic photoequilibrium is established.
3. Abiotic factors such as UV-B fluence rate and temperature affect the UVR8 photoequilibrium.

4. The UVR8 photoequilibrium is controlled by $UVR8^{dimer}$ regeneration rather than monomerisation.
5. RUP1 and RUP2 are vital in maintaining the UVR8 photoequilibrium.
6. The regeneration rate of UVR8 is affected by temperature through RUP activity.
7. Different ecotypes maintain different UVR8 photoequilibria with respect to UV-B fluence rate.
8. There is a huge degree of variability in *A. thaliana* sequence worldwide.
9. Proteins involved in the early transcriptional stages of UVR8 UV-B response are conserved and do not vary by altitude. Only COP1 and HY5 vary by geographical location.
10. UVR8, RUP1 and RUP2 vary based on both geographical and altitudinal location of origin.
11. Within UVR8, RUP1 and RUP2 there are changes which occur more frequently at high altitude. These are potential adaptations for high UV-B environments.

Based on these observations, it can be determined that the current model of UVR8 monomerisation and dimer regeneration is far too simple and needs to be extended to include the existence of a photoequilibrium; the influence of abiotic factors such as temperature; and the background ecotype used must also be considered.

6.9 Future Work

There are many opportunities for furthering the work presented in this thesis. While it has been shown that the RUP proteins influence the UVR8 photoequilibrium, the mechanism through which this is achieved has not been determined. Examination of the RUP protein amount found in the cell under different conditions and whether this correlates to changes in the UVR8 photoequilibrium would be a great place to start.

Investigation of the effect of protein structure on the UVR8 photoequilibrium has not been completed. The database analysis within this thesis gives an excellent starting point to determine whether the natural changes seen within *A. thaliana*

translate to changes in the UVR8 photoequilibrium. Furthermore, these results could help determine whether UVR8, RUP1 or RUP2 is the determining factor of the photoequilibrium balance. While BRET and FRET were not applicable to determine homodimer interaction, they could be very effectively used to study the interaction dynamics of UVR8, RUP1 and RUP2 as well as other proteins within the UVR8 photoreception complex such as COP1.

The effect of changes in UVR8 photoequilibrium also needs to be investigated. Once again using the data generated from the study of the 1001 Genomes Project it should be possible to pick ecotypes that contain different haplotypic combinations of UVR8, RUP1 and RUP2. UV-B response and sensitivity can then be investigated and correlated to UVR8 photoequilibrium. This should help to establish whether UVR8 photoequilibrium is key in determining UV-B tolerance or is a more fine-scale adjustment of UV-B response.

This project demonstrated that there was variation that occurred within UVR8, RUP1 and RUP2, however there are many more analyses that could be performed. Firstly, it would be good to compare the ratio of synonymous to non-synonymous changes for all of the gene studied. This could help determine whether genes were under purifying or diversifying selection. A linkage disequilibrium analysis could also help determine if there were haplotypes that frequently co-occur. Again, as it is hypothesed that the changes within UVR8, RUP1 and RUP2 may be related to protein-protein interaction, changes that co-occur may be indicative of changed protein relationships and binding competition. This could then be further examined experimentally by performing a pull down assay and checking the UVR8 photoequilibrium.

While studies have been performed on the cellular localisation of UVR8, this has been performed using UV-B naïve plants (Kaiserli and Jenkins, 2007). It would enlightening to determine whether the cellular distribution seen – from primarily cytoplasmic in the absence of UV-B to primarily nuclear in the presence of UV-B – continues when under more natural solar conditions. In addition, some of the changes observed within the UVR8 sequences studied were found within the N-terminal, which is essential for localisation of UVR8. Analysis of how this

affected nuclear localisation, and the effect this has on both UVR8 and its downstream responses would be interesting to investigate.

Further analysis can be done to determine genes involved in regulating the UVR8 photoequilibrium by taking two ecotypes with significantly different UVR8 photoequilibria balances and creating recombinant inbred lines. QTL analysis could then be undertaken to determine whether there are any unknown, minor genes involved in maintaining the equilibrium. It would also be interesting to utilise the 1001 Genomes Database further and investigate other photoreceptors and their key interactors such as PHY and the PIFs.

Finally, this study has focused only on *A. thaliana*, which is an annual plant. It would be interesting to look at the responses of UVR8 and the genetic variety of UVR8 and the RUPS within a variety of different plants. For example, as conifers do not drop their leaves, they have to be able to cope with accumulative UV-B exposure and damage. There are also other plants that are adapted to and specialised for high light environments. In order to achieve this, a polyclonal UVR8 antibody that can recognise UVR8 from a variety of plants would have to be developed. Furthermore, experimental techniques would have to be developed for plants that are grown exclusively in a field environment.

Appendix

Table A-4: The accessions that have been sequenced at the time of writing from the 1001 Genomes Project. Accessions are listed in alphabetical order. Included is the latitude and longitude at which the accession was originally found, from which the country, continent and altitude were extrapolated. The haplotype designations for UVR8, COP1, HY5, ELIP1, HYH, RUP1 and RUP2 for each accession are also included.

Accession	Latitude	Longitude	Country	Continent	Altitude	UVR8	COP1	HY5	ELIP1	HYH	RUP1	RUP2
11C1	55.8877	-3.21072	UK	Europe	228	2	1	2	1	1	5	2
ARGE-1-15	47.16	4.28	France	Europe	464	1	2	2	2	1	2	3
ARR-17	44.05	3.69	France	Europe	287	3	1	2	2	2	3	4
Aa-0	51	10	Germany	Europe	376	1	1	1	1	1	3	1
Abd-0	57.09	-2.05	UK	Europe	60	1	1	2	3	1	2	2
Adam-1	51.41	59.98	Russia	Europe	330	1	1	1	1	1	2	2
Aedal-1	62.8622	18.336	Sweden	Europe	88	1	1	2	2	1	4	2
Aedal-3	62.8622	18.336	Sweden	Europe	88	1	1	2	1	1	4	2
Ag-0	45	1.5	France	Europe	270	1	1	2	1	1	2	5
Agu-1	41.32	-1.34135	Spain	Europe	928	3	1	1	1	1	5	2
Aiell-1	39.13	16.17	Italy	Europe	393	1	1	2	1	3	2	6
Aitba-1	31.48	-7.45	Morocco	Africa	1396	4	1	2	1	1	6	2
Ak-1	48	8	Germany	Europe	250	1	1	2	1	1	3	2
Alc-0	40.31	-3.22	Spain	Europe	631	5	3	1	1	2	2	2
Ale-Stenar-44-4	55.3833	14.05	Sweden	Europe	19	1	1	2	1	1	2	2
Ale-Stenar-56-14	55.3833	14.05	Sweden	Europe	19	2	1	2	2	1	7	3
Ale-Stenar-64-24	55.3833	14.05	Sweden	Europe	19	2	1	2	1	1	2	2
Algutsrum	56.68	16.5	Sweden	Europe	10	2	1	2	1	1	8	2
Alst-1	54.8	-2.4	UK	Europe	372	1	1	1	1	1	3	7
Alt-1	48.59	9.22	Germany	Europe	405	1	1	1	1	1	1	2
Altai-5	46.4	96.25	Mongolia	Asia	2175	1	1	1	1	1	9	3
Amel-1	53.1	5.8	Netherlands	Europe	-1	1	1	1	1	1	2	2
An-1	51.5	4.5	Belgium	Europe	8	1	1	1	1	1	2	5
Ang-0	50	5	Belgium	Europe	437	1	1	1	1	1	2	2
Anholt-1	51.85	6.43	Germany	Europe	19	1	1	2	1	1	2	3
Ann-1	45.9	6.1	France	Europe	503	1	1	2	1	1	2	8
Anz-0	-2.52	36.12	Tanzania	Africa	1561	1	1	1	1	1	2	9
App1-12	56.3333	15.9667	Sweden	Europe	18	6	1	1	1	2	2	2
App1-14	56.3333	15.9667	Sweden	Europe	18	1	1	2	1	1	2	2
App1-16	56.3333	15.9667	Sweden	Europe	18	2	3	2	1	1	2	10
Appt-1	51.8	5.6	Netherlands	Europe	7	2	1	2	1	1	2	2
BEZ-9	44.12	3.77	France	Europe	370	3	1	3	1	1	2	4
Bl-4	48.4	8.77	Germany	Europe	422	1	1	1	1	1	10	2
BRE-14	48.85	4.45	France	Europe	91	1	1	1	1	1	2	3
BRI-2	50.68	3.52	France	Europe	46	1	1	1	4	1	2	2
Ba-1	52	-3.5	UK	Europe	209	1	1	1	1	1	2	1
Baa1-2	56.4	12.9	Sweden	Europe	183	7	1	1	1	1	1	2
Baa4-1	56.4	12.9	Sweden	Europe	183	2	4	2	1	1	2	2
Baa5-1	56.4	12.9	Sweden	Europe	183	2	4	2	1	1	2	2
Baa-1	51.3	6.1	Netherlands	Europe	27	2	1	1	1	1	11	2
Bach-7	48.41	8.84	Germany	Europe	469	8	1	1	1	1	2	2
Bach2-1	48.41	8.84	Germany	Europe	469	1	1	1	1	1	2	2
Bai-10	48.5	8.78	Germany	Europe	489	1	1	1	1	1	2	3
Bak-2	41.7942	43.4767	Georgia	Europe	1242	9	1	1	1	1	2	3

Accession	Latitude	Longitude	Country	Continent	Altitude	UVR8	COP1	HY5	ELIP1	HYH	RUP1	RUP2
Bak-7	41.7942	43.4767	Georgia	Europe	1242	9	1	1	1	1	12	11
Balan-1	51.82	79.48	Russia	Asia	195	1	1	1	2	1	5	2
Basta-1	51.82	79.48	Russia	Asia	195	1	1	4	1	1	9	3
Basta-2	51.82	79.48	Russia	Asia	195	1	1	4	1	1	9	6
Bay-0	49	11	Germany	Europe	535	1	1	1	1	1	2	12
Bch-1	53.5	10.5	Germany	Europe	44	1	1	1	1	1	2	3
Bd-0	52.5	13.5	Germany	Europe	39	1	1	1	1	1	3	13
Bela-1	48.47	18.94	Slovakia	Europe	935	1	1	2	1	1	9	3
Bela-2	48.47	18.94	Slovakia	Europe	935	1	1	1	1	1	13	2
Benk-1	52	5.7	Netherlands	Europe	46	1	1	2	1	1	7	2
Ber	55	12	Denmark	Europe	65	1	1	2	1	1	2	2
Berg-1	48.41	8.79	Germany	Europe	491	1	1	1	1	1	2	14
Bg-2	47.6479	-122.305	USA	North America	24	1	1	1	1	1	2	6
Bijisk-4	52.52	85.27	Russia	Asia	184	1	1	1	1	1	9	3
Bik-1	33.89	35.67	Lebanon	Asia	776	10	1	1	5	1	14	15
Bil-5	63.324	18.484	Sweden	Europe	55	3	11	2	1	1	4	2
Bil-7	63.324	18.484	Sweden	Europe	55	3	1	2	1	1	4	2
Bivio-1	39.13	16.17	Italy	Europe	393	11	1	2	6	1	2	3
Bl-1	44.5	11.5	Italy	Europe	34	1	1	2	1	1	2	2
Bla-1	41.68	2.8	Spain	Europe	81	1	1	1	1	1	1	1
Bla_1	41.68	2.8	Spain	Europe	81	1	1	2	1	1	15	7
Blh-1	48	19	Czech Republic	Europe	541	1	1	2	1	1	1	2
Boo2-1	55.86	13.51	Sweden	Europe	69	1	1	1	1	1	1	1
Boot-1	54.4	-3.3	UK	Europe	46	2	1	2	1	1	2	9
Bor-1	49.4	16.2	Czech Republic	Europe	514	1	1	2	1	1	2	2
Bor-4	49.4	16.2	Czech Republic	Europe	514	1	1	1	1	1	1	2
Borky1	49.4	16.2	Czech Republic	Europe	514	1	1	1	1	1	2	2
Br-0	49	16.5	Czech Republic	Europe	184	1	1	2	1	1	5	16
Boesarp-34-145	55.7167	14.1333	Sweden	Europe	41	1	3	1	1	1	1	2
Broet1-6	56.3	16	Sweden	Europe	14	2	1	2	1	1	7	2
Bs-1	47.5	7.5	Switzerland	Europe	334	3	1	2	1	1	3	1
Bsch-0	50.0167	8.6667	Germany	Europe	130	1	1	1	1	1	1	1
Bu-0	50.5	9.5	Germany	Europe	430	1	1	2	1	1	2	1
Buckhorn-Pass	41.3599	-122.755	USA	North America	1089	1	1	1	4	1	16	2
Bur-0	53.5	-8	Ireland	Europe	39	2	3	5	1	1	2	2
Bur_0	53.5	-8	Ireland	Europe	39	2	5	5	1	1	2	2
C24	40.2	-8.42	Portugal	Europe	45	1	1	1	1	1	2	2
CATS-6	50.79	2.69	France	Europe	98	2	1	2	2	1	2	2
CHA-41	42.3634	-71.1445	USA	North America	3	1	1	2	1	1	2	2
CIBC-17	51.4162	-0.67647	UK	Europe	74	1	1	1	1	1	17	3
CIBC-5	51.4162	-0.67647	UK	Europe	74	1	1	1	1	1	2	6
CON-7	47.24	4.43	France	Europe	476	2	1	2	2	1	2	2
CSHL-5	40.8585	-73.4675	USA	North America	14	1	1	2	2	1	5	2
CYR	47.4	0.68333	France	Europe	50	3	1	2	1	1	5	2
Ca-0	50.5	8.5	Germany	Europe	273	1	1	1	1	1	7	1
Cal-0	53.35	-2.75	UK	Europe	14	2	3	5	1	1	2	2
Can-0	29.2144	-13.4811	Canary Islands	Africa	433	1	1	2	1	1	2	17
Castelfed-1-197	46.34	11.29	Italy	Europe	358	1	1	2	1	1	2	18
Castelfed-4-211	46.34	11.29	Italy	Europe	358	3	1	6	1	1	2	2
Castelfed-4-214	46.34	11.29	Italy	Europe	358	3	1	1	1	1	2	2

Accession	Latitude	Longitude	Country	Continent	Altitude	UVR8	COP1	HY5	ELIP1	HYH	RUP1	RUP2
Cdm-0	39.7255	-5.74406	Spain	Europe	457	1	1	2	1	1	2	11
Cerv-1	41.9	12.5	Italy	Europe	55	5	1	2	1	1	18	6
Chaba-2	53.6	79.37	Russia	Asia	126	1	1	1	1	1	13	2
Chat-1	48.1	1.3	France	Europe	144	3	1	2	3	1	7	2
Chi-0	54	34	Russia	Europe	204	1	1	1	1	1	2	19
Cimin-1	39.58	16.21	Italy	Europe	158	3	1	2	1	1	2	2
Cnt-1	51.3	1.1	UK	Europe	10	1	1	1	1	1	2	2
Cnt_1	51.3	1.1	UK	Europe	10	1	1	1	1	1	2	2
Co	40.2077	-8.42639	Portugal	Europe	111	3	1	2	1	1	2	6
Co-1	40.5	-8.5	Portugal	Europe	48	1	1	1	1	1	2	2
Col-0	38.5	-92.5	USA	North America	264	1	1	1	1	1	1	1
Com-1	49.4	2.8	France	Europe	36	2	1	2	1	1	2	7
Corig-1	39.6	16.51	Italy	Europe	239	3	6	2	1	1	2	3
Ct-1	37.3	15	Italy	Europe	33	1	1	1	1	1	2	2
Cvi-0	15.0469	-23.6345	Cape Verde Islands	Africa	1225	5	7	1	7	1	19	2
Cvi_0	15.0469	-23.6345	Cape Verde Islands	Africa	1225	5	7	1	7	1	20	2
DIR-9	48.54	4.32	France	Europe	145	2	1	2	4	1	2	4
Da1-12	49.75	15.5	Czech Republic	Europe	465	1	1	1	1	1	21	2
Db-12	50.5	8.5	Germany	Europe	273	1	1	1	1	1	2	2
Del-10	44.9444	21.1828	Serbia	Europe	226	1	1	2	1	1	2	3
Dem-4	41.1876	-87.1923	USA	North America	202	1	1	1	4	1	16	2
Di-G	47.333	5.033	France	Europe	267	1	1	1	1	1	3	2
Dja-1	42.5833	73.6333	Kyrgyzstan	Asia	2682	1	1	1	1	1	9	20
Do-0	50.5	8	Germany	Europe	237	2	1	2	1	1	3	2
Doer-10	63.0167	17.4914	Sweden	Europe	125	12	1	2	1	1	4	2
Dog-4	38.3011	42.2239	Turkey	Asia	1487	3	1	1	1	1	22	21
Dolen-1.9697	41.62	23.94	Bulgaria	Europe	880	1	1	1	1	1	10	2
Dolna-1.9712	42.32	23.1	Bulgaria	Europe	570	1	1	2	2	1	10	3
Don-0	36.8323	-6.35981	Spain	Europe	3	1	1	1	1	1	2	22
Dospa-1	41.64	24.18	Bulgaria	Europe	1264	1	1	1	2	2	2	2
Doubravnik7	49.4211	16.3497	Czech Republic	Europe	349	1	1	1	1	1	2	23
Dr-0	51	13.5	Germany	Europe	397	1	1	2	1	1	2	2
Dra2-1	55.76	14.12	Sweden	Europe	63	1	3	1	1	1	1	2
Dra3-1	55.76	14.12	Sweden	Europe	63	1	1	2	1	1	4	2
DraII-6	49.4112	16.2815	Czech Republic	Europe	499	1	1	1	1	1	10	3
DraIII-1	49.4112	16.2815	Czech Republic	Europe	499	1	1	2	1	1	21	24
DraII-1	49.4112	16.2815	Czech Republic	Europe	499	1	1	1	1	1	2	12
DraIV.5893	49.4112	16.2815	Czech Republic	Europe	499	1	1	1	1	1	2	2
DraIV.5907	49.4112	16.2815	Czech Republic	Europe	499	1	1	1	1	1	21	2
DraIV.5950	49.4112	16.2815	Czech Republic	Europe	499	1	1	1	1	1	1	23
DraIV.5984	49.4112	16.2815	Czech Republic	Europe	499	1	1	1	1	1	2	3
DraIV.5993	49.4112	16.2815	Czech Republic	Europe	499	1	1	1	1	1	2	3
Dra-0	49.217	16.67	Czech Republic	Europe	312	1	1	1	1	1	21	2
Draha2	49.4112	16.2815	Czech Republic	Europe	499	1	1	2	1	1	10	3
Duk	49.1	16.2	Czech Republic	Europe	336	1	1	2	1	1	2	3
Durh	54.8	-1.6	UK	Europe	109	2	1	2	1	1	2	9
ENC-2-1	50.86	3.6	France	Europe	26	1	1	2	1	1	5	2
ESP-1-11	50.72	3.47	France	Europe	15	1	2	2	2	1	2	3
Eden-1	62.877	18.177	Sweden	Europe	40	1	1	2	1	1	23	2
Eden-2	62.877	18.177	Sweden	Europe	40	1	1	2	1	1	4	2
Eden-7	62.877	18.177	Sweden	Europe	40	1	1	2	1	1	4	2

Accession	Latitude	Longitude	Country	Continent	Altitude	UVR8	COP1	HY5	ELIP1	HYH	RUP1	RUP2
Eden-9	62.877	18.177	Sweden	Europe	40	1	1	2	1	1	4	2
Edi-0	55.9494	-3.16028	UK	Europe	42	1	1	1	1	1	24	2
Eds-1	62.9	18.4	Sweden	Europe	85	1	1	2	1	1	23	2
Eds-9	62.9	18.4	Sweden	Europe	85	1	1	2	1	1	23	2
Ei-2	50.5	6.5	Germany	Europe	518	1	1	1	1	1	2	2
El-0	51.5	9.5	Germany	Europe	265	1	1	7	1	1	1	2
Ema-1	51.3	0.5	UK	Europe	11	2	1	2	3	1	2	2
En-1	50	8.5	Germany	Europe	111	1	1	1	1	1	2	2
En-2	50	8.5	Germany	Europe	111	1	1	1	1	1	1	1
EN-D	48	37.75	Ukraine	Europe	212	1	1	1	1	1	2	2
Epidauros-1	37.6	23.08	Greece	Europe	348	11	1	2	1	1	5	3
Er-0	49.5	22	Germany	Europe	426	1	1	1	1	1	25	7
Erg2-6	48.5	8.8	Germany	Europe	489	1	1	1	1	1	2	2
Es-0	60	25	Finland	Europe	1	1	1	2	1	1	2	9
Est-1	58.5	25.5	Russia	Europe	96	1	1	1	1	1	2	1
Est	58.6656	24.9871	Germany	Europe	47	2	1	1	1	1	2	2
Et-0	44.65	2.57	France	Europe	271	1	1	2	1	1	3	2
Etna-2	38.08	13.23	Italy	Europe	582	3	1	1	1	1	2	25
Ey15-2	48.4345	8.76781	Germany	Europe	389	1	1	1	1	1	2	2
Faeb-2	63.0165	18.3174	Sweden	Europe	14	1	1	2	1	1	23	2
Faeb-4	63.0165	18.3174	Sweden	Europe	14	1	1	2	1	1	23	2
Fael-1	63.0165	18.3174	Sweden	Europe	14	1	1	2	1	1	4	2
Faneronemi-3	37.07	22.04	Greece	Europe	6	1	1	2	1	1	2	11
Fei-0	40.9233	-8.54213	Portugal	Europe	131	2	1	2	1	1	5	2
Fell1-10	48.43	8.79	Germany	Europe	528	1	1	1	1	1	2	2
Fell2-4	48.43	8.79	Germany	Europe	528	8	1	1	1	1	2	2
Fell3-7	48.43	8.79	Germany	Europe	528	1	1	1	1	1	2	2
Fi-0	50.5	8.5	Germany	Europe	273	1	1	2	1	1	2	3
Filet-1	40.68	14.87	Italy	Europe	64	3	1	2	1	1	2	11
Fjae1-1	56.06	14.29	Sweden	Europe	45	2	1	2	2	1	2	2
Fjae1-2	56.06	14.29	Sweden	Europe	45	2	1	2	1	1	3	3
Fjae1-5	56.06	14.29	Sweden	Europe	45	2	1	1	1	1	8	2
Fjae2-4	56.06	14.29	Sweden	Europe	45	1	1	2	1	1	2	2
Fly2-1	55.7509	13.3712	Sweden	Europe	23	2	1	1	1	1	2	2
Fly2-2	55.7509	13.3712	Sweden	Europe	23	2	1	1	1	1	2	2
Fondi-1	41.36	13.4	Italy	Europe	7	1	1	2	1	1	2	2
Fr-2	50	8.5	Germany	Europe	273	1	1	1	1	1	7	7
Fri-2	55.8106	14.2091	Sweden	Europe	4	2	1	2	1	1	26	26
Furni-1	45.14	25	Romania	Europe	438	1	1	1	1	1	13	27
GEN-8	50.59	3.3	France	Europe	69	1	1	1	1	1	2	2
Ga-0	50.5	8	Germany	Europe	273	1	1	2	1	1	2	3
Ge-0	46.5	6.08	Switzerland	Europe	1062	1	1	2	1	1	17	2
Geg-14	40.1408	44.8203	Armenia	Asia	1693	1	1	1	1	1	9	3
Gel-1	51	5.6	Netherlands	Europe	86	2	1	1	3	1	2	2
Gie-0	50.5	8.5	Germany	Europe	273	2	1	1	1	1	9	2
Giffo-1	38.44	16.13	Italy	Europe	401	3	1	2	1	1	2	2
Gifu-2	35.3	137.38	Japan	Asia	449	1	1	1	4	1	16	2
Gn-1	48.57	9.17	Germany	Europe	403	1	1	1	1	1	2	3
Gn2-3	48.58	9.18	Germany	Europe	422	8	1	1	1	1	1	3
Goced-1	41.57	23.85	Bulgaria	Europe	545	1	1	2	1	1	9	28
Gol-2	57.9672	-3.96722	UK	Europe	8	2	1	2	1	1	1	29
Got-22	51.5338	9.9355	Germany	Europe	156	3	3	2	1	1	2	2

Accession	Latitude	Longitude	Country	Continent	Altitude	UVR8	COP1	HY5	ELIP1	HYH	RUP1	RUP2
Got-7	51.5338	9.9355	Germany	Europe	156	3	3	2	1	1	2	2
Gr-5	47	15.5	Austria	Europe	334	3	8	1	1	1	2	2
Gr-1	47	15.5	Austria	Europe	334	2	1	1	1	1	27	2
Gradi-1	45.17	18.7	Croatia	Europe	85	1	1	1	1	2	28	3
Gre-0	43.178	-85.2532	USA	North America	257	1	1	1	4	1	16	2
Grivo-1	41.84	25.75	Bulgaria	Europe	225	1	1	2	1	1	2	2
Gro-3	62.6437	17.7339	Sweden	Europe	99	3	1	2	1	1	4	2
Groen-12	62.806	18.1896	Sweden	Europe	26	3	1	2	1	1	4	2
Groen-14	62.806	18.1896	Sweden	Europe	26	1	1	2	2	1	4	2
Groen-5	62.806	18.1896	Sweden	Europe	26	3	1	2	1	1	4	2
Gu-0	50.3	8	Germany	Europe	330	8	1	2	1	1	1	1
Gy-0	49	2	France	Europe	127	2	1	2	1	1	2	9
HE-1	48.55	8.99	Germany	Europe	507	1	1	1	1	1	2	2
HKT2	48.136	9.40332	Germany	Europe	558	8	1	1	1	1	2	2
HR10	51.4083	-0.6383	UK	Europe	73	1	1	1	3	1	2	2
HR5	51.5083	-0.6383	UK	Europe	73	2	1	1	1	1	2	2
HSm	49.33	15.76	Czech Republic	Europe	565	1	1	2	1	1	21	3
Ha-HBT1-2	48.54	9.02	Germany	Europe	418	1	1	2	2	1	2	2
Ha-HBT2-10	48.54	9.02	Germany	Europe	418	1	1	1	2	1	2	2
Ha-HBT3-11	48.54	9.02	Germany	Europe	418	1	1	2	1	1	2	2
Ha-P-13	48.54	9.02	Germany	Europe	418	1	1	2	2	1	2	2
Ha-P2-1	48.54	9.02	Germany	Europe	418	1	1	1	2	1	2	3
Ha-S-B	48.54	9.02	Germany	Europe	418	1	1	2	2	1	2	2
Ha-SP-2	48.54	9.02	Germany	Europe	418	1	1	1	1	1	2	3
Ha-0	52.5	9.5	Germany	Europe	41	2	1	1	1	1	2	3
Had-1	57.3263	15.8979	Sweden	Europe	108	1	1	1	1	1	2	2
Had-2	57.3263	15.8979	Sweden	Europe	108	1	3	2	1	1	2	2
Haes-1	48.6	9.2	Germany	Europe	441	1	1	1	2	1	2	6
Hag-2	56.5804	16.4063	Sweden	Europe	1	2	1	2	1	1	26	30
Hal-1	57.5089	15.0105	Sweden	Europe	244	2	9	2	2	1	29	2
Ham-1	55.4234	13.9905	Sweden	Europe	3	2	1	2	1	1	2	3
Hart-2	48.39	9.95	Germany	Europe	515	1	1	1	1	1	2	2
Hau-0	56	12	Denmark	Europe	10	1	4	1	1	1	3	19
Hel-3	57.8765	14.8549	Sweden	Europe	195	2	1	2	1	4	7	3
Hey-1	51.3	5.9	Netherlands	Europe	32	1	1	1	1	1	1	2
Hh-0	54.4167	9.8833	Germany	Europe	15	2	1	1	1	1	2	2
Hi-0	52	5	Netherlands	Europe	2	1	1	2	1	1	2	2
Hn-0	51.5	8.5	Germany	Europe	338	1	1	1	1	1	30	2
Hod	48.8	17.1	Czech Republic	Europe	158	1	1	1	1	1	2	2
Hof-1	48.41	8.85	Germany	Europe	464	1	1	2	1	1	2	2
Hola-1-1	55.7491	13.399	Sweden	Europe	29	1	1	1	1	1	2	2
Hola-2-2	55.7491	13.399	Sweden	Europe	29	1	1	1	1	1	2	2
Hola-1-2	55.7491	13.399	Sweden	Europe	29	1	1	1	1	1	2	2
Hov1-10	56.1	13.74	Sweden	Europe	60	1	1	2	1	1	1	2
Hov1-7	56.1	13.74	Sweden	Europe	60	1	1	1	8	1	1	2
Hov3-2	56.1	13.74	Sweden	Europe	60	2	1	1	1	1	1	1
Hov3-5	56.1	13.74	Sweden	Europe	60	2	1	1	1	1	3	2
Hov4-1	56.1	13.74	Sweden	Europe	60	2	1	1	1	1	1	2
Hovdala-2	56.1	13.74	Sweden	Europe	60	1	10	1	1	1	2	2
Hs-0	52.5	9.5	Germany	Europe	41	2	1	1	1	1	1	2
ICE1	44.4604	25.7356	Romania	Europe	111	1	1	1	1	1	31	31
ICE102	40.5711	15.3215	Italy	Europe	226	1	1	2	2	1	2	29

Accession	Latitude	Longitude	Country	Continent	Altitude	UVR8	COP1	HY5	ELIP1	HYH	RUP1	RUP2
ICE104	39.1776	16.2601	Italy	Europe	803	1	1	2	1	1	2	3
ICE106	38.3623	16.2304	Italy	Europe	44	1	1	2	1	1	2	3
ICE107	38.2782	16.2174	Italy	Europe	252	3	1	2	1	1	2	3
ICE111	40.2803	15.655	Italy	Europe	499	1	2	2	1	1	24	2
ICE112	39.831	16.1726	Italy	Europe	515	1	1	2	2	1	2	3
ICE119	39.2729	16.2677	Italy	Europe	448	1	1	2	6	1	2	3
ICE120	40.1763	16.4533	Italy	Europe	159	1	1	2	1	1	30	11
ICE127	51.3391	82.5724	Russia	Asia	497	1	1	1	1	5	9	6
ICE130	51.3184	82.5528	Russia	Asia	497	1	1	1	1	5	23	6
ICE134	51.3284	82.185	Russia	Asia	358	1	1	1	1	1	9	3
ICE138	51.655	80.8151	Russia	Asia	249	1	1	4	1	1	9	3
ICE150	41.45	70.05	Uzbekistan	Asia	922	1	1	1	1	1	9	20
ICE152	41.45	70.05	Uzbekistan	Asia	922	1	1	1	1	1	9	20
ICE153	41.45	70.05	Uzbekistan	Asia	922	1	1	1	1	1	9	20
ICE163	46.3716	11.2376	Italy	Europe	610	1	11	1	1	1	2	2
ICE169	46.513	11.331	Italy	Europe	642	1	1	1	1	2	2	3
ICE173	46.513	11.331	Italy	Europe	642	1	1	1	1	2	2	3
ICE181	46.3646	11.2835	Italy	Europe	238	1	1	2	1	1	2	2
ICE21	44.3386	21.4603	Serbia	Europe	161	1	1	2	1	1	3	6
ICE212	46.3378	11.2928	Italy	Europe	343	3	1	1	1	1	2	2
ICE213	46.3378	11.2928	Italy	Europe	343	5	1	1	1	1	2	2
ICE216	46.2543	11.167	Italy	Europe	297	3	1	1	1	1	2	3
ICE226	46.6295	10.8161	Italy	Europe	749	1	1	2	1	1	2	32
ICE228	46.6295	10.8161	Italy	Europe	749	1	1	2	1	1	2	32
ICE29	41.4275	23.6471	Bulgaria	Europe	1118	1	1	2	2	1	2	20
ICE33	41.588	25.1988	Bulgaria	Europe	754	3	1	2	1	1	5	2
ICE36	44.8373	20.1566	Serbia	Europe	73	1	1	2	1	1	2	3
ICE49	31.484	-7.4499	Morocco	Africa	1396	5	1	2	9	1	32	3
ICE50	31.4687	-7.41662	Morocco	Africa	1683	5	1	2	9	1	33	3
ICE60	54.0599	60.4789	Russia	Asia	260	1	1	1	1	1	2	3
ICE61	54.0599	60.4789	Russia	Asia	260	1	12	1	1	1	34	3
ICE63	46.1088	21.9523	Serbia	Europe	156	1	1	1	1	1	2	3
ICE7	41.428	23.4993	Romania	Europe	424	1	1	2	1	1	2	2
ICE70	53.0389	51.7457	Russia	Europe	73	1	1	1	1	1	9	3
ICE71	53.3328	49.4807	Russia	Europe	214	1	1	1	1	1	2	6
ICE72	53.332	49.4804	Russia	Europe	214	1	1	4	1	1	13	6
ICE73	51.3071	57.5612	Russia	Europe	325	1	1	1	1	1	13	6
ICE75	53.088	52.0001	Russia	Europe	135	1	1	1	1	1	9	3
ICE79	46.36	11.23	Italy	Europe	838	1	1	1	1	1	2	2
ICE91	38.6191	16.1678	Italy	Europe	216	1	1	1	1	1	2	3
ICE92	38.7631	16.2416	Italy	Europe	51	1	1	2	1	1	2	3
ICE93	39.0085	16.4678	Italy	Europe	832	1	1	2	1	1	2	2
ICE97	41.6156	12.8687	Italy	Europe	89	1	1	2	1	1	2	11
ICE98	41.6156	12.8687	Italy	Europe	89	1	1	2	1	1	2	33
IP-Adm-0	39.15	-4.54	Spain	Europe	643	1	1	2	1	1	2	3
AP-Ala-0	39.72	-6.89	Spain	Europe	218	1	1	2	1	1	2	34
IP-All-0	42.19	-7.8	Spain	Europe	468	1	1	1	1	1	2	3
IP-Alm-0	39.8848	-0.36401	Spain	Europe	679	13	1	1	1	1	5	3
IP-Alo-0	40.11	-7.47	Portugal	Europe	772	1	1	2	1	1	2	2
IP-Ang-0	50.3	5.3	Belgium	Europe	205	1	1	2	1	1	2	6
IP-Ara-4	41.7	-3.68	Spain	Europe	825	3	1	1	1	2	3	11
IP-Bar-1	41.43	2.13	Spain	Europe	318	1	1	1	1	1	2	6
IP-Bea-0	36.52	-5.27	Spain	Europe	161	1	1	2	1	1	2	11

Accession	Latitude	Longitude	Country	Continent	Altitude	UVR8	COP1	HY5	ELIP1	HYH	RUP1	RUP2
IP-Ben-0	38.37	-2.66	Spain	Europe	753	1	1	2	1	1	2	3
IP-Ber-0	55	12	Denmark	Europe	65	14	3	1	1	1	5	2
IP-Bis-0	42.4899	0.53657	Spain	Europe	1372	3	1	1	1	1	30	2
IP-Cab-3	41.54	2.39	Spain	Europe	208	3	1	2	1	1	5	3
IP-Cad-0	40.37	-5.74	Spain	Europe	48	1	1	2	1	1	2	3
IP-Cal-0	40.94	-1.37	Spain	Europe	1050	3	1	1	1	1	2	3
IP-Cap-1	36.97	-3.36	Spain	Europe	1418	1	1	1	1	1	2	3
IP-Car-1	38.25	-4.32	Spain	Europe	766	1	1	1	1	1	2	2
IP-Cdc-3	41.21	-4.54	Spain	Europe	787	3	1	2	1	1	2	3
IP-Cdo-0	42.23	-4.64	Spain	Europe	815	15	1	1	1	1	2	3
IP-Cem-0	41.15	-4.32	Spain	Europe	905	1	1	1	1	1	2	3
IP-Cmo-3	40.05	-4.65	Spain	Europe	402	3	1	2	1	1	2	2
IP-Coa-0	38.45	-7.5	Portugal	Europe	200	1	1	2	1	1	2	22
IP-Coc-1	42.31	3.19	Spain	Europe	156	3	1	1	1	1	5	1
IP-Cor-0	40.83	-2	Spain	Europe	1020	3	1	1	1	1	2	2
IP-Cum-1	38.07	-6.66	Spain	Europe	588	1	1	2	1	1	2	11
IP-Cur-4	43.12	-8.09	Spain	Europe	524	1	1	1	1	1	2	2
IP-Deh-1	40.29	-6.67	Spain	Europe	872	2	1	2	1	1	2	35
IP-Elb-0	41.81	2.34	Spain	Europe	1045	3	3	1	1	1	2	2
IP-Fue-2	38.26	-5.42	Spain	Europe	609	1	1	2	1	1	35	11
IP-Fun-0	40.79	-4.05	Spain	Europe	1466	1	13	1	1	1	36	11
IP-Gra-0	36.77	-5.39	Spain	Europe	1092	1	1	8	6	1	2	36
IP-Gua-1	39.4	-5.33	Spain	Europe	602	1	1	2	10	1	2	3
IP-Her-12	39.4	-5.78	Spain	Europe	564	1	1	1	1	1	2	3
IP-Hom-4	40.82	-1.68	Spain	Europe	1247	3	1	2	1	1	15	1
IP-Hor-0	41.67	2.62	Spain	Europe	468	1	1	1	1	2	5	6
IP-Hum-2	42.23	-4.69	Spain	Europe	823	3	13	1	1	1	2	2
IP-Iso-4	43.05	-5.37	Spain	Europe	1482	1	1	2	7	1	37	2
IP-Jim-1	42.28	-5.92	Spain	Europe	792	1	1	2	1	1	2	3
IP-Lab-7	40.89	-4.5	Spain	Europe	1031	1	1	2	1	1	2	3
IP-Ldd-0	41.58	-4.71	Spain	Europe	708	2	3	2	1	1	2	6
IP-Lso-0	38.86	-3.16	Spain	Europe	758	1	1	1	11	1	2	37
IP-Mar-1	39.58	-3.93	Spain	Europe	1000	1	1	1	1	1	2	3
IP-Men-2	39.66	-4.34	Spain	Europe	713	3	1	1	1	1	5	2
IP-Moa-0	42.4633	0.69882	Spain	Europe	1202	3	1	1	1	1	38	2
IP-Moc-11	41.57	-5.64	Spain	Europe	649	1	1	1	1	1	2	2
IP-Mon-5	38.06	-4.38	Spain	Europe	311	1	1	2	1	1	2	2
IP-Mos-1	40.04	-7.11	Portugal	Europe	593	1	1	2	1	1	2	38
IP-Mot-0	38.19	-6.24	Spain	Europe	518	1	1	2	1	1	2	39
IP-Mun-0	40.71	-5.04	Spain	Europe	1137	3	1	2	1	1	2	3
IP-Mur-0	41.67	2	Spain	Europe	750	3	1	1	1	1	5	2
IP-Nav-0	40.42	-4.65	Spain	Europe	756	1	1	1	1	1	2	2
IP-Nog-17	40.45	-1.6	Spain	Europe	1415	3	1	1	1	1	5	11
IP-Orb-10	42.97	-1.23	Spain	Europe	769	3	1	2	1	1	2	3
IP-Oso-0	42.44	-4.36	Spain	Europe	810	3	1	1	1	1	5	2
IP-Pal-0	42.34	1.3	Spain	Europe	1571	3	3	1	1	1	5	2
IP-Pan-0	42.7613	-0.23117	Spain	Europe	1656	3	1	1	1	1	5	2
IP-Pds-1	42.87	-6.45	Spain	Europe	846	1	1	1	1	1	2	2
IP-Pob-0	41.35	1.03	Spain	Europe	657	3	1	1	1	1	5	2
IP-Pro-0	43.28	-6.01	Spain	Europe	220	2	1	2	2	1	5	2
IP-Pue-0	42.75	-3.05	Spain	Europe	471	1	1	1	1	1	2	2
IP-Rds-0	41.86	2.99	Spain	Europe	313	3	1	1	1	1	2	11
IP-Rei-0	38.75	-7.59	Portugal	Europe	394	1	1	2	1	1	2	11

Accession	Latitude	Longitude	Country	Continent	Altitude	UVR8	COP1	HY5	ELIP1	HYH	RUP1	RUP2
IP-Rel-0	38.6	-2.7	Spain	Europe	787	3	1	1	1	1	2	3
IP-Ren-6	42.77	-4.21	Spain	Europe	906	3	1	1	1	1	5	3
IP-Rev-0	40.86	-4.11	Spain	Europe	1169	3	1	2	1	1	2	3
IP-Ria-0	42.34	2.17	Spain	Europe	1663	3	3	1	1	1	2	3
IP-Sac-0	42.13	-6.7	Spain	Europe	1080	3	1	1	1	1	2	2
IP-San-10	38.33	-3.51	Spain	Europe	701	1	1	2	1	1	2	3
IP-Scm-0	38.68	-3.57	Spain	Europe	702	3	1	2	1	1	2	3
IP-Sdv-3	42.84	-5.12	Spain	Europe	951	1	1	2	1	1	2	40
IP-Ses-0	41.48	-1.63	Spain	Europe	892	3	1	1	1	1	2	3
IP-Sne-0	37.09	-3.38	Spain	Europe	2476	1	13	1	12	1	2	2
IP-Stp-0	41.19	-3.58	Spain	Europe	1132	1	1	2	1	1	2	34
IP-Svi-0	43.4	-7.39	Spain	Europe	469	5	1	2	1	1	2	3
IP-Tam-0	41.03	-3.27	Spain	Europe	961	3	1	1	1	1	5	3
IP-Tdc-0	41.5	-1.88	Spain	Europe	830	3	1	1	1	1	2	3
IP-Tol-7	41.6639	-83.5552	USA	North America	186	3	3	1	1	1	5	2
IP-Tor-1	41.6	-2.83	Spain	Europe	978	1	1	1	1	1	2	3
IP-Trs-0	43.37	-5.49	Spain	Europe	279	3	3	2	1	1	2	4
IP-Vad-0	42.86	-3.59	Spain	Europe	590	2	1	1	1	1	3	2
IP-Vae-2	42.1	-5.44	Spain	Europe	738	1	1	1	1	1	2	2
IP-Vav-0	38.53	-8.02	Portugal	Europe	225	1	1	2	1	1	2	35
IP-Vaz-0	42.26	-2.99	Spain	Europe	1678	3	1	1	1	1	2	41
IP-Vdm-0	42.04	1.01	Spain	Europe	1067	3	3	1	1	1	5	2
IP-Vdt-0	40.89	-5.5	Spain	Europe	803	15	1	2	1	1	2	2
IP-Ver-5	41.95	-7.45	Spain	Europe	505	1	1	1	1	1	2	40
IP-Vid-1	38.22	-7.84	Portugal	Europe	234	1	3	2	1	1	2	11
IP-Vig-1	42.31	-2.53	Spain	Europe	609	3	1	1	1	1	5	3
IP-Vim-0	41.88	-6.51	Spain	Europe	652	1	13	1	1	6	2	3
IP-Vin-0	42.8	-5.77	Spain	Europe	1042	15	1	1	1	1	2	42
IP-Vis-0	39.85	-6.04	Spain	Europe	397	3	1	8	11	1	35	37
IP-Voz-0	41.85	-1.88	Spain	Europe	944	3	1	2	10	1	2	2
IP-Vpa-1	40.5	-3.96	Spain	Europe	651	15	3	2	1	2	2	40
ISS-20	43.92	3.71	France	Europe	143	1	1	2	1	1	24	2
IST-29	47.58	5.33	France	Europe	268	1	1	1	1	1	39	43
Iasi-1	47.16	27.59	Romania	Europe	62	1	14	1	1	1	2	3
In-0	47.5	11.5	Austria	Europe	1548	1	1	2	1	1	2	3
Is-0	50.5	7.5	Germany	Europe	261	1	1	2	1	1	1	1
Istisu-1	38.9786	48.5594	Azerbaijan	Asia	90	1	15	2	1	1	2	3
Je-0	51	11.5	Germany	Europe	242	2	1	9	1	1	1	3
Jea	43.6833	7.33333	France	Europe	54	3	1	2	1	1	40	2
J1-3	49.2	16.6	Czech Republic	Europe	234	1	1	2	1	1	2	2
Jm-0	49.07	16.25	Czech Republic	Europe	348	1	1	1	1	1	2	3
K-oze-1	51.35	82.18	Russia	Asia	358	1	1	1	1	1	41	6
K-oze-3	51.34	82.16	Russia	Asia	467	1	1	1	1	1	42	3
KBG1-14	48.53	9.01	Germany	Europe	394	1	1	1	2	1	1	44
KBG2-13	48.53	9.01	Germany	Europe	394	1	1	1	2	1	2	2
KYC-33	37.9169	-84.4639	USA	North America	295	1	1	2	1	1	24	2
Kaevlinge-1	55.9	13.1	Sweden	Europe	54	2	1	2	1	1	2	2
Kal-2	56.047	13.9519	Sweden	Europe	103	1	1	2	1	1	2	2
Kar-1	42.3	74.3667	Kyrgyzstan	Asia	116	1	1	1	1	1	9	45
Karag-1	51.37	59.44	Russia	Europe	304	1	1	1	1	1	2	6
Karag-2	51.37	59.44	Russia	Europe	304	1	1	1	1	1	2	46
Kas-1	35	77	India	Asia	1580	1	1	10	1	1	34	20

Accession	Latitude	Longitude	Country	Continent	Altitude	UVR8	COP1	HY5	ELIP1	HYH	RUP1	RUP2
Kas-2	35	77	India	Asia	1580	1	1	10	1	1	34	20
Kastel-1	44.6419	34.3814	Ukraine	Europe	390	1	15	1	1	2	2	3
Kb-0	50.1797	8.50861	Germany	Europe	263	1	1	2	1	1	1	6
Kelsterbach	50.0667	8.5333	Germany	Europe	111	1	1	2	1	1	2	1
Kent	51.15	0.4	UK	Europe	88	1	1	1	1	1	7	6
Kia-1	56.0573	14.302	Sweden	Europe	24	2	1	2	1	1	2	2
Kil-0	55.6395	-5.66364	UK	Europe	13	1	1	1	1	1	1	2
Kin-0	43.35	-84.42	USA	North America	214	1	1	2	1	1	4	2
Kl-5	51	7	Germany	Europe	45	1	1	2	1	1	1	6
Kn-0	54.5	23.5	Lithuania	Europe	83	1	1	1	1	1	2	2
Kni-1	55.66	13.4	Sweden	Europe	103	2	1	1	1	1	2	2
Knjas-1	43.54	22.29	Serbia	Europe	248	1	1	1	1	1	2	3
Knox-18	41.28	-86.65	USA	North America	225	1	1	1	1	1	2	7
Ko-2	55.5	11.5	Denmark	Europe	28	1	1	1	1	1	2	2
Koch-1	50.3553	29.3244	Ukraine	Europe	169	1	1	1	1	1	23	3
Kolar-1	41.37	23.14	Bulgaria	Europe	339	1	1	1	1	1	2	3
Kolar-2	41.37	23.14	Bulgaria	Europe	339	3	1	1	13	1	43	3
Koln	50.95	6.967	Germany	Europe	50	1	1	1	3	1	7	6
Kolyv-2	51.31	82.59	Russia	Asia	497	1	1	1	1	5	9	3
Kolyv-3	51.36	82.59	Russia	Asia	497	1	1	1	1	1	9	3
Kolyv-5	51.32	82.55	Russia	Asia	497	1	1	1	1	1	9	6
Kolyv-6	51.33	82.54	Russia	Asia	446	1	1	1	1	5	9	2
Kondara	38.5	68.5	Tajikistan	Asia	824	1	1	1	1	1	9	47
Kor-3	57.2746	16.1494	Sweden	Europe	72	1	1	2	1	1	3	3
Koren-1	41.83	25.69	Bulgaria	Europe	176	1	1	2	1	1	2	2
Kro-0	50.1	8.97	Germany	Europe	112	1	1	1	1	1	1	2
Kro_0	50.083	8.966	Germany	Europe	107	1	1	1	1	1	2	2
Krot-0	50.97	11.02	Germany	Europe	201	2	1	1	1	1	1	3
Kru-3	57.7215	18.3837	Sweden	Europe	4	2	1	1	1	1	4	2
Kulturen-1	55.705	13.196	Sweden	Europe	51	2	1	2	1	1	26	2
Kus2-2	48.52	9.11	Germany	Europe	431	1	1	1	19	2	2	3
Kyoto	35.25	135.75	Japan	Asia	479	1	1	1	1	1	2	2
Kz-9	49.6708	73.3344	Kazakhstan	Asia	560	1	1	1	1	1	2	48
LDV-18	48.5167	-4.06667	France	Europe	95	1	1	2	2	1	2	3
LDV-46	48.5167	-4.06667	France	Europe	95	1	1	2	2	1	2	3
LEC-25	43.91	4.14	France	Europe	268	1	1	1	1	1	2	3
LI-OF-065	40.7777	-72.9069	USA	North America	5	2	1	2	1	1	2	6
LL-0	41.59	2.49	Spain	Europe	299	1	1	1	1	1	2	6
LP3413	41.6862	-86.8513	USA	North America	192	2	1	2	1	1	1	4
La-0	53.2144	13.5148	Germany	Europe	77	1	1	1	1	1	3	1
Lag1-2	41.8296	46.2831	Georgia	Asia	477	1	1	2	1	2	2	6
Lag1-4	41.8296	46.2831	Georgia	Asia	477	1	1	2	1	2	44	6
Lag1-6	41.8296	46.2831	Georgia	Asia	477	9	1	2	1	1	44	3
Lag2	41.8296	46.2831	Georgia	Asia	477	1	1	11	1	2	12	49
Lan-1	55.9745	14.3997	Sweden	Europe	3	2	1	2	1	1	1	2
Lan-0	55.5	-3.5	UK	Europe	294	1	1	1	1	1	1	1
Le-0	52.5	4.5	Netherlands	Europe	4	1	1	1	1	1	1	1
Lebja-2	51.67	80.82	Russia	Asia	231	1	1	4	1	1	9	50
Lebja-4	51.63	80.83	Russia	Asia	238	1	1	4	1	1	9	3
Leo-1	41.7959	-3.11466	Spain	Europe	1021	1	1	1	1	1	2	2
Ler-0	47.984	10.8719	Germany	Europe	619	1	1	1	1	1	3	2

Accession	Latitude	Longitude	Country	Continent	Altitude	UVR8	COP1	HY5	ELIP1	HYH	RUP1	RUP2
Ler-1	47.984	10.8719	Germany	Europe	619	1	1	1	1	1	3	2
Ler_1	47.984	10.8719	Germany	Europe	619	1	1	1	1	1	3	1
Lerik1-3	38.7406	48.6131	Azerbaijan	Europe	269	3	1	11	1	1	2	3
Leska-1	41.54	24.98	Bulgaria	Europe	599	1	1	2	1	1	2	51
Lesno-1	53.04	51.9	Russia	Europe	92	1	1	1	1	1	42	6
Lesno-2	53.04	51.94	Russia	Europe	101	1	1	4	1	1	45	6
Lesno-4	53.04	51.96	Russia	Europe	108	1	1	1	1	1	42	6
Li-7	50.3833	8.0666	Germany	Europe	139	1	3	1	1	1	1	1
Li-2	50.5	8	Germany	Europe	237	16	1	2	1	1	10	2
Liarum	55.9473	13.821	Sweden	Europe	137	1	1	1	1	4	9	2
Lilloe-1	56.1494	15.7884	Sweden	Europe	3	1	1	2	14	1	4	2
Lip-0	50	19	Poland	Europe	241	3	1	2	1	1	3	2
Liri-1	41.41	13.77	Italy	Europe	36	1	1	4	1	1	9	3
Lis-2	56.0328	14.775	Sweden	Europe	10	1	1	2	1	4	2	2
Lis-3	56.0328	14.775	Sweden	Europe	10	1	1	1	1	1	1	2
Lisse	52.25	4.5667	Netherlands	Europe	-3	2	1	1	1	1	2	2
Litva	56	24	Lithuania	Europe	56	1	1	1	1	1	9	2
Lm-2	48	0.5	France	Europe	148	2	1	1	1	1	2	9
Lom1-1	56.09	13.9	Sweden	Europe	52	1	1	1	1	1	2	3
Lp2-2	49.9167	15.5333	Czech Republic	Europe	284	1	1	1	1	1	9	3
Lp2-6	49.38	16.81	Czech Republic	Europe	566	1	1	2	1	1	25	3
Lu-1	55.71	13.2	Sweden	Europe	48	1	1	2	1	1	16	2
Lu3-30	48.53	9.09	Germany	Europe	367	1	1	1	1	1	2	2
Lu4-2	48.54	9.09	Germany	Europe	430	1	1	1	1	1	2	52
Lund	55.71	13.2	Sweden	Europe	67	2	1	1	1	1	2	2
MAR-4-16	47.45	3.94	France	Europe	346	1	1	1	1	1	10	2
Mar2-3	47.45	3.93333	France	Europe	374	3	1	1	1	1	2	2
MIC-31	41.8266	-86.4366	USA	North America	234	2	1	1	4	1	16	2
MIL-2	48.52	4.7	France	Europe	132	1	1	1	2	1	2	1
MNF-Che-2	43.5251	-86.1843	USA	North America	215	1	1	1	4	1	5	2
MNF-Jac-12	43.5187	-86.1739	USA	North America	210	1	1	1	1	1	16	2
MNF-Pin-39	43.5356	-86.1788	USA	North America	215	1	1	1	1	1	2	3
MNF-Pot-21	43.595	-86.2657	USA	North America	250	1	1	1	1	1	16	2
MNF-Pot-75	43.595	-86.2657	USA	North America	250	1	1	1	1	1	16	2
MNF-Riv-21	43.5139	-86.1859	USA	North America	194	1	1	4	1	1	2	20
MOL-1	47.1	4.22	France	Europe	361	1	1	1	1	1	46	2
MOU2-25	43.98	4.31	France	Europe	83	11	1	2	1	1	15	3
Malii-1	43.71	22.3	Serbia	Europe	48	1	1	1	1	1	1	1
Marce-1	38.92	16.47	Italy	Europe	219	1	1	2	1	1	2	4
Mas1-1	54.13	81.31	Russia	Asia	48	1	16	4	15	1	47	3
Mc-0	57	-4	UK	Europe	283	2	1	1	7	1	2	2
Mdn-1	42.051	-86.509	USA	North America	190	2	1	2	2	1	2	2
Melic-1	38.45	16.04	Italy	Europe	116	17	1	2	16	1	2	3
Melni-2	41.53	23.39	Bulgaria	Europe	382	3	1	2	1	7	2	6
Mer-6	38.9159	-6.33764	Spain	Europe	231	1	1	2	1	1	2	6
Mh-0	53.5	20.5	Poland	Europe	130	1	1	2	1	1	1	1
Mir-0	44	12.37	Italy	Europe	92	3	1	2	1	1	2	3
Mitterberg-1-180	46.36	11.28	Italy	Europe	307	1	1	2	1	1	2	2
Mitterberg-1-182	46.36	11.28	Italy	Europe	307	1	1	2	1	1	2	2

Accession	Latitude	Longitude	Country	Continent	Altitude	UVR8	COP1	HY5	ELIP1	HYH	RUP1	RUP2
Mitterberg-1-183	46.36	11.28	Italy	Europe	307	1	1	2	1	1	2	2
Mitterberg-2-184	46.37	11.28	Italy	Europe	255	1	1	1	1	1	2	2
Mitterberg-2-185	46.37	11.28	Italy	Europe	255	1	1	2	1	1	2	2
Mitterberg-3-187	46.37	11.28	Italy	Europe	255	1	1	2	1	1	2	53
Mnz-0	50	8.5	Germany	Europe	111	1	1	1	3	1	2	6
Ms-0	55.45	37.36	Russia	Europe	155	1	1	1	1	1	2	47
Mt-0	32.34	22.46	Libya	Africa	283	8	1	1	1	1	2	1
Muh-2	48.42	8.76	Germany	Europe	388	1	1	1	1	1	2	2
Mv-0	41.3923	-70.6652	USA	North America	15	1	1	1	4	1	16	2
Mz-0	50.5	8.5	Germany	Europe	273	1	3	1	1	1	1	1
N13	61.36	34.15	Russia	Europe	206	1	1	1	10	1	9	2
NC-6	35	-79.18	USA	North America	77	1	1	2	1	1	16	2
NFA-10	51.4083	-0.6383	UK	Europe	73	2	1	2	3	1	2	2
NFA-8	51.4083	-0.6383	UK	Europe	73	2	1	1	1	1	2	2
NOZ-6	44.12	4.33	France	Europe	48	2	1	1	2	1	2	2
Naes-2	62.8815	18.4055	Sweden	Europe	39	1	1	2	2	1	4	2
Nc-1	48.615	6.255	France	Europe	231	1	1	2	1	1	2	6
Nd-1	50.3302	9.50243	Germany	Europe	194	1	1	1	1	1	1	1
Nemrut-1	38.6425	42.2394	Turkey	Asia	1910	1	1	1	1	1	23	3
Neo-6	37.35	72.4667	Tajikistan	Asia	3465	1	1	1	1	1	9	47
Nicas-1	38.97	16.34	Italy	Europe	310	1	1	2	1	1	2	2
Nie1-2	48.5179	8.80256	Germany	Europe	501	1	1	1	1	1	2	2
No-0	51.0581	13.2995	Germany	Europe	256	1	1	2	1	1	2	2
Nok-3	52	4	Netherlands	Europe	-3	1	1	1	1	1	16	2
Nosov-1	51.87	80.6	Russia	Asia	225	1	1	4	1	1	9	6
Noveg-1	51.75	80.82	Russia	Asia	231	1	1	1	1	1	9	31
Noveg-2	51.77	80.85	Russia	Asia	230	1	1	1	1	1	9	3
Noveg-3	51.73	80.86	Russia	Asia	230	1	1	1	1	1	9	3
Np-0	52.5	11.5	Germany	Europe	69	1	1	2	1	1	1	2
Nw-0	50.5	8.5	Germany	Europe	273	1	1	1	3	1	1	1
Ny1-13	62.9513	18.2763	Sweden	Europe	27	1	1	2	1	1	4	2
Ny1-2	62.9513	18.2763	Sweden	Europe	27	1	1	2	1	1	4	2
Ny1-7	62.9513	18.2763	Sweden	Europe	27	1	1	2	1	1	4	2
Nz-1	-2.667	36.2	Tanzania	Africa	1030	2	1	7	1	1	1	2
Ob-0	50.2	8.58	Germany	Europe	201	1	1	2	1	1	1	1
Obe1-15	48.45	8.87	Germany	Europe	456	8	1	1	1	1	2	3
Obh-13	48.39	8.96	Germany	Europe	525	1	1	1	1	1	2	2
Oede-2	62.8959	18.3659	Sweden	Europe	95	1	1	2	2	1	4	2
Oemoe1-7	56.1481	15.8155	Sweden	Europe	23	1	1	2	1	1	2	2
Oemoe2-1	56.1481	15.8155	Sweden	Europe	23	1	3	2	1	1	2	2
Oer-1	56.4573	16.1408	Sweden	Europe	1	2	3	2	1	1	2	2
Old-1	53	8	Germany	Europe	8	2	1	1	1	1	1	2
Olympia-2	37.63	21.62	Greece	Europe	50	1	1	2	1	1	2	2
Omn-1	62.9552	18.3109	Sweden	Europe	49	1	1	2	1	1	4	2
Omn-5	62.9552	18.3109	Sweden	Europe	49	1	1	2	1	1	2	2
Or-0	50.3827	8.01161	Germany	Europe	160	2	1	7	1	1	1	2
Orast-1	45.84	23.16	Romania	Europe	232	1	1	1	1	1	2	3
Ove-0	53.5	8.5	Germany	Europe	3	2	1	1	1	1	1	1
Oy-0	60.23	6.13	Norway	Europe	18	3	1	1	1	1	30	3
Oy_0	60.23	6.13	Norway	Europe	18	3	1	1	1	1	5	3
PHW-2	43.7703	11.2547	Italy	Europe	50	3	1	2	1	1	2	1

Accession	Latitude	Longitude	Country	Continent	Altitude	UVR8	COP1	HY5	ELIP1	HYH	RUP1	RUP2
PHW-34	48.6103	2.3086	France	Europe	74	3	1	1	1	1	3	5
PLO-1	48.58	4.46	France	Europe	158	1	1	1	1	1	1	1
PLY-20	48.59	4.24	France	Europe	107	2	1	1	1	1	5	2
PNA3	42.0945	-86.3253	USA	North America	220	1	1	2	19	1	2	2
PT2	41.3424	-86.7368	USA	North America	205	2	1	2	4	1	2	2
PYL-6	44.65	-1.16667	France	Europe	40	3	3	1	1	1	2	4
Panik-1	53.05	52.15	Russia	Europe	130	1	1	1	1	1	9	3
Panke-1	53.82	80.31	Russia	Asia	159	1	1	4	1	1	9	31
Parti-1	52.99	52.16	Russia	Europe	204	1	1	4	1	1	9	2
Paw-26	42.148	-86.431	USA	Europe	196	1	1	2	1	1	2	6
Ped-0	40.7385	-3.89783	Spain	Europe	1050	3	13	1	12	1	2	3
Per-1	58	56	Russia	Europe	104	1	1	1	1	1	34	19
Petergof	59	29	Russia	Europe	49	1	1	1	1	1	2	6
Pfn-10	48.54	9.09	Germany	Europe	430	1	1	2	1	1	2	3
Pfn-N2	48.56	9.11	Germany	Europe	448	1	1	1	1	1	2	2
Pi-0	47	11	Austria	Europe	1755	1	1	2	1	1	1	1
Pigna-1	41.18	14.18	Italy	Europe	65	1	1	2	1	1	2	3
Pla-0	41.5	2.5	Spain	Europe	2	3	1	2	1	1	15	8
Pna-10	42.167	-86.4525	USA	North America	191	1	1	1	4	1	1	3
Pna-17	42.167	-86.4525	USA	North America	191	1	1	1	4	1	1	2
Po-0	50.7167	7.1	Germany	Europe	82	3	1	1	1	1	2	6
Pog-0	49.2655	-123.206	Canada	North America	75	2	1	2	1	1	5	9
Pra-6	41.0504	-3.53949	Spain	Europe	1092	3	1	2	12	1	2	11
Pro-0	43.2355	-6.034	Spain	Europe	268	2	1	2	3	1	4	2
Pt-0	53.5	10.5	Germany	Europe	44	2	1	1	1	1	18	2
Pu2-23	49.41	16.37	Czech Republic	Europe	352	1	1	1	1	1	2	3
Pu2-7	49.41	16.37	Czech Republic	Europe	352	1	1	1	1	1	4	54
Pu2-8	49.41	16.36	Czech Republic	Europe	370	1	1	1	1	1	4	54
Puk-2	56.1633	14.6806	Sweden	Europe	10	2	1	1	1	1	1	2
QUI-8	44.07	4.08	France	Europe	118	1	1	1	1	1	1	1
Qar-8a	34.09	35.85	Lebanon	Asia	1007	10	1	1	1	1	49	55
Qui-0	42.6918	-6.93011	Spain	Europe	734	15	1	2	1	1	2	6
RAD-21	46.69	4.34	France	Europe	301	3	1	2	1	2	3	3
RMX3	42.036	-86.511	USA	North America	193	1	1	1	2	1	2	2
RRS-7	41.5888	-86.4119	USA	North America	225	1	1	1	10	1	1	3
RRs-10	41.5888	-86.4119	USA	North America	225	1	1	1	4	1	16	2
RUM-20	48.91	4.52	France	Europe	119	3	1	2	2	1	5	4
Ra-0	46	3	France	Europe	604	1	1	2	1	1	2	56
Ragl-1	54.6512	-3.41697	UK	Europe	96	1	1	1	1	1	9	20
Rak-2	49	16	Czech Republic	Europe	322	1	1	1	1	1	10	2
Rakit-1	51.87	80.06	Russia	Asia	188	1	1	1	1	1	9	3
Rakit-3	51.84	80.06	Russia	Asia	188	18	1	4	1	1	9	3
Rd-0	50.5	8.5	Germany	Europe	273	4	16	1	17	2	3	3
Rd_0	50.5	8.5	Germany	Europe	273	1	1	1	1	1	2	1
Ren-1	48.5	-1.41	France	Europe	48	1	1	2	1	1	2	29
Ren-11	48.5	-1.41	France	Europe	48	2	1	2	1	1	4	29
Rennes-1	48.5	-1.41	France	Europe	48	1	1	2	1	1	2	57
Rev-1	55.6942	13.4504	Sweden	Europe	39	2	1	1	1	1	2	2
Rev-2	55.6942	13.4504	Sweden	Europe	39	2	1	2	1	1	2	2
Rhen-1	52	5.6	Netherlands	Europe	5	2	1	1	1	1	1	2

Accession	Latitude	Longitude	Country	Continent	Altitude	UVR8	COP1	HY5	ELIP1	HYH	RUP1	RUP2
Ri-0	49.1632	-123.137	Canada	North America	5	1	1	2	1	1	30	2
Rld-1	56.25	34.31	Russia	Europe	190	1	1	1	1	1	9	3
Rmx-A02	41.897	-85.528	USA	North America	265	2	1	2	3	1	2	2
Rmx-A180	42.036	-86.511	USA	North America	193	2	1	2	3	1	2	2
Roed-17-319	62.8	18.2	Sweden	Europe	51	1	1	1	1	1	1	58
Rome-1	41.9	12.5	Italy	Europe	55	1	1	1	1	1	2	3
Rou-0	49.6	3	France	Europe	83	2	1	2	1	1	2	2
Rsch-4	56.3	34	Russia	Europe	181	1	1	1	1	1	3	6
Ru-2	48.56	9.16	Germany	Europe	335	1	1	1	1	1	2	3
Ru-N2	48.57	9.16	Germany	Europe	406	1	1	1	2	1	2	2
Ru4-16	48.57	9.16	Germany	Europe	406	1	1	2	1	1	1	3
Rubeznhoe-1	49.0158	38.3669	Ukraine	Europe	75	1	1	1	1	1	2	7
Rue3-1-31	48.564	9.15947	Germany	Europe	361	8	1	1	1	1	2	2
SAUL-24	47.43	5.21	France	Europe	245	1	1	1	1	1	3	2
SLSP-31	43.665	-86.496	USA	North America	180	3	1	2	2	1	5	2
SLSP-35	43.665	-86.496	USA	North America	180	3	1	1	2	1	5	2
Sakata	38.9	139.85	Japan	Asia	4	1	17	10	1	1	2	2
San-2	56.07	13.74	Sweden	Europe	85	2	1	2	1	1	2	2
Sanna-2	62.69	18	Sweden	Europe	4	3	1	2	1	1	4	2
Sap-0	49.49	14.24	Czech Republic	Europe	490	1	1	2	1	1	10	3
Sarno-1	40.84	14.57	Italy	Europe	30	1	1	2	1	1	5	33
Schip-1	42.72	25.33	Bulgaria	Europe	877	1	1	1	2	1	5	2
Schl-7	48.6	9.22	Germany	Europe	365	3	1	2	2	1	2	2
Se-0	41.5	2.5	Spain	Europe	2	3	1	2	1	1	15	11
Seattle-0	47	-122	USA	North America	483	1	1	2	1	1	4	2
Sei-0	46.5	11.5	Italy	North America	886	1	1	1	1	1	2	2
Set-1	54.1	-2.3	UK	Europe	226	1	1	2	1	1	3	2
Sever-1	52.1	79.31	Russia	Europe	144	1	1	4	1	1	9	3
Sf-2	41.7833	3.03333	Spain	Europe	4	3	1	2	1	1	2	2
Sf-1	41.7833	3.03333	Spain	Europe	4	3	1	2	1	1	2	11
Sg-1	47.6667	9.5	Germany	Europe	406	1	1	1	1	1	2	1
Sha	39.25	68.25	Tajikistan	Asia	3387	1	1	1	1	1	9	1
Shakdara	39.25	68.25	Tajikistan	Asia	3387	1	1	1	1	1	9	3
Si-0	51	8	Germany	Europe	417	1	1	2	1	1	2	1
Sim-1	55.5678	14.3398	Sweden	Europe	4	1	1	2	1	1	48	6
Slavi-2	41.42	23.67	Bulgaria	Europe	940	1	1	2	2	1	2	3
Smolj-1	41.55	24.75	Bulgaria	Europe	1136	1	1	1	1	1	2	3
Sorbo	38.82	69.487	Tajikistan	Asia	1563	1	1	1	1	1	9	3
Sp-0	52.5	13.5	Germany	Europe	39	19	1	1	1	1	3	1
Sparta-1	55.7097	13.2145	Sweden	Europe	65	1	1	2	1	1	2	3
Spr1-2	58.4168	14.1612	Sweden	Europe	117	1	1	2	2	1	2	3
Spr1-6	58.4168	14.1612	Sweden	Europe	117	2	1	1	1	1	3	3
Spro-1	57.2545	18.2109	Sweden	Europe	18	2	1	2	1	1	9	2
Spro-2	57.2545	18.2109	Sweden	Europe	18	1	1	1	1	1	1	3
Spro-3	57.2545	18.2109	Sweden	Europe	18	1	1	1	1	1	1	3
Sq-1	51.4083	-0.6383	UK	Europe	73	2	1	1	1	1	2	2
Sq-8	51.4083	-0.6383	UK	Europe	73	2	1	1	1	1	50	6
Sr:3	58.9	11.2	Sweden	Europe	26	1	1	2	1	2	4	2
Sr:5	58.9	11.2	Sweden	Europe	26	1	1	1	1	1	2	2
St-0	59	18	Sweden	Europe	19	1	1	1	1	1	2	2

Accession	Latitude	Longitude	Country	Continent	Altitude	UVR8	COP1	HY5	ELIP1	HYH	RUP1	RUP2
Star-8	48.4345	8.81672	Germany	Europe	522	1	1	2	2	1	2	1
Stara-1	42.49	25.61	Bulgaria	Europe	392	1	1	1	18	1	51	2
Staro-1	44.3	21.08	Serbia	Europe	114	1	1	1	2	1	2	2
Ste-0	52.6068	11.8558	Germany	Europe	33	2	1	2	1	1	2	2
Ste-2	57.8009	18.5162	Sweden	Europe	49	2	1	2	1	1	4	2
Ste-3	57.8009	18.5162	Sweden	Europe	49	2	1	2	1	1	2	2
Ste-4	57.8009	18.5162	Sweden	Europe	49	2	1	2	1	1	4	2
Stiav-1	48.46	18.9	Slovakia	Europe	607	1	1	2	1	1	2	3
Stilo-1	38.47	16.47	Italy	Europe	333	1	1	1	1	1	9	3
Stu1-1	58.4666	16.1284	Sweden	Europe	66	1	1	2	1	1	3	2
Stw-0	52.5	36.6	Russia	Europe	237	1	1	1	1	1	2	20
Su-0	53.5	-3	UK	Europe	19	1	1	1	1	1	50	2
Sus-1	42.1225	74.0619	Kyrgyzstan	Asia	2025	1	1	1	1	1	9	3
T1000	55.6525	13.2197	Sweden	Europe	14	2	1	2	1	1	2	2
T1020	55.6514	13.2233	Sweden	Europe	13	2	1	2	1	1	4	2
T1070	55.6481	13.2264	Sweden	Europe	52	1	1	2	1	1	2	3
T1080	55.6561	13.2178	Sweden	Europe	10	2	1	1	2	1	2	2
T1090	55.6575	13.2386	Sweden	Europe	16	3	1	1	14	1	2	2
T1110	55.6	13.2	Sweden	Europe	32	2	1	2	1	1	4	3
T1130	55.6	13.2	Sweden	Europe	32	12	1	2	1	1	2	2
T1160	55.7	13.2	Sweden	Europe	32	2	1	1	1	1	2	2
T460	55.7931	13.1186	Sweden	Europe	13	2	4	2	1	1	2	2
T470	55.7942	13.1222	Sweden	Europe	17	2	4	2	1	1	2	3
T480	55.7989	13.1206	Sweden	Europe	14	2	1	1	1	1	4	3
T530	55.7989	13.1219	Sweden	Europe	14	1	1	2	1	1	2	3
T540	55.7967	13.1044	Sweden	Europe	20	2	3	2	1	1	2	6
T550	55.8078	13.1028	Sweden	Europe	18	2	1	2	1	1	2	6
T570	55.8097	13.1342	Sweden	Europe	28	3	1	2	1	1	2	2
T710	55.8403	13.3106	Sweden	Europe	65	2	1	1	1	1	2	2
T720	55.8411	13.3047	Sweden	Europe	63	2	1	2	1	1	4	59
T740	55.8397	13.2881	Sweden	Europe	70	2	1	2	1	1	2	2
T780	55.8369	13.3181	Sweden	Europe	69	2	1	1	1	1	2	2
T790	55.8386	13.3186	Sweden	Europe	72	2	1	1	1	1	2	3
T800	55.8364	13.2906	Sweden	Europe	74	2	1	1	1	1	8	2
T840	55.9336	13.5519	Sweden	Europe	76	2	1	1	1	1	2	2
T850	55.9419	13.5603	Sweden	Europe	84	2	1	1	1	1	2	2
T860	55.9403	13.5511	Sweden	Europe	77	1	1	1	1	1	2	2
T880	55.9392	13.5539	Sweden	Europe	76	2	1	1	1	1	2	2
T900	55.9428	13.5558	Sweden	Europe	84	2	3	1	1	1	2	2
T930	55.9497	13.5533	Sweden	Europe	86	2	1	2	1	1	2	3
T960	55.9319	13.5508	Sweden	Europe	86	2	1	2	1	1	2	2
T980	55.9261	13.5319	Sweden	Europe	76	1	1	2	1	1	2	2
T990	55.6528	13.2244	Sweden	Europe	13	1	1	1	1	1	3	2
TAA-04	62.6422	17.7406	Sweden	Europe	92	3	1	2	1	1	4	2
TAA-14	62.6425	17.7356	Sweden	Europe	80	3	1	2	1	1	4	2
TAA-18	62.6425	17.7397	Sweden	Europe	82	3	1	2	1	1	4	2
TAAD-01	62.8714	18.3447	Sweden	Europe	33	1	1	2	1	1	26	2
TAAD-03	62.8717	18.3444	Sweden	Europe	87	1	1	2	1	1	4	2
TAAD-04	62.8717	18.3436	Sweden	Europe	20	1	1	2	1	1	52	2
TAAD-05	62.8717	18.3419	Sweden	Europe	33	1	1	2	1	1	52	2
TAAD-06	62.8719	18.3422	Sweden	Europe	33	1	1	2	1	1	26	2
TAAL-03	62.6322	17.69	Sweden	Europe	88	3	1	2	1	1	1	2
TAAL-07	62.6322	17.6906	Sweden	Europe	88	1	1	1	1	1	1	1

Accession	Latitude	Longitude	Country	Continent	Altitude	UVR8	COP1	HY5	ELIP1	HYH	RUP1	RUP2
TBO-01	62.8892	18.4522	Sweden	Europe	46	3	1	2	1	1	4	2
TDr-1	55.7683	14.1386	Sweden	Europe	59	1	1	1	1	1	53	1
TDr-13	55.7708	14.1331	Sweden	Europe	59	1	1	1	1	1	2	60
TDr-16	55.7719	14.1211	Sweden	Europe	78	2	3	2	1	1	2	2
TDr-17	55.7717	14.1206	Sweden	Europe	78	20	1	1	1	1	2	2
TDr-2	55.7686	14.1383	Sweden	Europe	59	1	1	1	1	1	2	2
TDr-7	55.7694	14.1347	Sweden	Europe	89	1	1	2	1	1	1	2
TDr-8	55.7706	14.1342	Sweden	Europe	89	2	3	2	1	4	1	2
TDr-9	55.7708	14.1342	Sweden	Europe	66	2	3	2	1	1	2	2
TEDEN-02	62.8836	18.1842	Sweden	Europe	77	1	1	2	1	1	4	2
TEDEN-03	62.8839	18.1836	Sweden	Europe	77	1	1	2	1	1	4	2
TFAE-06	63.0167	18.3283	Sweden	Europe	14	1	1	2	1	1	4	2
TFAE-07	63.0169	18.3283	Sweden	Europe	14	1	1	2	1	1	4	2
TFAR-08	63.0172	18.3283	Sweden	Europe	14	1	1	2	1	1	23	2
TOM-04	62.9619	18.35	Sweden	Europe	28	1	1	2	1	1	2	2
TOM-06	62.9622	18.35	Sweden	Europe	28	1	1	2	1	1	4	2
TOM-07	62.9614	18.3608	Sweden	Europe	75	1	1	2	1	1	4	61
TOU-A1-88	46.6667	4.11667	France	Europe	252	3	1	2	1	1	3	34
TOU-A1-89	46.6667	4.11667	France	Europe	252	3	1	2	1	1	3	3
TRAE-01	62.9169	18.4728	Sweden	Europe	10	1	1	2	1	1	4	2
TRE-1	48.86	4.1	France	Europe	113	3	1	2	1	1	2	11
TV-10	55.5796	14.3336	Sweden	Europe	14	2	1	2	1	1	2	6
TV-22	55.5796	14.3336	Sweden	Europe	14	1	1	2	1	1	26	6
TV-30	55.5796	14.3336	Sweden	Europe	14	1	1	2	1	1	26	6
TV-38	55.5796	14.3336	Sweden	Europe	14	1	3	1	1	1	2	2
TV-7	55.5796	14.3336	Sweden	Europe	14	1	1	2	1	1	26	6
Ta-0	49.5	14.5	Czech Republic	Europe	589	1	1	2	1	1	2	2
Tamm-2	59.82	23.58	Finland	Europe	19	22	1	2	1	1	23	3
Tamm_2	59.98	23.44	Finland	Europe	13	3	1	2	1	1	23	3
Tamm-27	60	23.5	Finland	Europe	27	3	1	2	1	1	23	3
Taeno-1	41.33	14.09	Italy	Europe	172	3	1	2	1	1	2	11
Teiu-2	44.69	25.17	Romania	Europe	208	1	1	1	1	1	2	6
Tgr-01	62.806	18.1896	Sweden	Europe	26	3	1	2	1	1	4	2
Tha-1	52.1	4.3	Netherlands	Europe	6	3	1	2	1	1	2	2
Ting-1	56.5	15	Sweden	Europe	144	1	1	2	1	4	54	3
Tny-04	62.96	18.2844	Sweden	Europe	37	1	1	2	1	1	4	2
Toc-1	46.01	22.33	Romania	Europe	162	1	1	2	1	1	2	2
Tol-0	41.66	-83.555	USA	North America	186	3	1	1	4	1	4	8
Tomegap-2	55.7	13.2	Sweden	Europe	39	1	1	2	1	1	55	2
Tottarp-2	55.95	13.85	Sweden	Europe	106	1	1	2	1	1	10	3
Ts-1	41.7194	2.93056	Spain	Europe	4	21	1	1	1	1	15	6
Ts-5	41.7194	2.93056	Spain	Europe	4	3	1	1	1	1	4	6
Tscha-1	47.1	9.9	Austria	Europe	1281	1	1	1	1	1	2	2
Tsu-0	34.43	136.31	Japan	Asia	164	1	1	2	1	1	2	3
Tsu-1	34.43	136.31	Japan	Asia	164	1	1	2	1	1	2	3
Tu-B1-2	48.52	9.08	Germany	Europe	318	1	1	2	2	1	2	2
Tu-B2-3	48.52	9.08	Germany	Europe	318	1	1	1	1	1	2	2
Tu-KB-6	48.52	9.05	Germany	Europe	344	2	3	1	1	1	2	2
Tu-KS-7	48.52	9.07	Germany	Europe	340	1	1	1	2	1	2	6
Tu-NK-12	48.52	9.05	Germany	Europe	344	1	1	1	1	1	2	1
Tu-PK-7	48.52	9.05	Germany	Europe	344	1	3	1	2	1	2	44
Tu-WH	48.55	9.06	Germany	Europe	372	1	1	1	1	1	2	2

Accession	Latitude	Longitude	Country	Continent	Altitude	UVR8	COP1	HY5	ELIP1	HYH	RUP1	RUP2
Tu-0	45	7.5	Italy	Europe	290	1	1	2	1	1	2	3
TueSB30-3	48.5334	9.05831	Germany	Europe	430	1	1	1	1	1	1	2
TueV13	48.5232	9.05198	Germany	Europe	330	2	3	1	1	1	2	2
TueWa1-2	48.5342	9.03452	Germany	Europe	458	1	1	2	1	1	2	6
Teuscha9	48.5344	9.05033	Germany	Europe	428	1	1	2	1	1	2	2
Tul-0	43.27	-85.25	USA	North America	265	1	1	1	4	1	56	2
Tur-4	57.6511	14.8043	Sweden	Europe	268	1	1	2	1	4	2	2
Ty-1	56.4	-5.2	UK	Europe	155	3	1	1	1	1	5	2
Ty-0	56.44	-5.23	UK	Europe	2	3	1	1	1	1	2	2
UKID107	52.9	-3.1	UK	Europe	260	1	3	2	1	1	2	3
UKID114	51.8	-0.6	UK	Europe	147	1	1	1	1	1	1	1
UKID63	52.1	-1.5	UK	Europe	109	2	1	1	1	1	24	3
UKID74	51	-3.1	UK	Europe	30	1	1	2	10	1	2	2
UKID96	57.4	-5.5	UK	Europe	35	1	1	1	1	1	1	2
UKNW06-003	54.5	-3	UK	Europe	200	1	1	2	2	1	2	2
UKNW06-403	54.7	-3.4	UK	Europe	119	2	1	2	2	1	2	2
UKNW06-481	54.4	-2.9	UK	Europe	204	3	1	2	2	1	5	6
UKSE06-118	51.3	0.5	UK	Europe	11	2	1	1	19	1	2	2
UKSE06-252	51.3	0.5	UK	Europe	11	1	1	1	1	1	1	2
UKSE06-325	52.2	-1.7	UK	Europe	61	3	1	1	2	1	5	2
UKSE06-362	51.3	0.4	UK	Europe	39	1	3	1	2	1	2	2
UKSE06-432	51.2	0.3	UK	Europe	25	2	1	1	1	1	2	2
UKSE06-470	51.2	0.4	UK	Europe	12	2	1	2	2	1	2	2
UKSE06-500	51.1	0.6	UK	Europe	66	1	1	1	1	1	2	2
UKSE06-533	51.3	1.1	UK	Europe	10	3	1	2	2	1	2	2
UKSW06-179	50.4	-4.9	UK	Europe	121	2	1	2	2	1	2	2
UKSW06-207	50.4	-4.9	UK	Europe	121	3	1	2	1	1	2	2
UKSW06-226	50.4	-4.9	UK	Europe	121	1	3	2	1	1	2	6
UKSW06-285	50.3	-4.9	UK	Europe	41	2	1	1	2	1	2	2
UKSW06-302	50.3	-4.8	UK	Europe	11	2	1	1	2	1	2	2
UKSW06-333	50.3276	-4.6	UK	Europe	50	1	1	1	4	1	56	2
UKSW06-360	50.5	-4.5	UK	Europe	193	1	1	2	1	1	3	3
Udul.6296	49.2771	16.6314	Czech Republic	Europe	448	1	1	1	1	1	9	2
Udul.6390	49.2771	16.6314	Czech Republic	Europe	448	1	1	2	1	1	2	2
Udul.6396	49.2771	16.6314	Czech Republic	Europe	448	1	1	2	1	1	2	2
Uk-1	48.0333	7.7667	Germany	Europe	207	1	1	2	1	1	2	1
Ulies-1	45.95	22.62	Romania	Europe	286	1	1	4	1	1	9	3
Ull-A-1	56.0648	13.9707	Sweden	Europe	29	1	1	1	1	1	1	2
Ull2-3	56.0648	13.9707	Sweden	Europe	29	2	1	1	1	1	2	2
Ull2-5	56.0648	13.9707	Sweden	Europe	29	2	1	1	1	1	2	2
Ullapool-8	57.9	-5.1525	UK	Europe	24	3	1	2	1	2	3	3
Uod-2	48.3	14.45	Austria	Europe	390	1	1	1	2	1	1	2
Uod-1	48.3	14.45	Austria	Europe	390	1	1	1	1	1	10	62
Uod-7	48.3	14.45	Austria	Europe	390	1	1	1	1	1	2	33
Utrecht	52.5	5.8	Netherlands	Europe	-5	1	1	1	1	1	2	2
VED-10	43.74	3.89	France	Europe	126	1	1	1	1	1	9	3
Vaar-1	55.5796	14.3336	Sweden	Europe	14	1	1	2	1	1	48	2
Vaar2-1	55.58	14.334	Sweden	Europe	14	1	1	2	1	1	48	6
Vaar2-6	55.58	14.334	Sweden	Europe	14	1	1	2	1	1	48	6
Vaestervik	57.75	16.6333	Sweden	Europe	24	2	1	1	1	1	2	2
Van-0	49.3	-123	Canada	North America	5	1	1	1	1	1	2	56
Vash-1	41.1908	46.4735	Georgia	Asia	371	1	1	2	1	2	57	3

Accession	Latitude	Longitude	Country	Continent	Altitude	UVR8	COP1	HY5	ELIP1	HYH	RUP1	RUP2
Ven-1	52	5.6	Netherlands	Europe	5	1	1	1	1	1	30	3
Vie-0	42.63	0.76	Spain	Europe	2164	3	3	1	1	1	30	11
Vimmerby	57.7	15.8	Sweden	Europe	114	1	1	1	1	4	2	2
Vind-1	55	-2.3	UK	Europe	209	1	1	1	4	1	2	2
Vinsloev	56.1	13.9167	Sweden	Europe	31	1	3	1	1	1	2	2
WAR	41.7302	-71.2825	USA	North America	9	1	1	1	1	1	2	2
WAV-8	50.65	2.99	France	Europe	39	2	1	2	2	1	2	1
Wa-1	52.3	21	Poland	Europe	83	1	1	1	1	1	2	2
WalhaesB4	48.5956	9.18553	Germany	Europe	440	1	1	1	1	1	1	3
Wc-1	53	10	Germany	Europe	86	2	1	1	1	1	1	64
Wei-0	47.416	8.433	Switzerland	Europe	407	3	1	2	1	1	2	6
Westkar-4	42.3	74	Kyrgyzstan	Asia	2448	1	1	1	1	1	9	47
Wil-2	54.6833	25.3167	Lithuania	Europe	134	1	1	1	1	1	2	3
Wil-1	54.6833	25.3167	Lithuania	Europe	134	1	1	1	1	1	2	2
Wl-0	48.5	8.5	Germany	Europe	737	1	1	1	1	1	9	3
Ws-0	52.3	30	Russia	Europe	158	1	1	1	1	1	25	6
Ws-2	52.5	30	Russia	Europe	141	1	1	1	1	1	9	20
Wt-5	52.5	9.5	Germany	Europe	41	1	1	1	1	1	1	1
Wu-0	49.7878	9.9361	Germany	Europe	187	1	1	1	1	1	2	2
Xan-1	38.6546	48.7992	Azerbaijan	Asia	1	1	1	2	1	2	2	3
Yeg-1	39.8692	45.3622	Armenia	Asia	1615	1	1	1	1	1	9	20
Yeg-2	39.8692	45.3622	Armenia	Asia	1615	1	1	1	1	1	9	3
Yeg-4	39.8692	45.3622	Armenia	Asia	1615	1	1	1	1	1	9	3
Yeg-5	39.8692	45.3622	Armenia	Asia	1615	1	1	1	1	1	9	20
Yeg-7	39.8692	45.3622	Armenia	Asia	1615	1	1	1	1	1	9	20
Yeg-8	39.8692	45.3622	Armenia	Asia	1615	1	1	1	1	1	9	20
Yo-0	37.6966	-119.675	USA	North America	1450	1	1	1	1	1	16	2
Yst-1	55.4242	13.8484	Sweden	Europe	48	2	1	2	1	1	2	2
Zagub-1	44.23	21.71	Serbia	Europe	274	1	1	2	19	1	1	33
Zal-1	42.8	76.35	Kyrgyzstan	Asia	2313	1	1	1	1	1	9	47
Zdarec3	49.3667	16.2667	Czech Republic	Europe	363	1	1	1	1	1	2	2
Zdrl.6424	49.3853	16.2533	Czech Republic	Europe	506	1	1	1	1	1	2	2
Zdrl.6434	49.3853	16.2533	Czech Republic	Europe	506	1	1	1	1	1	3	2
Zdrl.6445	49.3853	16.2533	Czech Republic	Europe	506	1	1	2	1	1	21	2
Zdr-1	49.1	16.35	Czech Republic	Europe	216	22	1	2	1	1	46	3
Zu-0	47.3667	8.55	Switzerland	Europe	426	3	1	2	1	1	3	2
Zu-1	47.3667	8.55	Switzerland	Europe	426	2	1	1	1	1	2	6
Zupan-1	45.07	18.72	Croatia	Europe	80	1	1	1	2	1	3	6
love-1	62.801	18.079	Sweden	Europe	27	3	1	2	1	1	4	64
love-5	62.801	18.079	Sweden	Europe	27	3	1	2	1	1	4	64

References

Alonso-Blanco, C., and Koorneef, M., (2000). Naturally occurring variation in *Arabidopsis*: an underexploited resource for plant genetics. *Trends in Plant Science*. 5(1): 22-29.

Alonso-Blanco, C., Bentsink, L., Hanhart, C.J., Beankestijn-de Vries, H., Koorneef, M., (2003). Analysis of natural allelic variation at seed dormancy loci of *Arabidopsis thaliana*. *Genetics* 164: 711-729.

Anwer, M., and Davis, S.J., (2013). An overview of natural variation studies in the *Arabidopsis thaliana* circadian clock. *Seminars in Cell and Developmental Biology*. 24: 422-429.

Angers, B., Castonguay, E., Massicotte, R., (2010). Environmentally induced phenotypes and DNA methylation: how to deal with unpredictable conditions until the next generation and after. *Molecular Ecology*. 19: 1283-1295.

Apel, K., Hirt, H., (2004). Reactive oxygen species: metabolism, oxidative stress, and signal transuction. *Annural Review of Plant Biology*. 55: 373-399.

Austen, R.A., (1968). Northwest Tanzania under German and British rule: colonial policy and tribal politics, 1889-1939. *New Haven*.

Ballaré, C.L., Mazza., C.A., Austin, A.T., Pierik, R,. (2012). Canopy Light and Plant Health. *Plant Physiology*. 160: 145-155.

Ballaré, C.L., (2014). Light Regulation of Plant Defence. *Annual Reviews of Plant Biology*. 65: 15.1-15.29.

Banaś, A.K., Aggarwal, C., Łabuz, J., Sztatelman, O, Gabryś, H., (2012). Blue light signalling in chloroplast movement. *Journal of Experimental Botany*. DOI 10.1093/jxb/err429.

Barnes, P.W., Flint, S.D., Ryel, R.J., Tobler, M.A., Barkley, A.E., Wargent, J.J., (2014). Rediscovering leaf optical properties: new insights into plant acclimation to solar UV radiation. *Plant Physiology and Biochemistry*. 93: 94-100.

Bates, D., Mächler, M., Bolker, B.M., Walker, S.C., (2014). Fitting linear mixed-effects models using lme4. *Journal of Statistical Software*. DOI: arXiv:1406.5823.

Beckmann, M., Václavík, T., Manceur, A.M., Šprtová, L., von Wehrden, H., Welk, E., Cord, A.F., (2014). glUV: a global UV-B radiation data set for macroecological studies. *Methods in Ecology and Evolution*. 5(4): 372-383.

Beggs, C.J., Stolzer-Jehle, A., Wellman, E., (1985). Isoflavonoid formation as an indicator of UV stress in bean (*Phaseolus vulgaris* L.) leaves the significance of photorepair in assessing potential damage by increased solar UV-B radiation. *Plant Physiology*. 79(3): 630-634.

Binkert, M., Kozma-Bognár, L., Terecskei, K., de Veylder, L., Nagy, F., Ulm, R., (2014). UV-B-responsive association of the *Arabidopsis* bZIP transcription factor ELONGATED HYPOCOTYL5 with target genes, including its own promoter. *The Plant Cell*. 26(10): 4200-4213.

Boccalandro, H., Rossi, M.C,. Saijo, Y., Deng, X-W., Casal, J.J., (2004). Promotion of photomorphogenesis by COP1. *Plant Molecular Biology*. 56(6): 905-915.

Bornman, J.F., Barnes, P.W., Robinson, S.A., Ballaré, C.L., Flint, S.D., Caldwell, M.M., (2014). Solar ultraviolet radiation and ozone depletion-driven climate change: effects on terrestrial ecosystems. *Photochemical & Photobiological Sciences*. DOI: 10.1039/c4pp0Q034k.

Briggs, G.C., Osmont, K.S., Shindo, C., Sibout, R., Hardtke, C.S., (2006). Unequal genetic redundancies in *Arabidopsis* – a neglected phenomenom? *TRENDS in Plant Science*. 11(10): 1360-1385.

Briknarová, K., Nasertorabi, F., Havert, M.L., Eggleston, E., Hoyt, D.W., Li, C., Olson, A.J., Vuori, K., Ely, K.R., (2005). The Serine-rich Domain from Crk-associated Substrate (p130^{cas}) Is a Four-helix Bundle. *The Journal of Biological Chemistry*. 280: 21908-21914.

Britt, A.B., (2004). Repair of DNA damage induced by solar UV. *Photosynthesis Research*. 81(2): 105-112.

Brosche, M., Strid, A., (2003). Molecular events following perception of Ultraviolet-B radiation by plants. *Physiologica Plantarum* 117: 1-10.

Brown B.A., Cloix C., Jiang G.H., Kaiserli E., Herzyk P., Kliebenstein D.J., Jenkins G.I., (2005). A UV-B-specific signaling component orchestrates plant UV protection. *PNAS* 102: 18225–18230.

Brown, B.A., Jenkins, G.I., (2008). UV-B signaling pathways with different fluence-rate response profiles are distinguished in mature Arabidopsis leaf tissue by requirement for UVR8, HY5, and HYH. *Plant Physiology* 146: 576-588.

Brown, B.A., Headland, L.R., Jenkins, G.I., (2009). UV-B action spectrum for UVR8-mediated *HY5* transcript accumulation in Arabidopsis. *Photochemistry and Photobiology*. 85: 1147-1155.

Bücherl, C., Aker, J., de Vries, S., Borst, J.W., (2010). Probing protein-protein interactions with FRET-FLIM. *Plant Developmental Biology, Methods in Molecular Biology 655*. DOI: 10.1007/978-1-60761-765-5_26.

Bücherl, C., Bader, A., Westphal, A.H., Laptenok, S.P., Borst, J.W., (2014). FRET-FLIM applications in plant systems. *Protoplasma*. 251: 282-294.

Buckler, E., Gore, M., (2007). An *Arabidopsis* haplotype map takes root. *Nature Genetics*. 39(9): 1056-1057.

Burke, M.J., Gusta, L.V., Quamme, H.A., Weiser, C.J., Li, P.H., (1976). Freezing and injury in plants. *Annual Review of Plant Physiology and Plant Molecular Biology*. 27: 507-528.

Carbonell-Bejerano, P., Diago, M-P., Martínez-Abaigar, J., Martínez-Zapater, J.M., Tardáguila, J., Núñez-Olivera, E., (2014). Solar ultraviolet radiation is necessary to enhance grapevine fruit ripening transcriptional and phenolic responces. *BMC Plant Biology*. 14:183.

Casati, P., Walbot, V., Rapid transcriptome responses of maize (*Zea mays*) to UV-B in irradiated and shielded tissues. *Genome Biology*. 5:R16.

Chen, M., Chory, J., Fankhauser, C., (2004). Light signal transduction in higher plants. *Annual Review of Genetics* 38.87-117.

Christie, J.M., (2007). Phototropin blue-light receptors. *Annual Review of Plant Biology*. 58: 21-45.

Christie, J.M., Arval, A.S., Baxter, K.J., Heilmann, M., Pratt, A.J., O'Hara, A., Kelly, S.M., Hothorn, M., Smith, B.O., Hitomi, K., Jenkins, G.I., and Getzoff, E.D., (2012). Plant UVR8 photoreceptor senses UV-B by tryptophan-mediated disruption of cross-dimer salt bridges. *Science* 335: 1492-1496.

Clark, R.M., Schweikert, G., Toomajian, C., Ossowski, S., Zeller, G., Shinn, P., Warthmann, N., Hu, T.T., Fu, G., Hinds, D.A., Chen, H., Frazer, K.A., Huson, D.H., Schölkopf, B., Nordborg, M., Rätsch, G., Ecker, J.R., Weigel, D., (2007). Common sequence polymorphisms shaping genetic diversity in *Arabidopsis thaliana*. *Science*. 317: 338-342.

Clerget, B., Rattunde, H.F.W., Weltzien, E., (2012). Why tropical sorghum sown in winter months has delayed flowering and modified morphogenesis in spite of prevailing short days. *Field Crops Research*. 125: 139-150.

Cloix, C., Jenkins, G.I., (2008). Interaction of the Arabidopsis UV-B-Specific signaling component UVR8 with chromatin. *Molecular Plant* 1: 118-128.

Cloix, C., Kaiserli, E., Heilmann, M., Baxter, K.J., Brown, B.A., O'Hara, A., Smith, B.O., Christie, J.M., Jenkins, G.I., (2012). C-terminal region of the UV-B photoreceptor UVR8 initiates signaling through interaction with the COP1 protein. *PNAS* 109: 16366-16370.

Cooley, N.M., Higgins, J.T., Holmes, M.G., Attridge, T.H., (2001). Ecotypic differences in responses of *Arabidopsis thaliana* L. to elevated polychromatic UV-A and UV-B + A radiation in the natural environment: a positive correlation between UV-B + A inhibition and growth rate. *Journal of Photochemistry and Photobiology B: Biology*. 60: 143-150.

Culligan, K.M., Robertson, C.E., Foreman, J., Doerner, P., Britt, A.B., (2006). ATR and ATM play both distinct and additive roles in response to ionizing radiation. *The Plant Journal*. 48(6): 947-961.

Davey, M.P., Susanti, N.I., Wargent, J.J., Findlay, J.E., Quick, W.P., Paul, N.D., Jenkins, G.I., (2012). The UV-B photoreceptor UVR8 promotes photosynthetic efficiency in *Arabidopsis thaliana* exposed to elevated levels of UV-B. *Photosynthesis Research*. 114(2): 121-131.

Demkura PV, Abdala G, Baldwin IT, Ballar´e CL. (2010). Jasmonate-dependent and -independent pathways mediate specific effects of solar ultraviolet-B radiation on leaf phenolics and antiherbivore defense. *Plant Physiology.* 152: 1084–95

Demkura, P.V., Ballaré, C.L., (2012). UVR8 mediates UV-B-induced *Arabidopsis* defense responses against *Botrytis cinerea* by controlling sinapte accumulation. *Molecular Plant*. 5(3): 642-652.

Deng, X-W. (1994). Fresh view of light signal transduction. *Cell* 76: 423-426.

Devlin, P.F., Christie, J.M., Terry, M.J., (2007). Many hands make light work. *Journal of Experimental Botany*. 58(12) 3071-3077.

Ding, S.T., Gális, I., Baldwin, I.T., (2012). UV-B radiation and HGL-DTGs provide durable resistance against mirid (*Tupiocoris notatus*) attack in field-grown *Nicotiana attenuata* plants. *Plant Cell & Environment*. 36: 590-606.

Fankhauser, C., Chory, J., (1997). Light control of plant development. *Annual Reviews in Cell Developmental Biology*. 13: 203-229.

Favory, J-J., Stec, A., Gruber, H., Rizzini, L., Oravecz, A., Funk, M., Albert, A., Cloix, C., Jenkins, G.I., Oakeley, E.J., Seidlitz, H., Nagy, F., Ulm, R., (2009). Interaction of COP1 and UVR8 regulates UV-B-induced Photomorphogenesis and Stress Acclimation in *Arabidopsis*. *The EMBO Journal*. 28: 591-601.

Filiault, D.L., Wessinger, C.A., Dinneny, J.R., Lutes, J., Borevitz, J.O., Wiegel, D., Chory, J., Maloof, J.M., (2008). Amino acid polymorphisms in *Arabidopsis* phytochrome B cause differential responses to light. *PNAS*. 105(8): 3157-3162.

Fioletov, V., Kerr, J.B., Fergusson, A., (2010). The UV Index: definition, distribution and factors affecting it. *Canadian Journal of Public Health*. 101(4): 15-19.

Frohnmeyer, H., Staiger, D., (2003). Ultraviolet-B radiation-mediated responses in plants. balancing damage and protection. *Plant Physiology* 133: 1420-1428.

Fuglevand, G., Jackson, J.A., and Jenkins, G.I., (1996). UV-B, UV-A and blue light signal transduction pathways interact synergistically to regulate chalcone synthase gene expression in Arabidopsis. *The Plant Cell* 8:2347-2357.

Fulcher, N., Teunbenbacher, A., Kerdaffrec, E., Farlow, A., Nordborg, M., Riha, K., (2015). Genetic Architechture of Natural Variation of Telomere Length in *Arabidopsis thaliana*. *GENETICS*. 199(2): 625-635.

Gangappa, S.N., Holm, M., Botto, J.F., (2013). Molecular interactions of BBX24 and BBX25 with HYH, HY5 HOMOLOG, to modulate Arabidopsis seedling development. *Plant Signaling & Behaviour*. 8:8, e25208, DOI: 10.4161/psb.25208.

Gao, Q., Zhang, L., (2008). Ultraviolet-B-induced oxidative stress and antioxidant defense system responses in ascorbate-deficient *vtc1* mutants of *Arabidopsis thaliana*. *Journal of Plant Physiology* 165:138-148.

Garcia, V., Bruchet, H., Camescasse, D., Granier, F., Bouchez, D., Tissier, A., (2003). AtATM is essential for meiosis and the somatic response to DNA damage in plants. *The Plant Cell*. 15(1): 119-132.

Gegas, V.C., Wargent, J.J., Pesquet, E., Granqvist, E., Paul, N.D., Doonan, J.H., (2014). Endopolyploidy as a potential alternative adaptive strategy for *Arabidopsis* leaf size variation in response to UV-B. *Journal of Experimental Botany*. DOI: 10.1093/jxb/ert473.

González Besteiro, M.A., Bartels, S., Ablert, A., Ulm, R., (2011). Arabidopsis MAP kinase phosphatase 1 and its target MAP kinases 3 and 6 antagonistically determine UV-B stress tolerance, independent of the UVR8 photoreceptor pathway. *The Plant Journal*. 68:727-737.

Gruber, H., Heijge, M., Heller, W., Albert, A., Seidlitz, H., Ulm, R., (2010). Negative feedback regulation of UV-B-induced photomorphogenesis and stress acclimation in *Arabidopsis*. *PNAS*. 107(46): 20132-20137.

Guy, L.C., (1990). Cold acclimation and freezing stress. *Annual Review of Plant Physiology and Plant Molecular Biology*. 41: 187-223.

Hayes, S., Velanis, C.N., Jenkins, G.I., Franklin, K.A., (2014). UV-B detected by the UVR8 photoreceptor antagonizes auxin signalling and plant shade avoidance. *PNAS*. 111(32): 11894-11899.

Hectors, K., Prinsen, E., de Coen, W., Jansen, M.A.K., Guisez, Y., (2007). *Arabidopsis thaliana* plants acclimated to low dose rates of ultraviolet B radiation show specific changes in morphology and gene expression in the absence of stress symptoms. *New Phytologist*. 175: 255-270.

Hectors, K,. van Oevelen, S., Geuns, J., Guisez, Y., Jansen, M.A.K., Prinsen, E., (2014). Dynamic changes in plant secondary metabolites during UV acclimation in *Arabidopsis thaliana*. *Physiologia Plantarum*. 152: 219-230.

Heijge, M., Ulm, R., (2012). UV-B photoreceptor-mediated signaling in plants. *Trends in Plant Science* 17: 4-11.

Heijge, M., Ulm, R., (2013). Reversion of the *Arabidopsis* UV-B photoreceptor UVR8 to the homodimeric ground state. *PNAS* 110: 1113-1118.

Heilmann M., and Jenkins G.I., (2013). Rapid reversion from monomer to dimer regenerates the ultraviolet-B photoreceptor UV RESISTANCE LOCUS8 in intact Arabidopsis plants. *Plant Physiology* 161: 547-555.

Hideg, E., Jansen, M.A.K., Strid, Å., (2013). UV-B exposure, ROS, and stress: inseparable companions or loosely linked associates? *Trends in Plant Sciences*. 19(2): 107-115.

Hilscher, J., Schlötterer, C., Hauser, M.T., (2009). A single amino acid replacement in ETC2 shapes trichome patterning in natural *Arabidopsis* populations. *Current Biology*. 19: 1747-1751.

Hoecker, U., Quail, P.H., (2001). The phytochrome A-specific signalling intermediate SPA1 interacts directly with COP1, a constitutive repressor of light signalling in Arabidopsis. 276(41): 38173-38178.

Holm, M., Hardtke C.S., Gaudet, R., Deng, X-W., (2001). Identification of a structural motif that confers specific interaction with the WD40 repeat domain of Arabidopsis COP1. *The EMBO Journal*. 20: 118-127.

Holm, M., Ma, L-G., Qu, L-J., Deng, X-W., (2002). Two interacting bZIP proteins are direct targets of COP1-mediated control of light-dependent gene expression in Arabidopsis. *Genes and Development*. 16: 1247-1259.

Horton, M.W., Hancock, A.M., Huang, Y.S., Toomajian, C., Atwell, S., Auton, A., Muliyati, N.W., Platt, A., Sperone, F.G., Vilhjálmsson, B.J,. Nordborg, M., Borevitz, J.O., Bergelson, J., (2012). Genome-wide patterns of genetic variation in worldwide *Arabidopsis thaliana* accession from the RegMap panel. *Nature Genetics*. 44(2): 212-216.

Hua, J., (2013). Modulation of plant immunity by light circadian rhythm and temperature. *Current Opinion in Plant Biology*. 16: 406-413.

Huang, X., Ouyang, X., Yang, P., Lau, O.S., Chen, L., Wei, N., Deng, X.W., (2013). Conversion from CUL4-based COP1-SPA E3 apparatus to UVR8-COP1-SPA complexes underlies a distinct biochemical function of COP1 under UV-B. *PNAS*. 110(41): 16669-16674.

Huang, X., Yand, P., Ouyang, X., Chen, L., Deng, X.W., (2014). Photoactivated UVR8-COP1 module determines photomorphogenic UV-B signalling output in *Arabidopsis*. *PLoS Genetics*. 10(3): e1004218.

Imaizumi, T., Schultz, T.F., Harmon, F.G., Ho, L.A., Kay, S.A., (2005). FKF1 F-box protein mediates cyclic degradation of a repressor of CONSTANS in Arabidopsis. *Science*. 309(5732): 293-297.

Izaguirre, M.M., Mazza, C.A., Biondini, M., Baldwin, I.T., Ballaré, C.L., (2003). Convergent responses to stress. Solar ultraviolet-B radiation and *Manduca sexta*

herbivory elicit overlapping transcriptional responses in field-grown plants of *Nicotiana longiflora*. *Plant Physiology*. 132: 1755-1767.

Jakoby, M., Weisshaar, B., Dröge-Laser, W., Vicente-Carbajosa, J., Tiedemann, J., Kroj, T., Parcy, F., (2002). bZIP transcription factors in Arabidopsis. *Trends in Plant Science*. 7(3): 106-111.

Jansen, M.A.K., Bornman, J.F., (2012). UV-B radiation: from generic stressor to specific regulator. *Physiologia Plantarum*. 145: 501-504.

Jenkins, G.I., (2009). Signal trasduction in responses to UV-B radiation. *Annual Review of Plant Biology* 60: 407-431.

Jenkins, G.I., (2014). The UV-B photoreceptor UVR8: from structure to physiology. *The Plant Cell*. 26: 21-37.

Jian, L., Li, S., (2015). Signaling cross talk under the control of plant photoreceptors. *Photobiology: The Science of Light and Life*. DOI: 10.1007/978-1-4939-1468-5_14.

Jonassen, E.M., Lea, U.S., Lillo, C., (2008). *HY5* and *HYH* are positive regulators of nitrate reductase in seedlings and rosette stage plants. *Planta*. 227: 559-564.

Jordan, B.R., (1996). The effects of Ultraviolet-B radiation on plants: a molecular perspective. *Advances in Botanical Reseach*. 22: 97-162.

Kaiserli, E., and Jenkins, G.I., (2007). UV-B promotes rapid nuclear translocation of the Arabidopsis UV-B specific signaling component UVR8 and activates its function in the nucleus. *The Plant Cell* 19:2662-2673.

Kami, C., Lorrain, S., Hornitschek, P., Fankhauser, C., (2010). Chapter Two – Light-Regulated Plant Growth and Development. *Current Topics in Developmental Biology*. 91: 29-66.

Kataria, S., Jojoo, A., Guruprasad, K.N., (2014). Impact of increasing Ultraviolet-B (UV-B) radiation on photosynthetic processes. *Journal of Photochemistry and Photobiology B: Biology*. 137: 55-66.

Kazan, K., Manners, J.M.M., (2011). The interplay between light and jasmonate signalling during defence and development. *Journal of Experimental Botany*. 62(12): 4087-4100.

Kilian, J., Whitehead, D., Horah, J., Wanke, D., Weinl, S., Batistic, O., D'Angelo, C., Bornberg-Bauer, E., Kudla, J., Harter, K., (2007). The AtGenExpress global stress expression data set: protocols, evaluation and model data analysis of UV-B light, drought and cold stress responses. *The Plant Journal*. 50: 347-363.

Kircher, S., Nobis, T., Nitschke, R., Kunkel, T., Bauer, D., (2004). Constitutive Photomorphogenesis 1 and multiple photoreceptors control degradation of phytochrome interacting factor 3, a transcription factor required for light signalling in Arabidopsis. *Control*. 16: 1433-1445.

Kliebenstein, D.J., Lim, J.E., Landry, L.G., Last, R.L., (2002). Arabidopsis UVR8 regulates Ultraviolet-B signal transduction and tolerance and contains sequence similarity to human *Regulator of Chromatin Condensation 1. Plant Physiology* 130:234-243.

Kobayashi, M., Kanto, T., Fujikawa, T., Yamada, M., Ishiwata, M., Satua, M., Hisamatsu, T., (2013). Supplemental UV radiation controls rose powdery mildew disease under the greenhouse conditions. *Environmental Control in Biology*. 51(4): 157-163.

Koorneef, M., Alonso-Blanco, C., Vreugdenhil, D., (2004). Naturally occurring genetic variation in *Arabidopsis thaliana*. *Annual Reviews in Plant Biology*. 55: 141-172.

Krizek, D.T., (2004). Influence of PAR and UV-A in determining plant sensitivity and photomorphogenic responses to UV-B radiation. *Photochemistry and Photobiology*. 79(4): 307-315.

Laubinger, S., Fittinghoff, K., Hoecker, U., (2004). The SPA quartet: a family of WD-repeat proteins with a central role in suppression of photomorphogenesis in arabidopsis. *Plant Cell*. 16(9): 2293-2306.

Laubinger, S., Hoecker, U., (2003). The SPA1-like proteins SPA3 and SPA4 repress photomorphogenesis in the light. *The Plant Journal*. 35(3): 373-385.

Li, J., Li, G., Wang, J., Deng, X.W., (2011). Phytochrome signalling mechanisms. *The Arabidopsis Book*. 9.

Liu, Z., Li, X., Zhong, F.W., Li, J., Wang, L., Shi, Y., Zhong, D., (2014). Quenching dynamics of Ultraviolet-light perception by UVR8 photoreceptor. *The Journal of Physical Chemistry Letters*. 5: 69-72.

Liscum, E., Hodgson, D.W., Campbell, T.J., (2003). Blue light signalling through the cryptochromes and phototropins. So that's what the blues is all about. *Plant physiology*. 133(4): 1429-1436.

Mackerness, S.A.H., John, C.F., Jordan, B., Thomas, B., (2001). Early signalling components in ultraviolet-B responses: distinct roles for different reactive oxygen species and nitric oxide. *FEBS Letters*. 489(2): 237-242.

Madronich, S., McKenzie, R.L., Björn, L.O., Caldwell, M.M., (1998). Changes in biologically active ultraviolet radiation reaching the Earth's surface. *Journal of Photochemistry and Photobiology B: Biology*. 46: 5-19.

Magrane, M., and Uniprot Consortium, (2011). UniProt Knowledgebase: a hub of integrated protein data. *Database*. DOI: 10.1093/database/bar009.

Maloof, J.N., Borevitz, J.O., Dabi, T., Lutes, J., Nehring, R.B., Redfern, J.L., Trainer, G.T., Wilson, J.M., Asami, T., Berry, C.C., Weigel, D., Chory, J., (2001). Natural variations in light sensitivity of *Arabidopsis*. *Nature*. 29: 441-446.

Martínez-Lüscher, J., Torres, N., Hilbert, G., Richard, T., Sánchez-Díaz, M., Delrot, S., Aguirreolea, J., Pascual, I., Gomés, E., (2014). Ultraviolet-B radiation modifies the quantitative and qualitative profile of flavonoid and amino acids in grape berries. *Phytochemistry*. 102: 106-114.

Mathes, T., Heilmann, M., Pandit, A., Zhu, J., Ravensbergen, J., Kloz, M., Fu, Y., Smith, B.O., Christie, J.M., Jenkins, G.I., Kennis, J.T.M., (2015). Proton-coupled electron transfer consititues the photoactivation mechanism of the

plant photoreceptor UVR8. *Journal of the American Chemical Society*. 135(5): 8113-8120.

Mazza, C.A., Ballaré, C.L., (2015). Photoreceptors UVR8 and phytochome B cooperate to optimize plant growth and defense in patchy canopies. *New Phytologist*. DOI: http://dx.doi.org/10/1111/nph/13332.

McClung, C.R., Salomé, P.A., Michael, T.P. (2002). The Arabidopsis circadian system. *The Arabidopsis Book*. 1.

McClung, C.R., (2011). The genetics of plant clocks. *Advanced Genetics*. 74(74): 105-139.

Méndez-Vigo, B., Picó, F.X., Ramiro, M., Martínez-Zapater, J.M., Alonso-Blanco, C., (2011). Altitudinal and climatic adaptiation is mediated by flowering traits FRI, FLC and PHYC genes in *Arabidopsis*. *Plant Physiology*. 157: 1942-1955.

Miyamori, T., Nakasone, T., Hitome, K., Christie, J.M., Getzoff, E.D., Terazime, M., (2015). Reaction dynamics of the UV-B photosensor UVR8. *Photochemical and Photobiological Science*. DOI: 10.1039/C5PP00012B.

Montaigu, A., Giokountis, A., Rubin, M., Tóth, R., Cremer, F., Sokolova, V., Porri, A., Reymond, M., Weinig, C., Coupland, G., (2015). Natural diversity in daily rhythms of gene expression contributes to phenotypic variation. *PNAS*. 112(3): 905-910.

Morales, L.O., Broshe, M., Vainonen, J., Jenkins, G.I., Wargent, J.J., Sipari, N., Strid, A., Lindfors, A.V., Tegelberg, R., and Aphalo, P.J., (2013). Multiple Roles for UV Resistance Locus8 in Regulating Gene Expression and Metaboliet Accumulation in Arabidopsis Under Solar Ultraviolet Radiation. *Plant Physiology* 161:744-759.

Möglich, A., Yang, X., Ayers, R.A., Moffat, K., (2010). Structure and function of plant photoreceptors. *Annual Review of Plant Biology*. 61: 21-47.

Müller-Xing, R., Xing, Q., Goodrich, J., (2014). Footprints of the sun: memory of UV and light stress in plants. *Frontiers in Plants Science*. 5(474): 1-12.

Nemhauser, J.L., (2008). Dawning of a new era: photomorphogenesis as an integrated molecular network. *Current Opinion in Plant Biology*. 11:4-8.

Nordborg, M., (2000). Linkage disequilibrium, gene trees and selfing: an ancestral recombination graph with partial self-fertilization. *Genetics*. 154: 923-929.

Nordborg, M., Hu, T.T., Ishino, Y., Jhaveri, J., Toomajian, C., Zheng, H., Bakker, E., Calbrese, P., Gladstone, J., Goyal, R., Jakobsson, M., Kim, S., Morozov, Y., Padhukasahasram, B., Plagnol, V., Rosenberg, N.A., Shah, C., Wall, J.D., Wang, J., Zhao, K., Kalbfleisch, T., Schulz, V., Kreitman, M., Bergelson, J., (2005). The pattern of polymorphism in *Arabidopsis thaliana*. *PLoS Biology*. 3(7): e196.

O'Hara, A., Jenkins, G.I., (2012). In vivo function of tryptophans in the *Arabidopsis* UV-B photoreceptor UVR8. *The Plant Cell*. 24: 3755-3766.

Osmond, C.B., Austin, M.P., Berry, J.A., Billings, W.D., Boyer, J.S., Dacey, J.W.H., Nobel, P.S., Smith, S.D., Winner, W.E., (1987). How plants cope: plant physiological ecology. *BioScience*. 37(1): 38-48.

Pacín, M., Legris, M., Casal, J.J., (2013). COP1 re-accumulates in the nucleus under shade. *The Plant Journal*. 75: 631-641.

Pedmale, U.V., Celaya, R.B., Liscum, E., (2010). Phototropism: mechanism and outcomes. *The Arabidopsis Book*. 8.

Perata, P., Armstrong, W., Voesenek, L.A.C.J., (2011). Commentary plants and flooding stress. *New Phytologist*. 190: 269-273.

Platt, A., Horton, M., Huang, Y.S., Li, Y., Anastasio, A.E,. Mulyati, N.W., Ågren, J., Bossdorf, O., Byers, D., Donohue, K., Dunning, M., Holub, E.B., Hudson, A., le Corre, V., Loudet, O., Roux, F., Warthmann, N., Weigel, D., Rivero, L., Scholl, R., Nordborg, M., Bergelson, J., Borevitz, J.O., (2010). The scale of population structure in *Arabidopsis thaliana*. *PLoS Genetics*. 6(2): e1000843.

Rausenberger, J., Tscheuschler, A., Nordmeier, W., Wüst, F., Timmer, J., Schäfer, E., Fleck, C., Hiltbrunner, A., (2011). Photoconversion and nuclear

trafficking cycles determine Phytochrome A's response profile to far-red light. *Cell*. 146: 813-825.

Rizzini, L., Favory, J., Cloix, C., Faggionato, D., O'Hara, A., Kaiserli, E., Baumeister, R., Schafer, E., Nagy, F., Jenkins, G.I., and Ulm, R., (2011). Perception of UV-B by the *Arabidopsis* UVR8 protein. *Science* 332:103-106.

Robson, T.M., Klem, K., Urban, O., Jansen, M.A.K., (2014). Re-interpreting plant morphological responses to UV-B radiation. *Plant, Cell & Environment*. DOI: 10.1111/pce.12374.

Saijo, Y., Sullivan, J.A., Wang, H., Yang, J., Shen, Y., Rubio, V., Ma, L., Hoechker, U., Deng, X-W., (2003). The COP1-SPA1 interaction defines a critical step in phytochrome A-mediated regulation of HY5 activity. *Genes & Development*. 17: 2642-2647.

Saijo, Y., Zhu, D., Li, J., Rubio, V., Zhou, Z., Shen, Y., Hoecker, U., Wang, H., Deng, X-W., (2008). Arabidopsis COP1/SPA1 complex and FHY1/FHY3 associate with distinct phosphorylated forms of phytochrome A in balancing light signalling. *Molecular Cell*. 31(4): 607-613.

Schulz, E., Tohge, T., Zuther, E., Fernie, A.R., Hincha, D.K., (2015). Natural variation in flavonol and anthocyanin metabolism during cold acclimation in *Arabidopsis thaliana* accessions. *Plant, Cell & Environment*. 38(8): 1658-1672.

Sedej, T.T., (2014). Broadleaf and conifer tree responses to long-term enhanced UV-B radiation in outdoor experiments: a review. *Acta Biologica Slovenica*. 52(2): 13-23.

Seo, H.S., Yang, J-Y., Ishikawa, M., Bolle, C., Ballesteros, M.L., Chua, N-H., (2003). LAF1 ubiquitination by COP1 controls photomorphogenesis and is stimulated by SPA1. *Nature*. 423: 995-999.

Sexton, J.P., McIntyre P.J., Angert, A.L., Rice, K.J., (2009). Evolution and ecology of species range limits. *Annual Review of Ecology, Evolution and Systematics*. 40: 415-436.

Sibout, R., Sukumar, P,. Hettiarachchi, C., Holm, M., Muday, G.K., Hardtke, C.S., (2006). Oppositie root growth phenotypes of *hy5* versus *hy5 hyh* mutants correlate with increased constitutive auxin signalling. *PLoS Genetics*. 2(11): e202.

Singh, S., Agrawal, S.B., Agrawal, M., (2014). UVR8 mediated plant protective responses under low UV-B radiation leading to photosynthetic acclimation. *Journal of Photochemistry and Photobiology B: Biology*. 137: 67-76.

Smirnoff, N., (1998). Plant resistance to environmental stress. Current Opinion in Biotechnology. 9: 214-219.

Somers, D.E., 2001. Clock-associated genes in Arabidopsis: a family affair. *Philosophical Transaction of the Royal Society of London. Series B, Biological Sciences*. 356(1415): 1745-1753.

Srivastava, P.K., Singh, V.P., Prasad, S.M., (2014). Low and high doses of UV-B differentially modulate chlorpyrifos-induced alterations in nitrogen metabolism of cyanobacteria. *Ecotoxicology and Environmental Safety*. 107: 291-299.

Stacey, M.G., Hicks, S.N., von Arnim, A.G., (1999). Discrete domains mediate the light-responsive nuclear and cytoplasmic localization of Arabidopsis COP1. *Plant Cell*. 11: 349-364.

Subramanian, C., Kim, B-H., Lyssenko, N.N., Xu, X., Johnson, C.H., von Arnim, A.G., (2004). The *Arabidopsis* repressor of light signalling, COP1, is regulated by nuclear exclusion: mutational analysis by bioluminescence resonance energy transfer. *PNAS*. 101(17): 6798-6802.

Swarup, K., Alonso-Blanco, C., Lynn, J.R., Michaels, S.D., Amasino, R.M., Koorneef, M., Millar, A.J., (1999). Natural allelic variation identifies new genes in the *Arabidopsis* circadian system. *The Plant Journal*. 20(1): 67-77.

Thomashow, M.F., (1999). Plant cold acclimation: freezing tolerance gene and regulatory mechanisms. *Annual Review of Plant Physiology and Plant Molecular Biology*. 50: 571-599.

Thomashow, M.F., (2001). So what's new in the field of plant cold acclimation? Lots! *Plant Physiology*. 125(1): 89-93.

Tilbrook, K., Arongaus, A.B., Binkert, M., Heijge, M., Yin, R., Ulm, R., (2013). The UVR8 UV-B photoreceptor: perception, signalling and response. *The Arabidopsis Book*. DOI: 10.1199/tab.0164.

Torabinejad, J., Caldwell, M.M., (2000). Inheritance of UV-B tolerance in seven ecotypes of *Arabidopsis thaliana* L. Heynh. and their F_1 hybrids. *The American Genetic Association*. 91: 228-233.

Torii, K.U., Stoop-Myer, C.D., Okamoto, H., Coleman, J.E., Matsui, M., Deng, X-W., (1999). The RING finger motif of photomorphogenic repressor COP1 specifically interacts with the RING-H2 motif of a novel Arabidopsis protein. *Journal of Biological Chemistry*. 274(39): 27674-27681.

Tossi, V., Lamattina, L., Jenkins, G.I., Cassia, R.O., (2014). Ultraviolet-B-induced stomatal closure in Arabidopsis is regulated by the UV RESISTANCE LOCUS8 photoreceptor in a nitric oxide-dependent mechanism. *Plant Physiology*. 164: 2220-2230.

Trewavas, A.J., Malhó, R., (1997). Signal perception and transduction: the origin of the phenotype. *The Plant Cell*. 9: 1181-1195.

Ulm, R., Baumann, A., Oravecz, A., Máté, Z., Ádám, É., Oakeley, E.J., Schäfer, Nagy, F., (2004). Genome-wide analysis of gene expression reveals function of the bZIP transcription factor HY5 in the UV-B response of *Arabidopsis*. *PNAS*. 101(5): 1397-1402.

Ulm, R., Nagy, F., (2005). Signalling and gene regulation in response to ultraviolet light. *Current Opinions in Plant Biology*. 8: 477-482.

Vandenbussche, F., Tilbrook, K., Fierro, A.C., Marchal, K., Poelman, D., van der Straeten, D., Ulm, R., (2014). Photoreceptor-mediated bending towards towards UV-B in *Arabidopsis*. *Molecular Plant*. 7: 1041-1052.

Vierstra, R.D., Zhang, J., (2011). Phytochrome signalling: solving the Gordian knot with microbial relatives. *TRENDS in Plant Science*. 16(8): 417-26.

Vinocur, B., Altman, A., (2005). Recent advances in engineering plant tolerance to abiotic stress: achievements and limitations. *Current Opinion in Biotechnology*. 16(2): 123-132.

Visser, E.J.W., Voesenek, L.A.C.J., Vartapetian, B.B., Jackson, M.B., (2003). Flooding and plant growth. *Annals of Botany*. 91: 107-109.

Voityuk, A.A., Marcus, R.A., Michel-Beyerle, M-E., (2014). On the mechanism of photoinduced dimer dissociation in the plant UVR8 photoreceptor. *PNAS*. 111(14): 5219-5224.

Wade, H. K., Bibikova, T.N., Valentine, W.J., and Jenkins, G.I., (2001). Interactions within a network of Phytochrome, Cryptochrome and UV-B phototransduction pathways regulate Chalcone Synthase gene expression in Arabidopsis leaf tissue. *The Plant Journal* 25:675-685.

Wang, W., Yang, D., Feldmann, K.A., (2011). *EFO1* and *EFO2*, encoding putative WD-domain proteins, have overlapping and distinct roles in the regulation of vegetative development and flowering of *Arabidopsis*. *Journal of Experimental Botany*. 62(3): 1077-1088.

Wargent, J.J., Gegas, V.C., Jenkins, G.I., Doonan, J.H., Paul, N.D., (2009). UVR8 in *Arabidopsis thaliana* regulates multiple aspects of cellular differentiation during leaf development in response to ultraviolet B radiation. *New Phytologist* 183:315-326.

Wargent, J.J., Nelson, B.C.W., McGhie, T.K., Barnes, P.W., (2014). Acclimation to UV-B radiation and visible in *Lactuca sativa* involves up-regulation of photosynthetic performance and orchestration of metabolome-wide responses. *Plant, Cell & Environment*. DOI: 10.1111/pce.12392.

Williamson, C.E., Zepp, R.G., Lucas, R.M., Madronich, S., Austin, A.T., Ballaré, C.L., Norval, M., Sulzberger, B., Bais, A.F., McKenzie, R.L., Robinson, S.A., Häder, D-P., Paul, N.D., Bornman, J.F., (2014). Solar ultraviolet radiation in a changing climate. *Nature Climate Change*. 4: 434-441.

Wrzaczek, M., Vainonen, J.P., Gauthier, A., Overmyer, K., Kangasjärvi, J., (2011). Reactive oxygen in abiotic stress perception – from genes to proteins. *ABIOTIC STRESS RESPONSE IN PLANTS – PHYSIOLOGICAL BIOCHEMICAL AND GENETIC PERSPECTIVES*. 27.

Wu, M., Grahn, E., Eriksson, L.A., Strid, Å., (2011). Computational evidence for the role of *Arabidopsis thaliana* UVR8 as UV-B photoreceptor and identification of its chromophore amino acids. *Journal of Chemical Information and Modeling*. 51: 1287-1295.

Wu, D., Hu, Q., Yan, Z., Chen, W., Yan, C., Huang, X., Zhang, J., Yang, P., Deng, H., Wang, J., Deng, X., and Shi, Y., (2012). Structural Basis of Ultraviolet-B Perception by UVR8. *Nature* 484:214-220.

Wu, M., Strid, Å., Eriksson, L.A., (2013). Interactions and stabilities of the UV RESISTANCE LOCUS8 (UVR8) protein dimer and its key mutants. *Journal of Chemical Information and Modeling*. 53: 1736-1746.

Wu, M., Eriksson, L.A., Strid, Å., (2013). Theoretical prediction of the protein-protein interaction between *Arabidopsis thaliana* COP1 and UVR8. *Theoretical Chemistry Accounts*. 132: 1371.

Wu, S., (2014). Gene Expression Regulation in Photomorphogenesis from the Perspective of the Central Dogma. *Annual Review of Plant Biology*. 65: 311-333.

Wu, M., Strid, Å., Eriksson, L.A., (2014). Photochemical reaction mechanism of UV-B-induced monomerization of UVR8 dimers as the first signaling event in UV-B-regulated gene expression in plants. *The Journal of Physical Chemistry B*. 118: 951-965.

Xu, C., and Min, J., (2011). Structure and function of WD40 domain proteins. *Protein Cell*. 2(3): 202-214.

Yoon, M.K., Kim, H.M., Choi, G., Lee, J.O., Choi, B.S., (2007). Structural basis for the conformational integrity of the Arabidopsis thaliana HY5 leucine zipper homodimer. *The Journal of Biological Chemistry*. 282: 12989-13002.

Yu, X., Liu, H., Klejnot, J., Lin, C., (2010). The Cryptochrome blue light receptors. *The Arabidopsis Book*. 8.

Yu, Y., Wang, J., Zhang, Z., Quan, R., Zhang, H., Deng, X.W., Ma, L., Huang, R., (2013). Ethylene promotes hypocotyl growth and HY5 degradation by enhancing the movement of COP1 to the nucleus in the light. *PLoS Genetics*. 9(12): e1004125.

Zavala, J.A., Mazza, C.A., Dillon, F.M., Chludil, H.D., Ballaré, C.L., (2014). Soybean resistance to stink bugs (*Nezara viridula* and *Piezodorus guildinii*) increases with exposure to solat UV-B radiation and correlates with isoflavonoid content in pods under field conditions. *Plant, Cell & Environment*. DOI: 10.1111/pce.12368.

Zhang, Y., Zheng, S., Zhongjuan, L., Wang, L., Bi, Y., (2011). Both HY5 and HYH are necessary regulators for low temperature-induced anthocyanin accumulation in *Arabidopsis* seedlings. *Journal of Plant Physiology*. 168: 367-374.